FACULDADE DE ENGENHARIA DA UNIVERSIDADE DO PORTO

Automating HVAC Implementation in Hospitals: Pressure Losses, Maintenance, and Life Cycle Cost Analysis

Isabel Martins Mendes Monteiro de Azevedo
up202006880

Master's Degree in Mechanical Engineering

FEUP Supervisor: Prof. José Joaquim da Mota Machado, PhD

ASL Supervisor: Eng.º Salvador Costa

June 28^{th}, 2025

Automating HVAC Implementation in Hospitals: Pressure Losses, Maintenance, and Life Cycle Cost Analysis

Isabel Martins Mendes Monteiro de Azevedo

up202006880

Master's Degree in Mechanical Engineering

June 28^{th}, 2025

Abstract

António Santos Lessa was founded in 2006 and has since grown significantly in the field of building project specialities. The firm operates in engineering and consulting, offering comprehensive services that include the design of architectural, electrical, structural, and mechanical systems. While it has worked on various building types, it has recently focused more on healthcare facilities such as hospitals, clinics, and treatment units.

This project was developed for the Mechanical Installations team to enhance the efficiency of HVAC system implementation in hospitals. It addressed three main challenges: calculating pressure losses in complex duct systems to correctly size equipment, creating a database and schedule for future maintenance, and developing a tool to assess life cycle costs and compare equipment options.

Different tools were applied to each task. The first, a custom tool was created using Revit's programming interface to automate pressure loss calculations. This reduced design time and human error significantly. Comparing manual and automated methods shows a time and cost reduction of more than 90% per duct system, based on calculations for the critical path only.

For the second task, Microsoft Power Apps was used to build a user-friendly platform for HVAC maintenance management. The app centralises equipment data and enables real-time tracking of maintenance, supporting operational decisions. Its full impact is not yet measurable, as the hospital is still under construction.

Finally, Microsoft Power BI was used to implement a Life Cycle Cost Analysis (LCCA) tool. It integrates acquisition and replacement costs, providing automated and visual analysis of long-term economic performance across HVAC assets.

In conclusion, the integration of digital tools such as Revit, Power Apps, and Power BI has been demonstrated to be highly effective in addressing the key challenges related to HVAC design and maintenance in healthcare facilities. The automation of pressure loss calculations has been demonstrated to ensure enhanced accuracy, whilst concomitantly delivering substantial savings in terms of both time and cost. The establishment of a maintenance platform utilising Power Apps established the foundation for enhanced efficiency and traceability in equipment management during the operational phase. Furthermore, the LCCA tool developed with Power BI yielded valuable long-term insights, facilitating strategic decision-making. Collectively, these tools facilitate a more streamlined, data-driven approach to hospital engineering design and lifecycle management.

Resumo

António Santos Lessa foi fundada em 2006 e desde então tem crescido significativamente no campo das especialidades de projectos de construção. A empresa opera na área da engenharia e consultoria, oferecendo serviços abrangentes que incluem a conceção de sistemas arquitectónicos, eléctricos, estruturais e mecânicos. Embora tenha trabalhado em vários tipos de edifícios, recentemente tem-se focado mais em instalações de saúde, tais como hospitais, clínicas e unidades de tratamento.

Este projeto foi desenvolvido para a equipa de Instalações Mecânicas para melhorar a eficiência da implementação de sistemas AVAC em hospitais. Abordou três desafios principais: calcular as perdas de pressão em sistemas de condutas complexos para dimensionar corretamente o equipamento, criar uma base de dados e um calendário para manutenção futura e desenvolver uma ferramenta para avaliar os custos do ciclo de vida e comparar opções de equipamento.

Para cada tarefa foram aplicadas diferentes ferramentas. A primeira, uma ferramenta personalizada, foi criada utilizando a interface de programação do Revit para automatizar os cálculos de perda de pressão. Isto reduziu significativamente o tempo de projeto e o erro humano. A comparação entre os métodos manual e automatizado mostra uma redução de tempo e custo de mais de 90% por sistema de condutas, com base em cálculos apenas para o caminho crítico.

Para a segunda tarefa, o Microsoft Power Apps foi utilizado para criar uma plataforma de fácil utilização para a gestão da manutenção de AVAC. A aplicação centraliza os dados do equipamento e permite o acompanhamento em tempo real da manutenção, apoiando as decisões operacionais. O seu impacto total ainda não é mensurável, uma vez que o hospital ainda está em construção.

Por último, o Microsoft Power BI foi utilizado para implementar uma ferramenta de análise do custo do ciclo de vida (LCCA). Esta integra os custos de aquisição e substituição, fornecendo uma análise automatizada e visual do desempenho económico a longo prazo dos activos de AVAC.

Em conclusão, a integração de ferramentas digitais como o Revit, Power Apps e Power BI demonstrou ser altamente eficaz na abordagem dos principais desafios relacionados com o projeto e manutenção de AVAC em instalações de cuidados de saúde. Foi demonstrado que a automatização dos cálculos de perda de pressão garante uma maior precisão, ao mesmo tempo que permite poupanças substanciais em termos de tempo e de custos. A criação de uma plataforma de manutenção utilizando o Power Apps estabeleceu a base para uma maior eficiência e capacidade de registo na gestão de equipamentos durante a fase operacional. Além disso, a ferramenta LCCA desenvolvida com o Power BI produziu conhecimentos valiosos a longo prazo, facilitando a tomada de decisões estratégicas. No seu conjunto, estas ferramentas facilitam uma abordagem mais simplificada e guiada por dados à conceção da engenharia hospitalar e à gestão do ciclo de vida.

Acknowledgments

Esta dissertação assinala o fim do meu percurso académico e o encerramento de um capítulo marcante da minha vida enquanto estudante. Foi um trajeto repleto de esforço, dedicação, desafios e superações, cujas memórias levarei para sempre comigo.

Em primeiro lugar, gostaria de expressar o meu sincero agradecimento à ASL pela oportunidade de desenvolver este trabalho num ambiente profissional tão enriquecedor. A possibilidade de aprender e colaborar com uma empresa com vasta experiência no setor representou um contributo inestimável para o meu crescimento técnico e profissional.

À equipa de Mecânica, que tão bem me acolheu ao longo destes meses, agradeço a disponibilidade, o apoio constante e a partilha de conhecimentos, que foram essenciais para a concretização deste projeto.

Um agradecimento especial ao Eng.º Salvador Costa e ao Eng.º Nuno Couto, pela orientação dedicada, paciência e generosidade na transmissão de saberes práticos, que muito enriqueceram esta experiência.

Ao Professor José Machado, manifesto o meu profundo reconhecimento pela motivação incansável, pelos conselhos valiosos e pela confiança depositada em mim ao longo de todo este processo. O seu apoio foi determinante para a realização deste trabalho.

Sou profundamente grata às minhas amigas por me terem acompanhado durante esta jornada, por todos os momentos e memórias partilhadas, por todos os sorrisos que tornaram esta experiência mais leve.

Um agradecimento enorme ao meu namorado, Miguel, por todo o carinho, compaixão e motivação durante estes últimos anos. Obrigada pelo amor e confiança constantes.

Por fim, obrigada do fundo do coração à minha família que é a verdadeira razão de ter conseguido completar esta etapa. Obrigada por serem um exemplo de força, dedicação e por me proporcionarem a oportunidade de alcançar este objetivo. Ficarei eternamente grata.

Isabel Martins Mendes Monteiro de Azevedo

Relevant Sustainable Development Goals (SDGs)

The present dissertation aligns with several United Nations Sustainable Development Goals (SDGs), reflecting its broader contribution to sustainable development in the context of engineering design, digital transformation, and healthcare infrastructure.

Firstly, the project directly supports SDG 9 – Industry, Innovation and Infrastructure – by developing innovative digital tools to improve the design and operational management of HVAC systems in hospital settings. The implementation of an automated pressure loss calculation tool within Autodesk Revit demonstrates the efficacy of automation in streamlining complex engineering tasks, the reduction of human error, and the enhancement of productivity and precision in the design of mechanical systems. Furthermore, the establishment of a maintenance management platform utilising Microsoft Power Apps signifies a substantial advancement in the digitalisation of facility management practices, thereby facilitating more dependable and data-driven decision-making processes during the operational phase of hospital infrastructure.

In addition to technological innovation, the project also indirectly advances SDG 3 – Good Health and Well-Being, due to its focus on the critical role that HVAC systems play in maintaining safe and healthy indoor environments in healthcare facilities. Adequate ventilation, air quality control, and thermal comfort must be ensured for the prevention of infection and the enhancement of patient and healthcare staff well-being. The project's contribution to the resilience and functionality of hospital environments is evident in its focus on the maintenance and monitoring of HVAC systems through a dedicated platform.

In conclusion, the incorporation of a Life Cycle Cost Analysis (LCCA) instrument is instrumental in achieving Sustainable Development Goal 12 (SDG 12) – Responsible Consumption and Production – by facilitating more sustainable decision-making throughout the life cycle of HVAC equipment. This tool encourages a more holistic and resource-efficient approach to infrastructure management by taking into account not only the initial cost but also the operational and replacement expenses of mechanical components. In doing so, the project fosters economic and environmental sustainability in the planning and maintenance of complex systems, particularly in energy-intensive sectors such as healthcare.

Representative figure of the Sustainable Development Goals.

Contents

List of Figures

List of Tables

Abbreviations and Symbols

Abbreviations

ADENE	Agency for Energy
AIM	Asset Information Model
AIR	Asset Information Requirements
ASHRAE	American Society of Heating, Refrigerating and Air-Conditioning Engineers
ATU	Air Treatment Unit
BCA	Building Condition Assessment
BEP	BIM Execution Plan
BIM	Building Information Modelling
BOQ	Bill of Quantities
CAD	Computer-Aided Design
CDE	Common Data Environment
CFD	Computational Fluid Dynamics
CMMS	Computerised Maintenance Management System
EIR	Exchange Information Requirements
HVAC	Heating, Ventilation and Air Conditioning
MEP	Mechanical, Eletrical and Plumbing Engineers
ML	Machine Learning
MTTF	Mean Time To Failure
NPV	Net Present Value
LCCA	Life Cycle Cost Analysis
LCC	Life Cycle Costs
LHV	Lower Heating Value
OIR	Organization Information Requirements
PACU	Post-Anesthesia Care Unit
PCS	Permanent Care Service
PIM	Project Information Model
PIR	Project Information Requirements
RH	Relative Humidity
WACC	Weighted Average Cost of Capital
WLF	Whole Life Costs

Symbols

Δp_t	Total pressure losses [Pa]
$\Delta p_{friction}$	Friction pressure losses [Pa]
$\Delta p_{dynamic}$	Dynamic pressure losses [Pa]
f	Friction factor
L	Length [m]
D	Diameter [m]
ρ	Density of the fluid [kg/m^3]
V	Velocity [m/s]
K_L	Loss coefficient of an equipment [-]
A	Area [m^2]
P	Perimeter [m]
Re	Reynolds number [-]
μ	Dynamic viscosity of the fluid [Pa.s]
ε	Equivalent roughness [-]
Dh	Hydraulic diameter [m]
De	Equivalent diameter [m]
a	Bigger axis in an oval duct [m]
b	Small axis in an oval duct [m]
R_t	Cash flow
N	Number of periods being analysed [-]
i	Discount rate [-]
n	Number of years between the time of analysis and time of expense [-]
E	Energy [kJ]
Q	Flow rate [m^3/s]

Chapter 1

Introduction

This dissertation is part of the Master's program in Mechanical Engineering at the Faculdade de Engenharia da Universidade do Porto (FEUP). This work was developed in a business environment at ASL & Associados. This project started on 10^{th} February 2025 and was completed on 11^{th} July 2025. The main objective of this dissertation was to automate Heating, Ventilation and Air Conditioning (HVAC) implementation in hospitals.

1.1 Objectives

The development of this project is driven by three overarching objectives. Primarily, the development of an automatic pressure loss calculation tool within Revit. This software facilitates the design of duct systems for HVAC installations; however, for a complex installation such as a Hospital Unit, the pressure loss calculations throughout the ducts can be a time-consuming task. The development of this tool is intended to accelerate the pressure loss calculations and reduce the potential errors that could be committed during this process.

Secondly, the creation of a platform for automating the maintenance process and routines of the HVAC equipment in the Hospital Unit through Microsoft Power App. The objective of this platform is to function as a repository for the data pertinent to the various equipment and to serve as a user-friendly tracking system. The platform is destined to be used during the operational phase of the hospital to facilitate the decision-making process regarding equipment replacement.

Finally, the maintenance model includes equipment purchase prices and also replacement costs, contributing to the creation of a Life Cycle Cost Analysis (LCCA) tool. The tool performs automatic calculations of the costs throughout the life cycle of a given piece of equipment. The purpose of the tool is to facilitate the analysis of the various costs associated with the utilisation of the equipment in question.

Figure 1.1 represents an introductory project diagram, highlighting the initial key questions addressed, the targets of this dissertation, and the metrics evaluated for comparison.

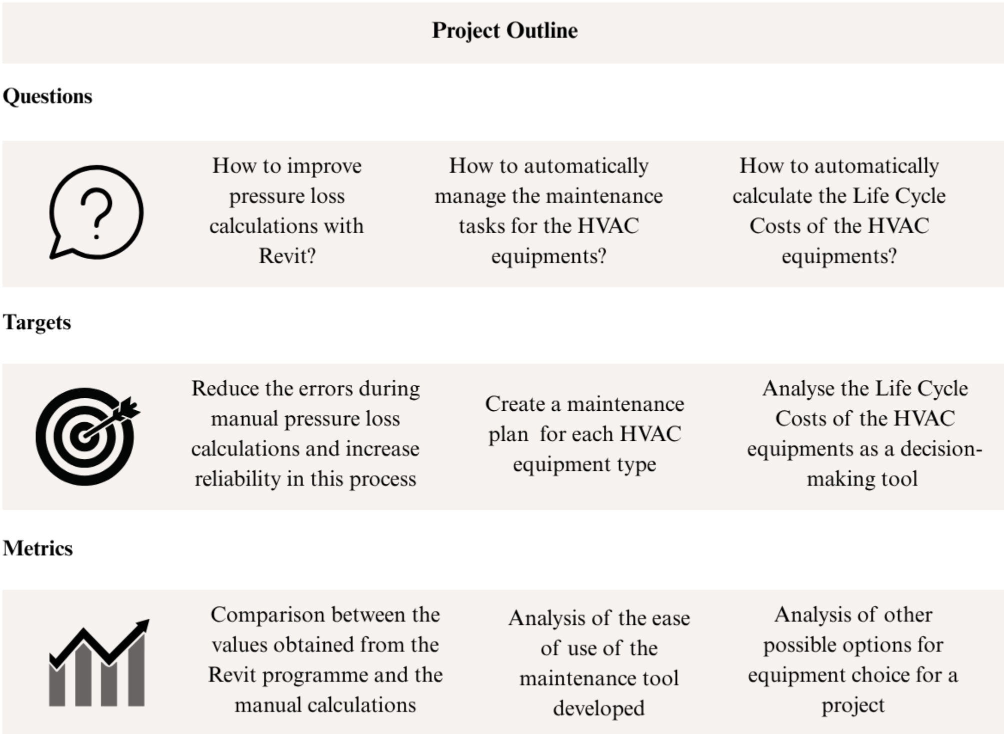

Figure 1.1: Project diagram illustrating the primary questions and objectives.

1.2 Methodology

This section delineates the methodology employed during this dissertation. The first stage of the process pertained to diagnosis, which entailed identifying the three problems that were to be addressed and corrected. The subsequent stages of each problem are the respective stages that were followed to present a solution to each problem.

The process began with defining the project's purpose and objectives, contributing to ensuring the desired outcomes. Three problem areas were defined in the implementation of HVAC systems in Hospital Units, and for each, strategies were outlined to solve them. These steps were executed in the implementation phase. Finally, at the end of each proposed task, the outcomes were evaluated to compare against the proposed objective. Figure 1.2 provides a visual representation of the project methodology.

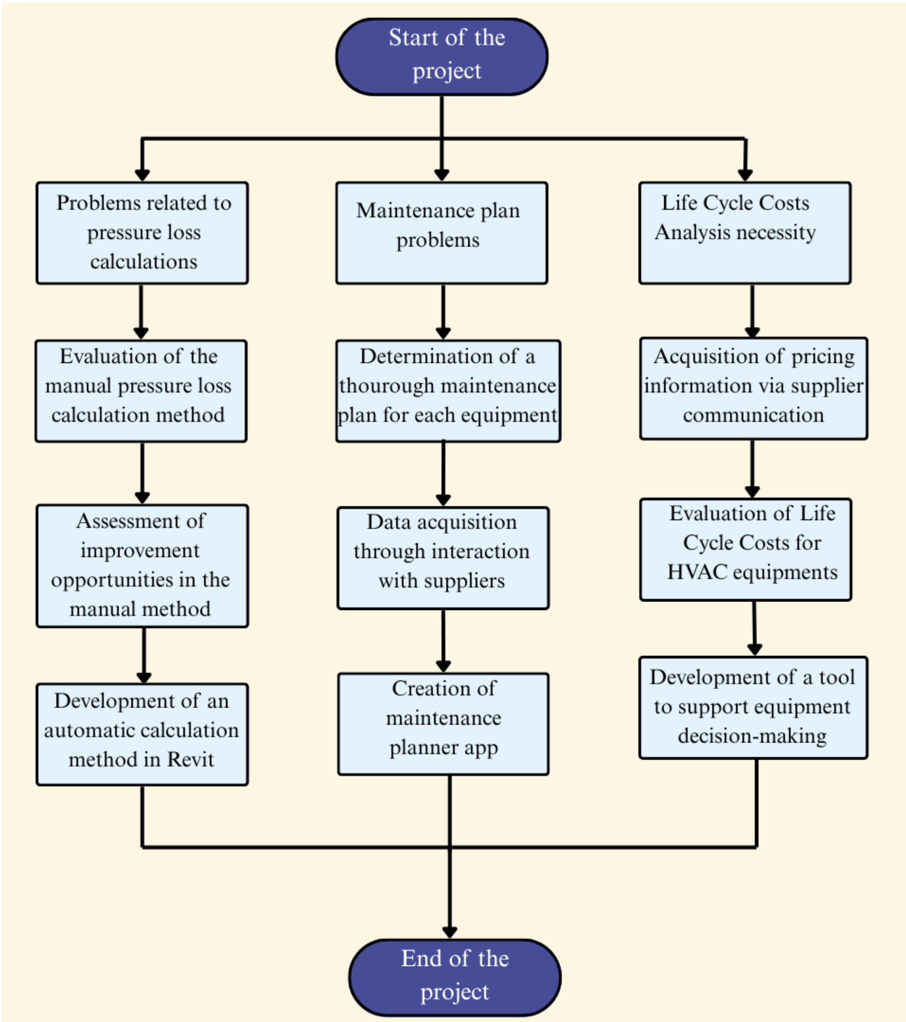

Figure 1.2: General flow chart of the project.

The process began with defining the project's purpose and objectives, contributing to ensuring the desired outcomes. Three problem areas were defined in the implementation of HVAC systems in Hospital Units, and for each, strategies were outlined to solve them.

As illustrated in Figure 1.3, the Gantt diagram provides a visual representation of the approximate timeline for the execution of the various tasks.

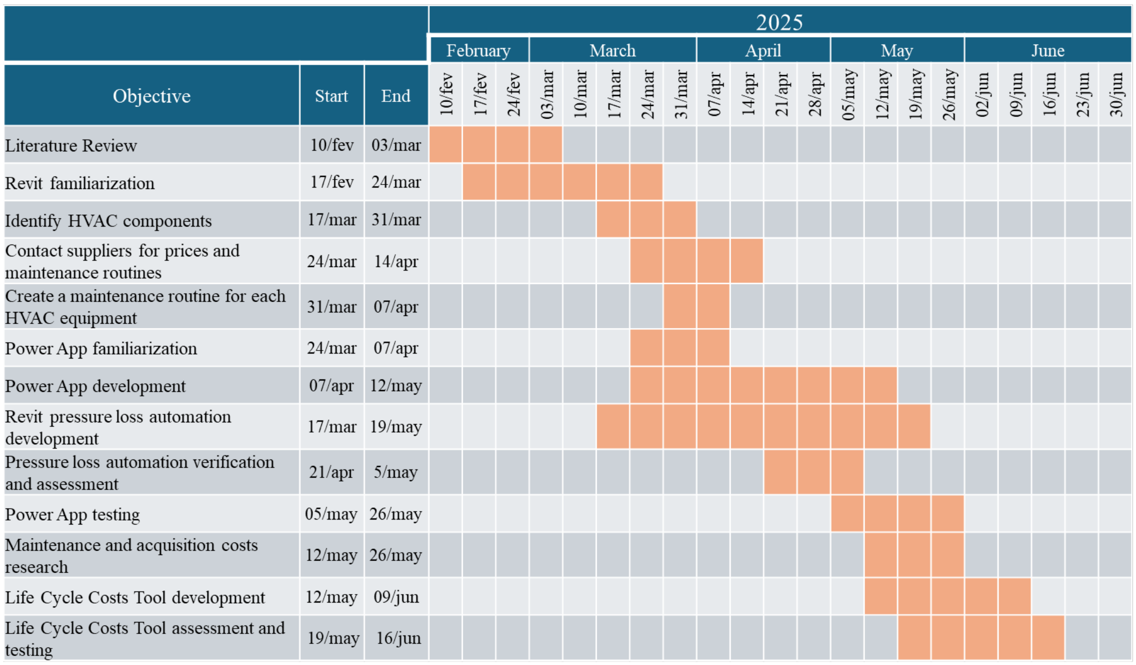

Figure 1.3: Gantt diagram of the project.

1.3 Hosting Company

The project under discussion was developed within the firm ASL. This firm is a subsidiary of the group ASL - António Santos Lessa & Associados, SGPS S.A. This group joins several firms that act fundamentally in the engineering services, investments, and real estate promotion fields. It currently owns six companies, including ASL, Gomes and Lessa investments, and Encke.

The firm was founded in 2006 by its current CEO, António Lessa, a civil engineer licensed by the Faculty of Engineering of Porto. Since then, the company has grown significantly and expanded its portfolio of projects. The company's core competencies lie in the areas of projects and consultancy. The multidisciplinary team contributes to speciality projects and project fiscalisation and management. Figure 1.4 shows the ASL logo.

Figure 1.4: ASL Firm logo.

The firm is currently headquartered in the Porto district, specifically in Matosinhos, and employs 60 collaborators.

The firm's team is divided into several specialities to contribute to all areas of a construction project. These areas collaborate to produce a comprehensive and unified proposal. The following areas of expertise are currently represented within the firm:

- Structures;

- Mechanical Installation;
- Thermal and Acoustic;
- Electrical Installations;
- Hydraulic and Gas Installations.

As the regulatory landscape about energy requirements in the construction industry evolves towards more stringent specifications, the firm has established a dedicated energy certification team. This is complemented by a construction fiscalisation team, which adds to its comprehensive array of specialisms.

The company's project legacy includes more than 5,000 clients, 12,000 energy certificates issued, and over 1,500 completed projects. The company acquired the "Great Place to Work" 2024 ranking in the previous year, thereby asserting its legacy as a great Portuguese company. This ranking is based on an evaluation of the general employee happiness index concerning their workplace, workplace organisational practices, and more. The firm possesses a yearly billing of 6 million euros.

The project has been directed towards the Mechanical Installations team, which is responsible for the design and project of HVAC systems. The team is composed of 10 mechanical engineers, including both junior and senior members, and a team leader.

1.4 Dissertation Structure

This dissertation is divided into six chapters.

Chapter 2 provides a project context about the Hospital Unit at work and the HVAC legislations that are in place for medical facilities.

Chapter 3 presents the literature review. This relates to the BIM methodology implemented in the hospital unit at work, including the Revit software used and its characteristics, the pressure losses calculation process, various maintenance procedures applicable to equipment such as HVAC systems, and an explanation of the Life Cycle Cost Analysis.

Chapter 4 is dedicated to the pressure losses that occur in the duct system in an HVAC system, highlighting its importance for the correct dimensioning of the project, and explaining the process of implementation of an automatic pressure loss calculator in Revit.

Chapter 5 is devoted to the HVAC equipment maintenance tasks, explaining the process of designing and developing the application and its functionalities.

Chapter 6 presents the Life Cycle Costs Analysis tool. It is dedicated to the explanation of the process used to calculate the costs of a certain equipment and the comparison with another possible model. It also presents the tool developed for this task and how it can be used for other cases.

Chapter 7 presents the conclusions of the project, summarising the results of the process of HVAC Implementation in Hospitals.

Chapter 2

Project Context

This chapter is dedicated to the Hospital Unit project, briefly describing the building and the spaces into which it is divided. In addition, a comprehensive inventory of the primary HVAC pieces of equipment selected for the structure, along with the pertinent legislative requirements for this construction type, has been compiled.

2.1 Hospital Unit

The project under consideration for this dissertation is a Hospital Unit within the *Trofa Saúde* Group, which is currently under construction in Maia, part of the Porto district, located at Avenida Dom Mendo and Avenida Eng.º António Bragança Fernandes. The following Figure 2.1 is the Google Earth satellite image that can be obtained for reference, with a highlighted area in red, showing the area destined for the hospital. The project has been developed from the ground up by the various specialities possessed by the firm.

Figure 2.1: Location of the building, from Google Earth.

The mechanical installations team was responsible for creating the Revit model for this subsystem of the hospital. The proposed work was for a hospital building comprising several health units, including dental clinics, physiotherapy, inpatient units, surgical blocks, and medical examination rooms. The structure was, then, divided into six floors:

- The -1 floor contained a car parking, a laundry room, a morgue, changing rooms, and a technical space for electrical installations, medical gases, generator sets, general waste rooms, and water pumping control stations.
- The first floor comprises a reception/waiting room, spaces for building administration (e.g., offices and meeting rooms), consultation rooms, diverse sanitary installations, consultation rooms, clinical analysis spaces, a nursing area, paediatrics, and more, and a kitchen and restaurant area.
- The second floor is characterised by spacious waiting rooms situated in the core of the building, in addition to consultation rooms, a gynaecology speciality room, medical examination rooms for X-rays and such, physiotherapy, and 2 gymnasiums.
- The third floor is dedicated to inpatient units, an on-site pharmacy, waiting rooms, and auxiliary rooms.
- The fourth floor contains ample waiting rooms situated in the core of the building, consultation rooms, dental speciality rooms, sanitary installations, and auxiliary rooms.
- The fifth floor is dedicated to surgical blocks and auxiliary spaces, including dressing rooms for staff members, storage for sterilised materials, recovery rooms, and post-operative care units. Sanitary installations are also present on this floor.

It was proposed that the hospital be equipped with a cold water (air-water) and hot water production system, to be installed separately. Two chillers are to be installed for the production of cold water, with a capacity of 440 kW each, and three boilers arranged in a cascade system, with a total capacity of 720 kW. It is important to note that these pieces of equipment were dimensioned to never work in their full potential, to safeguard their potential.

2.2 Heating, Ventilation and Air Conditioning Systems

The HVAC system in a hospital unit can be regarded as a complex installation. HVAC systems are the single largest energy consumer in utility buildings, such as large office spaces, shops, hotels, restaurants, and health-care facilities. These systems are designed to regulate environmental factors such as temperature, humidity, and air quality within buildings and specific locations. Central HVAC systems are comprised of three core components: a heating unit, which incorporates a boiler; a ventilation unit, which incorporates fans; and a cooling unit, which incorporates chillers (Figure 2.2) (Teke and Timur, 2014).

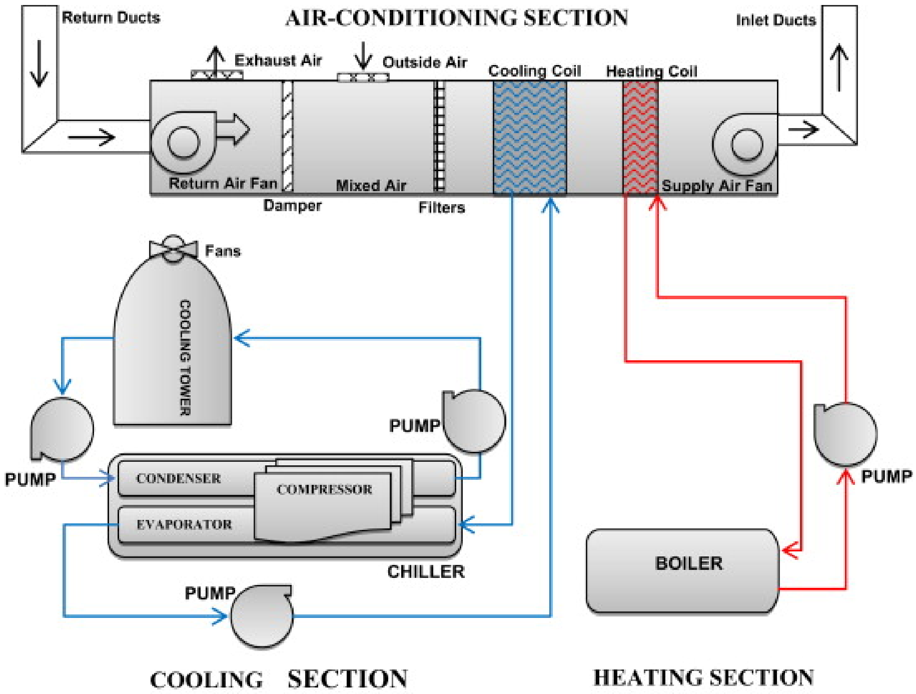

Figure 2.2: Schematic diagram of the conventional HVAC System (Zheng and Cao, 2020).

However, the scope of this dissertation does not encompass an exhaustive examination of all HVAC equipment, as significant variations exist in terms of their maintenance complexity and their function within the system. The focus of this study will be on the most essential and widely used equipment, with a detailed examination of the components present in the next sections.

2.2.1 Air Handling Units

An Air Handling Unit (AHU) represents a pivotal component in HVAC systems. These units are indispensable for the maintenance of indoor air quality, the regulation of temperature, and ensuring comfort. It is a mechanical device that has been designed to treat air and deliver it through duct systems. These devices find application in a variety of settings, including residential homes, office buildings, hospitals, and other such facilities. The process of air filtration, heating, or cooling is integral to the functioning of these systems, and the distribution of treated air to the designated rooms is a key aspect of their operation.

ATUs are comprised of multiple components, each with a specific role:

- Fan: designed to augment air pressure, thereby facilitating the movement of air and counteracting pressure drops that occur during its transit through the components and the duct system.

- Filters: air filters ensure healthy indoor air by removing harmful dust, bacteria, pollen, and other organic and inorganic materials. Filters contribute to ensuring hygienic and efficient operation.

- Heating and cooling elements: In ATUs, the heating and cooling elements are responsible for adjusting the air temperature as needed. Heating elements generally consist of electric coils or hot water pipes, and cooling elements consist of refrigeration coils.

- Humidification and dehumidification systems: Humidity is a parameter that can be controlled in an ATU through the use of humidifiers and dehumidifiers.

- Energy recovery systems: In circumstances where the outdoor air temperature deviates from the required supply air conditions, it is necessary to heat the air. Heat (or energy) recovery systems are applied to minimise energy consumption through heating by transferring the thermal energy of the extracted air to the outdoor air.

- Silencers: noise is typically generated by the duct and the components present in the circuit, but also by the fan. It is common practice to position silencers near the fan, as this is often the primary source of noise.

- Controls and sensors: modern ATUs typically have control systems and sensors that monitor temperature, humidity, air quality, and energy consumption for precise regulation of the HVAC operations.

ATUs are generally designed with a specific purpose in mind. The design of ATUs is informed by the specific conditions of the room and prevailing state of the outside air, with the design parameters being met according to these criteria. The components mentioned above can be combined for the specific solution necessary for to space in question. Figure 2.3 represents an example of an ATU from *EVAC* company.

Figure 2.3: Air Treatment Unit example (EVAC, 2024).

2.2.2 Boilers

Boilers represent a vital component within the broader framework of HVAC systems, assuming primary responsibility for the generation of hot water or steam, with the purpose of heating and supplying domestic hot water.

In the context of a hospital environment, where factors such as comfort, hygiene, and process reliability are of paramount importance, the role of boilers becomes particularly crucial in maintaining the thermal balance of the building. Figure 2.4 represents an example of a boiler from *Vaillant* company.

Figure 2.4: Boiler example (Vaillant, 2024).

2.2.3 Circulating Pumps

Circulating pumps are critical components in HVAC systems, responsible for ensuring the continuous flow of fluids, typically hot or chilled water, throughout the network of pipes, radiators, heat exchangers, and terminal units.

In hospital facilities, these pumps are pivotal in maintaining consistent temperature regulation in various zones, a necessity that is of both patient comfort and the proper functioning of medical equipment. Given their central role in the hydronic distribution system, any malfunction or degradation in performance can have a significant impact on system efficiency and occupant comfort. Figure 2.5 represents an example of circulating pumps from *Wilo* company.

Figure 2.5: Circulating pumps example (Wilo, 2024).

2.2.4 Chillers

Chillers represent a vital component in HVAC systems. The primary function of these devices is to extract heat from a building employing circulating chilled water to air handling units or terminal devices, where the process of heat absorption from the indoor air takes place.

In critical environments such as hospitals, chillers play a critical role in maintaining precise temperature and humidity levels, which are essential for patient safety, infection control, and the proper functioning of sensitive medical equipment. Figure 2.6 represents an example of a chiller from *Mitsubishi* company.

Figure 2.6: Chiller example (Mitsubishi, 2024).

2.2.5 Fan Coil Units

Fan Coil Units are a type of air conditioning system that functions in individual rooms or specific zones. These units comprise a heat exchanger, also known as a coil, and a fan that is positioned to blow air over the coil. This mechanism enables precise and localised temperature control. In the context of a hospital environment, these units assume a pivotal role in ensuring the comfort of patients in their rooms, as well as in offices and smaller service areas. Figure 2.7 represents an example of fan coil units from *Systemair* company.

Figure 2.7: Fan coil units example (Systemair, 2024).

2.2.6 Ventilators

Ventilators represent a fundamental component of HVAC systems, responsible for ensuring adequate air circulation, ventilation, and indoor air quality. In healthcare facilities, where the maintenance of air hygiene and pressure control is paramount, ventilators assume a pivotal role in ensuring a safe and comfortable environment. The improvement of air circulation, a function of ventilators, has been shown to reduce levels of dust and create a more pleasant environment.

A well-designed ventilation system is capable of effectively removing indoor pollutants and allergens. It can filter out dust, pollen, pet dander, and other allergens that are known to trigger allergies or respiratory issues. This is particularly beneficial in healthcare facilities where the maintenance of clean air is essential, such as hospitals. Figure 2.8 represents an example of a ventilator from *Sodeca* company.

Figure 2.8: Ventilator example (Sodeca, 2024).

2.2.7 Split Units

Split Units are versatile cooling systems commonly used in isolated rooms or small zones, consisting of two units, an indoor and an outdoor. These systems are used to control the temperature of a single room or area that has access to an exterior wall. The unit outside houses components such as a compressor and a condenser, which cool the air. On the contrary, the indoor unit contains an air filter and a cooling coil. These elements are responsible for distributing cool, filtered air into the room while maintaining proper airflow. The two units are connected through a network of insulated pipes that circulate refrigerant. They create a convenient solution for many office environments.

The aforementioned types of equipment offer several benefits, making them a popular choice for cooling systems. They are comparatively inexpensive to install, consume less energy than central air systems, require minimal space, and provide the ability to expand the system as needed, such as by installing and connecting additional units to the outside unit (within capacity limits). Figure 2.9 represents an example of a split unit from *Daikin* company.

Figure 2.9: Split units example (Daikin, 2024).

2.2.8 Conditions of the Hospital Unit's Rooms

To correctly dimension the equipment for each room, the thermal balance has to be calculated. External characteristics were taken into consideration for both the winter and summer seasons. For the winter season, the dry bulb temperature was recorded at 0.5 ºC, with the corresponding relative humidity (RH) at 90 %. Conversely, for the summer season, the dry bulb temperature was recorded at 34 ºC, with a relative humidity of 40 %. These figures were recommended by the National Institute of Meteorology and Geophysics for the Porto region. This data was taken into account for the calculation of the external gains.

On the contrary, the internal gains caused by the occupants were determined based on the American Society of Heating, Refrigeration and Air-Conditioning Engineers (ASHRAE) Handbook Chapter 18 (ASHRAE, 2019a), with values depending on the type of activity being conducted in the space. According to the established norm, for sedentary activities, the sensible heat per occupant is 70 W, and the latent heat is 60 W.

Furthermore, the internal gains caused by the lighting features were considered to be 10 W/m^2, as a way to simplify this parameter for the calculations.

The internal conditions for the rooms were selected based on the conventional temperature or Relative Humidity (RH) values for thermal comfort or other specific requirements that were stipulated. The subsequent Table 2.1 delineates the temperature and RH parameters for the majority of the spaces. These conditions were determined by the Mechanical Installations team for the different areas of the Hospital Unit.

Table 2.1: Temperature and relative humidity conditions for most spaces of the Hospital.

Area	**Space**	**Temperature and Humidity Conditions**
Endoscopic	Endoscopic Examination Room	20–25°C and 30–60% RH
	Recovery Room	20–25 °C
	Disinfecting Room (dirty)	18–25 °C
	Disinfecting Room (clean)	20–25 °C and 30–60 % RH
Imaging	Ultrasound/Mammography/CT Scan/Orthopantomography Room	22–25 °C
	Preparation and Recovery Room	20–25 °C
	MRI Room	20–25 °C
Physical Medicine and Rehabilitation	Treatment Room	22–25 °C
	Therapeutic Gym	20–25 °C
PCS and Emergency Room	Observation/Treatment Room	22–25 °C
	Recovery Room	20–25 °C
	Small Surgery Room	20–26 °C and 60 % RH
Hospitalization	Rooms	20–25 °C
	Offices	22–25 °C
	Cafeteria	22–25 °C
Operating Room	Operation Room	20–26 °C and 30–60 % RH
	Post-Anesthesia Care Unit (PACU)	23–25 °C and 40–60 % RH
Intermediate Care Unit	Open Room	23–25 °C and 40–60 % RH
Storage Pharmacy	18–25 °C	
Remaining Spaces	20–25 °C and 50 % RH (not controlled)	

2.3 Heating, Ventilation and Air Conditioning Legislation for Hospital Units

Medical advances have created a constant need for research and development of air conditioning in hospitals and medical facilities. While the impact of air conditioning on clinical outcomes is a subject of ongoing research, its role in protecting against harmful occupational exposures is well-established. Consequently, there is a necessity for effective and precise design and operation of ventilation systems, as outlined in the ASHRAE Handbook (ASHRAE, 2019b).

For hospitals to be safe environments for patients and staff, several regulations must be implemented and considered during the design and construction phases. HVAC systems in these environments must meet strict standards of air temperature and humidity, ventilation rates, strict guidelines for air changes and pressure differentials, etc. These standards are in place to ensure the safe operation of healthcare and similar environments. Air handling and distribution systems provide a means to dilute and remove contaminants but also provide a comfortable environment (ASHRAE, 2021).

The project in question follows some guidelines set by the Portuguese government and regulatory bodies:

- **Decree-Law Nº 101-D/2020** (Portugal, 2020): Works to optimise the energy efficiency of buildings in Portugal, establishing the technical requirements for energy certification and emission reduction. Establishes requirements for ventilation, heating, and cooling. Emphasises the need for new buildings to have near-zero energy consumption and to ensure that air quality is maintained through proper ventilation. Outlines the responsibilities of the ADENE (*Agência Nacional de Energia*) in the management and validation of the energy certification system.

- **Regulation Nº 90/2024/1** (Portugal, b): Establishes the minimum requirements for the licensing, installation, organisation, operation, human resources, and technical equipment of residential units managed by public bodies, military institutions, private social solidarity institutions, and private entities in Portugal. Provides specific guidelines to improve the management and operation of these units. Also includes some guidelines for room layout and ventilation rates depending on the purpose of the room.

- **Regulation Nº 138-I/2021** (Portugal, 2021): Sets minimum energy performance requirements for the building envelope and the minimum requirements for technical systems. The aim is to improve energy efficiency and sustainability. The regulation prioritises natural ventilation and the use of mechanical systems where necessary, and introduces requirements for air quality control, proper insulation, and temperature regulation in HVAC systems.

- **Regulation Nº 353-A/2013** (Portugal, 2013): This regulation establishes the minimum requirements for fresh airflows in commercial and service buildings, and specifies the protection limits for indoor air pollutants. It provides calculation methods for airflows and specific airflow requirements for sanitary installations and pollutant protection thresholds.

- **Regulation Nº 292/2000** (Portugal, 2000): Regulates noise, the prevention of noise pollution, distinguishing thresholds depending on the zone analysed (sensitive or mixed).

In addition, Regulation Nº 88/2024/1 (Portugal, 2024a) and Regulation Nº 92/2024/1 (Portugal, 2024b), which overlap with Regulation nº 90/2024/1 described above, are also applied in this hospital unit. These regulations have similar purposes and help to define guidelines for rooms according to their use. Figure 2.10 represents a schematic summary of the regulations mentioned above.

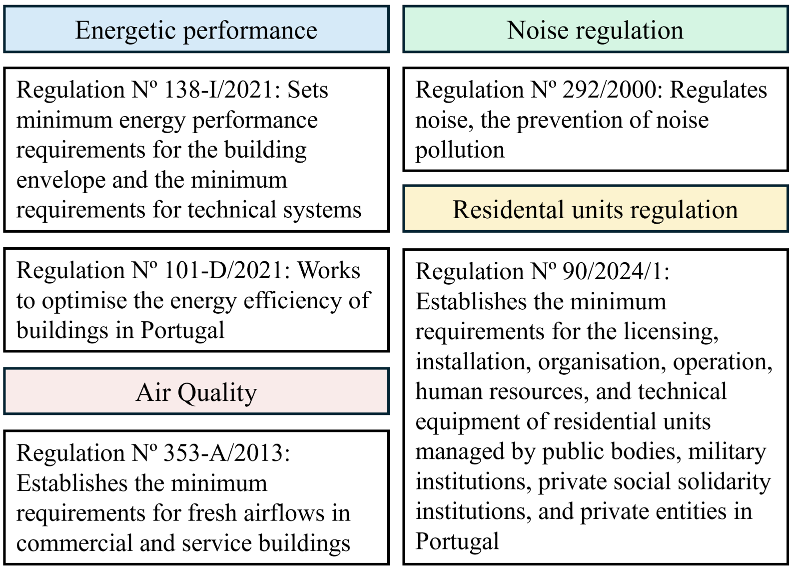

Figure 2.10: Schematic summary of the regulations applied to Hospital Units in Portugal.

Finally, as mentioned in the previous section, some considerations from the ASHRAE Handbook for internal occupant gains were taken into account (ASHRAE, 2019b).

Chapter 3

Literature Review

This chapter is dedicated to the literature review of: the Building Information Modelling (BIM) methodology, the Revit software used, and its differences when compared to AutoCAD, the different types of maintenance that can be applied to equipment, especially HVAC systems, and a brief review of LCCA.

3.1 Building Information Modelling Methodology

BIM is the foundation of digital transformation in the Architecture, Engineering and Construction (AEC) industry. It is the process of creating and managing information for a built asset. By integrating diverse, multidisciplinary data, BIM facilitates the creation of detailed digital representations managed in the cloud. Teams can connect their Revit models via the cloud, giving all the stakeholders visibility and access to accurate information whenever they need it, always synchronised. For example, engineers and architects can quickly access the same information to find better solutions and deliver projects faster. This cloud-based model is part of the Common Data Environment (CDE) approach that BIM software follows.

BIM supports the creation of smart data that can be used throughout the lifecycle of a building project or infrastructure. This approach improves transparency, promotes sustainable options and efficiency in AEC projects (Autodesk, 2024b). It can be defined as a shared digital representation of a built asset that is used to facilitate design, construction, and operation processes. The project under discussion can be said to reach the digital twin concept, which is a complete virtual representation of a real building, including its spatial aspects and the physical objects within it.

The CDE is a digital platform that gathers together information as part of the typical BIM workflow. It can encompass a multitude of information, including details about the project contract, delivery schedules, and other pertinent documentation. In essence, it encompasses any data that is generated during a project. The CDE is equipped with mechanisms to regulate the dissemination of information, ensuring that construction documents are made available to the project team only after undergoing rigorous approval and release processes (Autodesk, 2024a).

The development of ISO 19650 (ISO, 2018) was initiated to establish a quality standard for BIM building processes and regulate the information management related to the life cycle of an asset. It defined information requirements in a BIM project, such as (Ashworth et al., 2022):

- Organisational Information Requirement (OIR): this encompasses the information necessary to comply with strategic business activities, asset management, portfolio planning, and more. It is instrumental in ensuring that the information and objectives are appropriately delineated at the project's inception, thereby enabling the team to prioritise the client's information needs. It should be regularly reviewed to ensure that it remains aligned with the organisation's needs.

- Asset Information Requirement (AIR): It contains important information to address specific needs during the operational and management phase of the asset. All pertinent data must be systematically collected and easily accessible, facilitating efficient transfer into the operational systems.

- Project Information Requirement (PIR): This refers to the information to be provided by the appointed party at specific project milestones. The appointing party is empowered to make decisions for the following project stages with access to this information. It should be specific to each project. The Project Information Requirement (PIR), in conjunction with the Asset Information Requirement (AIR) and the Organisational Information Requirement (OIR), constitutes the information basis for the preparation of the Exchange Information Requirement (EIR).

- Exchange Information Requirement (EIR): It defines management, commercial, and technical aspects of producing project information. It specifies what information is required at what time. It is a contractual document requiring the appointed party to create their BIM Execution Plan (BEP). The BEP is an execution plan that outlines how the team will use BIM tools and techniques.

In addition, ISO 19650 (ISO, 2018) yielded two information models: the Project Information Model (PIM) and the Asset Information Model (AIM) (Salzano et al., 2023). These can be defined as the combination of graphical and non-graphical data and documents related to a building or construction project, that can be managed in a CDE.

The PIM is the construction information model. It is developed during the design and construction phase of a project in response to requirements set out in the EIR. It is initially formulated as the "design intent" model and undergoes subsequent development. It encompasses the historical development of all project information (NBS, 2024a).

Upon completion of the building, the PIM is transferred to the AIM, which is defined as the set of information gathered from all sources that supports the ongoing management of an asset. The AIM is defined as a unified repository of validated and approved information about a constructed asset, utilised during the operational phase of a building. The AIM is designed to meet the needs of the building's end users or clients, equipping them with the necessary data to manage their activities effectively. The information included in the AIM must be updated regularly to account for any changes, such as repairs, refurbishments, or maintenance (NBS, 2024b).

As illustrated in Figure 3.1, the hierarchy of the information requirements is delineated, along with the relationships between them and the corresponding information models. When information requirements are clearly defined, the delivery team can understand the project's requirements. The OIR is thus the foundational element upon which the AIR and PIR are defined. These elements contribute directly to the EIR. The purpose of the EIR is to provide instructions to the appointed delivery team about the client's information needs and how these should be delivered. This ensures that the team can correctly deliver the PIM, aligning with the organisation's business and strategic plan. The final step in this process is the creation of the AIM, with the information from the PIM.

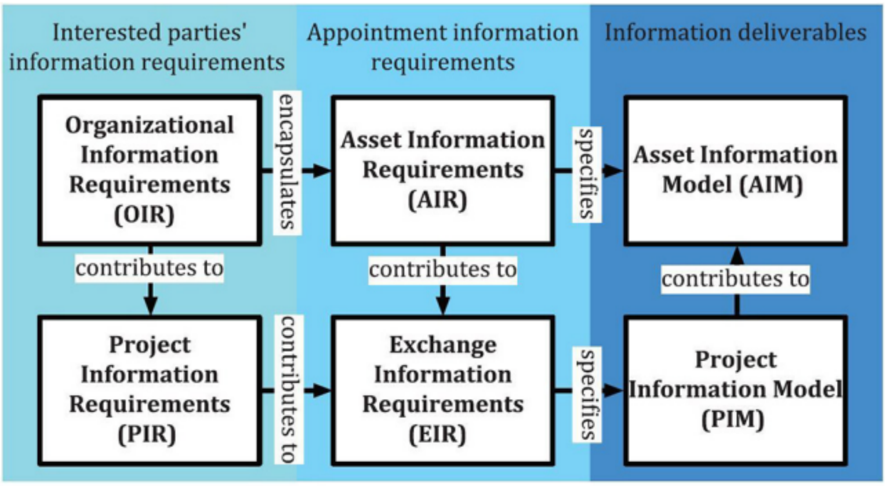

Figure 3.1: Relationship of information requirements and information models.

3.2 Revit Software

Revit is a BIM software that is available for commercial use. It was created by the company Autodesk (Figure 3.2).

Figure 3.2: Revit Software logo.

It is employed by a diverse range of professionals, including architects, structural engineers, Mechanical, Electrical, and Plumbing Engineers (MEP), designers, and contractors. Revit facilitates the creation, editing, and review of 3D models with exceptional detail (Figure 3.3).

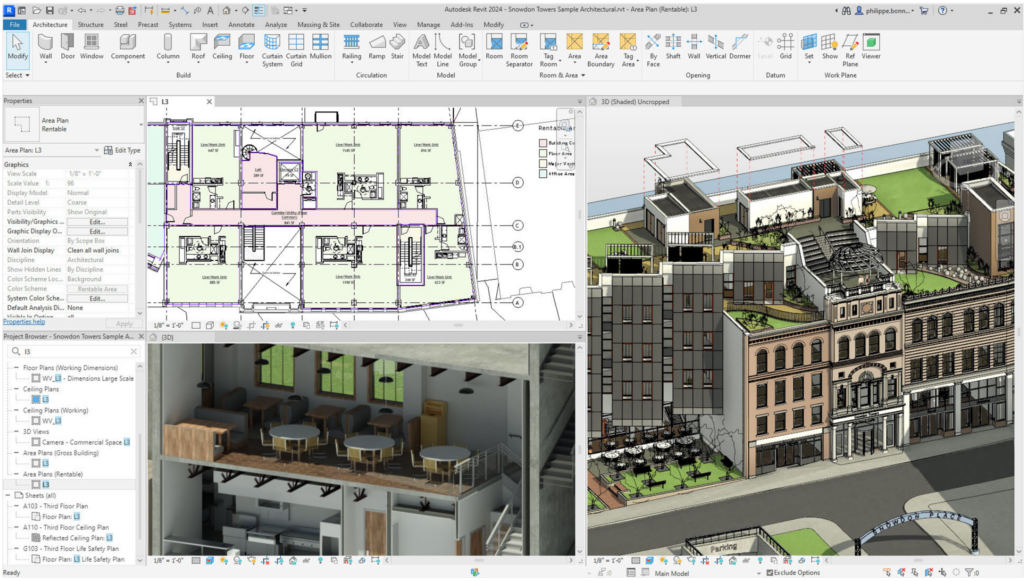

Figure 3.3: Project example in Revit (Autodesk, 2024c).

Revit allows for the insertion of real-world information necessary for the project, such as:

- Architectural design: Add architectural elements such as walls, doors, and windows, and render with high precision to accurately visualise the building;

- Structural Engineering: Computational design of structures and use of analysis tools to assess and adapt as the model develops;

- Mechanical, Electrical, and Plumbing Engineering: Design complex duct and pipe systems as well as perform preliminary load calculations before modelling electrical components;

- Construction: Add accurate and manufacturable building product templates into your designs for immediate validation and faster design cycles.

The Portuguese government promulgated the Decree-Law Nº 10/2024 (Portugal, a) on 8^{th} January 2024, which stipulates that, with effect from 1^{st} January 2030, the submission of architecture projects in Portugal is to be subjected to the BIM methodology. The enactment of this Decree-Law has led to the urgent need for expeditious implementation of this methodology across the various specialities involved in the construction industry. However, it is important to acknowledge the inherent challenges associated with transitioning to a new software system, which is a process that is not without a learning curve. Revit and AutoCAD possess very different working spaces and processes, with advantages and disadvantages in each case. The subsequent Table 3.1 offers a concise evaluation of the software's performance in multiple categories.

Table 3.1: Revit vs AutoCAD comparison.

Feature	AutoCAD	Revit
Primary Purpose	The software is principally utilised for two-dimensional drafting, yet it is also compatible with three-dimensional modelling. Moreover, it is well-suited for precise technical drawings and schematics.	It is employed within the BIM methodology, a comprehensive approach to architecture, structural engineering, and design that integrates the entire building process, from design to construction.
Usage	Used in many industries, including architecture, engineering, and manufacturing, to create blueprints and detailed drawings.	Used mainly by engineers, architects, MEP professionals, and construction teams.
Modelling Type	AutoCAD can be used for both 2D and 3D modelling, although the latter requires additional tools to manage complex models.	Revit is used specifically for 3D BIM modelling, updating the entire model when a parameter is changed.
Collaboration	AutoCAD doesn't allow for real-time collaboration, so multiple users have to manage separate copies of the files.	Revit creates a centralised model that allows for all teams to collaborate and see changes in real time.
File Type	AutoCAD uses Drawing (DWG) files, which can be 2D or 3D, and can be converted into various formats for compatibility with other software.	Revit uses RVT files, which contain the building data, geometry, and documentation for a project, but the files are less widely accepted than those that are DWG.
Learning Curve	AutoCAD is generally easier to learn for basic drafting tasks, but 3D modelling requires a lot of time and effort, and sometimes even external software.	Revit is a software program that requires a significant time investment to become proficient in, due to the advanced nature of its functionality.
Interdisciplinary Work	AutoCAD doesn't provide tools for managing building components and ensuring design consistency.	Revit ensures that any changes made to a model are available throughout the project, so that all specialities can work together seamlessly.

The features presented are just a few examples of the differences that can be expected when working with the two software packages. The main difference in using Revit as a project tool is the ability to incorporate real-world information, unlike AutoCAD software. The BIM software can include structural and engineering information, allowing calculations to be performed on the model.

However, Revit and AutoCAD software can be used together. In many Revit projects today, the CAD tool is still present and working as a support for the final model (Revit vs. AutoCAD).

3.3 Pressure Losses Calculation Method

This chapter introduces the concept of pressure losses and the respective pressure drop calculation methods used.

Pressure drop is defined as the reduction in air pressure as it moves through the ductwork of an HVAC system. This phenomenon is of particular significance in HVAC and air handling systems, as it has been demonstrated to have a detrimental effect on energy efficiency, because it results in a reduction of airflow and, by extension, system performance, potentially resulting in inadequate heating or cooling. This, in turn, has the potential to generate inadequate heating or cooling. These calculations are of paramount importance when selecting the most appropriate equipment, as the model selected must be capable of overcoming the pressure drop and delivering the requisite capacity to the system.

These losses are caused by friction between the air and the duct surfaces. It has been demonstrated that an increase in pipe length is directly proportional to an increase in pressure losses. Additionally, the presence of rougher duct surfaces has been shown to generate greater levels of friction, which in turn leads to increased pressure losses. Changes in direction and cross-sectional area, such as elbows, bends, or sudden increases or decreases in duct size, induce local pressure drops.

In the design of such systems, it is imperative to undertake meticulous calculations to account for these losses. The total pressure loss in a duct can be obtained with the sum of the friction loss of the ductwork and the dynamic loss of the component (Equation 3.1) (Behls, 2021).

$$\Delta p_t = \Delta p_{fricton} + \Delta p_{dynamic} \tag{3.1}$$

The Darcy-Weisbach Equation is the most widely accepted for calculating pressure losses in any steady and incompressible pipe flow system, with these losses being based on fluid velocity, density, duct roughness, diameter, and length. Equation 3.2 calculates the resistance to airflow caused by friction.

$$\Delta p_{friction} = f \left(\frac{L}{D} \right) \frac{\rho V^2}{2} \tag{3.2}$$

The friction factor f, which is dependent on the Reynolds number and the duct relative roughness, is utilised. L is the total length that is travelled by the air inside the ducts, D is the duct diameter, ρ is the fluid density, and V is the fluid velocity. The Darcy-Weisbach equation is applied to the lengths of the ducts; however, for the majority of existing duct systems, there are components and curves along the path of the fluid that cause losses. The Darcy-Weisbach equation can thus be modified to account for these local losses induced by equipment, bends in the ducts, and T-fittings (Equation 3.3).

$$\Delta p_{dynamic} = \frac{1}{2} K_L \, \rho \, V^2 \tag{3.3}$$

The coefficient of loss induced by a certain component is denoted by K_L. This coefficient is fundamentally dependent on the geometry of the component. Typical values for the K_L coefficient corresponding to the component in question are presented in Figure 3.4.

Component	K_L
a. Elbows	
Regular 90°, flanged	0.3
Regular 90°, threaded	1.5
Long radius 90°, flanged	0.2
Long radius 90°, threaded	0.7
Long radius 45°, flanged	0.2
Regular 45°, threaded	0.4
b. 180° return bends	
180° return bend, flanged	0.2
180° return bend, threaded	1.5
c. Tees	
Line flow, flanged	0.2
Line flow, threaded	0.9
Branch flow, flanged	1.0
Branch flow, threaded	2.0
d. Union, threaded	0.08
***e. Valves**	
Globe, fully open	10
Angle, fully open	2
Gate, fully open	0.15
Gate, $\frac{1}{4}$ closed	0.26
Gate, $\frac{1}{2}$ closed	2.1
Gate, $\frac{3}{4}$ closed	17
Swing check, forward flow	2
Swing check, backward flow	∞
Ball valve, fully open	0.05
Ball valve, $\frac{1}{3}$ closed	5.5
Ball valve, $\frac{2}{3}$ closed	210

Figure 3.4: Loss coefficients for pipe components (Gerhart et al., 2018).

The supplier can provide the specific value for the K_L coefficient of a certain component; the aforementioned values are simply provided as a reference.

It is established that with the flow rate passing through a duct and its section area, the velocity of the fluid can be determined (Equation 3.4)

$$\dot{Q} = V \times A \tag{3.4}$$

where $\dot{Q}$ is the fluid flow rate in m^3/s, V is the velocity in m/s, and A is the area in m^2.

The friction factor is contingent on the Reynolds number and the duct relative roughness. The Reynolds number, a dimensionless quantity, is employed to evaluate the flow regime of a fluid, distinguishing between laminar and turbulent. It is a quantitative measure of the interplay between inertial and viscous forces within the fluid. The Reynolds number can be calculated through the following Equation 3.5 (Gerhart et al., 2018):

$$Re = \frac{\rho V D}{\mu} \tag{3.5}$$

The dynamic viscosity of the fluid, denoted by the symbol μ, is a key factor in this equation. The Reynolds number is a critical factor in determining the nature of fluid flow, categorising it as turbulent or laminar flow. For Reynolds numbers below 2100, the flow is laminar; for Reynolds numbers above 4000, the flow is turbulent. The calculation of the friction factor is contingent upon the Reynolds number. For laminar flows the Equation 3.6 can be employed (Gerhart et al., 2018):

$$f = \frac{64}{Re} \tag{3.6}$$

In this flow regime, the friction factor is independent of the roughness of the pipe. However, for flows exhibiting a higher Reynolds number, the determination of this factor becomes more intricate. The Colebrook Equation 3.7 delineates the dependency of the friction factor on the roughness (ε) for this category of Reynolds numbers (Gerhart et al., 2018).

$$\frac{1}{\sqrt{f}} = -2.0\, log\left(\frac{\varepsilon/D}{3.7} + \frac{2.51}{Re\sqrt{f}}\right) \tag{3.7}$$

The issue with this equation is that it necessitates an iterative process due to the implicit dependence of f. However, modern computers and calculators can easily solve it. To enhance its accessibility, the Haaland Equation 3.8 can be solved for f explicitly, once again invoking the Reynolds number and the rugosity of the pipe.

$$\frac{1}{\sqrt{f}} = -1.8\, log\left[\left(\frac{\varepsilon/D}{3.7}\right)^{1.11} + \frac{6.9}{Re}\right] \tag{3.8}$$

There is, however, another formula that can be used to calculate the friction factor. The Churchill Equation 3.9 was developed as an explicit formula that estimates the friction factor across all Reynolds number ranges, laminar and turbulent. It was originally designed to describe the Moody Chart, which plots the Darcy-Weisbach friction factor against the Reynolds number (Benavides-Muñoz, 2024)

$$f = 8\left[\left(\frac{8}{Re}\right)^{12} + \frac{1}{(A+B)^{\frac{3}{2}}}\right]^{\frac{1}{12}} \tag{3.9}$$

where A can be calculated through the following Equation 3.10:

$$A = \left[2.457 ln\left(\frac{1}{\left(\frac{7}{Re}\right)^{0.9} + 0.27\left(\frac{\varepsilon}{D}\right)}\right)\right]^{16} \tag{3.10}$$

and B through Equation 3.11:

$$B = \left(\frac{37530}{Re}\right)^{16} \tag{3.11}$$

This equation is the one utilised for the automation process due to its explicit formulation and the capacity to encompass the entirety of Reynolds number ranges.

The effective roughness is represented through the symbol ε. It is feasible to obtain a measure of the roughness of typical pipes, in common materials, and thus to obtain the friction factor. The relative rugosity is obtained by dividing the value of ε by the hydraulic diameter of the duct (Equation 3.12).

$$\text{Relative Rugosity} = \frac{\varepsilon}{D_h} \tag{3.12}$$

The duct system for the Hospital Unit was galvanised iron, so the ε value used for this project's calculations was 1.5×10^{-4}, as mentioned in Figure 3.5.

	Equivalent Roughness, ε	
Pipe	**Feet**	**Millimeters**
Riveted steel	0.003–0.03	0.9–9.0
Concrete	0.001–0.01	0.3–3.0
Wood stave	0.0006–0.003	0.18–0.9
Cast iron	0.00085	0.26
Galvanized iron	0.0005	0.15
Commercial steel or wrought iron	0.00015	0.045
Drawn tubing	0.000005	0.0015
Plastic, glass	0.0 (smooth)	0.0 (smooth)

Figure 3.5: Typical roughness values for new pipes (Gerhart et al., 2018).

In the case of non-circular ducts, like rectangular and oval, the diameter used for the calculations must be adapted and is referred to by an alternative designation, namely the equivalent diameter. This diameter is used across all calculations for non-circular ducts. It can be defined as the equivalent diameter of a non-circular duct to a circular duct, which for rectangular ducts is calculated through Equation 3.13

$$D_e = 1{,}3\frac{(a \times b)^{0{,}625}}{(a+b)^{0{,}25}} \tag{3.13}$$

where a and b are the width and height of the duct. In the case of an oval duct, this equation is slightly different (Equation 3.14)

$$D_e = 1{,}55\frac{A^{0{,}625}}{P^{0{,}25}} \tag{3.14}$$

where A is the area and P is the perimeter. They can be calculated, respectively, by the following Equations 3.15 and 3.16, where a is the bigger axis and b is the smaller axis.

$$A = \frac{\pi \times b^2}{4} + b \times (a - b) \tag{3.15}$$

$$P = \pi \times b + 2(a - b) \tag{3.16}$$

3.4 Industrial Maintenance

Maintenance, as defined in the standard EN 13306 (da Qualidade, 2021), is described as the combination of all the technical, administrative and managerial actions carried out during a given element's life cycle, with the objective being the maintenance and restoration of the conditions necessary to ensure that it fulfils the required function (Coandă et al., 2020).

Maintenance costs can account for a large proportion of a facility's expenditure. In the past, maintenance costs were regarded as a necessary expense with little or no possibility of reduction. The maintenance strategy used, run-to-failure, involved running the equipment to operate until a system component failed, causing it to stop working. This method is the most expensive type of maintenance that can be carried out (Engineering, 2004). This approach is both ineffective and extremely expensive, as typically breakdown maintenance will cost three to four times more than the same repair when well planned (Mobley et al., 2008).

3.4.1 Maintenance Types

Nonetheless, maintenance procedures have, nowadays, been recognised as necessary to maintain the operational performance and ensure production levels. Maintenance policies are diverse and modelled based on the respective needs of the industry or equipment (da Costa and Cavalcante, 2022). Figure 3.6 represents a schematic representation of the different maintenance types that can be executed.

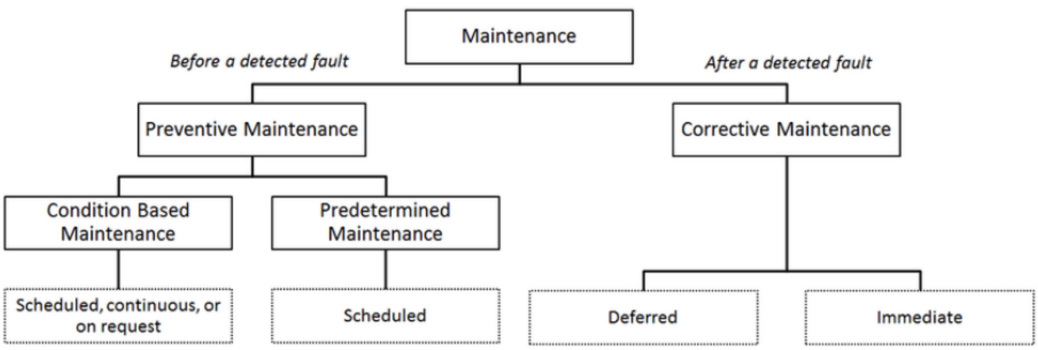

Figure 3.6: Types of maintenance (Coandă et al., 2020).

Maintenance can be categorised into two distinct types: preventive and corrective. The former is implemented before a failure is detected, and the latter is a correction after a failure has been detected.

As a more cost-effective and proactive option, preventive maintenance focuses on tasks that contribute to extending the useful life of the equipment, with a good cost-benefit ratio. A comprehensive preventive maintenance program will utilise regular evaluation of critical plant equipment, machinery, and systems to detect potential problems and immediately schedule maintenance tasks that will prevent degradation in operating condition. This type of maintenance is generally performed during a downtime of the machine (Ostachowicz et al., 2016).

This approach follows a time-based view of maintenance needs and can be represented by a "Bathtub curve": a graphical model that suggests that a new machine has a higher probability of failure (due to installation problems) and that this probability decreases over it's normal life until it increases again as the equipment wears out (Figure 3.7) (Engineering, 2004).

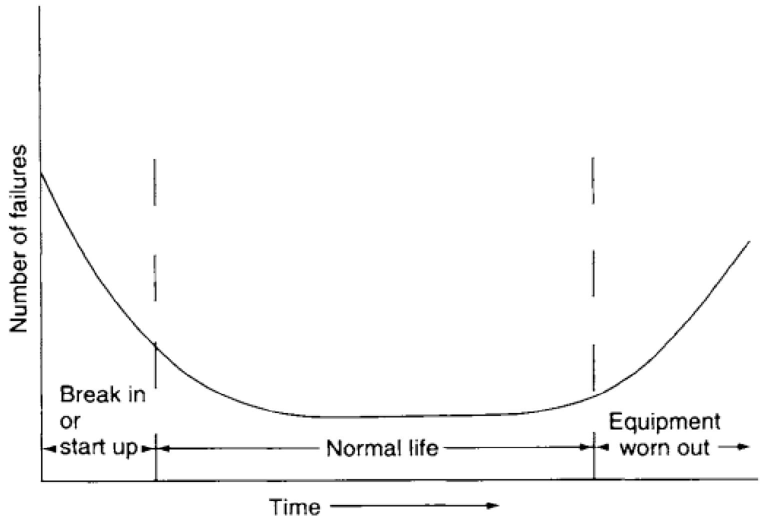

Figure 3.7: Bathtub curve (Source: Engineering (2004)).

To establish the frequency or interval of a task, it is necessary to ascertain the existence of applicable operational experience data that can suggest an effective interval for task accomplishment. Information relevant to this data can be obtained from one or more of the following sources (Mobley et al., 2008):

- Prior knowledge from other similar equipment, which shows that a scheduled maintenance task has offered substantial evidence of being applicable, effective, and economically worthwhile.
- Manufacturer/supplier test data, which indicates that a scheduled maintenance task will be applicable and effective for the item being evaluated.
- Reliability data and predictions.

When establishing the maintenance intervals, it is imperative to give due consideration to safety and cost factors. It is recommended that scheduled inspections and replacement intervals coincide whenever possible, and that tasks are grouped to minimise operational impact (Mobley et al., 2008).

Finally, the concept of predictive maintenance is also relevant in the context of modern maintenance policies. Predictive maintenance is a technique to schedule the maintenance tasks of equipment based on distributed sensors and a knowledge of the normal behaviour of the machine. The machine is monitored and, using Machine Learning (ML) algorithms or the Digital Twins concept, the normal behaviour is tracked. There are several advantages to using these methods, as the systems provide reliable information for the industry (Álvarez García and Salgado, 2022).

A comprehensive predictive maintenance program can and should use a variety of techniques, including:

- Vibration Monitoring (Chu et al., 2024): Vibration monitoring or analysis is a very commonly used technique applicable to either rotating or non-rotating equipment. Machines produce oscillatory movements during their operation, and this reflects their condition. The vibrations depend on the machine and the conditions of the operation. When there are above-normal vibrations, the machine will suffer accelerated wear and premature failure. These can be tracked as each possesses a different vibration pattern.

- Thermography (Venegas et al., 2022): This is a technique that is employed to measure temperature from a distance in a variety of applications. The temperature is indicative of the quantity of heat exchanged. The device utilises the principle of thermometry to measure the amount of infrared energy being emitted and subsequently converts this to a temperature reading. A significant proportion of failures result in substantial temperature changes, thus making this technique a valuable tool for identifying problems at an early stage.

- Tribology (Moleda et al., 2023): A methodical examination of the chemistry of oil may yield indicators of machine component wear and lubrication quality. A systematic analysis of oil enables the determination of the state of wear of machine elements and the planning of preventive actions, such as the replacement of oil or filters. A thorough examination of properties such as viscosity, contamination, oxidation and solid content is the most effective method of determining the quality of the lubricating performance. Such an examination is also capable of detecting leaks, corrosion or abnormal wear.

- Process parameters (Mobley et al., 2008): This technique is predicated on the hypothesis that machinery that is operating below acceptable efficiency parameters can limit productivity. Although vibration monitoring and thermography can provide information regarding the condition of the equipment, neither of these techniques provides data on operating efficiency. Consequently, process parameters monitoring should encompass all machinery and systems within the plant process that have the potential to impact its production capacity.

- Visual Inspection (Shukla et al., 2022): This method is one of the most used strategies to detect faults without using any machines. It can be useful in cases where the other processes did not detect failures. Defects can include: stains, dirt accumulation, scratches and cracks.

3.4.2 Computerised Maintenance Management Systems

Industrial Maintenance has been recognised as a function with a significant impact on the overall results of industrial companies. The concept of industrial maintenance has undergone numerous transformations over time. At present, maintenance can be regarded as a complex management process that is associated with several organisational processes, including production, quality, the environment, risk analysis, and safety (Lopes et al., 2016). Planning, scheduling of maintenance is one of the ways of optimising the use of this resource (Mobley et al., 2008).

Maintenance management can be defined as a set of objectives, strategies, and responsibilities. Information systems designed to support the maintenance function are referred to as Computerised Maintenance Management Systems (CMMS) (Lopes et al., 2016).

A CMMS is a software application designed to collate and centralise data relevant to the management of maintenance operations. The primary function of a CMMS is to facilitate the optimisation of efforts and the efficient allocation of time resources in the execution of maintenance tasks. Figure 3.8 illustrates a selection of the primary functions of a CMMS (INFRASPEAK, 2024).

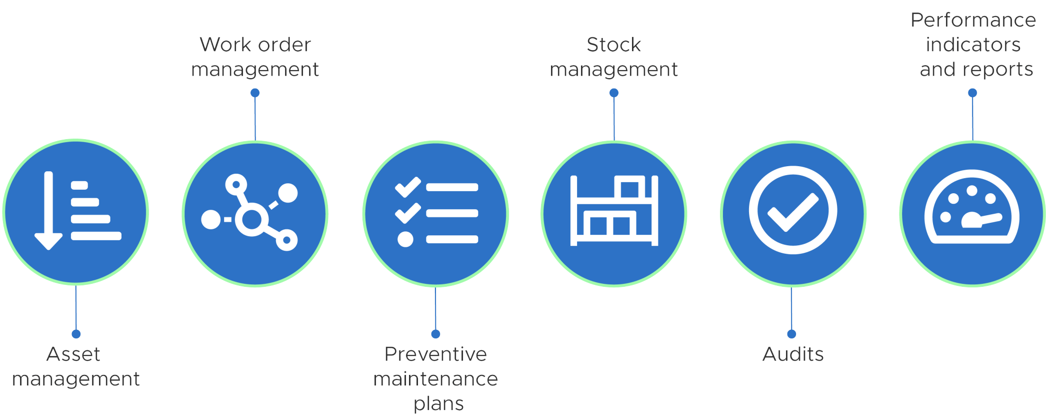

Figure 3.8: Examples of CMMS functions (INFRASPEAK, 2024).

The fundamental principle of a CMMS is based on the concept of a "work order", which can be defined as a maintenance request. This request can be managed, tracked in real time, and archived within the software. In conjunction with this function, the system can also generate a report about the operation.

The CMMS adheres to a very straightforward workflow. The process begins with creating a maintenance request for a required maintenance task, scheduling it for a specific date and time, and assigning it to a technician. The task is marked as resolved when the technician has completed the task and closed it, Figure 3.9.

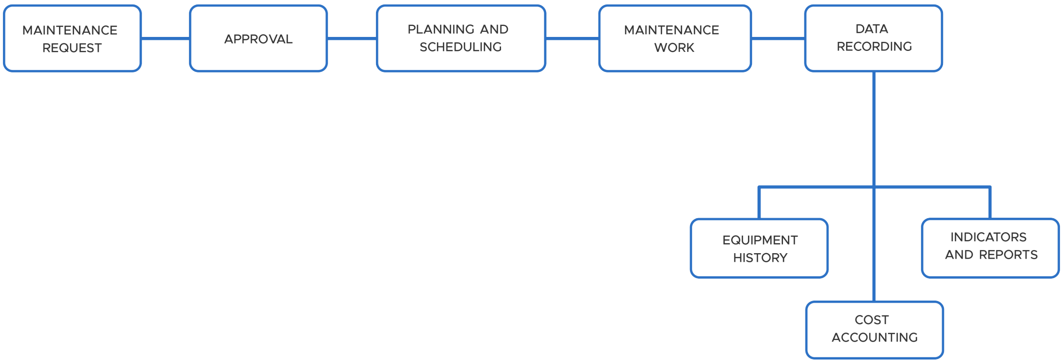

Figure 3.9: CMMS workflow (INFRASPEAK, 2024).

The utilisation of the CMMS by companies has been demonstrated to engender several advantageous outcomes, including (INFRASPEAK, 2024):

- Centralisation of information;
- Facilitation of agile communication;
- Increased productivity;
- Reduction of downtime;
- Cost control;
- Increase in asset lifespan.

An increasing number of facility managers are opting for platforms that facilitate the integration and coordination of teams, assets, maintenance, and other functions. However, the systems available on the market are not perfectly suited to each company's needs, and as a result, many companies prefer to develop their software rather than purchase commercial packages (INFRASPEAK, 2024).

3.5 Life Cycle Costs Analysis

LCCA is a method of assessing all the relevant costs of a project, product, or activity over time. This is a technique of combining both capital and operating costs to determine the net economic effect of an investment (Kubba, 2010). A LCCA is a valuable tool when comparing project alternatives that fulfil the same performance requirements, but differ concerning initial costs and operating costs (Khan et al., 2023). This analysis can assist in selecting the alternative that maximises net savings (Krus, 2004).

According to ISO (2017), there are only a few categories that should be included in the LCCA. Figure 3.10 exemplifies the costs that are considered in this analysis. Wider costs and incomes should not be considered for this analysis, as they are part of the wider category of Whole Life Costs (WLC).

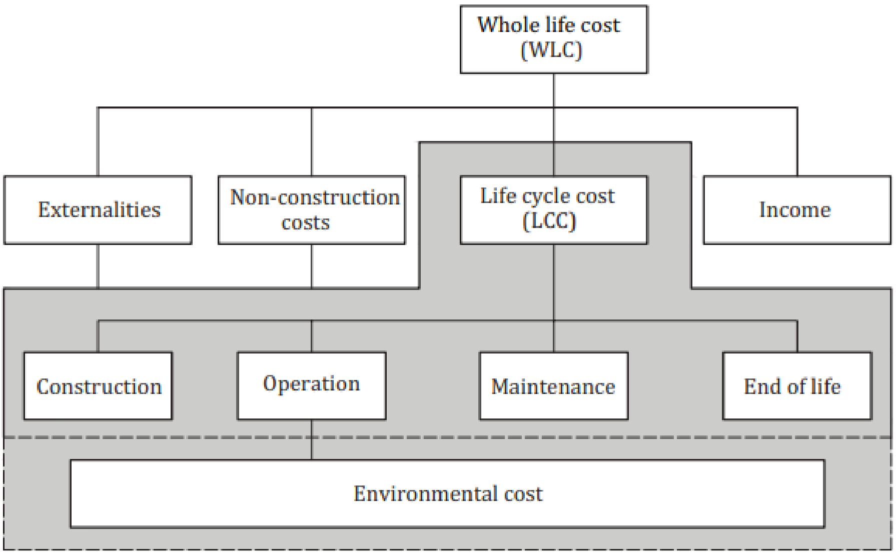

Figure 3.10: The distinction between Whole Life Costs and Life Cycle Costs (ISO, 2017).

The ASHRAE has developed a cost model for the analysis of life cycle costs of HVAC systems. It is important to note that this particular method of analysis involves the comparison of the cumulative total of costs relating to design, construction, acquisition, operation and maintenance, and disposal (Greeff, 2004). The total costs are amortised over the life of the system or the loan repayment period. After the analytical period, the costs and investments are subject to a discount and displayed as the total combined life-cycle cost. Table 3.2 presents the main life cycle cost elements, based on ASHRAE (Krus, 2004).

Table 3.2: Life-Cycle Cost Elements (Krus, 2004).

Pillars of Life Cycle Cost	**Elements**
Operating and Maintenance Cost	Utilities
	Consumables
	Fuel
	Waste
	Spares
	Equipment life
	Planned Maintenance
	Unplanned Repairs
	Labour Costs
	Cost of Parts
	Maintenance Management

Continued on the next page

Table 3.2 – Life-Cycle Cost Elements (Krus, 2004) (End).

Pillars of Life Cycle Cost	**Elements**
Design and Construction Cost	Engineering Installation Training
Acquisition, Renewal, And Disposal Costs	Procurement Administration Environmental Demolition

The data required for the evaluation of life cycle cost, as outlined, may be categorised into two distinct groups: annual costs and one-time costs. The one-time costs category encompasses both the initial construction costs and the periodic replacement costs incurred throughout the supported facility's lifespan. The yearly expenses encompass maintenance and repair costs, operating costs (i. e. the cost of the energy consumed in the production process), and other miscellaneous expenses. Both of these categories must be thoroughly evaluated. The following Equation 3.17 can be used to sum all the costs.

$$LCC = IC + OC \tag{3.17}$$

where "IC" is the initial cost of the equipment and "OC" is the operating cost. The initial cost of the equipment can be obtained through suppliers and includes the acquisition price of the machine and other necessities, such as accessories for the system to be complete. The operating cost can be calculated as the sum of the "EC" or energy cost and "MC" or maintenance cost, Equation 3.18 (Al-Ghamdi and Al-Gahtan, 2022).

$$OC = EC + MC \tag{3.18}$$

The most commonly used LCC methods are the net present value (NPV) and the uniform annualised cost method. The present value method, used in this dissertation, relies on determining the present value of future expenses by taking into account the anticipated inflation of present dollars and discounting that amount by a predicted rate over the period between the anticipated time of future expenses and the present time, Equation 3.19 (Rahman and Vanier, 2004).

$$NPV = FV\left[\frac{1}{(1+i)^n}\right] \tag{3.19}$$

where NPV is the net present value, FV is the future value of expenses, n is the number of years between the time of analysis and the time of expense, and i is the discount rate. It is also possible to calculate the NPV, for example, in a year, through the following Equation 3.20, which can be used to calculate this value. In this equation, i denotes the discount rate over a certain period (e.g., one year), t represents the total cash flow time, R_t indicates the cash flow, and N is the total number of periods being analysed (Altaf et al., 2025).

$$NPV = \sum_{i=0}^{N} \left[\frac{R_t}{(1+i)^t} \right] \quad (3.20)$$

The discount rate is determined by a range of factors. It is usually in the 5-10% range, depending on the application (Lecamwasam et al., 2012). When evaluating potential investment projects, the discount rate can be obtained by determining the Weighted Average Cost of Capital (WACC). It serves as the cost of capital from the investors' perspective. It allows the company to understand the minimum return it needs to generate from its operations to meet the expectations of its capital provider. This factor reflects the firm's required return in a project (Majka, 2024).

To undertake a LCCA of a designated project, it is imperative first to ascertain the study duration. This is required to facilitate the subsequent evaluation of the components' cost during the specified time interval. The longer the interval, the higher the number of replacements and maintenance activities executed.

3.6 Analysis of Case Studies

In this section of the dissertation, a detailed examination and comparison of case studies that have researched the pressure losses in ducts is conducted, Table 3.3. The purpose of this section is to gather relevant studies and present a full summary of the case studies analysed.

Table 3.3: Pressure Losses Case Studies.

Authors	**Description and Conclusions**
de Carvalho (2010)	This study focuses on the pressure losses in ducts with 90º curves, utilising simulations in Computational Fluid Mechanics (CFD) to evaluate the behaviour of the flow in different Reynolds number regimes. The main purpose was to evaluate how the loss coefficients vary as a function of the Reynolds number and the ratio between the curve radius and the duct diameter. Results showed that for laminar flows with Reynolds numbers lower than 50, the losses are friction-based, and as this number increases, the flow transitions to turbulent, and there is the creation of separation zones.
Guimarães (2010)	This study analyses the effects of overpressure in ducts and the efficiency of scape valves as a solution to mitigate these impacts. The study focuses on sudden pressure variations in supply water duct systems. Through simulations, the study demonstrates that air release valves, when correctly dimensioned and positioned, significantly contribute to reducing pressure losses.

Continued on the next page

Table 3.3 – Pressure Losses Case Studies (End).

Authors	**Description and Conclusions**
Abushakra et al. (2002)	This study consisted of evaluating the pressure drop characteristics of residential duct system components. The tests were designed to imitate cases typically found in residential and light commercial installations. The results showed that the published references tend to underestimate the effects of compression in flexible ducts, enabling the pressure drop to be 9 times bigger than estimated. Diffusers can also increase the pressure drop by up to twice in discharge fittings. The study emphasises the importance of the project engineer being aware of these factors.
Lin et al. (2022)	This study provides a broad view of the methods and techniques used to measure pressure losses in duct systems. It details different components that contribute to the pressure losses beyond friction. It mentions the existing measuring methods, discussing their respective advantages and disadvantages
Ali and Hamad (2018)	This study analysed the pressure drops in duct systems, considering different tube lengths, diameters, connections, elbows, and valves. It was compared the real pressure drops versus the theoretical ones. The study concluded that the pressure losses are significantly influenced by the length of the tube, diameter, connection type, and flow regime. The experimental measures showed a good concordance with the theoretical ones.

Chapter 4

Pressure Loss Automation

This chapter introduces the pressure drop calculation method and explains the implementation of an automatic pressure drop tool in Revit. In the context of a complex HVAC system, such as the one proposed for the hospital unit under consideration, pressure losses assume a particular significance and must be correctly calculated. This variable is of key importance during the decision-making phase of the project development, as it is instrumental in determining the most appropriate equipment for each particular situation.

Given the current development of the Hospital Project in Revit, a software programme that includes an automatic pressure drop calculation tool would be of significant practical value. It was designed to be applicable in every situation where pressure losses can be calculated.

4.1 Problem Description

Currently, the firm performs duct dimensioning by calculating pressure losses manually. To facilitate and expedite the process, Excel spreadsheets have been developed. Said spreadsheets have been developed in such a way that they replicate the manual methodology, incorporating all necessary formulas and input parameters. The input parameters that are typically included are the airflow rate (in m^3/h), the geometric shape of the duct (circular, rectangular, or oval), and its corresponding dimensions. It is the contention of this study that, in conjunction with the selected duct shape and the input data, the Excel sheet performs the calculation of the velocity of the airflow and subsequently undertakes the computation of pressure loss.

Despite the utilisation of spreadsheets, the process remains challenging due to the inherent complexity of many HVAC projects. These projects frequently entail the construction of extensive duct networks, comprising a substantial number of components (e.g., elbows, dampers, transitions) and substantial total duct lengths. Consequently, manual calculations are time-consuming, labour-intensive, and susceptible to human error.

To manage this complexity, the engineering team has developed a methodology for estimating the most critical duct path. This is defined as the segment with the highest cumulative pressure losses and is determined based on the number and type of pressure-reducing elements present and their length. Once identified, the path is analysed manually using the Excel tool to estimate the total pressure loss. It is standard practice to apply a safety margin of approximately 10% to 15% to the final result, to account for uncertainties and ensure the reliability of the system.

While this method has proven to be functional, it is still considered rudimentary and inefficient, especially for large-scale or intricate systems. The utilisation of manual calculations and approximations can result in the over-dimensioning of ductwork, which has the potential to increase costs and reduce overall system efficiency.

The proposed objective of this solution is to automate the identification of the critical path within the duct system and calculate its total pressure loss with precision. The aforementioned action eliminates the necessity for conservative safety margins, thereby enabling precise and optimised system dimensioning. This will enhance the accuracy of the design and significantly reduce the time required for calculations. It will also mitigate the risks associated with manual data handling.

As demonstrated in Appendix D, the Excel spreadsheet currently employed to facilitate the manual calculation process is illustrated.

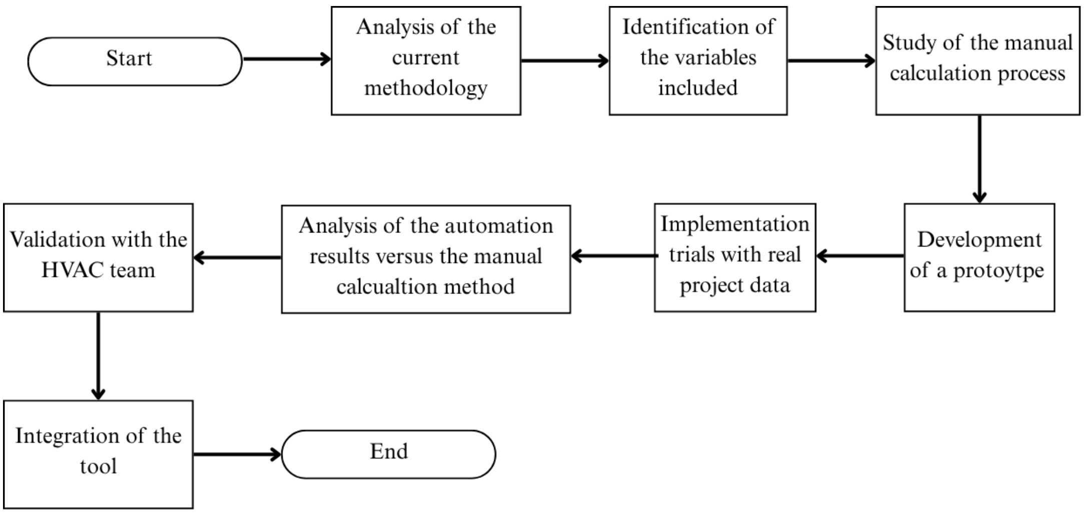

Figure 4.1: Pressure loss automation development process.

4.2 Revit Automation

The methodology of pressure loss calculation is designed to analyse the critical path along the circuit of the fluid. This approach is particularly relevant in determining the most critical airflow route, which is often the longest or the one with the most local losses. This, in turn, determines the system's total pressure drop, a crucial factor in selecting fans and sizing ducts.

This automation was created as a plug-in, custom programmed in C#. Microsoft developed this language as a general-purpose, high-level, and object-oriented solution, as part of the .NET initiative. Programming a plug-in in Revit works through an API that allows other applications to interact with the software. This allows for different applications to communicate with each other, essentially.

The plug-in contains the formulas for the pressure losses mentioned in Chapter 3. The formula used to calculate the friction factor was the Churchill equation. Another equation could have been considered, but has the team was used to utilising this equation, it was the one chosen.

When designing a project in Revit, values such as the flow rate and diameter of the duct are inserted. The details of the project are determined by the mechanical installations team. The software gathers the properties of the duct system and determines the value for the pressure losses for each section.

Figure 4.2 presents the menu bar that can be seen when the Revit software is opened. On the main menu bar, there is a tab that contains all the plug-ins created by the firm. In the mechanical engineering section, it is possible to find the plug-in with the text *"Calcular perdas de carga"*.

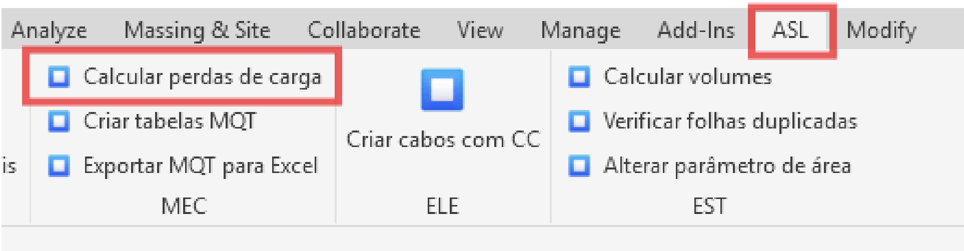

Figure 4.2: Interface of the "ASL" tab in Autodesk Revit, highlighting the "Calculate pressure drops" tool.

The plug-in is initialised at a location selected by the user. This point marks the location at which the equipment is to be inserted (the beginning of the air supply), and the total pressure losses are to be taken into consideration to ensure the appropriate sizing of the equipment. The plug-in simulates every possible path for the air to run in the ductwork, following the direction that was determined during the project phase. Then it calculates the pressure loss in each duct section, and sums the values for all the sections that are part of that respective path.

The ductwork in the Revit project should contain the respective size, such as the diameter, length, flow rate, and direction of flow, etc. The model considers the losses of the air flowing through the ducts, as well as the local losses, and determines the highest pressure loss path. The maximum pressure loss is the critical path, and it is the maximum pressure loss that the chosen equipment must overcome.

The plug-in under consideration employs a straightforward calculation method, based on the equations that influence pressure losses in ductwork. The type of element present plays a significant role, as an elbow or sharp turn creates more pressure loss than a straight duct of equal length. Figure 3.4 represents some local loss coefficients for pipe components, and Appendix A is a comprehensive list of all the ASHRAE coefficients, used as a source for this automation.

The plug-in also generates a text file containing the possible paths and the pressure losses of each respective one. Appendix B presents an example of a *.txt* file that was generated for the fourth case study is presented.

Moreover, it is also necessary to consider the pressure loss that a component, such as a diffuser at the exit of the duct, inflicts on the duct system. For this value, the supplier catalogues have to be consulted. There is, however, an issue given the large number of types of equipment available on the market. For this dissertation, only the main types of equipment present in the Hospital Unit were considered, like:

- Diffusers;
- Grilles;
- Fire dampers;
- Automatic Flow Control Dampers (VAV/VAC systems);
- Acoustic Attenuators.

Starting with the diffusers installed, all from the brand Koolair. There is more than one type of diffuser: circular, rectangular, high-reach, etc.

4.3 Automation Testing

Proceeding onwards to the actual testing of the Revit automation. Illustrated in Figure 4.3 and Figure 4.4 are the duct systems utilised to conduct an experimental investigation into the efficacy of the proposed automation system in the next sections of the dissertation. Both of these systems are from the Hospital Unit project.

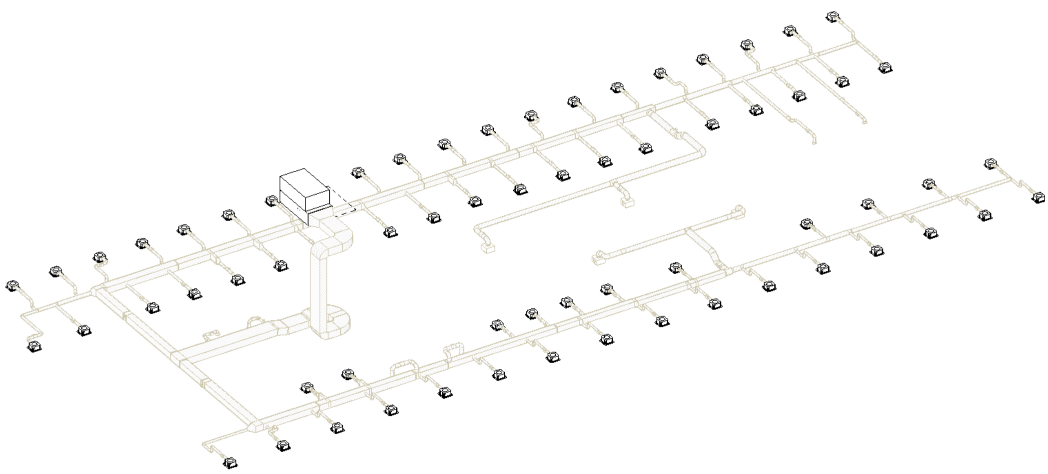

Figure 4.3: Revit project example one of a duct system in Revit.

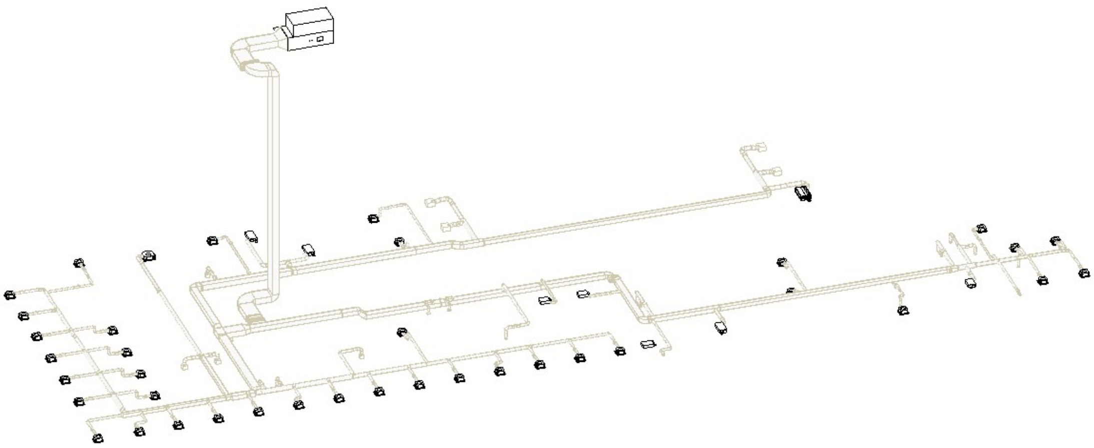

Figure 4.4: Revit project example two of a duct system in Revit.

The plug-in was also designed to generate a text file at the end of the calculations, which is saved in the same environment as the file being used. This text file comprises a comprehensive description of all potential pathways within the Revit project, with the values for each variable quantity, including velocity, diameter, flow rate, local losses attributable to components, frictional pressure drops, and the total losses experienced along each specified pathway. This is useful for verifying whether the critical path is indeed the one with the highest pressure loss and also to analyse specific sections of the path, if necessary.

When the calculations are done, the path determined as critical is highlighted, as represented in Figure 4.5 for the first duct system example, and the text file is generated and available.

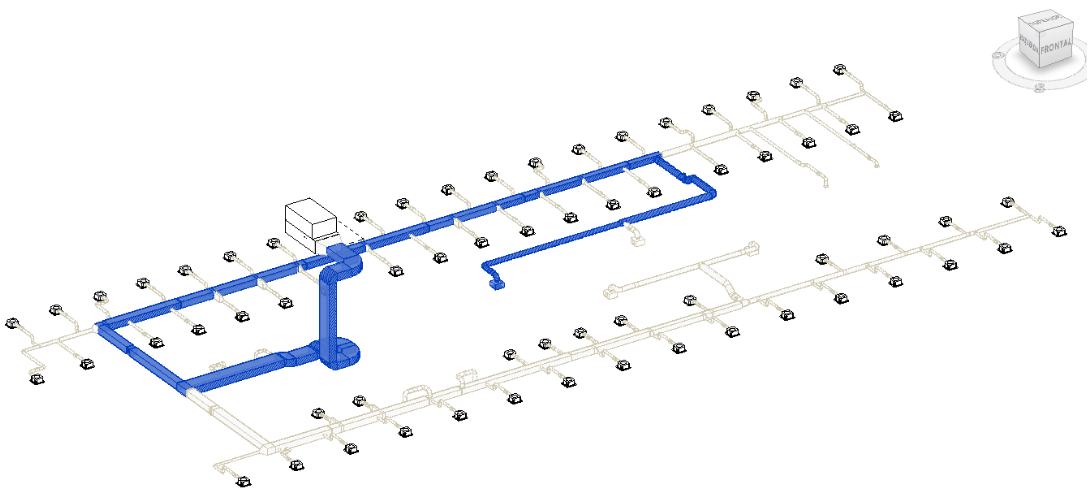

Figure 4.5: Critical path highlighted in blue.

The formulas utilised are mostly described in detail in Chapter 3. Any expression not yet addressed will be mentioned in this section.

In Table 4.1, the values employed for certain constants in the pressure loss calculations are presented. These values were utilised in both the manual and the programmed calculations to ensure the uniformity of the calculations. The air density under consideration is for an air temperature of 20°C, and the material considered is galvanised iron.

Table 4.1: Values for constants used in the pressure loss calculation.

Constants	Value
Air Density (ρ) [kg/m^3]	1.2013
Air Viscosity (μ) [Pa s]	1.81×10^{-5}
Rugosity [m]	1.50×10^{-4}

In the case of a duct system exhibiting distinct characteristics, such as those of the duct material, it is necessary to adjust the rugosity to align it with the specific material characteristics. To develop this thesis, it was considered that the duct systems were composed of galvanised iron. This is because galvanised iron offers resistance to rust and corrosion, facilitates inspections, and ensures a long life for the ducts. It is a very versatile material, with applications in many industries.

To analyse the difference between the values, it is valuable to calculate the error of the Revit number compared to the manual method, through the application of Equation 4.1.

$$Error(\%) = \frac{|\text{Value Calculated Manually - Value Calculated in Revit}|}{\text{Value Calculated Manually}} \times 100\% \tag{4.1}$$

Some approximations will be made to simplify the code behind the calculations. This includes, for example, dynamic loss coefficients, given the numerous variations inherent in each. The values for these coefficients are from the ASHRAE Fitting Loss Coefficients guide, Appendix A.

To prove the accuracy of the Revit plug-in, it is interesting to compare the values obtained through it and the values obtained when using the equations in Chapter 3. This comparison will be obtained by choosing case studies from a system and evaluating their results from both methods. Figure 4.6 represents a scheme containing the case studies presented in the following sections.

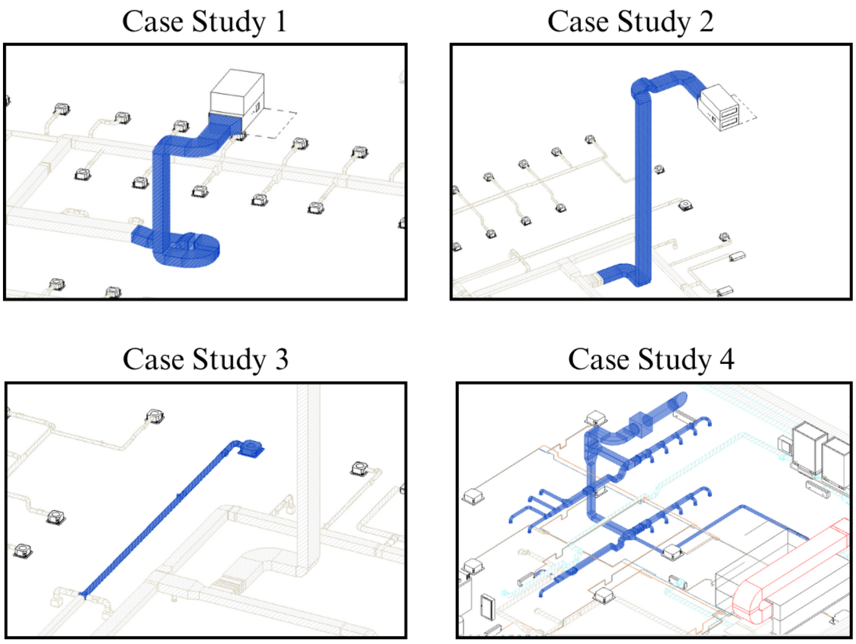

Figure 4.6: Diagram presenting the case studies used.

In the next sections of the dissertation, these case studies will be evaluated. The first two are simple sections directly after the respective equipment, and with only friction-related losses. The third case study possesses equipment-related losses, and the final one tests the tool in a complex gymnasium duct system.

4.3.1 Case Study 1 - Supply Air Duct Section

This section of the dissertation is dedicated to the first case study that will be analysed. This section is from the first duct system example, presented previously (Figure 4.3). As illustrated in Figure 4.7, the duct section highlighted can be analysed using data from Revit, which is presented in Table 4.2. This data was also utilised to conduct manual pressure loss calculations.

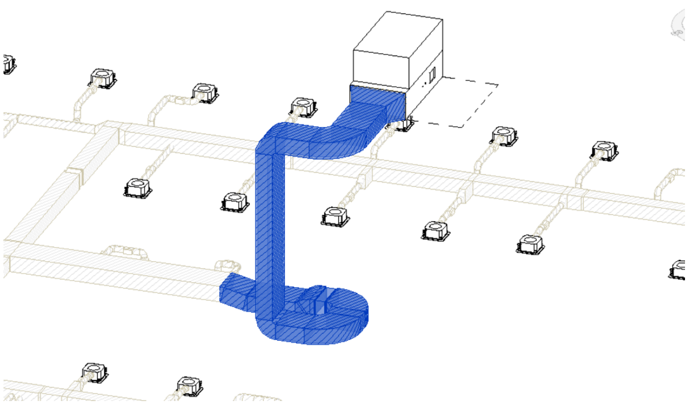

Figure 4.7: Duct section for the first case study, highlighted in blue.

The width and height of the ducts are determined when designing, and the program automatically sums the length of the ducts for each section.

Table 4.2: Case Study 1 Data.

Section number	289
Width of the duct [mm]	1000
Height of the duct [mm]	450
Length [m]	18.94
Flow rate [m^3/h]	8000

Section 289, highlighted in Figure 4.7, possesses several different transitions and elbows that contribute to the dynamic pressure losses. It contains nine elbows and a 45º transition between ducts. Each duct elbow was considered to produce a dynamic loss with a coefficient of 0.33 (Figure 4.8). The elbows present were considered to be 90º angles, as a simplification. The 45º transition between ducts was determined to have a coefficient equal to 0.22 (Figure 4.9). The total dynamic loss coefficient for this duct is 3.19.

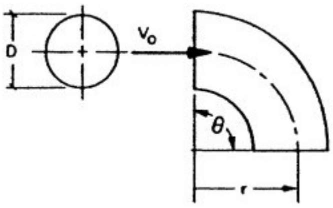

$$C_o = K_q C'_o$$

Coefficients for 90° Elbows

r/D	0.5	0.75	1.0	1.5	2.0	2.5
C'_o	0.71	$\boxed{0.33}$	0.22	0.15	0.13	0.12

Angle Correction Factors K_q (Idelchik et al. 1986, Diagram 6-1):

θ, degrees	0	20	30	45	60	75	90	110	130	150	180
K_θ	0	0.31	0.45	0.60	0.78	0.90	1.00	1.13	1.20	1.28	1.40

Figure 4.8: Dynamic loss coefficient for elbows.

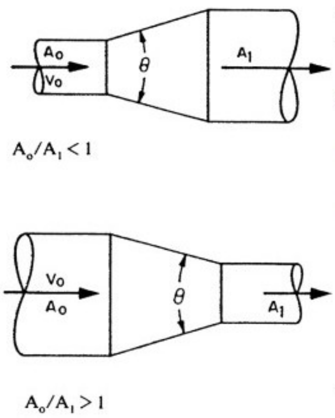

	C_o									
	θ, degrees									
A_o/A_1	10	15	20	30	45	60	90	120	150	180
0.06	0.21	0.29	0.38	0.60	0.84	0.88	0.88	0.88	0.88	0.88
0.1	0.21	0.28	0.38	0.59	0.76	0.80	0.83	0.84	0.83	0.83
0.25	0.16	0.22	0.30	0.46	0.61	0.68	0.64	0.63	0.62	0.62
0.5	0.11	0.13	0.19	0.32	0.33	0.33	0.32	0.31	0.30	0.30
1	0	0	0	0	0	0	0	0	0	0
2	0.20	0.20	0.20	0.20	$\boxed{0.22}$	0.24	0.48	0.72	0.96	1.0
4	0.80	0.64	0.64	0.64	0.88	1.1	2.7	4.3	5.6	6.6
6	1.8	1.4	1.4	1.4	2.0	2.5	6.5	10	13	15
10	5.0	5.0	5.0	5.0	6.5	8.0	19	29	37	43

Figure 4.9: Dynamic loss coefficient for a 45º transition.

Table 4.3 presents a comparison for the duct section in Figure 4.7, between the values obtained from the Revit plug-in and values obtained manually from the equations mentioned previously.

Table 4.3: Comparison between the Revit values and the manual calculation values for the first case study.

Variable	**Revit Value**	**Manual Calculation Value**	**Error (%)**
Area [m^2]	0.41	0.41	0
Hydraulic Diameter [m]	0.72	0.72	0
Velocity [m/s]	5.50	5.47	0.55
Friction Pressure Loss [Pa]	7.96	7.96	0
Dynamic Pressure Loss [Pa]	54.80	57.96	5.45
Total Pressure Loss [Pa]	62.76	65.92	4.79

As demonstrated in Table 4.3, several Revit values correspond to those derived manually. The values for the velocity and the hydraulic diameter are equal. A minor discrepancy is observed between the two velocity values, 5.5 m/s for the Revit value versus 5.47 m/s for the manual value, corresponding to a 0.55 % error.

The pressure loss resulting from the existing friction is equal for both methods, but the dynamic pressure losses vary. The Revit-generated value was found to be slightly lower than the manually obtained value, with an error value of 5.45 %. This error is acceptable as the differences between the values are negligible. The total pressure loss also presents a 4.79 % error, consistent with the accumulated differences.

In general, this case study produced very satisfactory values. There are some mathematical approximations, like the flow rate used for the manual calculations (7800 m^3/h), which can justify the error when in comparison. Overall, when comparing the manual and the Revit values, the error percentage produced was small. This indicates that the programme can accurately calculate the losses like the manual procedure.

4.3.2 Case Study 2 - Supply Air Duct Section

This section of the dissertation is dedicated to the second case study to test the Revit software model created (Figure 4.10). This section was obtained from the second duct system example (Figure 4.4).

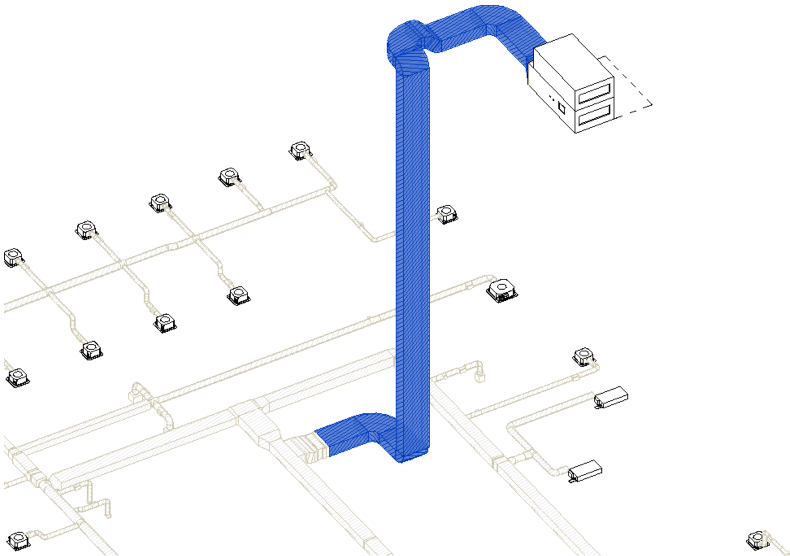

Figure 4.10: Duct section for the second case study, highlighted in blue.

As in the previous case, Table 4.4 presents the base information for the calculations of the pressure losses.

Table 4.4: Case Study 2 Data.

Section number	145
Width of the duct[mm]	1100
Height of the duct[mm]	450
Length [m]	27.32
Flow rate [m^3/h]	9130

Like the previous section, this one presents elements that contribute to the pressure losses along the duct. The dynamic loss coefficient for this section is again the sum of the coefficients for all the curves and elbows present. It totals 2.53 for this section.

Table 4.5 presents the values obtained through the Revit software and the manual calculations.

Table 4.5: Comparison between the Revit values and the manual calculation values for the second case study.

Variable	**Revit Value**	**Manual Calculation Value**	**Error (%)**
Area [m^2]	0.44	0.44	0
Hydraulic Diameter [m]	0.75	0.75	0
Velocity [m/s]	5.75	5.73	0.35
Friction Pressure Loss [Pa]	11.85	11.85	0
Dynamic Pressure Loss [Pa]	53.24	49.89	6.71
Total Pressure Loss [Pa]	65.09	61.77	5.38

Like the previous case study, the values produced by the two methods are similar. The area and hydraulic diameter are equal. The velocity possesses a slight difference, 5.75 m/s for the Revit method versus 5.73 m/s for the manual process. This difference can be justified as the flow rate used in the manual calculations (9130 m^3/h) is an approximation.

The friction pressure loss is also identical, which indicates that both methods consistently used the Darcy-Weisbach method with similar inputs. The dynamic pressure losses show a slightly larger discrepancy «, with the manual calculation yielding a 6.71 % lower value. This can result from differences in the estimation of loss coefficients (K values) and also the differences in the velocity value. The total pressure loss presents a final value with only a 5.38 % difference, which is still relatively small and acceptable.

4.3.3 Case Study 3 - Final Section of a Duct Section

This section of the dissertation is dedicated to the third case study. This section is from the first duct section example (Figure 4.3). It presents a section with an accessory present that has to be accounted for when calculating the pressure losses (Figure 4.11).

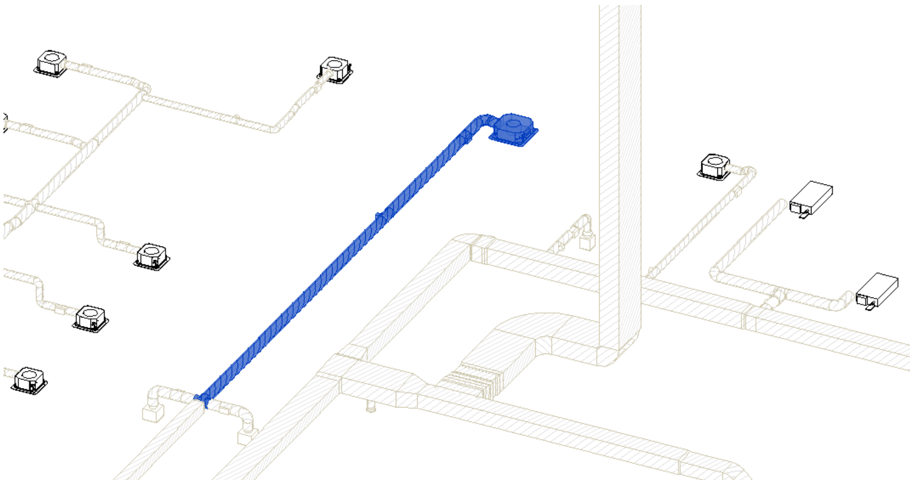

Figure 4.11: Duct section for the third case study, highlighted in blue.

As this section is circular, it is only important to consider the diameter of the duct for the calculations, and the hydraulic diameter is no longer relevant. Table 4.6 presents the data used for the calculations for the third case study.

Table 4.6: Case Study 3 Data.

Section number	86
Diameter [mm]	200
Length [m]	14.64
Flow rate [m^3/h]	230

In this section, there are some devices present that contribute to the pressure losses. These will be separated from the dynamic and friction pressure losses. For this section, the accessories present are fire dampers and airflow control dampers.

However, there are still elbows and tees present in the section. The dynamic loss coefficient is approximately 1.5 for this section. As in the previous cases, most of the elements present are elbows, except for a cross.

Table 4.7 presents the manual values obtained versus the Revit automation.

Table 4.7: Comparison between the Revit values and the manual calculation values for the third case study.

Variable	**Revit Value**	**Manual Calculation Value**	**Error (%)**
Area [m^2]	0.031	0.031	0
Velocity [m/s]	2.25	2.03	10.84
Friction Pressure Loss [Pa]	5.68	4.62	22.90
Dynamic Pressure Loss [Pa]	4.43	3.72	19.19
Accessories Pressure Loss [Pa]	51.4	51.4	0
Total Pressure Loss [Pa]	61.52	59.74	2.98

Firstly, the area is equal for both methods. This was also verified in the previous cases, as the formula is very direct and is not dependent on other variables. The velocity contains an error of almost 11 %. This can be justified by the approximations that the Revit automation is doing. The plug-in was based on the calculus sheets that the HVAC team was using, and, for simplification purposes, the velocity was always approximated in excess to the nearest quarter (0.25). This can justify the difference in the velocity value and the larger error obtained. It is also crucial to emphasise that, given the relatively low velocity value, any discrepancy between the two values is more significant than for higher values.

The friction pressure losses present an error of about 23 %. Once again, the difference present in the velocity is exacerbated and increases the error. Furthermore, there can be some approximations in the friction factor that also contribute negatively. This error can be considered high, especially when compared with the rest.

The dynamic pressure losses, even though smaller than the friction-related ones, possess a higher error value as well. This is aligned with the already higher difference present in the velocity values. Even though the error is not ideal for these calculations, the results are in agreement.

About the accessories pressure losses, it is related to the equipment present in the duct that, when air flows through, it causes a reduction in the overall energy of the flow. This can be diffusers, grilles, extraction valves, and more. Their respective induced pressure loss values are present in the catalogues of the company. In the case of this duct system, the brand used for the equipment was mostly *Koolair*.

Figure 4.12 represents a typical extraction valve from *Koolair* that is present in this duct system, and the selection table that is present on the *Koolair* company's website for this type of valve.

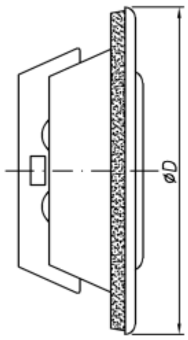

Size	Flow rate (m^3/h)	ΔP_t (Pa)
80	45	18
	60	28
	70	43
100	65	36
	75	49
	90	68
125	110	27
	135	38
	160	55
150	120	25
	145	37
	160	50
160	125	26
	150	37
	170	52
200	215	31
	250	45
	290	58

Figure 4.12: Technical diagram of the extraction valve (on the left) and the selection table from Koolair (on the right).

The diameter mentioned in the previous figure is related to their size. For a valve with a diameter of 125 mm (size 125) and a flow rate of about 90 m^3/h, the loss can be estimated at 20 Pa. As there are only values for a flow rate of 110 m^3/h for this model, it is necessary to estimate the pressure loss that it will cause. This was the value inserted in the Revit automation for this equipment.

The value for the accessories pressure loss is directly calculated from the Koolair website and, as such, is identical in both processes. In conclusion, the total pressure loss is 61.52 Pa by the Revit automation and 59.74 Pa by the manual process. This corresponds to only a difference of 2.98 % between the values. The greater error values obtained in the preceding calculations have been eliminated in the overall value of pressure loss. This indicates that the tool is capable of calculating total pressure loss with a high degree of accuracy, despite potential discrepancies in intermediate values.

4.3.4 Case Study 4 - Duct System of a Gymnasium

As a final stage of validation, the plug-in was applied to a complex and realistic ductwork system from an ongoing project within the company. This is the duct system projected for a gymnasium. This system encompasses multiple interconnected networks, each operating in coordination with distinct HVAC subsystems. The specific network selected for analysis is highlighted in Figure 4.13.

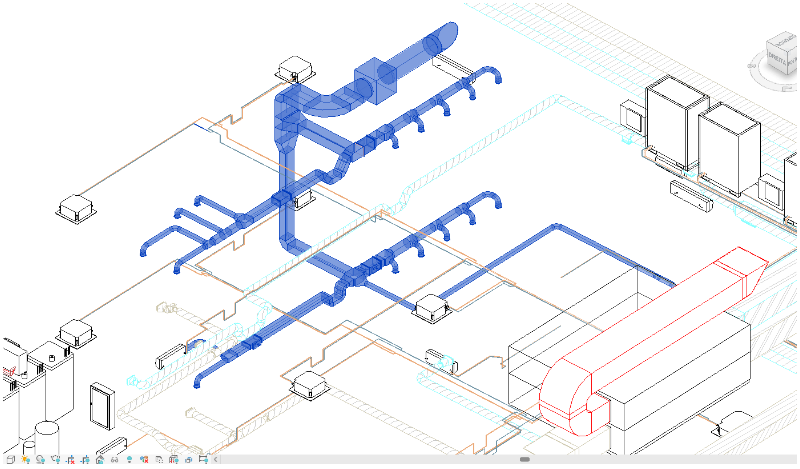

Figure 4.13: Revit model of the duct system for the fourth case study.

This particular configuration includes an ATU, which served as the reference point for sizing purposes. The network was deliberately chosen due to its intricate topology, featuring numerous branches, each containing distinct terminal equipment. This level of complexity results in increased cumulative pressure losses across the system, presenting a more challenging scenario than the previously analysed case studies. Consequently, it serves as an ideal benchmark for demonstrating the robustness and practical applicability of the plug-in in real-world design environments.

The system under analysis comprises circular diffusers, extraction valves, and constant air flow dampers. This network presents a particularly compelling case for evaluation due to its configuration. Based on conventional assumptions typically employed in the determination of the critical path, such as uniform flow distribution and pressure loss patterns, it would be reasonable, at first glance, to anticipate a behaviour analogous to that illustrated in Figure 4.14.

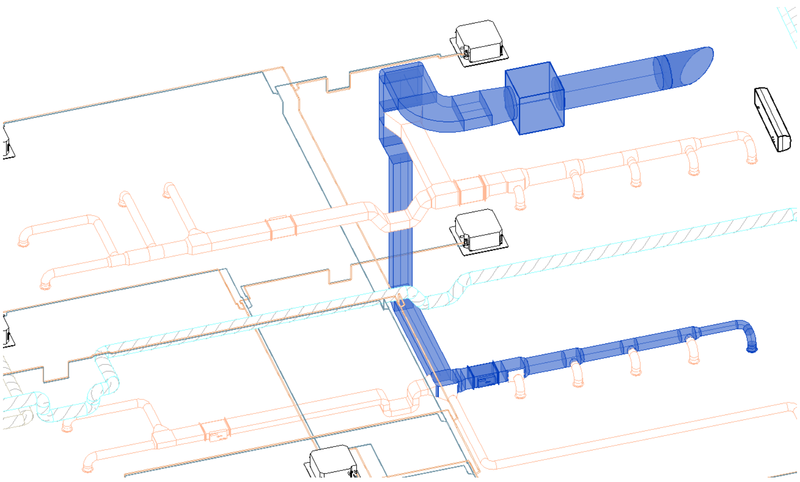

Figure 4.14: Estimated critical path, highlighted in blue.

Nonetheless, a more detailed assessment reveals a deviation from this initial expectation. Specifically, due to the considerably lower airflow velocities observed in the lower section of the system, the most significant pressure losses are concentrated at the intermediate level, as depicted in Figure 4.15. This counterintuitive outcome highlights the importance of rigorous, data-informed analysis in the design and evaluation of HVAC systems.

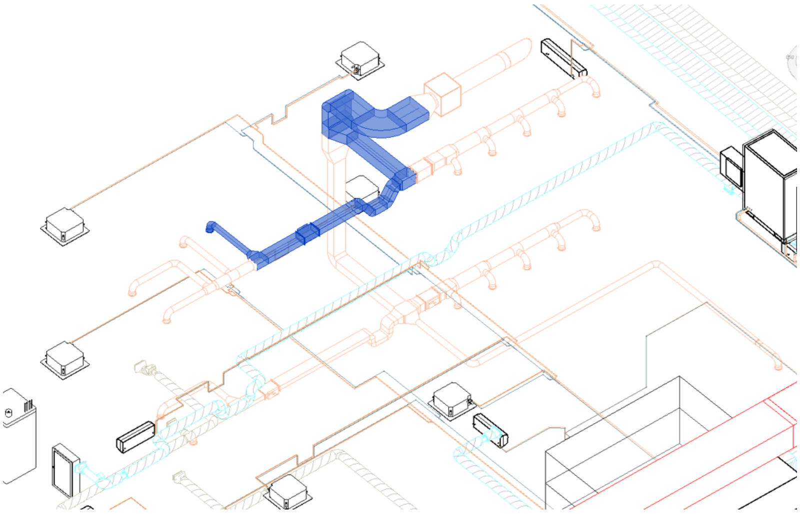

Figure 4.15: Actual critical path, highlighted in blue.

This programme allows the user to verify situations like this one and correctly assess the losses in the system. This particular configuration was deliberately selected to demonstrate such nuances. The application developed enables users to identify and correctly evaluate cases where intuitive estimations may lead to inaccurate conclusions. It thereby reinforces the necessity of precise simulation tools in accurately characterising pressure losses and determining the true critical path within a distribution network.

Appendix B presents the text file report that is created when the plug-in is run for this specific duct system.

4.4 Estimating Pressure Loss from Technical Catalogues

As previously stated, the equipment manufactured by Koolair is utilised extensively. Consequently, the company's website is frequently consulted to obtain equipment catalogues and information regarding pressure losses. In order to reduce the time spent with pressure losses in a duct system even further, the automation created for Revit software also includes a methodology for calculating the loss induced by a specific piece of equipment.

The current method commences with the identification of the pieces of equipment that are present on the duct system. The next step involves searching the *Koolair* website for the specified equipment. The flow rate of the respective equipment is then utilised to estimate the loss through a linear interpolation to calculate the appropriate value.

When the plug-in is initialised, the following interface is opened, a sort of form (Figure 4.16). As it is possible to see, the software gathers all the equipment in the duct system and creates a list with each respective flow rate, obtained from the project. This window is specific to the first duct system (Figure 4.3).

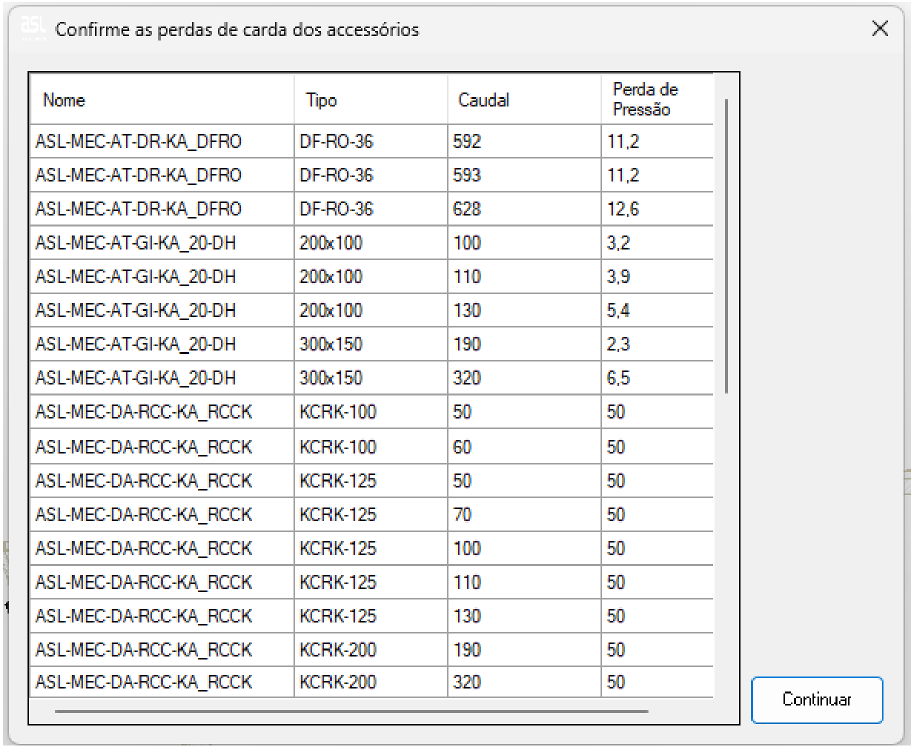

Nome	Tipo	Caudal	Perda de Pressão
ASL-MEC-AT-DR-KA_DFRO	DF-RO-36	592	11,2
ASL-MEC-AT-DR-KA_DFRO	DF-RO-36	593	11,2
ASL-MEC-AT-DR-KA_DFRO	DF-RO-36	628	12,6
ASL-MEC-AT-GI-KA_20-DH	200x100	100	3,2
ASL-MEC-AT-GI-KA_20-DH	200x100	110	3,9
ASL-MEC-AT-GI-KA_20-DH	200x100	130	5,4
ASL-MEC-AT-GI-KA_20-DH	300x150	190	2,3
ASL-MEC-AT-GI-KA_20-DH	300x150	320	6,5
ASL-MEC-DA-RCC-KA_RCCK	KCRK-100	50	50
ASL-MEC-DA-RCC-KA_RCCK	KCRK-100	60	50
ASL-MEC-DA-RCC-KA_RCCK	KCRK-125	50	50
ASL-MEC-DA-RCC-KA_RCCK	KCRK-125	70	50
ASL-MEC-DA-RCC-KA_RCCK	KCRK-125	100	50
ASL-MEC-DA-RCC-KA_RCCK	KCRK-125	110	50
ASL-MEC-DA-RCC-KA_RCCK	KCRK-125	130	50
ASL-MEC-DA-RCC-KA_RCCK	KCRK-200	190	50
ASL-MEC-DA-RCC-KA_RCCK	KCRK-200	320	50

Figure 4.16: Confirmation window of the pressure losses induced by each equipment.

This window functions as a confirmation form for the user to verify the flow rates and pressure losses, or to make any necessary changes to the values presented.

In instances where the flow rate falls outside the range of values specified on the brand's website, either at the lower or upper limit, the programme utilises extrapolation to calculate the relation between them and determines the value. This way, even for values not represented, a linear relation is extrapolated and used.

This automation has been demonstrated to be a highly efficient use of time, with the programme generating the pressure loss automatically for each piece of equipment. This automatic step saves the user time on calculations.

4.5 Automatic Pressure Loss Calculation on Revit

Within the "Analyse" bar of Revit, an option exists to calculate the pressure losses automatically. It is hypothesised that, if the tool is functioning properly, it should produce results equal to those of the automation created during this dissertation. As illustrated in Figure 4.17, the menu is displayed with the aforementioned bar open, and the option to calculate the pressure losses highlighted.

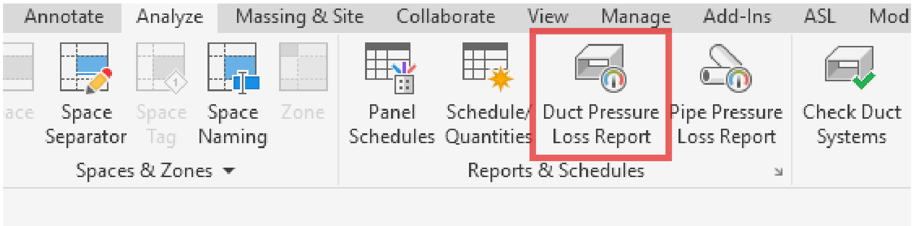

Figure 4.17: Interface of Autodesk Revit showing the built-in "Duct Pressure Loss Report" tool under the Analyse tab.

This tool's purpose is the same as the one proposed, so it will be tested in the same duct system for easier comparison. The values for density, dynamic viscosity, and roughness are specified in the properties browser of the software. Revit also uses the Darcy-Weisbach equation to compute the pressure drop on pipe segments, fittings, and accessories. The friction factor can be calculated by the Haaland or Colebrook method.

When the calculations are selected, an option box appears to select the systems present to calculate the pressure losses. Choosing all the systems present and proceeding with the method, the following window opens (Figure 4.18). This represents the fields that will be present in the report. It can be tailored to show the necessary fields. When clicking the "Generate" button, a report is generated and can be saved on the device. Appendix C presents the report that was produced in the first duct system example (Figure 4.3).

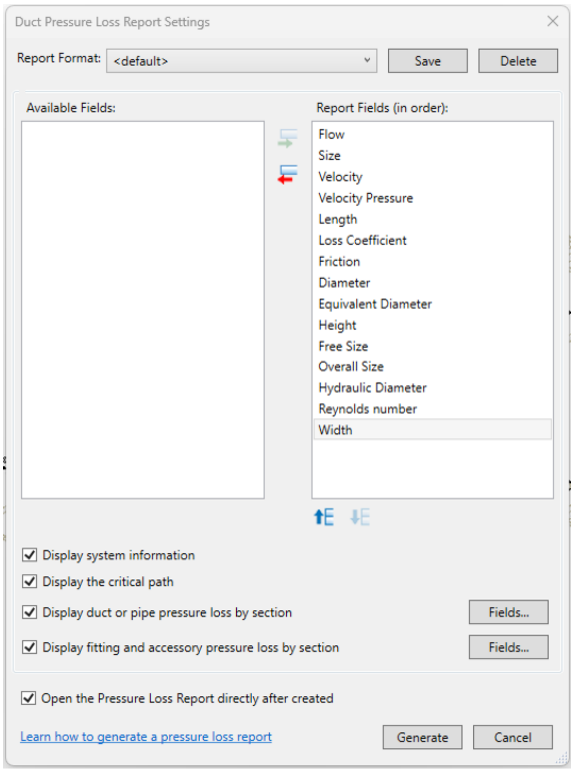

Figure 4.18: Duct Pressure Loss Report Settings.

This method could be a possibility for calculating the pressure losses in a duct system. However, the method presented in Revit does not produce interesting results. The values obtained manually and through this method are not compatible and present bigger differences than the automated ones.

The calculation method is, theoretically, the same as that employed in the manual method. Nevertheless, the simulation does not produce usable values. Each duct in the Revit model possesses the respective diameter and flow rate attributed. The software then calculates the remaining parameters, including the Reynolds number, relative roughness, hydraulic diameter (if applicable), and friction factor.

As it is possible to see by Appendix C, even though the software possesses values to calculate, the report created does not present any values or indicate the critical path. This tool was then discarded due to its inability to fulfil its respective function.

4.6 Summary

The chapter under discussion comprehensively explicated the automation developed for Revit and implemented through a plug-in, and some conclusions were gathered and will be presented.

Initially, the plug-in was analysed using four different case studies. A discrepancy was observed between the values present across these. It was found that, in general, the error remained within an acceptable range, with some exceptions to this rule that will be discussed in the following section.

Secondly, the accessories and duct components, such as elbows, were all accounted for in terms of pressure losses induced. This was achieved by utilising the ASHRAE document for fitting loss coefficients and from the suppliers' catalogues for the units, such as fan-coils and diffusers. The accurate calculation of the equipment's losses is essential for ensuring the system's dimensions align closely with actual requirements, thereby preventing unnecessary over-dimensioning of components.

The geometrical values, including the hydraulic diameter and, consequently, the duct area, were found to be equivalent in both methods. This confirmed that the automation was correctly reading the duct geometry. Nevertheless, each quantity has to be evaluated.

Secondly, discrepancies between the manual value and the Revit calculations can be attributed to certain approximations. Firstly, the velocity calculated through the Revit automation is approximated to the nearest quarter (0.25). For example, in the third case study, there is an approximation from 2.03 m/s to 2.25 m/s. This difference creates the bigger error values that can be presented. Although this is not ideal for those values, this method of approximating the velocity is used as it facilitates the analysis of the noise produced. This can be determined as one of the main sources of error in the automation.

Thirdly, the automation is highly practical in terms of its ease of use and seamless integration into the existing calculation process. The integration of the tool in the Revit software, which is currently the main one used for projects, is highly beneficial. The user does not need to open a second tool to calculate the pressure losses. In addition to enhancing precision, the automation reduced the time spent calculating and the tool used for that purpose. The integration of pressure loss analysis into BIM environments is a potential avenue for the automation of this process, to enable real-time feedback during the design phase and the streamlining of review and approval cycles.

This automation has been demonstrated to reduce the time taken for calculation and iteration by the Mechanical Installations team. In the context of a complex duct system, as illustrated in Case Study 4, the evaluation of the critical path can be accomplished in approximately two minutes. This time frame encompasses solely the execution of the plug-in and the acquisition of results. If the team were to undertake the calculation of pressure losses manually, assuming that they would calculate it for the critical path, the time taken would be approximately one hour. This represents a 96.7 % reduction in the time spent on the calculations. However, the reduction is even more pronounced in cases where the critical path is not clear and multiple paths have to be tested. Considering the hourly cost of an engineer analysing a complex path, the cost savings achieved are proportional to the time reduction, both amounting to about 96.7 %.

The tool was presented to the Mechanical Installations team, and it is currently being utilised by the team. The presentation utilised to illustrate the methodology for calculating pressure losses in a duct system can be found in Appendix E.

Chapter 5

HVAC Equipment Maintenance Tasks Automation

This chapter is dedicated to automating the maintenance tasks required by the HVAC equipment in the hospital unit. This automation was created using the Microsoft Power App software.

Microsoft Power Apps provides applications, services, and connectors as a rapid development environment for building custom applications. Apps built with the software can run seamlessly in the browser and on mobile devices. A notable advantage of this software is that it enables users to build custom apps without extensive coding knowledge. It also allows users to share the created app with others in the organisation, specifying which users and groups can run it and whether they can make alterations or not.

Power App provides a blank canvas where users can design the interface that is most convenient for the business model in question. Furthermore, the software facilitates the integration of data from a diverse range of sources, encompassing Microsoft applications such as Excel.

The automation was designed in Portuguese to facilitate future maintenance team use.

5.1 Problem Definition and Goals

This section of the dissertation is meant to explain the different objectives for this automation, but also to explain the difficulties encountered when working with preventive maintenance procedures. Figure 5.1 outlines the phases for the development of the Power App.

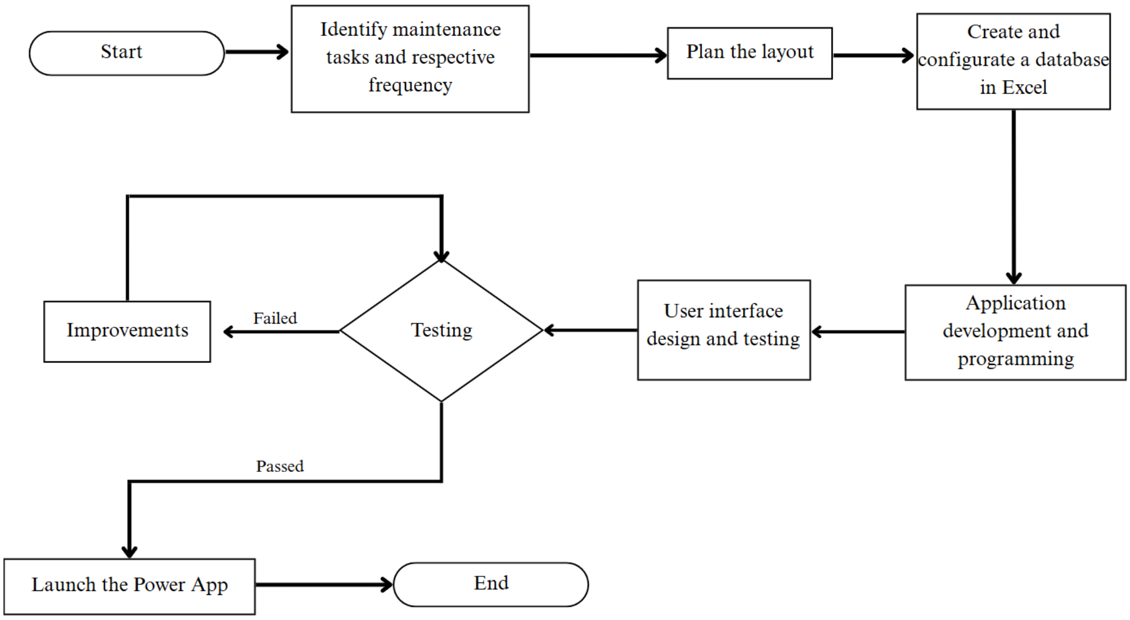

Figure 5.1: Power App development process.

As a first step, it was necessary to identify the tasks that each component required. As it was mentioned previously, this was executed with the use of maintenance sheets from previous projects and maintenance schedules recommended by suppliers. Appendix E presents a typical table that can be found in the suppliers' manuals.

The subsequent step involved thoroughly analysing and defining the desired layout for the application. This means deciding what type of features the application requires to perform the different objectives.

Parallel to this, it was also developed a database of the equipment's information that was mentioned before. This database was developed in Excel and served as a central reference point throughout the project, ensuring consistency and facilitating the organisation, analysis, and eventual integration of data into the application.

The following stage was inherently iterative, to develop and program the application. It was characterised by a trial-and-error approach, as it required continuous refinement and the integration of new features to enhance functionality. Throughout this process, the design and structure of the application evolved significantly, paralleling the increasing understanding and familiarity with the program's capabilities and potential. This ongoing development ensured that the final layout was not only functional but also well-adapted to the users' needs and the application's objectives.

The interface was then configured for the best user performance.

The design of the user interface was a key aspect of the application's development, aiming to ensure an intuitive and user-friendly experience. Special attention was given to clarity, simplicity so that users could navigate the application with ease and access information quickly. The layout was structured logically and coherently, with visual elements such as buttons, icons, and labels designed to be consistent and self-explanatory.

As the application evolved, the interface was also refined through multiple iterations based on usability testing and feedback, ensuring that it met both functional requirements and aesthetic standards.

The application was tested multiple times throughout the development process, and improvements were implemented whenever the initial objectives were not fully achieved or when potential enhancements were identified. This iterative testing allowed for continuous refinement and adaptation, ensuring the application aligned with both functional requirements and user expectations.

Concluding these steps, the application was determined to be ready to be launched.

5.2 Work Standardization

Standardisation is one of the tools that can be applied in the continuous improvement of an organisation. The standardisation strategy is predicated on the development and utilisation of consistent designs to align project stakeholders, objectives, and scope to capture and optimise schedule, cost, and value. Standardisation facilitates the replication of designs, procedures, and practices (Choi et al., 2023). It has been demonstrated that processes that follow this methodology are more readily controllable and comparable. This facilitates the documentation of best practice, for instance (Wolfa et al., 2022).

The standards delineate optimal methodologies for the execution of the work. The objective is to execute the task correctly on the initial attempt, without incurring errors or adverse effects on humans and the surrounding environment (Mĺkvaa et al., 2016). The following observations can be made concerning the use of the aforementioned devices:

- The reduction of variation and error correction;
- Improved safety;
- Facilitate communication;
- Visibility problems;
- Assistance in training and education;
- Increasing labour discipline;
- Facilitating the response to challenges;
- Clarification of the working procedures.

The standards precisely describe the necessary steps for the job, i.e., each step sequence (Mĺkvaa et al., 2016). The standard is required to exhibit the following characteristics:

- The text is concise and contains only the instructions that are indispensable for the operator to process;

- The simplicity and visual nature of the instructions enables the worker to locate and comprehend them with minimal effort;
- Exists potential for rapid alterations to be made to process parameters;
- Clarity, ensuring that every worker has all the relevant activities in the process;
- The ability to supervise the execution of standards and their effect on the process parameters (MÍkvaa et al., 2016).

This standardisation was applied to the maintenance tasks mentioned previously, Chapter 3, to create maintenance order sheets. These sheets would be available for the maintenance team to use as a checklist and an organisational method.

5.3 Maintenance of Heating, Ventilation and Air Conditioning Systems

The operating phase of facilities typically extends longer than other phases, and can account for up to 80% of the total life cycle cost of a building (Moradabadi et al., 2024). Because of this, the maintenance of the systems present in a building gains a very big weight on the total cost of that.

The current project (a hospital unit) relies heavily on the HVAC systems installed to ensure a safe environment. The maintenance of this equipment should correctly reflect its importance and be directly related to its specific type. For example, a boiler has different maintenance requirements from an ATU (Air Treatment Unit). For each equipment type, a maintenance checklist and frequency of maintenance must be created. This process can be facilitated by obtaining the necessary information from suppliers. The recommended maintenance procedures for each type of HVAC equipment are presented in the following sections, along with a description of the main characteristics and functions of that respective component.

The procedures are based on maintenance schedules from previous building projects and from some suppliers' catalogues, and were compiled during this dissertation's development. The maintenance procedures should be registered. It is beneficial to set up maintenance registries of equipment that has a significant impact on energy and water consumption, to prevent extra costs (Lecamwasam et al., 2012).

5.3.1 Maintenance Tasks of Air Treatment Units

Air Treatment Units are responsible for important functions within an HVAC system. They contain several components, such as dehumidifiers, humidifiers and filters, depending on the conditions of the room. The maintenance tasks can be tailored specifically to the ATU in question. Table 5.1 presents a general list of maintenance tasks that will be considered for ATUs for the maintenance tool under development.

Table 5.1: Maintenance tasks for Air Treatment Units.

Maintenance task	**Frequency**
Check for abnormal noises and vibrations from the pump	Monthly
Check for possible water leaks and condensate drainage	Monthly
Inspect and adjust transmission belts and pulleys	Monthly
Clear air filters and condensate tray with disinfectant	Monthly
Purge the heating/cooling oil	Monthly
Measure air inlet and outlet temperatures	Monthly
Check operation of the entire control system	Every six months
Perform mechanical and electrical tightening	Every six months
General cleaning, lubrication, and corrosion control	Every six months
Measure motor current draw	Every six months
Adjust and align transmission pulleys and check supports	Every six months
Check operation or airflow control dampers	Annual
Replace air mats or filters (if necessary)	Annual
Clean water filters	Annual
Clean cooling and heating coils with water or compressed air jet	Annual

5.3.2 Maintenance Tasks of Boilers

These systems operate under conditions of high temperature and pressure, necessitating strict adherence to safety and maintenance protocols. Regular maintenance is imperative to ensure operational efficiency and safety. Adherence to these procedures is imperative to ensure optimal efficiency, reduce energy consumption, and mitigate the risk of failure, which can disrupt hospital operations. Consequently, the establishment of a systematic maintenance programme for boilers is therefore crucial not only to maximise the longevity of the equipment but also to guarantee the uninterrupted and secure provision of heating services throughout the facility (Vaillant, 2024). Table 5.2 presents the maintenance tasks that will be considered for boilers for the maintenance tool under development.

Table 5.2: Maintenance tasks for boilers.

Maintenance task	**Frequency**
Check burner operation	Monthly
Check gas supply pressure	Monthly
Check pressure regulator efficiency (gas)	Monthly
Check gas valve operation	Monthly
Check main combustion components	Monthly
Check for abnormal noises or vibrations	Monthly

Continued on the next page

Table 5.2 – Maintenance tasks for boilers (End).

Maintenance task	**Frequency**
Check for leaks in the hydraulic circuit and automatic filling kit	Monthly
Check water flow switch operation	Monthly
Check water pressure and adjust if necessary	Monthly
Check water inlet and outlet temperatures	Monthly
Check operation of automatic devices and control/regulation equipment	Monthly
Analyse exhaust gases	Every six months
Perform tests on control and command instruments	Annual
Clean gas filters	Annual
Clean the tube bundle	Annual
General cleaning inside and outside	Annual
Burner tuning	Annual
Clean flue pipes and chimney (from the base)	Annual
Measure and record data for energy balance to determine boiler efficiency	Annual

5.3.3 Maintenance Tasks of Circulating Pumps

Consequently, the regular maintenance of circulating pumps is imperative. The implementation of a preventative maintenance programme has been shown to result in several benefits for facilities, including a reduction in energy usage, the avoidance of costly repairs, and the extension of the lifespan of the pumps. This, in turn, ensures the uninterrupted operation of the HVAC system (Wilo, 2024).

Table 5.3 presents the maintenance tasks that will be considered for circulating pumps for the maintenance tool under development.

Table 5.3: Maintenance tasks for circulating pumps.

Maintenance task	**Frequency**
Check pump noises and vibrations	Monthly
Check mechanical seal and gasket tightness	Monthly
Check alignment and fastening of pump chassis	Monthly
Check bearing condition	Monthly
Check for abnormal overheating	Monthly
Check cooling system	Monthly
Perform purging	Monthly
Alternate pump operation	Monthly

Continued on the next page

Table 5.3 – Maintenance tasks for circulating pumps (End).

Maintenance task	**Frequency**
Record water pressure (inlet/outlet)	Monthly
Measure and record motor absorbed current and compare with nominal values	Monthly
Check lubricant level (where applicable)	Every six months
Check for corrosion	Every six months
Perform verification tests on pressure and flow switches	Every six months
Lubricate bearings	Every six months
Perform general cleaning	Every six months
Clean water filters	Annual
Touch-up or complete paintings (if necessary)	Annual

5.3.4 Maintenance Tasks of Chillers

In the event of a failure or inefficiency in chiller performance, the consequences can be significant, including thermal discomfort, increased energy consumption, and even operational disruptions. Ensuring the reliability of chillers necessitates regular maintenance. The monitoring of temperature differentials, flow rates, and vibration levels can facilitate the identification of early indications of wear or inefficiency. Adherence to a comprehensive preventative maintenance plan is therefore essential for facilities, as it enhances chiller efficiency, reduces downtime, and extends the lifespan of the equipment. This, in turn, ensures the optimal performance of the HVAC system (Mitsubishi, 2024).

Table 5.4 presents the maintenance tasks that will be considered for chillers for the maintenance tool under development.

Table 5.4: Maintenance tasks for chillers.

Maintenance task	**Frequency**
Check for leaks	Monthly
Check compressor oil level and pressure	Monthly
Check the tightness of refrigeration circuits for traces of oil or freon	Monthly
Check refrigerant charge	Monthly
Check refrigerant humidity	Monthly
Check temperatures and pressures	Monthly
Check water flow in the evaporator	Monthly
Check compressor noise and mounting	Monthly
Check operation of crankcase heaters	Monthly

Continued on the next page

Table 5.4 – Maintenance tasks for chillers (End).

Maintenance task	**Frequency**
Check the tightness of piping and joints	Monthly
Check operation of condenser fan motors	Monthly
Check vibration and tightening of electrical components	Monthly
Record inlet/outlet water temperature	Monthly
Check operation of electrical and electronic valves	Every six months
Perform safety thermostat tests	Every six months
Perform LP and HP thermostat tests	Every six months
Clean condenser fins	Every six months
Perform general cleaning and lubrication, and prevent corrosion	Every six months
Measure compressor absorbed current	Every six months
Measure compressor oil acidity	Annual
Perform electrical and mechanical retightening	Annual
Clean water filters	Annual
Test measuring instruments	Annual
Touch up painting	Annual
Check for equipment label stating: "Contains fluorinated greenhouse gases covered by the Kyoto Protocol". Apply if missing	Annual
Check for label showing the quantities (kg and tons of CO_2) and type of refrigerant gas in the equipment (factory charge + additions = total). Apply if missing	Annual
Check bearing noise of fan motors	Annual

5.3.5 Maintenance Tasks of Fan-Coils

Due to their distributed nature and direct contact with indoor air, they are more prone to accumulating dust, microbial growth, and mechanical wear. Consequently, regular maintenance is imperative to prevent performance deterioration, reduce noise levels, and avert air quality concerns.

Table 5.5 presents the maintenance tasks that will be considered for fan-coils for the maintenance tool under development.

Table 5.5: Maintenance tasks for fan-coils.

Maintenance Task	**Frequency**
Clean air filters	Every three months
Functional tests of the unit and noise verification	Every three months
Check for leaks (Motorised Valves/Flow Modulating Valves)	Every three months
Check for corrosion (Motorised valves)	Every three months

Continued on the next page

Table 5.5 – Maintenance tasks for fan-coils (End).

Maintenance task	Frequency
Check for signs of corrosion	Every six months
Check fan noise	Every six months
Check and functionally test the actuator (Motorised Valves/Flow Modulation)	Every six months
Detect leaks in water circuits	Every six months
Check thermostat operation	Every six months
Check the condition of coils	Every six months
Check and clean condensate trays	Every six months
Check the condition of the condensate pump	Every six months
Check connections to the condensate drainage system	Every six months
Check the condition and operation of shut-off valves	Every six months
Check and clean water filters	Every six months
Clean coils	Annual
Check fan blade condition	Annual
Replace air filters	Every two years
Check the condition of thermal insulation	Annual
Lubricate moving parts if necessary	Annual
Clean and disinfect the interior of the equipment	Annual
Check and tighten electrical connections	Annual

5.3.6 Maintenance Tasks of Ventilators

These units typically operate continuously, which renders them particularly susceptible to wear, contamination, and mechanical fatigue. Accumulated dust, misaligned pulleys, and degraded filters can lead to reduced efficiency and problematic air quality. The proactive maintenance of ventilators is of great benefit not only in extending the life of the equipment's lifespan, but also in protecting the health of the occupants by ensuring consistent and hygienic airflow (Sodeca, 2024).

Table 5.6: Maintenance tasks for ventilators.

Maintenance task	Frequency
Check condition, measure and record pre-filter differential pressure	Monthly
Check pre-filters whenever differential pressure is below clogging threshold	Monthly
Check for impurities obstructing fresh air inlets or exhaust air outlets	Monthly

Continued on the next page

Table 5.6 – Maintenance tasks for ventilators (End).

Maintenance task	**Frequency**
Check fan operation	Every three months
Check pulley alignment	Every three months
Check for corrosion, contamination, odours, and signs of leaks	Every three months
Replace filter if defective	Every three months
Clean water deposits or stains	Every six months
Clean inside of equipment	Every six months
Measure and record electric current	Every six months
Check for contamination, deterioration, and corrosion	Every six months
Clean fan parts in contact with air	Every six months
Check the condition of motor supports and fan blades	Every six months
Check condition and tension of belts	Every six months
Check contamination of air intake elements, mosquito net or bird guard	Annual
Check operation and clean variable frequency drive	Annual
Clean and retighten the electric motor	Annual
Replace belts	Annual
Check motor mounting supports	Annual
Lubricate dynamic components	Annual
Clean unit's exterior structure	Annual
Check fan blade rotation and balance	Annual
Replace all filters	Annual
Replace filter seals	Annual
Check bearing condition and lubricate if needed	Annual

5.3.7 Maintenance Tasks of Split Units

Their performance depends heavily on regular maintenance, especially in high-demand environments like hospitals. Ensuring these units operate reliably helps maintain consistent comfort levels and reduce the risk of unplanned failures.

Table 5.7: Maintenance tasks for split units.

Maintenance task	**Frequency**
Clean air filters	Every three months
Check for fan noises	Every three months
Check controller commands	Every three months
Check for corrosion	Every six months

Continued on the next page

Table 5.7 – Maintenance tasks for split units (End).

Maintenance task	**Frequency**
Check thermostat operation	Every six months
Check coil condition	Every six months
Check and clean condensate trays	Every six months
Check condensate pump condition	Every six months
Check connections to the condensate drainage system	Every six months
Clean coils	Annual
Check the condition of fan blades	Annual
Check thermal insulation condition	Annual
Lubricate moving parts, if necessary	Annual
Clean and disinfect unit interior	Annual
Check and tighten electrical connections	Annual
Check for abnormal noises	Annual
Record compressor absorbed current	Annual
Check for possible freezing points	Annual
Replace air filters	Every two years

5.4 Power App Automation

The maintenance application developed during this dissertation is meant to function as a CMMS, specifically tailored to the hospital unit's maintenance needs (Chapter 3).

The automation desired during its project phase had several objectives. Primarily, the objective was to establish a comprehensive database encompassing all components utilised within the hospital environment. The components mentioned in the preceding chapter are the ones being analysed. The second task was to gather the maintenance routines from suppliers and create a calendar in the Power App that holds all scheduled tasks. This calendar is designed to serve as an alert system, displaying tasks that need to be completed along with their due dates. As tasks are done, employees can check them off a checklist.

The components were organised by category in the Power App, facilitating access to each component type and its characteristics. These characteristics include supplier, price, model name, power, fluid flow rates, and other specific parameters relevant to the respective component. The maintenance team is expected to utilise this information to gain comprehensive knowledge of each component when the building is operational.

The project was initiated with the identification of the maintenance tasks for each respective component and their respective frequency. This process entailed establishing communication with the relevant suppliers and obtaining the maintenance plans for the various equipment items. Moreover, as previously stated, the firm's existing maintenance plans were reviewed to facilitate a comparison of the recommended tasks and frequencies. It was possible to obtain several important pieces of information from these contacts. These include the prices and specific technical specifications of the equipment.

In the course of the application's development, Excel files were created to support the app and facilitate the organisation and storage of data. Each equipment category possessed an individual category for the management of specifications and acquisition prices. A comprehensive directory has been compiled, collating the maintenance procedures for all equipment in a centralised manner. This approach has been adopted to facilitate efficiency by bringing together all necessary tasks in one accessible location, thus eliminating the need for their dispersal across multiple calendars.

The maintenance tasks specified in Chapter 3 were consolidated into a single table within an Excel file for importation into the Power App software, thereby establishing a database for the routine programming. The frequency in each respective task was counted in the time unit of days to create uniformity across the frequencies.

- Monthly - equivalent to 30 days;
- Every three months - equivalent to 90 days;
- Every six months - equivalent to 180 days;
- Annually - equivalent to 365 days;
- Every two years - equivalent to 730 days.

These time frames are respective to each task and start counting from the day that the hospital starts operations. To facilitate the testing process, the maintenance tasks were scheduled to commence on the 1st of April. The tasks are to be initiated upon the establishment of hospital operations. The initial date for the beginning of the tasks should be adjusted once the Hospital Unit possesses a finish date.

After the data was structured in Excel, the development of the application began. The application consists of 11 screens, which will be described next.

- **Loading screen:** the introductory screen serves to welcome the user to the program (Figure 5.2). The design is minimalist and serves only as a loading screen to let the user into the program. It possesses two input fields for the user to insert their name and email to log in. After these are inserted, the button can then be pressed to enter the application.

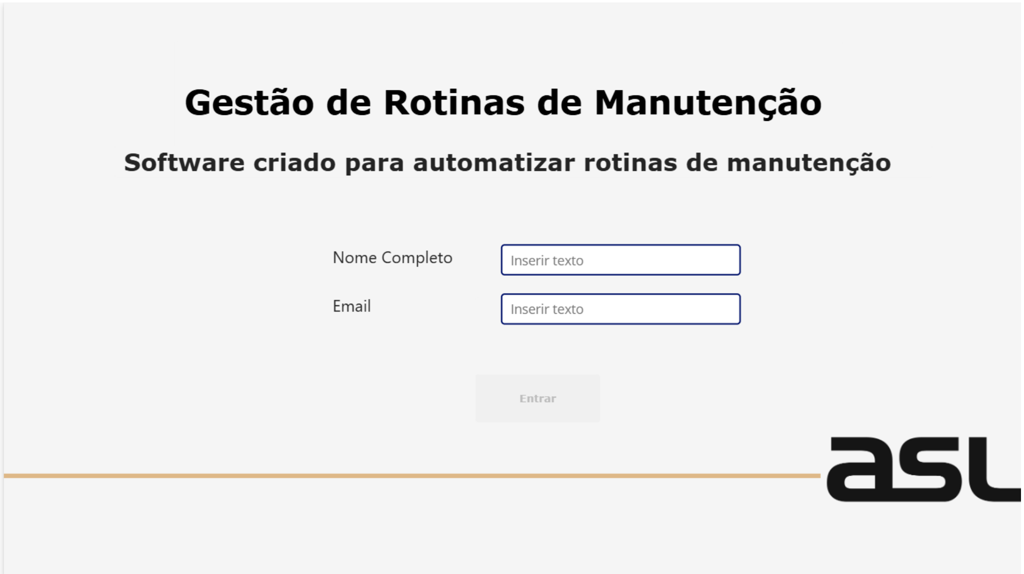

Figure 5.2: Loading screen of the maintenance management application.

- **Home screen:** meant to give a thorough overview and assist in quick navigation throughout the program (Figure 5.3). It is composed of several integral components that allow access to other important screens.

  Firstly, on top of the page is the header presenting the title of the page and also greeting the user who logged in on the previous screen. This login will then be registered, and a piece of important information for the maintenance records.

  Secondly, on the left side of the screen, there is a menu presenting the main options available and a small container for warnings. The first item on the menu is a Calendar icon, which, when pressed, leads to a dedicated screen that shows a calendar of the current month. This screen enables the visualisation of the whole month and the tasks that are scheduled each day. It enables the user to create a plan for the whole month. After that, there is an option box that will lead the user to a screen containing the technical sheets of the respective equipment type. When selecting the equipment type desired, the corresponding screen is prompted to open, thereby presenting the specifications pertinent to each equipment in the designated equipment category. Lastly, there is a button that leads the user to a screen with the pending tasks and the necessary steps to complete each respective task. This is part of the work standardisation mentioned earlier and will be explained later in the respective screen section.

  The warning section of the screen is meant to serve as a quick visualisation of the assigned tasks for the current day, the following week, or the following month. This helps the maintenance team know of the tasks and plan them without having to open the whole calendar. By choosing the respective option, the number of pending tasks is shown.

  Finally, two containers are presented. Arguably, the most beneficial section of the Home screen is the planning of these maintenance tasks, which is highly pertinent to the tool.

The first container presents the subsequent scheduled tasks, accompanied by the respective equipment category of that task. There is also an option box to filter the scheduled tasks by equipment category. The software has been configured in such a way that tasks that have exceeded their designated resolution date are displayed in red. This serves to convey an increased sense of urgency concerning their completion. The second container presents the completed tasks. The programme removes the task when it is marked as completed from the pending tasks, the first container. The completion of tasks is to be documented in the execution guides screen (Figure 5.7). This subject is addressed in greater detail subsequently. The second container also shows the user who marked it, as well as the date.

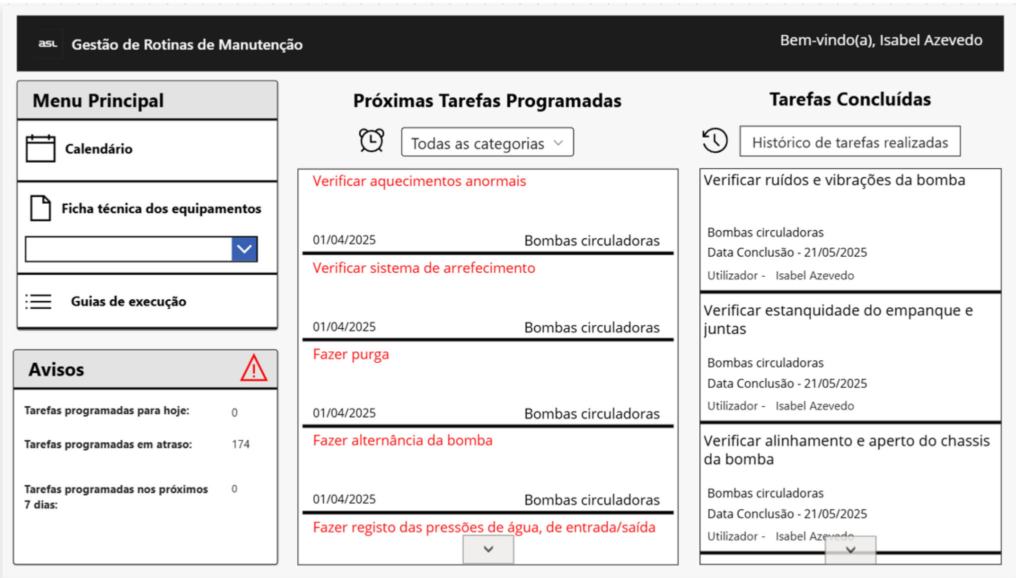

Figure 5.3: Home screen of the maintenance management application.

- **Calendar screen:** this screen presents a monthly calendar. The programme has been configured to ensure precise synchronisation between weekdays and the corresponding numerical day of the month, thereby reflecting the actual calendar. As previously indicated, the top left of the screen contains a return arrow to the Home screen. It is also indicated the current month, as the calendar is set to open on the current month. Moreover, two arrows are present, the function of which is to alternate the display of the month.

As illustrated in Figure 5.4, each table cell represents a weekday that has been correctly identified. In the case of the current day, this is indicated by the use of a different colour in the cell. The day of the month on which tasks are allocated is denoted by the colour red to attract the user's attention. This screen allows the user to visualise the whole month by scrolling down.

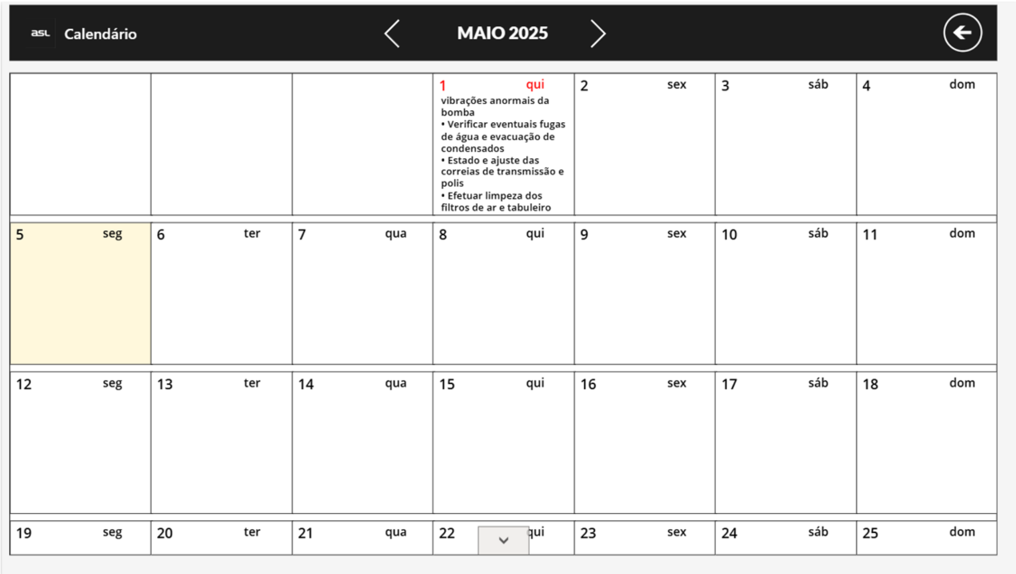

Figure 5.4: Calendar screen with May 2025.

Nevertheless, there are instances in which a given day encompasses multiple tasks. In the presence of more intricate tasks, it becomes challenging to fully observe the comprehensive list of tasks for that specific day. As illustrated in Figure 5.5, the expansion container is revealed upon clicking on a day with allocated tasks. The tasks are presented sequentially, with each task being displayed successively as the user scrolls down the page. Each task is categorised into its respective category, thereby facilitating efficient navigation and organisation. The container can then be closed when it is no longer necessary, returning to the previous Calendar screen.

Figure 5.5: Calendar with task container expanded.

- **Section screens:** Upon selection of the equipment category, the application directs the user to the relevant screen. The configuration of these screens was designed to facilitate the management of equipment inventory, encompassing a range of specifications, including but not limited to price, supplier, hospital location, and other pertinent parameters.

  Figure 5.6 shows, as an example, the dedicated screen for the inventory of ventilators. As illustrated on the left side of the screen, there is a list containing all the ventilators that are to be installed in the hospital unit. The list includes the ventilators' respective designations, model, and floor location. The nomenclature employed (e.g, VE -1.1) corresponds to the designated nomenclature of the project. Upon consideration of the ventilator, the tables on the right are immediately filled with the ventilator's specifications as illustrated in Figure 5.6, the ventilator designated as VE-1.1 has been selected for analysis. As is demonstrated by the tables on the side, the parameters of the equipment can be rapidly visualised, such as supplier, model, price, location in the building, and more.

  In the lower section of the screen, a gallery contains all the maintenance tasks relevant to ventilators, along with the respective frequency of each task. This database has been designed to serve as a comprehensive resource for the team, providing a centralised platform for the management and organisation of tasks by equipment.

  Lastly, at the top of the screen, a return arrow forwards the user to the last screen (Figure 5.3), enabling the selection of another equipment category.

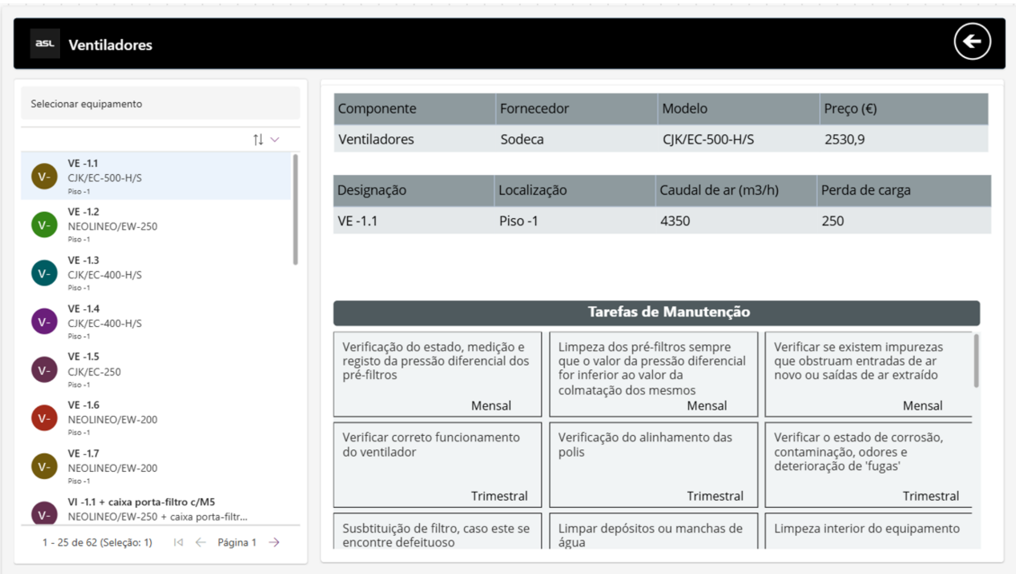

Figure 5.6: Section screen example for ventilators.

Each equipment category possesses a dedicated screen like the one just presented, with the inventory, specifications, and dedicated maintenance tasks. These screens occupy the majority of the program.

- **Guide screen for each maintenance task:** Upon selection of the execution guide, the application refers the user to the following screen (Figure 5.7). This screen's purpose is to create the work standardisation mentioned previously for each maintenance task. The workers who will use this tool later only need to follow the steps presented on this screen.

  The screen is divided into three containers. The first one contains the scheduled maintenance tasks, with the respective category and scheduled date. This can be filtered by category, like the Home screen.

  The following container depends on the selected task, as it changes to show the procedure list for each task selected. Like Figure 5.7 shows, the chosen task is highlighted in a light beige to ease the user's visualisation. As the user follows the procedure, the verification boxes can be checked, to, at the end, save the maintenance records. If necessary, there is an input text box in case the user needs to add observations to the task that was just concluded. By pressing the button at the end of the container, a register is added to the third container. The pending tasks are automatically updated to exclude a task when it is marked as done, adding that respective one to the list of concluded. This verification of the task completed receives a push notification (*"Tarefa Concluída com sucesso!"*) for the user to visually confirm that the task got correctly marked as done correctly.

  The third container presents the maintenance records created by the previous container's button, respectively specifying the task done, the category, the registry date, and the respective user. If the observation field is filled, it will also appear. Lastly, the third container also presents a button to send a report of the monthly tasks accomplished. This report is sent to the email that is currently logged in to the application, and presents a list of the tasks executed with the same information as presented in the third container. Like the task completion process, when the user clicks the button to send the email, a notification is presented on the screen to inform the user (*"Email enviado com sucesso!"*). Appendix G presents the format in which the user receives the report in the inserted email. All the tasks in this example were marked as done to represent a typical use of the application.

  As mentioned previously, the tasks present in the Home screen (Figure 5.3) are automatically updated by this screen. This contributes to uniformity, ensuring there are no tasks marked as completed without following the proper procedure.

Figure 5.7: Guide for maintenance tasks procedure screen.

5.5 Summary

This section of the chapter presents the conclusions that can be drawn from the tool. The primary objective of the system's design was to serve as a management instrument for the execution of maintenance operations within the framework of the Hospital Unit project.

As per the initial design, the tool was to encompass three core functions: a database for the equipment installed, a planner for the necessary maintenance tasks, and a tracking system for operations realised.

The development of this Power App application has been demonstrated to be an effective solution for the organisation and automation of preventive maintenance tasks. As the process unfolded, it became evident that the integration of a well-structured database with a user-friendly interface significantly enhanced the efficiency of maintenance planning and execution.

The application's primary accomplishment was the consolidation of equipment-related data, thereby facilitating expedited access to maintenance requirements and mitigating the risk of errors. The interface, conceived with simplicity and usability as guiding principles, enabled intuitive interaction with the system. This was further refined through iterative enhancements derived from user testing and feedback.

Furthermore, the adaptability of the platform enabled the integration of novel functionalities as the project progressed, demonstrating its capacity to evolve in response to real-world requirements and limitations. The iterative nature of the development process ensured that the final version of the application was not only aligned with the original objectives but also capable of evolving with future requirements.

However, despite the progress achieved throughout the development process, it is important to highlight that the application could not be tested in a real operational context with the maintenance team that is expected to use it. This is a consequence of the fact that, at the time of development, the designated maintenance team had not yet been established. Consequently, despite the thorough testing of the application in a controlled environment, its performance under actual working conditions remains to be validated once the team is in place.

In conclusion, the application successfully addressed the challenges associated with preventive maintenance by offering a digital and automated solution that is both practical and scalable. This development signifies a substantial basis for subsequent enhancements, including the incorporation of notifications, analytics, and potentially predictive maintenance tools through the expanded utilisation of Power Platform functionalities.

Chapter 6

Life Cycle Costs Analysis

This chapter of the dissertation is dedicated to the last automation tool developed: the Life Cycle Cost Analysis. This tool was created using the Power BI software, which is part of the same system as Power Apps. Power BI connects data sources and helps develop reports and dashboards. It enables users to transform data and combine it into a data model, allowing them to create visuals.

This tool's primary objective is to enable users to easily create a life cycle cost analysis for various types of equipment.

6.1 Life Cycle Costs Analysis Tool Development

As previously stated in Chapter 3, the life cycle cost of an asset can be defined as the total cost in present value or annual value. This encompasses the preliminary expenses, maintenance costs, repair costs, and renewal costs (MR&R) throughout the service life or a designated life cycle (Rahman and Vanier, 2004).

The development of this tool consisted of several stages. The first step was to create a methodology to evaluate the Life Cycle Costs of a specific piece of equipment, for example. Following that, it was necessary to identify all the costs correlated with that equipment's life cycle. These costs were collected from suppliers. The tool was developed with the use of the software Power BI and used to calculate the results, such as the Net Present Value. After the calculations are done, it is only necessary to analyse the values and compare the results, qualitatively. Figure 6.1 is a scheme explaining this process.

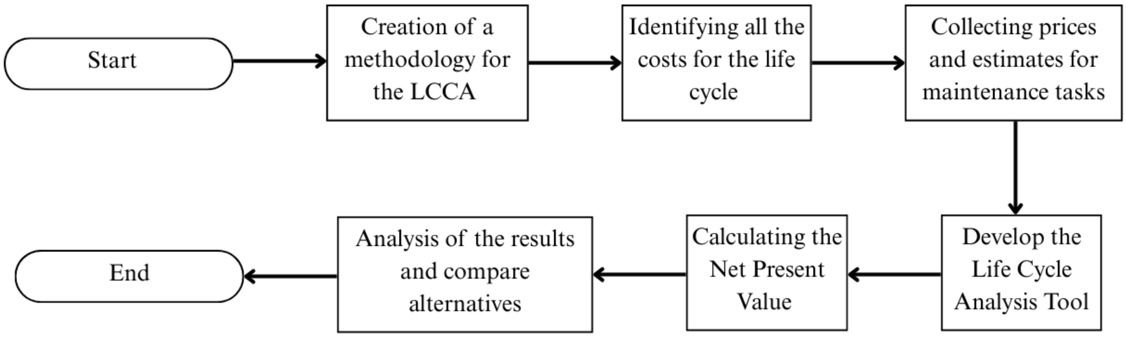

Figure 6.1: LCCA tool development process.

As stated in Chapter 5, the costs of the equipment selected for the hospital unit had already been obtained from the relevant supplier. However, further research is required to ascertain the costs associated with item substitution and labour. This information was also obtained from the suppliers.

The objective of the tool is to enable the user to modify the data underlying the calculations and adapt it to their specific case. The calculations thus generated can be adapted to suit any given piece of equipment. The model was created in Power BI, yet it is connected to an Excel file. It should be noted that the values contained in this file are directly connected to the model and can be updated to align with the particular case in question.

The model possesses several inputs and outputs to calculate the costs accurately. The inputs of the tool are:

- Analysis period (in years);
- Acquisition costs;
- Energy consumption costs;
- Useful life (in years);
- Maintenance material costs;
- Labour costs and estimated necessary time;
- Discount rate.

The outputs are calculated through the respective formulas mentioned in Chapter 3 and they are:

- Acquisition costs;
- Annual maintenance costs;
- Accumulated costs after a certain period.

The acquisition costs are considered at year zero of the Hospital Unit and every time the useful life of the equipment is exceeded.

The annual maintenance costs considered in this study encompass both labour and materials costs, which were obtained by contacting the supplier of the equipment. It is acknowledged that the values under consideration are subject to a certain degree of approximation. The suppliers provided values for the material kits used when replacing a component, and also an estimation of the time and cost for the team. These values are estimations of the real costs, as they are very variable and depend on market fluctuations and the maintenance team.

The accumulated costs refer to the sum of the costs incurred from the beginning of the analysis up to the year that is being analysed.

6.2 Case Study for the Life Cycle Costs Analysis Tool

In consideration of the temporal constraints imposed on the development of the present tool, it became essential to select the equipment that would be the focus of our analytical examination. The equipment selected for the evaluation process was the boilers in operation, due to several factors. The building is equipped with three boilers, the cost of which is a significant proportion of the total investment due to the high initial cost of the equipment. The equipment under consideration will serve as the test for the LCCA tool developed, but the objective is for it to be possible to change the equipment, just by changing the acquisition prices and life cycle.

The project's chosen boiler model is from the brand *Vaillant* and is the *ecoCRAFT exclusiv VKK 2406/3-E HL R1*. The following Table 6.1 represents some technical characteristics of the respective model.

Table 6.1: Technical data for this model of boiler.

Model	ecoCRAFT exclusiv VKK 2406/3-E HL R1
Heat output, average temp. 80º/60ºC (kW)	47 - 236.2
Heat output, del./ret. temp. 60º/40ºC (kW)	48.2 - 241.2
Nominal heat power (kW)	240
Electric power absorbed (W)	320
Stand-by power absorbed (W)	8

This is the boiler that will be analysed with the tool developed and compared with an alternative option in the following section.

Acquisition Costs

The supplier was consulted, and the acquisition cost of the new equipment was obtained. As illustrated in Figure 6.2, an extract from the budget that was received and that will be considered is presented.

Item	Descrição	Referência	Un.	Qtd.	Unit (€)	Total (€)
	RESUMO					
I	Caldeiras Gás Natural					53 988,00 €
II	Acessórios					11 982,00 €
	TOTAL					65 970,00 €

Figure 6.2: Boiler and necessary accessories price from supplier Vaillant.

Figure 6.3 represents the Excel table in the Excel file that is used to insert the initial data of the equipment, like the acquisition prices and the useful life of a boiler. As mentioned in Khan et al. (2023), the useful life of a boiler can be considered of about 15 years. The acquisition cost was then programmed to be considered at 15-year intervals.

	Preços de aquisição	Vida útil (anos)
Dados de entrada	65 970,00 €	15

Figure 6.3: Excel table for the initial data of the equipment.

Annual Maintenance Costs

As previously mentioned, the tool is connected to an Excel file that can be updated to include further maintenance costs. These are incorporated within the calculations of the tool for this category of annual costs. Figure 6.4 represents the Excel table that includes these costs.

Custos de manutenção					
Periodicidade	Vezes por ano	Custo material	Custo por hora	Horas de operação	Custo da tarefa
Bianual	2	61,00 €	50,00 €	4,00	522,00
Anual	1	62,00 €	75,00 €	2,00	212,00
					734,00 €

Figure 6.4: Excel table for the material and labour costs for the maintenance tasks.

The tool developed in Power BI gathers the data from this table and calculates the task cost with the following Equation 6.1. This method considers the material costs, the labour costs and the number of times per year the task is performed.

$$\text{Total Cost} = (\text{Material Costs} + \text{Hourly Costs} \times \text{Hours of Operation}) \times \text{Times per Year} \tag{6.1}$$

This was the calculation process to determine the annual maintenance cost of each task. In the years without acquisition costs, the only cost that will be considered is this one.

Operation Costs

The costs under discussion are those associated with operating the equipment. Given that the subject of analysis is a boiler, the operation costs taken into consideration are those of electrical power and fuel consumption (Khan et al., 2023). The boiler under scrutiny is utilising natural gas as fuel, with a flow rate of 25.4 m^3/h. The electrical power consumed is 320 W (Appendix H). Through conversion, the associated costs of energy consumption can be determined.

Starting with the fuel consumption, the flow rate should be converted to MWh, as this is the standard unit in which fuel consumption price is typically presented. Equation 6.2 presents the conversion that can be applied to determine the energy consumed by the boiler.

$$E(MWh) = \frac{\dot{Q}(m^3/h) \times LHV(MJ/m^3)}{3600}. \tag{6.2}$$

E is used to denote the energy consumed, in MWh, Q is the flow rate of the gas consumed, in m^3/h, and LHV represents the Lower Heating Value for natural gas. This represents the amount of heat that is released when a fuel is combusted, excluding the latent heat of vaporisation of any water produced, in MJ/m^3 (Boyce, 2012).

In hospital units, equipment such as boilers is required to operate continuously. Notwithstanding the existence of circumstances in which the boiler is not required to operate and generate heat, the building nevertheless has a constant heat requirement (Rivera et al., 2024). The calculations will be conducted for the scenario in which the system operates on a 24-hour basis, accounting for the worst-case scenario.

For a flow rate of 25.4 m^3/h, a LHV of 35 MJ/m^3, and the boiler with a continuous consumption as mentioned previously, the energy consumed is approximately 2164 MWh. This is the annual energy consumption for the boiler of natural gas.

As of June 2025, the average natural gas price, according to the Spanish supplier of energy REN, is 35.17 €/MWh. However, the market fluctuates, and the prices undergo alterations, and, as the energy calculated is relative to the yearly consumption, an average of the monthly prices can be used. As such, the price used is 41 €/MWh as the yearly average (REN, 2024). The total cost of natural gas consumption is approximately 88,724 € per year.

For the consumption of electricity, the same process is used. The boiler absorbs 320 W from the grid to produce heat. Following the same consumption pattern as before, 24 hours of continuous operation, the total energy per year can be calculated. Equation 6.3 shows this calculation.

$$0.32 \text{ kW} \times 24 \text{ hours} \times 365 \text{ days} = 2803.2 \text{ kWh/year} \tag{6.3}$$

This is 2.803 MWh of energy consumed yearly. As previously mentioned, the supplier REN possesses yearly values for the electricity prices being practised, 61.11 €/MWh. The yearly cost is about 171.3 €.

In conclusion, every year the building has to support a cost of about 88,895.3 € to be able to run the boiler continuously. Although this is the worst-case scenario, the analysis of the Life

Cycle Costs will be performed with these values.

Accumulated Costs

The comparison between the equipment can be made after a determined number of years. The total accumulated costs can be calculated by adding together the costs mentioned above, as well as the costs of acquisition, maintenance, and operation for each year until the limit is reached. This cost is a particularly salient one when comparing two options for the equipment, as the long-term costs of a model can be lower than others, even with higher initial costs.

The tool allows the user to estimate the total costs for years and compare the two options accordingly. This cost is represented in the tool as a bar graph to illustrate its evolution over time (Figure 6.5).

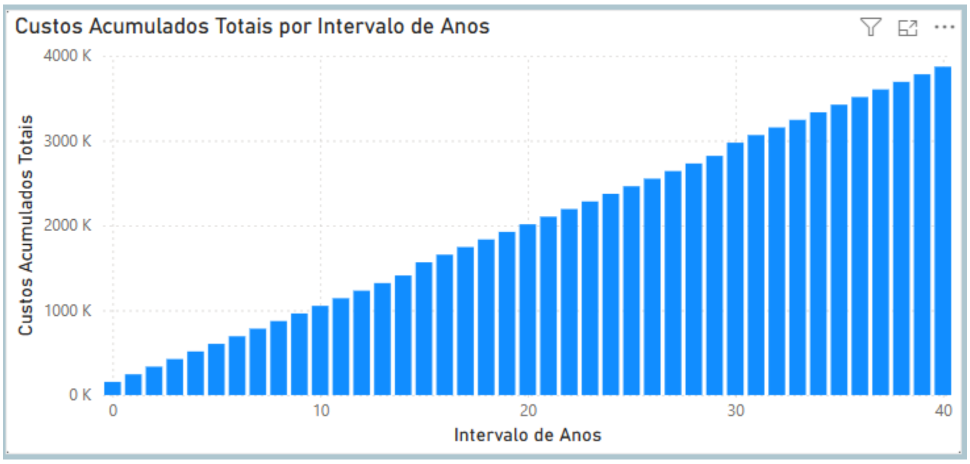

Figure 6.5: Accumulated costs graph for the ecoCRAFT exclusiv VKK 2406/3-E model.

Appendix I presents the LCCA tool developed in Power BI. The user is required to update the acquisition, maintenance and energy costs for the equipment they are evaluating.

6.3 Summary

In summary, this instrument is designed to estimate the costs incurred throughout the life cycle of a given piece of equipment. It incorporates acquisition, maintenance, and energy costs, offering a comprehensive overview of the total expenses associated with the equipment. Users can adjust input values to match the specific conditions of their case study and assess the resulting cost distribution accordingly.

Firstly, the platform includes acquisition costs, treating them as time-dependent. Based on the defined life cycle, the model assumes that the equipment will be replaced at the end of each cycle, and these replacement costs are added to the annual expenditure.

Secondly, the tool factors in energy consumption costs. Since energy prices are subject to market fluctuations, the updating feature allows users to simulate the impact of these variations on the total cost over time.

Thirdly, labour and equipment replacement costs are also considered. These depend on the specific characteristics of the maintenance team and materials used, and may vary significantly over the years.

Ultimately, the tool enables users to forecast total costs annually or across the entire operational lifespan of the equipment, supporting more informed and cost-effective decision-making. It contributes to reducing the costs and the time spent on the decision-making process. Moreover, it highlights the impact cost variations—such as increasing long-term maintenance expenses—can have on overall financial planning.

Chapter 7

Conclusion

The present work is focused on automating tools for the implementation of HVAC systems in Hospital Units. These systems constitute an integral part of the good functioning of these health units, and, as such, possess complex characteristics that make them challenging for engineers. The objectives of this dissertation are to facilitate the implementation of such systems, specifically in Hospitals. This addresses not only the technical difficulties encountered when designing a system like the one for the Hospital Unit mentioned, but also the economic and operational challenges present.

The development and evaluation of three integrated solutions was driven by three overarching objectives: the creation of a Power Apps-based application for maintenance planning, the development of a Revit plug-in to automate pressure loss calculation, and the conception of a life cycle cost analysis tool. Each solution meticulously addressed specific challenges within the maintenance, design, and cost management domains.

The Power Apps application was designed to serve as a digital management tool for preventive maintenance activities in the context of a hospital infrastructure project. Through the integration of a structured database, a task scheduler, and an operation tracker, the system significantly enhanced the organisation and automation of maintenance routines. Its usability and adaptability allowed iterative refinements based on user feedback, and although full validation under real operational conditions was not yet possible due to the absence of the designated maintenance team, the foundation for future implementation was solidly established.

The second contribution involved the development of a Revit plug-in that automates the calculation of pressure losses in HVAC duct systems. The tool was subjected to rigorous testing using a series of case studies, which demonstrated its remarkable precision in calculating losses, with minor deviations primarily attributable to the rounding methods employed for velocity calculations. Most notably, the automation led to a dramatic reduction in calculation time – up to 96.7 % in complex scenarios – while seamlessly integrating into existing BIM workflows. This serves to illustrate the potential of incorporating analytical tools directly into design environments, thereby facilitating faster and more informed decision-making.

The final section of the dissertation centred on the development of an LCCA instrument to estimate the long-term costs associated with equipment ownership. The tool evaluated acquisition, energy, and maintenance costs over time, and enabled users to customise input parameters for case-specific analysis. It further demonstrated the impact that cost variations, such as rising energy prices or long-term maintenance needs, can have on overall financial planning, supporting more sustainable and economically sound choices throughout the project's lifecycle.

Notwithstanding the distinct nature of the tools developed, they share a common objective: to improve accuracy, reduce manual workload, and enhance strategic decision-making through the use of digital technologies. The collective effect of these solutions represents a progression towards a more integrated and intelligent approach to facility management and building design, aligning with industry trends such as Building Information Modelling, predictive maintenance, and cost transparency.

Future research could concentrate on extending the functionality of these tools. To illustrate this point, the Power Apps application could be integrated with real-time notifications, analytics, and predictive maintenance features through Power BI and AI capabilities.

The Revit plug-in has the potential to evolve to support a greater number of complex system types and dynamic simulations. Different friction factor equations could have been tested to analyse the error that each produced in the calculations. Another development could include the interpolation process to determine more precise dynamic pressure losses.

Concurrently, the Life Cycle Costs Analysis tool stands to benefit from more profound integration with building data sources, thereby facilitating automated input collection and supporting scenario forecasting.

In conclusion, this dissertation successfully delivered practical and scalable digital tools that contribute to solving real-world engineering challenges. Furthermore, it established the foundations for subsequent advancements and integration of sophisticated technologies in the realm of building lifecycle management, thereby providing a robust foundation for engineering practices that are characterised by intelligence, efficiency, and sustainability.

References

Bass Abushakra, Iain S. Walker, and Max H. Sherman. A study of pressure losses in residential air distribution systems. *Proceedings of the ACEEE Summer Study on Energy Efficiency in Buildings, Pacific Grove, CA*, 2002.

Mohammed A. Al-Ghamdi and Khalid S. Al-Gahtan. Integrated value engineering and life cycle cost modelling for hvac system selection. *Sustainability*, February 2022.

Seror Atalah Khaleefa Ali and Huda T. Hamad. Study of pressure losses in piping system. *International Journal of Science and Research*, 2018.

Muhammad Altaf, Rabeea Jaffari, Wesam Salah Alalaoul, Muhammad Ali Musarat, and Syed Ammad. Developing an automated strategy of life cycle cost analysis (lcca) with building information modelling (bim) integration for building projects. *Results in Engineering*, January 2025.

ASHRAE. *2019 ASHRAE Handbook - HVAC Applications*, chapter Chapter 18. ASHRAE, 2019a.

ASHRAE. *2019 ASHRAE Handbook - HVAC Applications*, chapter Chapter 9. ASHRAE, 2019b.

ASHRAE. *Ventilation of Health Care Facilities*. ASHRAE, 2021.

Simon Ashworth, Michelle Dillinger, and Karsten Körkemeye. Bim guidance to optimise the operational phase: defining information requirements based on iso 19650. *Emeral Insight*, October 2022.

Autodesk. Iso 19650, the common data environment, and autodesk construction cloud. https://www.autodesk.com/autodesk-university/article/ISO-19650-Common-Data-Environment-and-Autodesk-Construction-Cloud, 2024a. Accessed on: 11 February 2025.

Autodesk. Building information modelling. https://www.autodesk.com/solutions/aec/bim, 2024b. Accessed on: 13 February 2025.

Autodesk. Autodesk revit: software bim para projetar e criar qualquer coisa. https://www.autodesk.com/br/products/revit/overview, 2024c. Accessed on: 8 April 2025.

Herman Behls. *Duct Systems Design Guide*. ASHRAE, 2021.

Holger Manuel Benavides-Muñoz. Modification and improvement of the churchill equation for friction factor calculation in pipes. *MDPI*, 2024.

Meherwan P. Boyce. *Gas Turbine Engineering Handbook (Fourth Edition)*, chapter 10. American Society of Mechanical Engineers, 2012.

Jin Ouk Choi, Young Hoon Kwak, and Seokho Chi. Key tasks for facility standardization work process in capital projects. *KSCE Journal of Civil Engineering*, 2023.

Thuy Chu, Tan Nguyen, Hyunsang Yoo, and Jihoon Wang. A review of vibration analysis and its applications. *Heliyon*, 2024.

P Coandă, M Avram1, and V Constantin. A state of the art of predictive maintenance techniques. *IOP Conference Series: Materials Science and Engineering*, 2020.

Lucas Q. M. da Costa and Cristiano Cavalcante. A review on the study of maintenance effectiveness. *ResearchGate*, 2022.

Instituto Português da Qualidade. *NP EN 13306:2021*. Instituto Português da Qualidade, 2021.

Daikin. *Daikin*, 2024. Accessed: 17 June 2025.

Nelson Pedro Magalhães de Carvalho. Perdas de carga e escoamento laminar tridimensional em condutas com curvatura de 90. Master's thesis, Faculdade de Engenharia da Universidade do Porto, 2010.

Plant Engineering. *Maintenance Fundamentals (Second Edition)*, chapter Chapter 1, Chapter 2. Butterworth-Heinemann, 2004.

EVAC. *UTA-Gama ZL*, 2024. Accessed: 17 June 2025.

Philip M. Gerhart, Andrew L. Gerhart, and John I. Hochstein. *Fundamentals of Fluid Mechanics*, chapter Chapter 7 and Chapter 8. Wiley, 2018.

Gerhard Greeff. *Practical E-Manufacturing and Supply Chain Management*, chapter Production capability management. Gerhard Greeff, 2004.

Cristina Filipa Guerreiro Guimarães. O efeito de sobrepressões em condutas. modelação da sua redução através da utilização de válvulas de escape. Master's thesis, Faculdade de Engenharia da Universidade do Porto, 2010.

INFRASPEAK. Guia completo do cmms para 2025. https://blog.infraspeak.com/pt-pt/cmms/, 2024. Accessed on: 21 February 2025.

ISO. *ISO 15686-5*, chapter Buildings and constructed assets — Service life planning — Part 5:Life-cycle cost. ISO, 2017.

ISO. Iso 19650-1:2018. https://www.iso.org/obp/ui/en/#iso:std:68078:en, 2018. Accessed on: 3 March 2025.

Umara Khan, Ron Zevenhoven, Lydia Stougie, and Tor-Martin Tveit. Life cycle cost analysis (lcca) of stirling-cycle-based heat pumps vs. conventional boilers. *Cleaner environmental systems*, 2023.

Christopher James Krus. Analysis of life cycle cost methods for heating, ventilation, and air conditioning systems in hospitals. Master's thesis, University of Texas at Austin, 2004.

Sam Kubba. *Green Construction Project Management and Cost Oversight*, chapter Green Design and Construction Economics. Green Design, 2010.

Lasath Lecamwasam, John Wilson, and David Chokolich. *Guide to Best Practice Maintenance Operation of HVAC Systems for Energy Efficiency*. Department of Climate Change and Energy Efficiency, 2012.

Lingnan Lin, Marylia Duarte Batista, and Natascha S. Milesi-Ferretti. Measurement methods and techniques for pressure losses in pipe fittings. *2022 ASHRAE Annual Conference*, 2022.

Isabel Lopes, Patrícia Senra, Sandrina Vilarinho, Vera Sá, Catarina Teixeira, João Lopes, Anabela Alves, José A. Oliveira, and Manuel Figueiredo. Requirements specification of a computerised maintenance management system – a case study. *Procedia CIRP*, 2016.

Marcin Majka. Weighted average cost of capital. *Engineering*, 2024.

Mitsubishi. *Mitsubishi*, 2024. Accessed: 17 June 2025.

R. Keith Mobley, Lindley R. Higgins, and Darrin J. Wikoff. *Maintenance Engineering Handbook, Seventh Edition*. McGraw-Hill Handbooks, 2008.

Marek Moleda, Bozena Malysiak-Mrozek, Weiping Ding, Vaidy Sunderam, and Dariusz Mrozek. From corrective to predictive maintenance—a review of maintenance approaches for the power industry. *Science and Technology*, 2023.

Bahram Moradabadi, Esmatullah Noorzai, and Saman Abbasi. Bim-based optimization approach to reduce life cycle costs by focusing on the integration of construction and operation phases in office-commercial buildings. *Journal of Building Engineering*, 2024.

Miroslava MÍkvaa, Vanessa Prajováa, Boris Yakimovichb, Alexander Korshunovb, and Ivan Tyurinc. Standardization - one of the tools of continuous improvement. *International Conference on Manufacturing Engineering and Materials*, 2016.

NBS. Building information modelling: What information is in the model? https://www.thenbs.com/knowledge/building-information-modelling-what-information-is-in-the-model, 2024a. Accessed on: 19 February 2025.

NBS. What is the asset information model (aim). https://www.thenbs.com/knowledge/what-is-the-asset-information-model-aim, 2024b. Accessed on: 18 February 2025.

Wiesław Ostachowicz, Malcolm McGugan, Jens-Uwe Schröder-Hinrichs, and Marcin Luczak. *New Materials and Reliability in Offshore Wind Turbine Technology*, chapter 15 - Reliability and Preventive Maintenance. Springer Open, 2016.

Portugal. Decree-law nº 292/2000. https://diariodarepublica.pt/dr/detalhe/decreto-lei/292-2000-615046, December 2000. Accessed on: 26 February 2025.

Portugal. Regulation nº 353-a/2013. https://diariodarepublica.pt/dr/detalhe/portaria/353-a-2013-331868, December 2013. Accessed on: 26 February 2025.

Portugal. Decree-law n.º 101-d/2020. https://diariodarepublica.pt/dr/detalhe/decreto-lei/101-d-2020-150570704, December 2020. Accessed on: 26 February 2025.

Portugal. Regulation nº 138-i/2021. https://diariodarepublica.pt/dr/detalhe/portaria/138-i-2021-166296492, July 2021. Accessed on: 27 February 2025.

Portugal. Decreto-lei n.º 10/2024, de 8 de janeiro. https://diariodarepublica.pt/dr/detalhe/decreto-lei/10-2024-836222484, Regulation nº 10/2024/1 2024a. Accessed on: 17 Abril 2025.

Portugal. Regulation nº.88/2024/1. https://diariodarepublica.pt/dr/detalhe/portaria/88-2024-854635718, December 2024a. Accessed on: 28 February 2025.

Portugal. Regulation nº 90/2024/1. https://diariodarepublica.pt/dr/detalhe/portaria/90-2024-854635720, Regulation nº 90/2024/1 2024b. Accessed on: 27 February 2025.

Portugal. Regulation nº.92/2024/1. https://diariodarepublica.pt/dr/detalhe/portaria/92-2024-854635722, December 2024b. Accessed on: 28 February 2025.

S. Rahman and D.J. Vanier. Life cycle cost analysis as a decision support tool for managing municipal infrastructure. *NRC Publications Archive (NPArC)*, 2004.

REN. Ren data hub: Market. https://datahub.ren.pt/en/natural-gas/market/, 2024. Accessed on: 13 June 2025.

Revit vs. AutoCAD, 2025. Accessed on: 24 February 2025.

Alex Rivera, William Quitiaquez, Isaac Simbaña, and René Patricio Quitiaquez Sarzosa. Study of steam generation and distribution in a hospital to improve energy efficiency using thermography, ultrasound, and gas analyzer. *Revista Técnica Energía*, 2024.

Antonio Salzano, Claudia Mariaserena Parisi, Giovanna Acampa, and Maurizio Nicolella. Existing assets maintenance management: Optimising maintenance procedures and costs through bim tools. *Automation in Construction*, February 2023.

Khyati Shukla, Samia Nefti-meziani, and Steve Thomas Davis. A heuristic approach on predictive maintenance techniques: Limitations and scope. *Advances in Mechanical Engineering*, 2022.

Sodeca. *Sodeca*, 2024. Accessed: 17 June 2025.

Systemair. *Systemair*, 2024. Accessed: 17 June 2025.

Ahmet Teke and Oğuzhan Timur. Assessing the energy efficiency improvement potentials of hvac systems considering economic and environmental aspects at the hospitals. *Renewable and Sustainable Energy Reviews*, 2014.

Vaillant. *Vaillant*, 2024. Accessed: 17 June 2025.

Pablo Venegas, Eugenio Ivorra, Mario Ortega, and Idurre Sáez de Ocáriz. Towards the automation of infrared thermography inspections for industrial maintenance applications. *MDPI*, 2022.

Wilo. *Wilo*, 2024. Accessed: 17 June 2025.

Yannic Wolfa, Lennard Sielaff, and Dominik Luckeb. A standardized description model for predictive maintenance use cases. *16th CIRP Conference on Intelligent Computation in Manufacturing Engineering*, 2022.

Zhanying Zheng and Jingyu Cao. Thermodynamic and feasibility analysis of air conditioning waste heat recovery via power generation cycles. *Energy Reports*, 2020.

Francisco Javier Álvarez García and David Rodríguez Salgado. An approach for predictive maintenance decisions for components of an industrial multistage machine that fail before their mttf: A case study. *Data Driven Decision-Making for Complex Production Systems*, 2022.

Appendix A

Fitting Loss Coefficients

Online Supplemental Material Accompanying
Principles of Heating, Ventilating, and Air Conditioning, Ninth Edition

FITTING LOSS COEFFICIENTS

This material provides coefficients for various fittings and loss-inducing components of a duct system. Covering both rectangular and circular ducting, this material references many sources and provides the most commonly used items in each category. The categories of fittings in this material are linked here for ease of navigation:

- **Entries**
- **Exits**
- **Elbows**
- **Transitions**
- **Junctions (Tees, Wyes, Crosses)**
- **Obstructions**
- **Fan-System Connections**

Note that for actual projects, use of the *ASHRAE Duct Fitting Database* (DFDB) is recommended. The DFDB includes more than 220 round, rectangular, and flat oval fittings. It is available in electronic form and has the capability to be linked to duct design programs.

1 ENTRIES

1-1 Duct Mounted in Wall (Hood, Nonenclosing, Flanged, and Unflanged) (Idelchik et al. 1986, Diagram 3-1)

General. If entry has a screen, use Fitting 6-7 to calculate screen resistance.

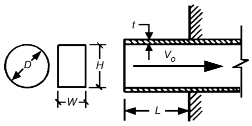

Rectangular: $D = 2HW/(H + W)$

	C_o						
	L/D						
t/D	**0**	**0.002**	**0.01**	**0.05**	**0.2**	**0.5**	**≥1.0**
≈0	0.50	0.57	0.68	0.80	0.92	1.0	1.0
0.02	0.50	0.51	0.52	0.55	0.66	0.72	0.72
≥0.05	0.50	0.50	0.50	0.50	0.50	0.50	0.50

1-2 Smooth Converging Bellmouth Without End Wall (Idelchik et al. 1986, Diagram 34)

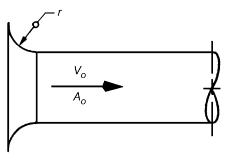

r/D	0	0.01	0.02	0.03	0.04	0.05
C_o	1.0	0.87	0.74	0.61	0.51	0.40
r/D	0.06	0.08	0.10	0.12	0.16	≥0.20
C_o	0.32	0.20	0.15	0.10	0.06	0.03

© 2021 ASHRAE (www.ashrae.org). For personal use only. Additional reproduction, distribution, or transmission in either print or digital form is not permitted without ASHRAE's prior written permission.

1-3 Smooth Converging Bellmouth with End Wall (Idelchik et al. 1986, Diagram 3-4)

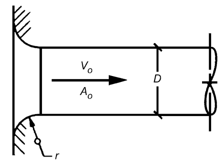

r/D	0	0.01	0.02	0.03	0.04	0.05
C_o	0.50	0.44	0.37	0.31	0.26	0.22
r/D	0.06	0.08	0.10	0.12	0.16	≥0.20
C_o	0.20	0.15	0.12	0.09	0.06	0.03

1-4 Conical Converging Bellmouth Without End Wall, Round and Rectangular

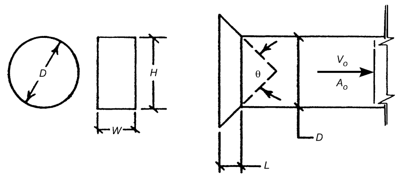

Rectangular: $D = 2HW/(H + W)$

	C_o									
	θ, degrees									
L/D	**0**	**10**	**20**	**30**	**45**	**60**	**90**	**120**	**150**	**180**
0.025	1.0	0.96	0.93	0.90	0.85	0.80	0.72	0.64	0.57	0.50
0.05	1.0	0.93	0.86	0.80	0.73	0.67	0.60	0.56	0.52	0.50
0.10	1.0	0.80	0.67	0.55	0.46	0.41	0.41	0.43	0.46	0.50
0.25	1.0	0.68	0.45	0.30	0.21	0.17	0.21	0.28	0.38	0.50
0.60	1.0	0.46	0.27	0.18	0.14	0.13	0.19	0.27	0.37	0.50
1.0	1.0	0.32	0.20	0.14	0.11	0.10	0.16	0.24	0.35	0.50

© 2021 ASHRAE (www.ashrae.org). For personal use only. Additional reproduction, distribution, or transmission in either print or digital form is not permitted without ASHRAE's prior written permission.

1-5 Conical Converging Bellmouth with End Wall, Round and Rectangular (Idelchik et al. 1986, Diagram 3-7)

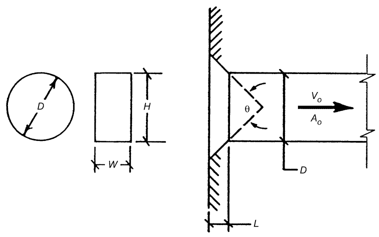

Rectangular: $D = 2HW/(H + W)$

	C_o									
	θ, degrees									
L/D	**0**	**10**	**20**	**30**	**45**	**60**	**90**	**120**	**150**	**180**
0.025	0.50	0.47	0.45	0.43	0.41	0.40	0.42	0.44	0.46	0.50
0.05	0.50	0.45	0.41	0.36	0.32	0.30	0.34	0.39	0.44	0.50
0.075	0.50	0.42	0.35	0.30	0.25	0.23	0.28	0.35	0.43	0.50
0.10	0.50	0.39	0.32	0.25	0.21	0.18	0.25	0.33	0.41	0.50
0.15	0.50	0.37	0.27	0.20	0.16	0.15	0.23	0.31	0.40	0.50
0.60	0.50	0.27	0.18	0.13	0.11	0.12	0.20	0.30	0.40	0.50

1-6 Intake Hood (Idelchik et al. 1986, Diagram 3-18)

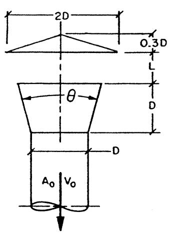

	C_o								
θ,	L/D								
degrees	**0.1**	**0.2**	**0.3**	**0.4**	**0.5**	**0.6**	**0.8**	**1.0**	**4.0**
0	2.63	1.83	1.53	1.39	1.31	1.19	1.08	1.06	1.0
15	1.32	0.77	0.60	0.48	0.41	0.30	0.28	0.25	0.25

© 2021 ASHRAE (www.ashrae.org). For personal use only. Additional reproduction, distribution, or transmission in either print or digital form is not permitted without ASHRAE's prior written permission.

1-7 Hood, Tapered, Flanged or Unflanged (Brandt and Steffy 1946)

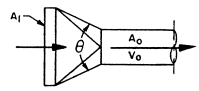

$A_1 \geq 2A_o$

θ is major angle for rectangular hoods

Hood Shape: Round										
θ, degrees	0	20	40	60	80	100	120	140	160	180
C_o	1.0	0.11	0.06	0.09	0.14	0.18	0.27	0.32	0.43	0.50
Hood Shape: Square or Rectangular										
θ, degrees	0	20	40	60	80	100	120	140	160	180
C_o	1.0	0.19	0.13	0.16	0.21	0.27	0.33	0.43	0.53	0.62

1-8 Orifice, Sharp-Edged, Inlet Duct (Idelchik et al. 1986; Diagrams 3-12, 3-14, and 4-19)

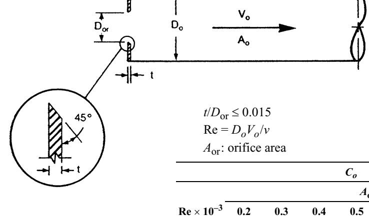

$t/D_{or} \leq 0.015$
$Re = D_oV_o/v$
A_{or}: orifice area

	C_o							
	A_{or}/A_o							
Re × 10^{-3}	**0.2**	**0.3**	**0.4**	**0.5**	**0.6**	**0.7**	**0.8**	**0.9**
4	45	18	7.9	3.9	2.3	1.3	0.83	0.51
10	49	20	9.2	4.4	2.7	1.5	0.96	0.59
20	50	21	9.3	4.9	2.9	1.6	1.1	0.65
100	55	23	11.0	5.6	3.3	1.9	1.2	0.75

2 EXITS

General. If exit has a screen, use Fitting 6-7 to calculate screen resistance.

2-1 Exit, Abrupt, Round and Rectangular (Idelchik et al. 1986, Diagram 11-1)

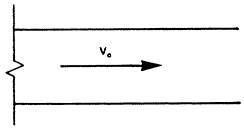

Uniform Velocity Distribution

$C_o = 1.0$

Exponential, Sinusoidal, Asymmetrical, and Parabolic Velocity Distribution

C_o varies from 1.0 to 3.67. For details, consult Idelchik et al. (1986), Diagram 11-1.

© 2021 ASHRAE (www.ashrae.org). For personal use only. Additional reproduction, distribution, or transmission in either print or digital form is not permitted without ASHRAE's prior written permission.

2-2 Exit, Abrupt, Round and Rectangular, with End (Idelchik et al. 1986, Diagrams 5-2 and 5-4)

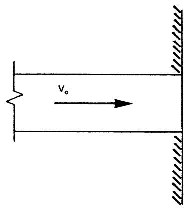

$C_o = 0.88$

2-3 Exit, Duct Flush with Wall, Flow along Wall (Idelchik et al. 1986, Diagram 11-2)

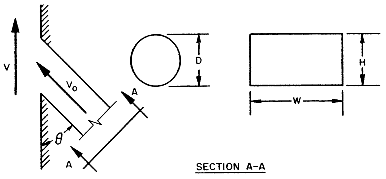

Round

	C_o				
	V/V_o				
θ, degrees	0	0.5	1.0	1.5	2.0
≤45	1.0	1.0	1.1	1.3	1.6
60	1.0	0.90	1.1	1.4	1.6
90	1.0	0.80	0.95	1.4	1.7
120	1.0	0.80	0.95	1.3	1.7
150	1.0	0.82	0.83	1.0	1.3

Rectangular

		C_o				
		V/V_o				
Aspect Ratio (H/W)	θ, degrees	0	0.5	1.0	1.5	2.0
≤0.2	≤90	1.0	0.95	1.2	1.5	1.8
	120	1.0	1.1	1.1	1.4	1.9
	150	1.0	0.95	0.95	1.4	1.8
0.5–2.0	≤45	1.0	1.0	1.1	1.3	1.6
	60	1.0	0.90	1.1	1.4	1.6
	90	1.0	0.80	0.95	1.4	1.7
	120	1.0	0.80	0.95	1.3	1.7
	150	1.0	0.82	0.83	1.0	1.3
≥5	45	1.0	0.92	0.93	1.1	1.3
	60	1.0	0.87	0.87	1.0	1.3
	90	1.0	0.82	0.80	0.97	1.2
	120	1.0	0.80	0.76	0.90	0.98

© 2021 ASHRAE (www.ashrae.org). For personal use only. Additional reproduction, distribution, or transmission in either print or digital form is not permitted without ASHRAE's prior written permission.

2-4 Exit, Round, Diverging (Idelchik et al. 1986, Diagram 11-3)

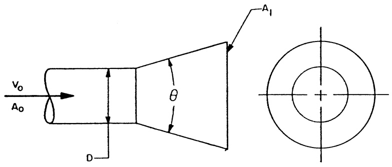

	C_o						
	θ, degrees						
A_1/A_o	8	10	14	20	30	45	≥60
2	0.36	0.33	0.37	0.51	0.90	1.0	1.0
4	0.24	0.21	0.28	0.40	0.70	0.99	1.0
6	0.20	0.19	0.26	0.37	0.67	0.99	1.0
10	0.18	0.16	0.24	0.36	0.68	0.99	1.0
16	0.16	0.16	0.20	0.36	0.66	0.99	1.0

2-5 Exit, Round, with End Wall Transition (Idelchik et al. 1986, Diagram 5-8)

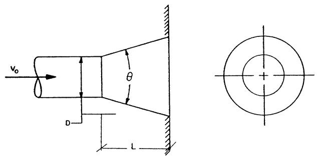

θ = optimum angle

L/D	0.5	1.0	2.0	3.0	4.0	5.0	6.0	8.0	10	12	14
θ, degrees	34	24	16	13	11	10	9	8	7	6	6
C_o	0.41	0.32	0.24	0.20	0.17	0.15	0.14	0.12	0.11	0.11	0.10

© 2021 ASHRAE (www.ashrae.org). For personal use only. Additional reproduction, distribution, or transmission in either print or digital form is not permitted without ASHRAE's prior written permission.

2-6 Exit, Rectangular, Two Sides Parallel, Diverging, Symmetrical (Idelchik et al. 1986, Diagram 11-6)

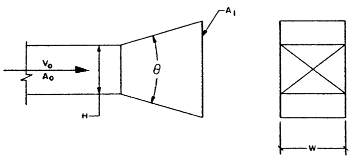

$0.5 \le H/W \le 2.0$

	C_o						
	θ, degrees						
A_1/A_o	8	10	14	20	30	45	≥60
2	0.50	0.51	0.56	0.63	0.80	0.96	1.0
4	0.34	0.38	0.48	0.63	0.76	0.91	1.0
6	0.32	0.34	0.41	0.56	0.70	0.84	0.96

2-7 Exit, Rectangular, with Wall, Two Sides Parallel, Symmetrical, Diverging (Idelchik et al. 1986, Diagram 5-10)

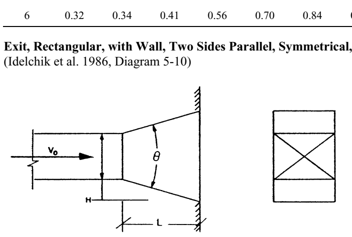

θ = optimum angle

L/H	0.5	1.0	2.0	3.0	4.0	5.0	6.0	8.0	10	12	14
θ, degrees	50	35	25	21	18	16	15	13	12	11	10
C_o	0.53	0.44	0.35	0.31	0.28	0.25	0.24	0.22	0.20	0.19	0.19

© 2021 ASHRAE (www.ashrae.org). For personal use only. Additional reproduction, distribution, or transmission in either print or digital form is not permitted without ASHRAE's prior written permission.

2-8 Exit, Rectangular, Pyramidal, Diverging (Idelchik et al. 1986, Diagram 11-5)

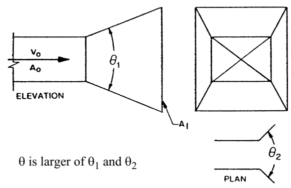

θ is larger of θ_1 and θ_2

	C_o						
	θ, degrees						
A_1/A_o	8	10	14	20	30	45	≥60
2	0.65	0.68	0.74	0.82	0.92	1.1	1.1
4	0.53	0.60	0.69	0.78	0.90	1.0	1.1
6	0.50	0.57	0.66	0.77	0.91	1.0	1.1
10	0 45	0.53	0.64	0.74	0.85	0.97	1.1

2-9 Exit, Rectangular, with Wall, Pyramidal, Diverging (Idelchik et al. 1986, Diagram 5-9)

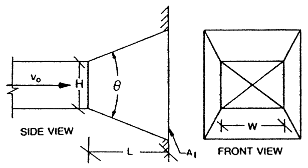

$D = 2HW/(H + W)$

θ = optimum angle

L/D	0.5	1.0	2.0	3.0	4.0	5.0	6.0	8.0	10	12	14
θ, degrees	26	19	13	11	9	8	7	6	6	5	5
C_o	0.49	0.40	0.30	0.26	0.23	0.21	0.19	0.17	0.16	0.15	0.14

© 2021 ASHRAE (www.ashrae.org). For personal use only. Additional reproduction, distribution, or transmission in either print or digital form is not permitted without ASHRAE's prior written permission.

2-10 Exit, Discharge to Atmosphere from a 90° Elbow, Rectangular and Round (Note: Elbow Loss Included) (Idelchik et al. 1986, Diagram 11-14)

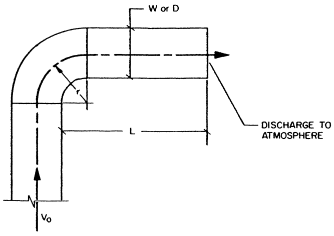

Rectangular

	C_o									
	L/W									
r/W	**0**	**0.5**	**1.0**	**1.5**	**2.0**	**3.0**	**4.0**	**6.0**	**8.0**	**12.0**
0	3.0	3.1	3.2	3.0	2.7	2.4	2.2	2.1	2.1	2.0
0.75	2.2	2.2	2.1	1.8	1.7	1.6	1.6	1.5	1.5	1.5
1.0	1.8	1.5	1.4	1.4	1.3	1.3	1.2	1.2	1.2	1.2
1.5	1.5	1.2	1.1	1.1	1.1	1.1	1.1	1.1	1.1	1.1
2.5	1.2	1.1	1.1	1.0	1.0	1.0	1.0	1.0	1.0	1.0

Round (r/D = 1.0)

L/D	0.9	1.3
C_o	1.5	1.4

2-11 Exhaust Hood (Idelchik et al. 1986, Diagram 11-16)

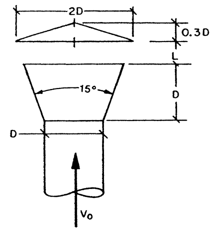

L/D	**0.1**	**0.2**	**0.25**	**0.3**	**0.35**	**0.4**	**0.5**
C_o	2.6	1.2	1.0	0.80	0.70	0.65	0.60

Poor Design—Should Not Be Used

© 2021 ASHRAE (www.ashrae.org). For personal use only. Additional reproduction, distribution, or transmission in either print or digital form is not permitted without ASHRAE's prior written permission.

2-12 Stackhead (Idelchik et al. 1986, Diagram 11-23)

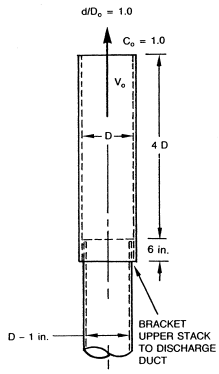

d/D	**0.3**	**0.4**	**0.5**	**0.6**	**0.7**	**0.8**	**0.9**	**1.0**
C_o	130	41	17	8.1	4.4	2.6	1.6	1.0

3 ELBOWS

3-1 Elbow, Smooth Radius (Die Stamped), Round (Locklin 1950, Equation A-10)

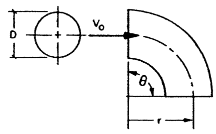

$$C_o = K_q C'_o$$

Coefficients for 90° Elbows

r/D	0.5	0.75	1.0	1.5	2.0	2.5
C'_o	0.71	0.33	0.22	0.15	0.13	0.12

Angle Correction Factors K_q (Idelchik et al. 1986, Diagram 6-1):

θ, degrees	0	20	30	45	60	75	90	110	130	150	180
K_θ	0	0.31	0.45	0.60	0.78	0.90	1.00	1.13	1.20	1.28	1.40

© 2021 ASHRAE (www.ashrae.org). For personal use only. Additional reproduction, distribution, or transmission in either print or digital form is not permitted without ASHRAE's prior written permission.

3-2 Elbows; 5-, 4-, and 3-Pieces, Round (Locklin 1950, Figure 10)

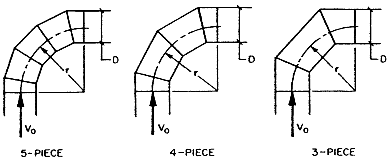

Coefficients for 90° Elbows (C'_o)

No. of Pieces	r/D 0.75	1.0	1.5	2.0
5	0.46	0.33	0.24	0.19
4	0.50	0.37	0.27	0.24
3	0.54	0.42	0.34	0.33

Angle Correction Factors K_q (Idelchik et al. 1986, Diagram 6-1)

θ, degrees	0	20	30	45	60	75	90	110	130	150	180
K_θ	0	0.31	0.45	0.60	0.78	0.90	1.00	1.13	1.20	1.28	1.40

3-3 Elbow, Mitered, Round (Idelchik et al. 1986, Diagram 6-5)

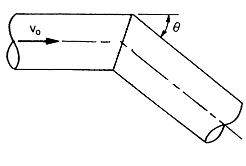

$$C_o = K_{Re} C'_o$$

θ, degrees	20	30	45	60	75	90
C'_o	0.08	0.16	0.34	0.55	0.81	1.2

Reynolds Number Correction Factors: *M/hc*

Re × 10^{-4}	**1**	**2**	**3**	**4**	**6**	**8**	**10**	**≥14**
K_{Re}	1.40	1.26	1.19	1.14	1.09	1.06	1.04	1.0

3-4 Elbows, 30,° Z-Shaped, Round

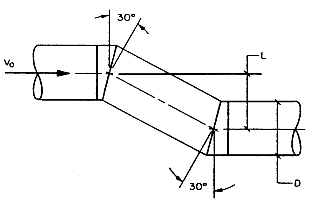

$$C_o = K_{Re} C'_o$$

L/D	0	0.5	1.0	1.5	2.0	2.5	3.0
C'_o	0	0.15	0.15	0.16	0.16	0.16	0.16

Reynolds Number Correction Factors

Re × 10^{-4}	**1**	**2**	**3**	**4**	**6**	**8**	**10**	**≥14**
K_{Re}	1.40	1.26	1.19	1.14	1.09	1.06	1.04	1.0

© 2021 ASHRAE (www.ashrae.org). For personal use only. Additional reproduction, distribution, or transmission in either print or digital form is not permitted without ASHRAE's prior written permission.

3-5 Elbow, Without Vanes, Rectangular (Idelchik et al. 1986, Diagram 6-1)

Smooth Radius

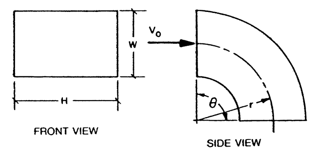

$$C_o = K_\theta K_{Re} C'_o$$

90°, Sharp Throat Radius Heel (r/W = 0.5)

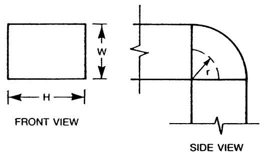

$$C_o = K_{Re} C'_o$$

Coefficients for 90° Elbows (C'_o)

	H/W										
r/W	**0.25**	**0.5**	**0.75**	**1.0**	**1.5**	**2.0**	**3.0**	**4.0**	**5.0**	**6.0**	**8.0**
0.5	1.3	1.3	1.2	1.2	1.1	1.0	1.0	1.1	1.1	1.2	1.2
0.75	0.57	0.52	0.48	0.44	0.40	0.39	0.39	0.40	0.42	0.43	0.44
1.0	0.27	0.25	0.23	0.21	0.19	0.18	0.18	0.19	0.20	0.21	0.21
1.5	0.22	0.20	0.19	0.17	0.15	0.14	0.14	0.15	0.16	0.17	0.17
2.0	0.20	0.18	0.16	0.15	0.14	0.13	0.13	0.14	0.14	0.15	0.15

Angle Correction Factor

θ, degrees	0	20	30	45	60	75	90	110	130	150	180
K_θ	0	0.31	0.45	0.60	0.78	0.90	1.00	1.13	1.20	1.28	1.40

Reynolds Number Correction Factor (K_{Re})

	Re × 10^{-4}								
r/W	**1**	**2**	**3**	**4**	**6**	**8**	**10**	**14**	**≥20**
0.5	1.40	1.26	1.19	1.14	1.09	1.06	1.04	1.0	1.0
≥0.75	2.0	1.77	1.64	1.56	1.46	1.38	1.30	1.15	1.0

© 2021 ASHRAE (www.ashrae.org). For personal use only. Additional reproduction, distribution, or transmission in either print or digital form is not permitted without ASHRAE's prior written permission.

3-6 Elbow, Mitered, Rectangular (Idelchik et al. 1986, Diagram 6-5)

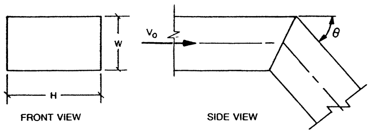

$C_o = K_{Re} C'_o$

	C'_o										
	H/W										
θ, degrees	**0.25**	**0.5**	**0.75**	**1.0**	**1.5**	**2.0**	**3.0**	**4.0**	**5.0**	**6.0**	**8.0**
20	0.08	0.08	0.08	0.07	0.07	0.07	0.06	0.06	0.05	0.05	0.05
30	0.18	0.17	0.17	0.16	0.15	0.15	0.13	0.13	0.12	0.12	0.11
45	0.38	0.37	0.36	0.34	0.33	0.31	0.28	0.27	0.26	0.25	0.24
60	0.60	0.59	0.57	0.55	0.52	0.49	0.46	0.43	0.41	0.39	0.38
75	0.89	0.87	0.84	0.81	0.77	0.73	0.67	0.63	0.61	0.58	0.57
90	1.3	1.3	1.2	1.2	1.1	1.1	0.98	0.92	0.89	0.85	0.83

Reynolds Number Corrections Factors

Re × 10^{-4}	**1**	**2**	**3**	**4**	**6**	**8**	**10**	**≥14**
K_{Re}	1.40	1.26	1.19	1.14	1.09	1.06	1.04	1.0

3-7 Elbow, Smooth Radius with Splitter Vanes, Rectangular
(Locklin 1950, Equation 10; Madison and Parker 1936)

a. One Splitter Vane

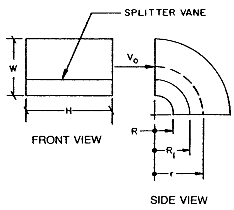

$C_o = K_\theta C'_o$
$R_1 = R/CR$
where
R = throat radius
R_1 = splitter vane radius
CR = curve ratio (values from Table 3-7.a)
K_θ = angle factor (see Fitting 3-1 for values)

Table 3-7.a Coefficients for Elbows with One Splitter Vane

			C'_o										
			H/W										
R/W	***r/W***	**CR**	**0.25**	**0.5**	**1.0**	**1.5**	**2.0**	**3.0**	**4.0**	**5.0**	**6.0**	**7.0**	**8.0**
0.05	0.55	0.218	0.52	0.40	0.43	0.49	0.55	0.66	0.75	0.84	0.93	1.0	1.1
0.10	0.60	0.302	0.36	0.27	0.25	0.24	0.30	0.35	0.39	0.42	0.46	0.49	0.52
0.15	0.65	0.361	0.28	0.21	0.18	0.19	0.20	0.22	0.25	0.26	028	0.30	0.32
0.20	0.70	0.408	0.22	0.16	0.14	0.14	0.15	0.16	0.17	0.18	0.19	0.20	0.21
0.25	0.75	0.447	0.18	013	0.11	0.11	0.11	0.12	0.13	0.14	0.14	0.15	0.15
0.30	0.80	0.480	0.15	0.11	0.09	0.09	0.09	0.09	0.10	0.10	0.11	0.11	0.12
0.35	0.85	0.509	0.13	0.09	0.08	0.07	0.07	0.08	0.08	0.08	0.08	0.09	0.09
0.40	0.90	0.535	0.11	0.08	0.07	0.06	0.06	0.06	0.06	0.07	0.07	0.07	0.07
0.45	0.95	0.557	0.10	0.07	0.06	0.05	0.05	0.05	0.05	0.05	0.06	0.06	0.06
0.50	1.00	0.577	0.09	0.06	0.05	0.05	0.04	0.04	0.04	0.05	0.05	0.05	0.05

b. Two Splitter Vanes

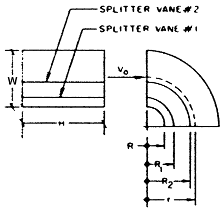

$C_o = K_\theta C'_o$
$R_1 = R/CR$
$R_2 = R_1/CR = R/CR^2$
where
R = throat radius
R_1 = splitter vane # l radius
R_2 = splitter vane # 2 radius
CR = curve ratio (value from Table 3-7.b)
K_θ = angle factor (see Note 3 for values)

Table 3-7.b Coefficients for Elbow with Two Splitter Vanes

			C'_o										
			H/W										
R/W	***r/W***	**CR**	**0.25**	**0.5**	**1.0**	**1.5**	**2.0**	**3.0**	**4.0**	**5.0**	**6.0**	**7.0**	**8.0**
0.05	0.55	0.362	0.26	0.20	0.22	0.25	0.28	0.33	0.37	0.41	0.45	0.48	0.51
0.10	0.60	0.450	0.17	0.13	0.11	0.12	0.13	0.15	0.16	0.17	0.19	0.20	0.21
0.15	0.65	0.507	0.12	0.09	0.08	0.08	0.08	0.09	0.10	0.10	0.11	0.11	0.11
0.20	0.70	0.550	0.09	0.07	0.06	0.05	0.06	0.06	0.06	0.06	0.07	0.07	0.07
0.25	0.75	0.585	0.08	0.05	0.04	0.04	0.04	0.04	0.05	0.05	0.05	0.05	0.05
0.30	0.80	0.613	0.06	004	0.03	0.03	0.03	0.03	0.03	0.03	0.04	0.04	0.04

c. Three Splitter Vanes

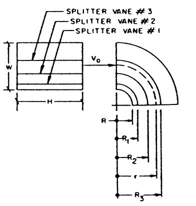

$C_o = K_\theta C'_o$
$R_1 = R/CR$
$R_2 = R_1/\mathrm{CR} = R/\mathrm{CR}^2$
$R_3 = R_2/\mathrm{CR} = R/\mathrm{CR}^3$
where
R = throat radius
R_1 = splitter vane # l radius
R_2 = splitter vane # 2 radius
R_3 = splitter vane # 3 radius
CR = curve ratio (value from Table 3-7.c)
K_θ = angle factor (see Note 3 for values)

Table 3-7.c Coefficients for Elbow with Three Splitter Vanes (C'_o)

			H/W										
R/W	***r/W***	***CR***	**0.25**	**0.5**	**1.0**	**1.5**	**2.0**	**3.0**	**4.0**	**5.0**	**6.0**	**7.0**	**8.0**
0.05	0.55	0.467	0.11	0.10	0.12	0.13	0.14	0.16	0.18	0.19	0.21	0.22	0.23
0.10	0.60	0.549	0.07	0.05	0.06	0.06	0.06	0.07	0.07	0.08	0.08	0.08	0.09

3-8 Elbow, Mitered, with Single-Thickness Vanes, Rectangular (Rozell 1974)

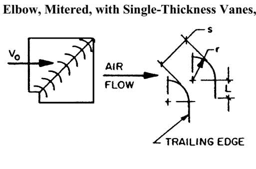

Design No.	**Dimensions, in.** *r*	*s*	*L*	C_o
1[a]	2.0	1.5	0.75	0.12
2	4.5	2.25	0	0.15
3	4.5	3.25	1.60	0.18

[a] When extension of trailing edge is not provided for this vane, losses are approximately unchanged for single elbows, but increase considerably for elbows in series.

3-9 Elbow, Mitered, with Double-Thickness Vanes, Rectangular (Rozell 1974)

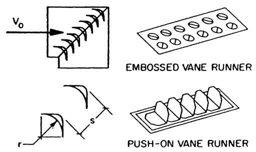

			C_o				
	Dimensions, in.		**Velocity V_o, fpm**				
Design No.	**r**	**s**	**1000**	**2000**	**3000**	**4000**	**Vane Runner**
1	2.0	1.5	0.27	0.22	0.19	0.17	Embossed
2	2.0	1.5	0.33	0.29	0.26	0.23	Push-On
3	2.0	2.13	0.38	0.31	0.27	0.24	Embossed
4	4.5	3.25	0.26	0.21	0.18	0.16	Embossed

3-10 Elbow, Variable Inlet/Outlet Areas, Rectangular (Idelchik et al. 1986, Diagram 6-4)

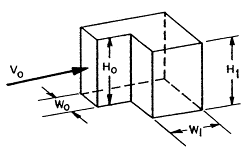

	C'_o					
	W_1/W_o					
H_o/W_o	**0.6**	**0.8**	**1.2**	**1.4**	**1.6**	**2.0**
0.25	1.8	1.4	1.1	1.1	1.1	1.1
1.0	1.7	1.4	1.0	095	0.90	0.84
4.0	1.5	1.4	0.81	0.76	0.72	0.66
∞	1.5	1.0	0.69	0.63	0.60	0.55

Reynolds Number Correction Factor

Re × 10^{-4}	1	2	3	4	6	8	10	≥14
K_{Re}	1.40	1.26	1.19	1.14	1.09	1.06	1.04	1.0

3-11 Elbows, 90°, Z-Shaped, Rectangular (Idelchik et al. 1986, Diagram 6-11)

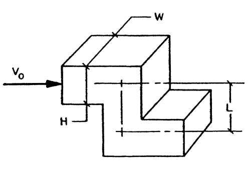

$C = K\,K_{Re} C'_o$

Coefficients for *W/H* = 1.0

L/H	0	0.4	0.6	0.8	1.0	1.2	1.4	1.6	1.8	2.0
C'_o	0	0.62	0.90	1.6	2.6	3.6	4.0	4.2	4.2	4.2
L/H	2.4	2.8	3.2	4.0	5.0	6.0	7.0	9.0	10.0	¥
C'_o	3.7	3.3	3.2	3.1	2.9	2.9	2.8	2.7	2.5	2.3

Reynolds Number Correction Factor

Re × 10^{-4}	1	2	3	4	6	8	10	≥14
K_{Re}	1.40	1.26	1.19	1.14	1.09	1.06	1.04	1.0

Apply the Following Factor for Other Than *H/W* = 1.0

W/H	0.25	0.50	0.75	1.0	1.5	2.0	3.0	4.0	6.0	8.0
K	1.10	1.07	1.04	1.0	0.95	0.90	9.83	0.78	0.72	0.70

3-12 Combined 90° Elbows Lying in Different Planes, Rectangular (Idelchik et al. 1986, Diagram 6-11)

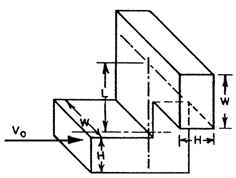

$C_o = K\,K_{Re} C'_o$

Coefficients for Square Ducts

L/W	0	0.4	0.6	0.8	1.0	1.2	1.4	1.6	1.8	2.0
C'_o	1.2	2.4	2.9	3.3	3.4	3.4	3.4	3.3	3.2	3.1
L/W	2.4	2.8	3.2	4.0	5.0	6.0	7.0	9.0	10.0	¥
C'_o	3.2	3.2	3.2	3.0	2.9	2.8	2.7	2.5	2.4	2.3

Reynolds Number Correction Factor

Re × 10^{-4}	1	2	3	4	6	8	10	≥14
K_{Re}	1.40	1.26	1.19	1.14	1.09	1.06	1.04	1.0

Apply the Following Factor for Other Than *H/W* = 1.0

H/W	0.25	0.50	0.75	1.0	1.5	2.0	3.0	4.0	6.0	8.0
K	1.10	1.07	1.04	1.0	0.95	0.90	0.83	0.78	0.72	0.70

3-13 Offset, S-Shaped (Gooseneck), Rectangular and Round (Idelchik et al. 1986, Diagram 6-16)

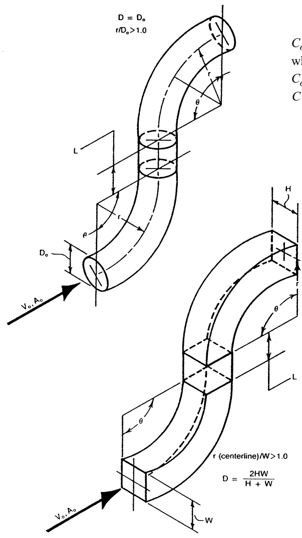

$C_o = KC'_o$

where

C_o = offset loss coefficient

C'_o = single elbow loss coefficient (see Fittings 3-1, 3-2, and 3-5)

	K														
θ,	***L*/*D***														
degrees	**0**	**1**	**2**	**3**	**4**	**6**	**8**	**10**	**12**	**14**	**16**	**18**	**20**	**25**	**≥40**
15	0.20	0.42	0.60	0.78	0.94	1.16	1.20	1.15	1.08	1.05	1.02	1.00	1.10	1.25	2.0
30	0.40	0.65	0.88	1.16	1.20	1.18	1.12	1.06	1.06	1.15	1.28	1.40	1.50	1.70	2.0
45	0.60	1.06	1.20	1.23	1.20	1.08	1.03	1.08	1.17	1.30	1.42	1.55	1.65	1.80	2.0
60	1.05	1.38	1.37	1.28	1.15	1.06	1.16	1.30	1.42	1.54	1.66	1.76	1.85	1.95	2.0
75	1.50	1.58	1.46	1.30	1.27	1.30	1.37	1.47	1.57	1.68	1.75	1.80	1.88	1.97	2.0
90	1.70	1.67	1.40	1.37	1.38	1.47	1.55	1.63	1.70	1.76	1.82	1.88	1.92	1.98	2.0

© 2021 ASHRAE (www.ashrae.org). For personal use only. Additional reproduction, distribution, or transmission in either print or digital form is not permitted without ASHRAE's prior written permission.

3-14 Offset, S-Shaped in Two Planes 90° Apart, Rectangular and Round (Idelchik et al. 1986, Diagram 6-16)

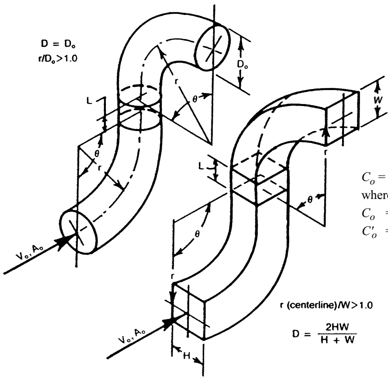

$C_o = KC'_o$

where

C_o = offset loss coefficient

C'_o = single elbow loss coefficient (see Fittings 3-1, 3-2, and 3-5)

	K												
θ,	***L*/*D***												
degrees	**0**	**1**	**2**	**3**	**4**	**6**	**8**	**10**	**12**	**14**	**20**	**25**	**40**
60	2.0	1.90	1.50	1.35	1.30	1.20	1.25	1.50	1.63	1.73	1.85	1.95	2.0
90	2.0	1.80	1.60	1.55	1.55	1.65	1.80	1.90	1.93	1.98	2.0	2.0	2.0

3-15 Elbows (4), 45°, Smooth Radius, Rectangular, Arranged to Go Around an Obstruction (SMACNA 1981, Table 6-14K)

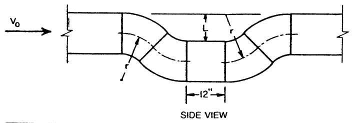

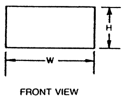

$W/H = 4$, $r/H = 1.5$, $L = 1.5H$

V_o, fpm	800	1200	1600	2000	2400
C_o	0.18	0.22	0.24	0.25	0.26

© 2021 ASHRAE (www.ashrae.org). For personal use only. Additional reproduction, distribution, or transmission in either print or digital form is not permitted without ASHRAE's prior written permission.

4 TRANSITIONS

4-1 Transition, Round (Idelchik et al. 1986, Diagrams 5-2 and 5-22)

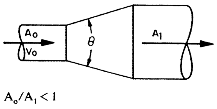

$A_o/A_1 < 1$

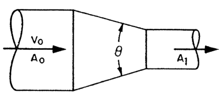

$A_o/A_1 > 1$

	C_o									
	θ, degrees									
A_o/A_1	**10**	**15**	**20**	**30**	**45**	**60**	**90**	**120**	**150**	**180**
0.06	0.21	0.29	0.38	0.60	0.84	0.88	0.88	0.88	0.88	0.88
0.1	0.21	0.28	0.38	0.59	0.76	0.80	0.83	0.84	0.83	0.83
0.25	0.16	0.22	0.30	0.46	0.61	0.68	0.64	0.63	0.62	0.62
0.5	0.11	0.13	0.19	0.32	0.33	0.33	0.32	0.31	0.30	0.30
1	0	0	0	0	0	0	0	0	0	0
2	0.20	0.20	0.20	0.20	0.22	0.24	0.48	0.72	0.96	1.0
4	0.80	0.64	0.64	0.64	0.88	1.1	2.7	4.3	5.6	6.6
6	1.8	1.4	1.4	1.4	2.0	2.5	6.5	10	13	15
10	5.0	5.0	5.0	5.0	6.5	8.0	19	29	37	43

4-2 Transition, Rectangular, Two Sides Parallel, Symmetrical (Idelchik et al. 1986, Diagram 5-5)[a]

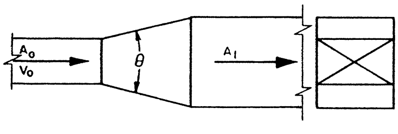

	C_o									
	θ, degrees									
A_o/A_1	**10**	**15**	**30**	**30**	**45**	**60**	**90**	**120**	**150**	**180**
0.06	0.26	0.27	0.40	0.56	0.71	0.86	1.00	0.99	0.98	0.98
0.1	0.24	0.26	0.36	0.53	0.69	0.82	0.93	0.93	0.92	0.91
0.25	0.17	0.19	0.22	0.42	0.60	0.68	0.70	0.69	0.67	0.66
0.5	0.14	0.13	0.15	0.24	0.35	0.37	0.38	0.37	0.36	0.35
1	0	0	0	0	0	0	0	0	0	0
2	0.23	0.20	0.20	0.20	0.24	0.28	0.54	0.78	1.0	1.1
4	0.81	0.64	0.64	0.64	0.88	1.1	2.8	4.4	5.7	6.6
6	1.8	1.4	1.4	1.4	2.0	2.5	6.6	10	13	15
10	5.0	5.0	5.0	5.0	6.5	8.0	19	29	37	43

[a] $A_o/A_1 > 1$ is tentative (adapted from Fitting 4-l data).

© 2021 ASHRAE (www.ashrae.org). For personal use only. Additional reproduction, distribution, or transmission in either print or digital form is not permitted without ASHRAE's prior written permission.

4-3 Transition, Rectangular, Three Sides Straight[a]

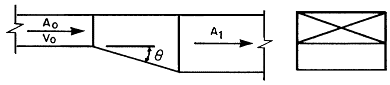

	C_o						
	θ, degrees						
A_o/A_1	**10**	**15**	**20**	**30**	**45**	**60**	**90**
0.06	0.26	0.27	0.40	0.56	0.71	0.86	1.00
0.1	0.24	0.26	0.36	0.53	0.69	0.82	0.93
0.25	0.17	0.19	0.22	0.42	0.60	0.68	0.70
0.5	0.14	0.13	0.15	0.24	0.35	0.37	0.38
1	0	0	0	0	0	0	0
2	0.23	0.20	0.20	0.20	0.24	0.28	0.54
4	0.81	0.64	0.64	0.64	0.88	1.1	2.8
6	1.8	1.4	1.4	1.4	2.0	2.5	6.6
10	5.0	5.0	5.0	5.0	6.5	8.0	19

[a]Tentative (assumed same as Fitting 4-2 data).

4-4 Transition, Rectangular, Pyramidal (Idelchik et al. 1986, Diagram 5-4)[a]

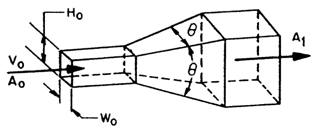

	C_o									
	θ, degrees									
A_o/A_1	**10**	**15**	**20**	**30**	**45**	**60**	**90**	**120**	**150**	**180**
0.06	0.26	0.30	0.44	0.54	0.53	0.65	0.77	0.88	0.95	0.98
0.1	0.24	0.30	0.43	0.50	0.53	0.64	0.75	0.84	0.89	0.91
0.25	0.20	0.25	0.34	0.36	0.45	0.52	0.58	0.62	0.64	0.64
0.5	0.14	0.15	0.20	0.21	0.25	0.30	0.33	0.33	0.33	0.32
1	0	0	0	0	0	0	0	0	0	0
2	0.23	0.22	0.21	0.20	0.22	0.2	0.49	0.74	0.99	1.1
4	0.84	0.68	0.68	0.64	0.88	1.1	2.7	4.3	5.6	6.6
6	1.8	1.5	1.5	1.4	2.0	2.5	6.5	10	13	15
10	5.0	5.0	5.1	5.0	6.5	8.0	19	29	37	43

[a] A_o/A_1 >1 is tentative (adapted from Fitting 4-1 data).

© 2021 ASHRAE (www.ashrae.org). For personal use only. Additional reproduction, distribution, or transmission in either print or digital form is not permitted without ASHRAE's prior written permission.

4-5 Transition, Round/Rectangular (Idelchik et al. 1986, Diagram 5-27)

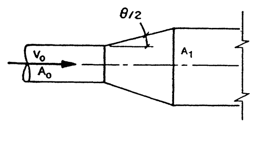

	C_o								
	θ, degrees								
A_1/A_o	**8**	**10**	**14**	**20**	**30**	**45**	**60**	**90**	**180**
2	0.14	0.15	0.20	0.25	0.30	0.33	0.33	0.33	0.30
4	0.20	0.25	0.34	0.45	0.52	0.58	0.62	0.64	0.64
6	0.21	0.30	0.42	0.53	0.63	0.72	0.78	0.79	0.79
≥10	0.24	0.30	0.43	0.53	0.64	0.75	0.84	0.89	0.88

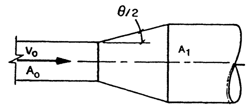

4-6 Transition, Rectangular to Round (Idelchik et al. 1986, Diagram 5-26)

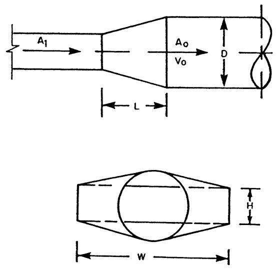

Re = DV_o/ν
$B = W/H(A_o/A_1)^2$

© 2021 ASHRAE (www.ashrae.org). For personal use only. Additional reproduction, distribution, or transmission in either print or digital form is not permitted without ASHRAE's prior written permission.

C_o for $A_o > A_1$ and $H < D$

Re × 10^{-4}	L/D	B: **0.1**	**0.5**	**1**	**2**	**5**	**10**	**20**	**50**
1	1	0.46	0.48	0.50	0.55	0.70	0.94	1.4	2.9
	1.5	0.46	0.47	0.49	0.53	0.64	0.82	1.2	2.3
	2	0.46	0.47	0.48	0.50	0.58	0.71	0.98	1.8
	3	0.45	0.46	0.46	0.48	0.51	0.57	0.69	1.0
	4	0.45	0.46	0.46	0.46	0.48	0.51	0.56	0.73
	5	0.45	0.46	0.46	0.47	0.49	0.53	0.61	0.84
2	1	0.41	0.43	0.46	0.51	0.66	0.90	1.4	2.9
	1.5	0.41	0.43	0.45	0.48	0.59	0.78	1.1	2.2
	2	0.41	0.42	0.44	0.46	0.54	0.67	0.93	1.7
	3	0.41	0.42	0.42	0.43	0.47	0.53	0.64	0.99
	4	0.41	0.41	0.41	0.42	0.44	0.46	0.52	0.69
	5	0.41	0.41	0.42	0.43	0.45	0.49	0.57	0.80
5	1	0.31	0.33	0.35	0.40	0.55	0.79	1.3	2.8
	1.5	0.31	0.32	0.34	0.38	0.49	0.67	1.0	2.1
	2	0.31	0.32	0.33	0.36	0.43	0.57	0.83	1.6
	3	0.30	0.31	0.31	0.33	0.36	0.42	0.54	0.88
	4	0.30	0.31	0.31	0.31	0.33	0.36	0.41	0.58
	5	0.30	0.31	0.31	0.32	0.34	0.38	0.46	0.70
10	1	0.19	0.21	0.23	0.28	0.43	0.68	1.2	2.6
	1.5	0.19	0.20	0.22	0.26	0.37	0.55	0.92	2.0
	2	0.19	0.20	0.21	0.24	0.31	0.45	0.71	1.5
	3	0.19	0.19	0.20	0.21	0.24	0.30	0.42	0.77
	4	0.18	0.19	0.19	0.19	0.21	0.24	0.29	0.46
	5	0.18	0.19	0.19	0.20	0.22	0.26	0.34	0.58
20	1	0.07	0.09	0.12	0.17	0.31	0.56	1.1	2.5
	1.5	0.07	0.09	0.10	0.14	0.25	0.43	0.80	0.9
	2	0.07	0.08	0.09	0.12	0.20	0.33	0.59	1.4
	3	0.07	0.07	0.08	0.09	0.13	0.18	0.30	0.65
	4	0.07	0.07	0.07	0.08	0.10	0.12	0.18	0.34
	5	0.07	0.07	0.08	0.08	0.11	0.15	0.22	0.46
50	1	0.01	0.03	0.05	0.10	0.25	0.30	0.99	2.5
	1.5	0.01	0.02	0.04	0.08	0.19	0.37	0.74	1.8
	2	0.01	0.02	0.03	0.06	0.13	0.27	0.53	1.3
	3	0	0.01	0.02	0.03	0.06	0.12	0.24	0.58
	4	0	0.01	0.01	0.01	0.03	0.06	0.11	0.28
	5	0	0.01	0.01	0.02	0.04	0.08	0.16	0.40

C_o for $A_o < A_1$ and $H < D$

Re × 10^{-4}	L/D	B: **0.1**	**1**	**5**	**10**	**20**	**50**
1	1	0.27	0.27	0.28	0.29	0.31	0.37
	3	0.27	0.27	0.28	0.29	0.30	0.33
	4	0.27	0.27	0.28	0.28	0.29	0.32
	5	0.27	0.27	0.27	0.27	0.27	0.27
2	1	0.25	0.25	0.26	0.27	0.29	0.35
	3	0.25	0.25	0.25	0.26	0.28	0.33
	4	0.25	0.25	0.25	0.26	0.27	0.30
	5	0.25	0.25	0.25	0.25	0.25	0.25
5	1	0.18	0.18	0.19	0.20	0.22	0.28
	3	0.18	0.18	0.19	0.20	0.22	0.27
	4	0.18	0.18	0.19	0.19	0.20	0.23
	5	0.18	0.18	0.18	0.18	0.18	0.18
10	1	0.11	0.11	0.12	0.13	0.15	0.21
	3	0.11	0.11	0.12	0.13	0.14	0.19
	4	0.11	0.11	0.12	0.12	0.13	0.16
	5	0.11	0.11	0.11	0.11	0.11	0.11
20	1	0.04	0.04	0.05	0.06	0.08	0.14
	3	0.04	0.04	0.05	0.06	0.07	0.12
	4	0.04	0.04	0.05	0.05	0.06	0.09
	5	0.04	0.04	0.04	0.04	0.04	0.04
50	1	0	0	0.01	0.02	0.04	0.10
	3	0	0	0.01	0.02	0.04	0.09
	4	0	0	0.01	0.01	0.02	0.05
	5	0	0	0	0	0	0

© 2021 ASHRAE (www.ashrae.org). For personal use only. Additional reproduction, distribution, or transmission in either print or digital form is not permitted without ASHRAE's prior written permission.

4-7 Transition, Rectangular to Round, Stepped, Conical (Idelchik et al. 1986, Diagram 4-9)

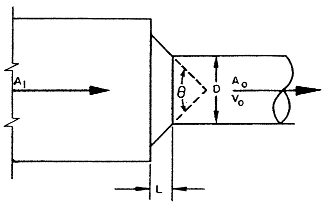

		C_o									
		θ, degrees									
A_o/A_1	L/H	**0**	**10**	**20**	**30**	**45**	**60**	**90**	**120**	**150**	**180**
0.1	0.025	0.46	0.43	0.42	0.40	0.38	0.37	0.38	0.40	0.43	0.46
	0.05	0.46	0.42	0.38	0.33	0.30	0.28	0.31	0.36	0.41	0.46
	0.075	0.46	0.39	0.32	0.28	0.23	0.21	0.26	0.32	0.39	0.46
	0.1	0.46	0.36	0.30	0.23	0.19	0.17	0.23	0.30	0.38	0.46
	0.15	0.46	0.34	0.25	0.18	0.15	0.14	0.21	0.29	0.37	0.46
	0.3	0.46	0.31	0.22	0.16	0.13	0.13	0.20	0.28	0.37	0.46
	0.6	0.46	0.25	0.17	0.12	0.10	0.11	0.19	0.27	0.36	0.46
0.25	0.025	0.40	0.38	0.36	0.35	0.33	0.32	0.33	0.35	0.37	0.40
	0.05	0.40	0.36	0.33	0.29	0.26	0.24	0.27	0.31	0.35	0.40
	0.075	0.40	0.34	0.28	0.24	0.20	0.19	0.23	0.28	0.34	0.40
	0.1	0.40	0.31	0.26	0.20	0.17	0.14	0.20	0.26	0.33	0.40
	0.15	0.40	0.30	0.22	0.16	0.13	0.12	0.18	0.25	0.32	0.40
	0.3	0.40	0.27	0.19	0.14	0.11	0.11	0.18	0.25	0.32	0.40
	0.6	0.40	0.22	0.14	0.10	0.09	0.10	0.16	0.24	0.32	0.40
0.5	0.025	0.30	0.28	0.27	0.25	0.24	0.24	0.25	0.26	0.27	0.30
	0.05	0.30	0.27	0.24	0.21	0.19	0.18	0.20	0.23	0.26	0.30
	0.075	0.30	0.25	0.21	0.18	0.15	0.14	0.17	0.21	0.25	0.30
	0.1	0.30	0.23	0.19	0.15	0.12	0.11	0.15	0.19	0.24	0.30
	0.15	0.30	0.22	0.16	0.12	0.09	0.09	0.13	0.18	0.24	0.30
	0.3	0.30	0.20	0.14	0.10	0.08	0.08	0.13	0.18	0.24	0.30
	0.6	0.30	0.16	0.11	0.08	0.07	0.07	0.12	0.17	0.23	0.30
0.8	0.025	0.15	0.14	0.13	0.13	0.12	0.12	0.12	0.13	0.14	0.15
	0.05	0.15	0.13	0.12	0.11	0.10	0.09	0.10	0.12	0.13	0.15
	0.075	0.15	0.13	0.10	0.09	0.08	0.07	0.08	0.10	0.13	0.15
	0.1	0.15	0.12	0.10	0.07	0.06	0.05	0.07	0.10	0.12	0.15
	0.15	0.15	0.11	0.08	0.06	0.05	0.04	0.07	0.09	0.12	0.15
	0.3	0.15	0.10	0.07	0.05	0.04	0.04	0.07	0.09	0.12	0.15
	0.6	0.15	0.08	0.05	0.04	0.03	0.04	0.06	0.09	0.12	0.15

© 2021 ASHRAE (www.ashrae.org). For personal use only. Additional reproduction, distribution, or transmission in either print or digital form is not permitted without ASHRAE's prior written permission.

5 JUNCTIONS (Tees, Wyes, Crosses)

5-1 Wye, 30°, Converging (Idelchik et al. 1986, Diagram 7-1)

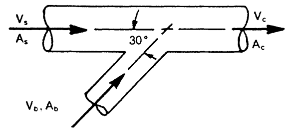

$A_s = A_c$

Branch, $C_{c,b}$

	A_b/A_c						
Q_b/Q_c	**0.1**	**0.2**	**0.3**	**0.4**	**0.6**	**0.8**	**1.0**
0	–1.0	–1.0	–1.0	–0.9	–0.9	–0.9	–0.9
0.1	0.21	–0.46	–0.57	–0.51	0.53	–0.54	–0.54
0.2	3.1	0.37	–0.06	–0.16	0.23	–0.24	–0.28
0.3	7.6	1.5	0.50	0.15	0.04	–0.06	–0.08
0.4	14	3.0	1.2	0.42	0.19	0.13	0.12
0.5	21	4.6	1.8	0.53	0.24	0.19	0.15
0.6	30	6.4	2.6	0.77	0.35	0.25	0.17
0.7	41	8.5	3.4	0.99	0.42	0.28	0.22
0.8	54	12	4.2	1.2	0.47	0.29	0.25
0.9	58	14	5.3	1.4	0.49	0.29	0.22
1.0	84	17	6.3	1.6	0.49	0.21	0.15

Main, $C_{c,s}$

	A_b/A_c						
Q_b/Q_c	**0.1**	**0.2**	**0.3**	**0.4**	**0.6**	**0.8**	**1.0**
0	0	0	0	0	0	0	0
0.1	0.02	0.11	0.13	0.15	0.16	0.17	0.17
0.2	–0.33	0.01	0.13	0.19	0.24	0.27	0.29
0.3	–1.1	–0.25	–0.01	0.10	0.22	0.30	0.35
0.4	–2.2	–0.75	–0.30	–0.05	0.17	0.26	0.36
0.5	–3.6	–1.4	–0.70	–0.35	0	0.21	0.32
0.6	–5.4	–2.4	–1.3	–0.70	–0.20	0.06	0.25
0.7	–7.6	–3.4	–2.0	–1.2	–0.50	–0.15	0.10
0.8	–10	–4.6	–2.7	–1.8	–0.90	–0.43	–0.15
0.9	–13	–6.2	–3.7	–2.6	–1.4	–0.80	–0.45
1.0	–16	–7.7	–4.8	–3.4	–1.9	–1.2	–0.75

5-2 Wye, 45° Converging, Round (Idelchik et al. 1986, Diagram 7-2)

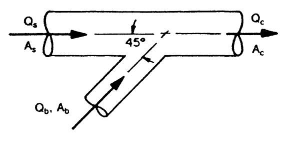

$A_s = A_c$

© 2021 ASHRAE (www.ashrae.org). For personal use only. Additional reproduction, distribution, or transmission in either print or digital form is not permitted without ASHRAE's prior written permission.

$C_{c,b}$							
	A_b/A_c						
Q_b/Q_c	0.1	0.2	0 3	0.4	0.6	0.8	1.0
0	– 1.0	–1.0	–1.0	–0.90	–0.90	–0.80	–0.90
0.1	0.24	–0.45	–0.56	–0.50	–0.52	–0.53	–0.53
0.2	3.2	0.54	–0.02	–0.14	–0.21	–0.23	–0.23
0.3	8.0	1.6	0.60	0.23	0.06	0	–0.02
0.4	14	3.2	1.3	0.52	0.25	0.18	0.15
0.5	22	5.0	2.1	0.65	0.33	0.25	0.22
0.6	32	7.0	3.0	0.91	0.81	0.61	0.51
0.7	43	9.2	3.9	1.2	0.56	0.39	0.33
0.8	56	12	4.9	1.5	0.66	0.39	0.36
0.9	71	15	6.2	1.8	0.72	0.44	0.35
1.0	87	19	7.4	2.0	0.78	0.44	0.32

$C_{c,s}$							
	A_b/A_c						
Q_b/Q_c	0.1	0.2	0.3	0.4	0.6	0.8	1.0
0	0	0	0	0	0	0	0
0.1	0.05	0.12	0.14	0.16	0.17	0.17	0.17
0.2	–0.20	0.17	0.22	0.27	0.27	0.29	0.31
0.3	–0.76	–0.13	0.08	0.20	0.28	0.32	0.40
0.4	–1.7	–0.50	–0.12	0.08	0.26	0.36	0.41
0.5	–2.8	–1.0	–0.49	–0.13	0.16	0.30	0.40
0.6	–4.3	–1.7	–0.87	–0.45	–0.04	0.20	0.33
0.7	–6.1	–2.6	–1.4	–0.85	–0.25	0.08	0.25
0.8	–8.1	3.6	–2.1	–1.3	–0.55	–0.17	0.06
0.9	–10	4.8	–2.8	–1.9	–0.88	–0.40	–0.18
1.0	–13	–6.1	–3.7	–2.6	–1.4	–0.77	–0.42

5-3 Tee, Converging, Round (Idelchik et al. 1986, Diagram 7-4)

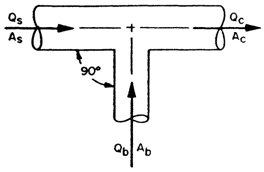

$A_s = A_c$

Branch, $C_{c,b}$							
	A_b/A_c						
Q_b/Q_c	0.1	0.2	03	0.4	0.6	0.8	1.0
0	–1.0	–1.0	–1.0	–0.90	–0.90	–0.90	–0.90
0.1	0.40	–0.37	–0.51	–0.46	–0.50	–0.51	–0.52
0.2	3.8	0.72	0.17	–0.02	–0.14	–0.18	–0.24
0.3	9.2	2.3	1.0	0.44	0.21	0.11	–0.08
0.4	16	4.3	2.1	0.94	0.54	0.40	0.32
0.5	26	6.8	3.2	1.1	0.66	0.49	0.42
0.6	37	9.7	4.7	1.6	0.92	0.69	0.57
0.7	43	13	6.3	2.1	1.2	0.88	0.72
0.8	65	17	7.9	2.7	1.5	1.1	0.86
0.9	82	21	9.7	3.4	1.8	1.2	0.99
1.0	101	26	12	4.0	2.1	1.4	1.1

Main											
Q_s/Q_c	0	0.1	0.2	0.3	0.4	0.5	0.6	0.7	0.8	0.9	1.0
$C_{c,s}$	0	0.16	0.27	0.38	0.46	0.53	0.57	0.59	0.60	0.59	0.55

© 2021 ASHRAE (www.ashrae.org). For personal use only. Additional reproduction, distribution, or transmission in either print or digital form is not permitted without ASHRAE's prior written permission.

5-4 Wye, 30° Converging, Round, Conical Main (Sepsy and Pies 1973)

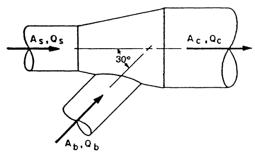

Branch, $C_{c,b}$											
		Q_b/Q_s									
A_s/A_c	A_b/A_c	0.2	0.4	0.6	0.8	1.0	1.2	1.4	1.6	1.8	2.0
0.3	0.2	–2.4	–0.11	1.8	3.4	4.8	6.0	7.1	8.0	8.9	9.7
	0.3	–2.8	–1.3	0.14	0.72	1.4	2.0	2.4	2.8	3.2	3.5
0.4	0.2	–1.4	0.61	2.3	3.8	5.2	6.3	7.3	8.3	9.1	9.8
	0.3	–1.8	–0.54	0.42	1.2	1.8	2.3	2.7	3.1	3.4	3.7
	0.4	–1.9	–0.89	–0.17	0.36	0.76	1.1	1.3	1.5	1.7	1.9
0.5	0.2	–0.82	0.97	2.6	4.0	5.3	6.4	7.4	8.3	9.1	9.9
	0.3	–1.2	–0.15	0.71	1.4	2.0	2.5	2.9	3.3	3.6	3.9
	0.4	– 1.4	–0.54	0.06	0.50	0.85	1.1	1.3	1.5	1.7	1.8
	0.5	–1.4	–0.66	–0.15	0.21	0.48	0.68	0.84	0.97	1.1	1.2
0.6	0.2	–0.52	1.2	2.7	4.1	5.3	6.4	7.4	8.3	9.1	9.9
	0 3	–0.93	0.06	0.85	1.5	2.1	2.6	3.0	3.4	3.7	4.0
	0.4	–1.1	–0.37	0.16	0.55	0.86	1.1	1.3	1.4	1.6	1.8
	0.5	–1.1	–0.49	–0.06	0.25	0.48	0.66	0.79	0.90	1.0	1.1
	0.6	– 1.2	–0.55	–0.15	0.12	0.31	0.45	0.56	0.65	0.71	0.77

Branch, $C_{c,b}$											
		Q_b/Q_c									
A_s/A_c	A_b/A_c	0.2	0.4	0.6	0.8	1.0	1.2	1.4	1.6	1.8	2.0
0.8	0.2	–0.27	1.3	2.7	4.0	5.2	6.3	7.3	8.2	9.0	9.7
	0.3	–0.67	0.18	0.90	1.5	2.0	2.5	2.9	3.3	3.6	4.0
	0.4	–0.85	–0.27	0.16	0.49	0.75	0.97	1.2	1.3	1.4	1.6
	0.5	–0.90	–0.40	–0.07	0.18	0.36	0.50	0.61	0.70	0.78	0.84
	0.6	–0.92	–0.46	–0.16	0.04	0.18	0.29	0.37	0.44	0.49	0.53
	0.7	–0.93	–0.49	–0.21	–0.03	0.10	0.19	0.25	0.30	0.34	0.37
	0.8	–0.93	–0.50	–0.24	–0.07	0.05	0.13	0.19	0.23	0.27	0.29
1.0	0.2	–0.26	1.2	2.6	3.9	5.1	6.1	7.1	8.0	8.8	9.5
	0.3	–0.65	0.12	0.79	1.4	1.9	2.4	2.8	3.1	3.5	3.8
	0.4	–0.83	–0.34	0.04	0.33	0.58	0.78	0.95	1.1	1.2	1.3
	0.5	–0.89	–0.48	–0.20	0	0.15	0.27	0.37	0.45	0.51	0.57
	0.6	–0.91	–0.54	–0.31	–0.14	–0.03	0.06	0.12	0.18	0.22	0.25
	0.8	–0.91	–0.59	–0.38	–0.25	–0.16	–0.10	–0.06	–0.03	–0.01	0.01
	1.0	–0.93	–0.60	–0.40	–0.28	–0.20	–0.14	–0.11	–0.08	–0.07	–0.06

© 2021 ASHRAE (www.ashrae.org). For personal use only. Additional reproduction, distribution, or transmission in either print or digital form is not permitted without ASHRAE's prior written permission.

Main, $C_{c,s}$											
		Q_b/Q_c									
A_s/A_c	A_b/A_c	0.2	0.4	0.6	0.8	1.0	1.2	1.4	1.6	1.8	2.0
0.3	0.2	4.5	2.8	1.5	0.56	–0.17	–0.74	–1.2	–1.6	–1.9	–2.1
	0.3	4.6	3.1	2.0	1.2	0.57	0.08	–0.30	–0.62	–0.89	–1.1
0.4	0.2	1.6	0.85	0.16	–0.43	–0.92	–1.3	–1.7	–1.9	–2.2	–2.4
	0.3	1.7	1.1	0.58	0.13	–0.24	–0.56	–0.82	–1.1	–1.3	–1.4
	0.4	1.8	1.3	0.80	0.42	0.11	–0.15	–0.37	–0.55	–0.72	–0.86
0.5	0.2	0.67	0.18	–0.33	–0.79	–1.2	–1.5	–1.8	–2.1	–2.3	–2.5
	0.3	0.75	0.42	0.07	–0.25	–0.54	–0.80	–1.0	–1.2	–1.4	–1.5
	0.4	0.80.	0.55	0.28	0.03	–0.20	–0.40	–0.57	–0.73	–0.86	–0.98
	0.5	0.82	0.62	0.41	0.20	0.02	–0.15	–0.29	–0.42	–0.53	–0.63
0.6	0.2	0.26	–0.11	–0.54	–0.95	–1.3	–1.6	–1.9	–2.1	–2.4	–0.25
	0.3	0.34	0.13	–0.14	–0.42	–0.67	–0.90	–0.11	–0.13	–0.14	–0.16
	0.4	0.39	0.25	0.06	–0.14	–0.33	–0.51	–0.66	–0.80	–0.93	–1.0
	0.5	0.41	0.32	0.18	0.03	–1.2	–0.26	–0.38	–0.50	–0.60	–0.69
	0.6	0.43	0.37	0.26	0.14	0.02	–0.09	–0.19	–0.29	–0.37	–0.45
0.8	0.2	–0.01	–0.30	–0.67	–1.1	–1.4	–1.7	–2.0	–2.2	–2.4	–2.6
	0.3	0.07	–0.07	–0.29	–0.58	–0.76	–0.97	–1.2	–1.3	–1.5	–1.6
	0.4	0.11	0.05	–0.09	–0.26	–0.42	–0.58	–0.72	–0.85	–0.97	–1.1
	0.5	0.14	0.12	0.03	–0.09	–0.21	–0.34	–0.45	–0.55	–0.64	–0.73
	0.6	0.15	0.17	0.11	0.02	–0.07	–0.17	–0.26	–0.34	–0.42	–0.49
	0.7	0.17	0.21	0.17	0.11	0.03	–0.05	–0.12	–0.19	–0.26	–0.32
	0.5	0.17	0.23	0.22	0.17	0.11	0.05	–0.02	–0.07	–0.13	–0.18
1.0	0.2	–0.05	–0.33	–0.70	–1.1	–1.4	–1.7	–2.0	–2.2	–2.4	–2.6
	0.3	0.03	–0.10	–0.31	–0.55	–0.78	–0.98	–1.2	–1.3	–1.5	–1.6
	0.4	0.07	0.02	–0.12	–0.28	–0.44	–0.59	–0.73	–0.86	–0.98	–1.1
	0.5	0.09	0.09	0.01	–0.11	–0.23	–0.35	–0.46	–0.56	–0.65	–0.74
	0.6	0.11	0.14	0.09	0	–0.09	–0.18	–0.27	–0.35	–0.43	–0.50
	0.8	0.13	0.20	0.19	0.15	0.09	0.03	–0.03	–0.08	–0.14	–0.19
	1.0	0.14	0.24	0.25	0.24	0.20	0.16	0.12	0.08	0.04	0

© 2021 ASHRAE (www.ashrae.org). For personal use only. Additional reproduction, distribution, or transmission in either print or digital form is not permitted without ASHRAE's prior written permission.

5-5 Wye, 45°, Converging, Round, Conical Main (Sepsy and Pies 1973)

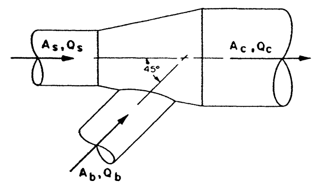

Branch, $C_{c,b}$											
		Q_b/Q_s									
A_s/A_c	A_b/A_c	0.2	0.4	0.6	0.8	1.0	1.2	1.4	1.6	1.8	2.0
0.3	0.2	–2.4	–0.01	2.0	3.8	5.3	6.6	7.8	8.9	9.8	11
	0.3	–2.8	–1.2	0.12	1.1	1.9	2.6	3.2	3.7	4.2	4.6
0.4	0.2	–1.2	0.93	2.8	4.5	5.9	7.2	8.4	9.5	10	11
	0.3	–1.6	–0.27	0.81	1.7	2.4	3.0	3.6	4.1	4.5	4.9
	0.4	–1.8	–0.72	0.07	0.66	1.1	1.5	1.8	2.1	2.3	2.5
0.5	0.2	–0.46	1.5	3.3	4.9	6.4	7.7	8.8	9.9	11	12
	0.3	–0.94	0.25	1.2	2.0	2.7	3.3	3.8	4.2	4.7	5.0
	0.4	–1.1	–0.24	0.42	0.92	1.3	1.6	1.9	2.1	2.3	2.5
	0.5	–1.2	–0.38	0.18	0.58	0.88	1.1	1.3	1.5	1.6	1.7
0.6	0.2	–0.55	1.3	3.1	4.7	6.1	7.4	8.6	9.6	11	12
	0.3	–1.1	0	0.88	1.6	2.3	2.8	3.3	3.7	4.1	4.5
	0.4	–1.2	–0.48	0.10	0.54	0.89	1.2	1.4	1.6	1.8	2.0
	0.5	–1.3	–0.62	–0.14	0.21	0.47	0.68	0.85	0.99	1.1	1.2
	0.6	–1.3	–0.69	–0.26	0.04	0.26	0.42	0.57	0.66	0.75	0.82
0.8	0.2	0.06	1.8	3.5	5.1	6.5	7.8	8.9	10	11	12
	0.3	–0.52	0.35	1.1	1.7	2.3	2.8	3.2	3.6	3.9	4.2
	0.4	–0.67	–0.05	0.43	0.80	1.1	1.4	1.6	1.8	1.9	2.1
	0.6	–0.75	–0.27	0.05	0.28	0.45	0.58	0.68	0.76	0.83	0.88
	0.7	–0.77	–0.31	–0.02	0.18	0.32	0.43	0.50	0.56	0.61	0.65
	0.8	–0.78	–0.34	–0.07	0.12	0.24	0.33	0.39	0.44	0.47	0.50
1.0	0.2	0.40	2.1	3.7	5.2	6.6	7.8	9.0	11	11	12
	0.3	–0.21	0.54	1.2	1.8	2.3	2.7	3.1	3.7	3.7	4.0
	0.4	–0.33	0.21	0.62	0.96	1.2	1.5	1.7	2.0	2.0	2.1
	0.5	–0.38	0.05	0.37	0.60	0.79	0.93	1.1	1.2	1.2	1.3
	0.6	–0.41	–0.02	0.23	0.42	0.55	0.66	0.73	0.80	0.85	0.89
	0.8	–0.44	–0.10	0.11	0.24	0.33	0.39	0.43	0.46	0.47	0.48
	1.0	–0.46	–0.14	0.05	0.16	0.23	0.27	0.29	0.30	0.30	0.29

© 2021 ASHRAE (www.ashrae.org). For personal use only. Additional reproduction, distribution, or transmission in either print or digital form is not permitted without ASHRAE's prior written permission.

Main, $C_{c,s}$

		Q_b/Q_s									
A_s/A_c	A_b/A_c	0.2	0.4	0.6	0.8	1.0	12	1.4	1.6	1.8	2.0
0.3	0.2	5.3	–0.01	2.0	1.1	0.34	–0.20	–0.61	–0.93	–1.2	–1.4
	0.3	5.4	3.7	2.5	1.6	1.0	0.53	0.16	–0.14	–0.38	–0.58
0.4	0.2	1.9	1.1	0.46	–0.07	–0.49	–0.83	–1.1	–1.3	–1.5	–1.7
	0.3	2.0	1.4	0.81	0.42	0.08	–0.20	–0.43	–0.62	–0.78	–0.92
	0.4	2.0	1.5	1.0	0.68	0.39	0.16	–0.04	–0.21	–0.35	–0.47
0.5	0.2	0.77	0.34	–0.09	–0.48	–0.81	–1.1	–1.3	–1.5	–1.7	–1.8
	0.3	0.85	0.56	0.25	–0.03	–0.27	–0.48	–0.67	–0.82	–0.96	–1.1
	0.4	0.88	0.66	0.43	0.21	0.02	–0.15	–0.30	–0.42	–0.54	–0.64
	0.5	0.91	0.73	0.54	0.36	0.21	0.06	–0.06	–0.17	–0.26	–0.35
0.6	0.2	0.30	0	–0.34	–0.67	–0.96	–1.2	–1.4	–1.6	–1.8	–1.9
	0.3	0.37	0.21	–0.02	–0.24	–0.44	–0.63	–0.79	–0.93	–1.1	–1.2
	0.4	0.40	0.31	0.16	–0.1	–0.16	–0.30	–0.43	–0.54	–0.64	–0.73
	0.5	0.43	0.37	0.26	0.14	0.02	–0.09	–0.20	–0.29	–0.37	–0.45
	0.6	0.44	0.41	0.33	0.24	0.14	0.05	–0.03	–0.11	–0.18	–0.25
0.8	0.2	–0.06	–0.27	–0.57	–0.86	–1.1	–1.4	–1.6	–1.7	–1.9	–2.0
	0.3	0	–0.08	–0.25	–0.43	–0.62	–0.78	–0.93	–1.1	–1.2	–1.3
	0.4	0.04	0.02	–0.08	–0.21	–0.34	–0.46	–0.57	–0.67	–0.77	–0.85
	0.5	0.06	0.08	0.02	–0.06	–0.16	–0.25	–0.34	–0.42	–0.50	–0.57
	0.6	0.07	0.12	0.09	0.03	–0.04	–0.11	–0.18	–0.25	–0.31	–0.37
	0.7	0.08	0.15	0.14	0.10	0.05	–0.01	–0.07	–0.12	–0.17	–0.22
	0.8	0.09	0.17	0.18	0.16	0.11	0.07	0.02	–0.02	–0.07	–0.11
1.0	0.2	–0.19	–0.39	–0.67	–0.96	–1.2	–1.5	–1.6	–1.8	–2.0	–2.1
	0.3	–0.12	–0.19	–0.35	–0.54	–0.71	–0.87	–1.0	–1.2	–1.3	–1.4
	0.4	–0.09	–0.10	–0.19	–0.31	–0.43	–0.55	–0.66	–0.77	–0.86	–0.94
	0.5	–0.07	–0.04	–0.09	–0.17	–0.26	–0.35	–0.44	–0.52	–0.59	–0.66
	0.6	–0.06	0	–0.02	–0.07	–0.14	–0.21	–0.28	–0.34	–0.40	–0.46
	0.8	–0.04	0.06	0.07	0.05	0.02	–0.03	–0.07	–0.12	–0.16	–0.20
	1.0	–0.3	0.09	0.13	0.13	0.11	0.08	0.06	0.03	–0.01	–0.03

© 2021 ASHRAE (www.ashrae.org). For personal use only. Additional reproduction, distribution, or transmission in either print or digital form is not permitted without ASHRAE's prior written permission.

5-6 Tee, Converging, Rectangular (Idelchik 1986, Diagram 7-11)

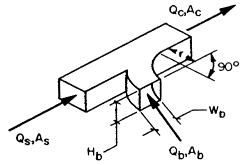

$r/w_b = 1$

Branch, $C_{c,b}$

		Q_c/Q_c								
A_b/A_s	A_b/A_c	0.1	0.2	~0.3	0.4	0.5	0.6	0.7	0.8	0.9
0.33	0.25	–1.2	–0.40	0.40	1.6	3.0	4.8	6.8	8.9	11
0.5	0.5	–0.50	–0.20	0	0.25	0.45	0.70	1.0	1.5	2.0
0.67	0.5	–1.0	–0.60	–0.20	0.10	0.30	0.60	1.0	1.5	2.0
1.0	0.5	–2.2	– 1.5	–0.95	–0.50	0	0.40	0.80	1.3	1.9
1.0	1.0	–0.60	–0.30	–0.10	–0.04	0.13	0.21	0.29	0.36	0.42
1.33	1.0	–1.2	–0.80	–0.40	–0.20	0	0.16	0.24	0.32	0.38
2.0	1.0	–2.1	–1.4	–0.90	–0.50	–0.20	0	0.20	0.25	0.30

Main, $C_{c,s}$

		Q_b/Q_s								
A_b/A_s	A_b/A_c	0.1	0.2	0.3	0.4	0.5	0.6	0.7	0.8	0.9
0.33	0.25	0.30	0.30	0.20	–0.10	–0.45	–0.92	–1.5	– 2.0	–2.6
0.5	0.5	0.17	0.16	0.10	0	–0.08	–0.18	–0.27	–0.37	–0.46
0.67	0.5	0.27	0.35	0.32	0.25	0.12	–0.03	–0.23	–0.42	–0.58
1.0	0.5	1.2	1.1	0.90	0.65	0.35	0	–0.40	–0.80	–1.3
1.0	1.0	0.18	0.24	0.27	0.26	0.23	0.18	0.10	0	–0.12
1.33	1.0	0.75	0.36	0.38	0.35	0.27	0.18	0.05	–0.08	–0.22
2.0	1.0	0.80	0.87	0.80	0.68	0.55	0.40	0.25	0.08	–0.10

5-7 Tee, Converging, Round Tap to Rectangular Main (SMACNA 1981, Table 6-9C)

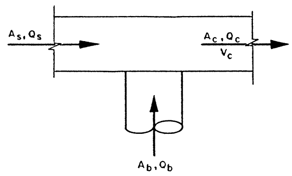

A_b/A_s	A_s/A_c	A_b/A_c
0.5	1.0	0.5

© 2021 ASHRAE (www.ashrae.org). For personal use only. Additional reproduction, distribution, or transmission in either print or digital form is not permitted without ASHRAE's prior written permission.

Branch, $C_{c,b}$

	Q_b/Q_c									
V_c, fpm	0.1	0.2	0.3	0.4	0.5	0.6	0.7	0.8	0.9	1.0
<1200	–0.63	–0.55	0.13	0.23	0.78	1.30	1.93	3.10	4.88	5.60
>1200	–0.49	–0.21	0.23	0.60	1.27	2.06	2.75	3.70	4.93	5.95

For main coefficient ($C_{c,s}$), see Fitting 5-3.

5-8 Tee, Converging, Rectangular Main and Tap (SMACNA 1981, Table 6-9D)

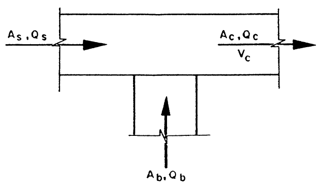

A_b/A_s	A_s/A_c	A_b/A_c
0.5	1.0	0.5

Branch, $C_{c,b}$

	Q_b/Q_c									
V_c, fpm	0.1	0.2	0.3	0.4	0.5	0.6	0.7	0.8	0.9	1.0
<1200	–0.75	–0.53	–0.03	0.33	1.03	1.10	2.15	2.93	4.18	4.78
>1200.	–0.69	–0.21	0.23	0.67	1.17	1.66	2.67	3.36	3.93	5.13

For main coefficient ($C_{c,s}$), see Fitting 5-3.

5-9 Converging, Rectangular Main and Tap (45° Entry) (SMACNA 1981, Table-9F)

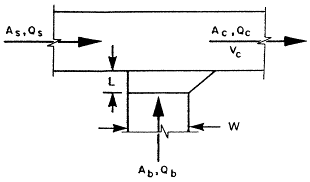

$L = 0.25\ W$, 3 in. min.

A_b/A_s	A_s/A_c	A_b/A_c
0.5	1.0	0.5

Branch, $C_{c,b}$

	Q_b/Q_c									
V_c, fpm	0.1	0.2	0.3	0.4	0.5	0.6	0.7	0.8	0.9	1.0
<1200	–0.83	–0.68	–0.30	0.28	0.55	1.03	1.50	1.93	2.50	3.03
>1200	–0.72	–0.52	–0.23	0.34	0.76	1.14	1.83	2.01	2.90	3.63

For main coefficient ($C_{c,s}$), see Fitting 5-3.

© 2021 ASHRAE (www.ashrae.org). For personal use only. Additional reproduction, distribution, or transmission in either print or digital form is not permitted without ASHRAE's prior written permission.

5-10 Tee, Diverging, Round, Conical Branch (Jones and Sepsy 1969, Figure 12)

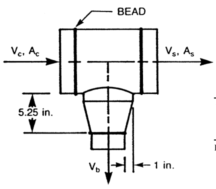

$A_c = A_s$

Branch

V_b/V_s	0	0.2	0.4	0.6	0.8	1.0	1.2	1.4	1.6	1.8	2.0
$C_{c,b}$	1.0	0.85	0.74	0.62	0.52	0.42	0.36	0.32	0.32	0.37	0.52

For main loss coefficient ($C_{c,s}$), see Fitting 5-23.

5-11 Wye, 45°, Diverging, Round, Conical Branch (Jones and Sepsy 1969, Figure 14)

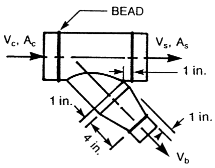

$A_c = A_s$

Branch

V_b/V_c	0	0.2	0.4	0.6	0.8	1.0	1.2	1.4	1.6	1.8	2.0
$C_{c,b}$	1.0	0.84	0.61	0.41	0.27	0.17	0.12	0.12	0.14	0.18	0.27

For main loss coefficient ($C_{c,s}$), see Fitting 5-23.

5-12 Tee, Diverging, Round, with 90° Elbow, Branch 90° to Main (Jones and Sepsy 1969, Figure 17)

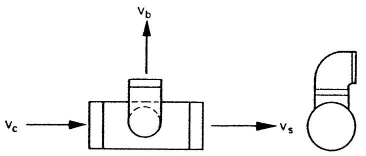

$A_r = A_s$

Branch

V_b/V_c	0	0.2	0.4	0.6	0.8	1.0	1.2	1.4	1.6	1.8	2.0
$C_{c,b}$	1.0	1.03	1.08	1.18	1.33	1.56	1.86	2.2	2.6	3.0	3.4

For main loss coefficient ($C_{c,s}$), see Fitting 5-23.

© 2021 ASHRAE (www.ashrae.org). For personal use only. Additional reproduction, distribution, or transmission in either print or digital form is not permitted without ASHRAE's prior written permission.

5-13 Tee, Diverging, Round, with 45° Elbow, Branch 90° to Main (Jones and Sepsy 1969, Figure 18)

$A_c = A_s$

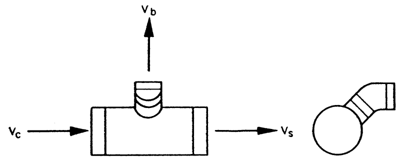

Branch											
V_b/V_c	0	0.2	0.4	0.6	0.8	1.0	1.2	1.4	1.6	1.8	2.0
$C_{c,b}$	1.0	1.32	1.51	1.60	1.65	1.74	1.87	2.0	2.2	2.5	2.7

For main loss coefficient ($C_{c,s}$), see Fitting 5-23.

5-14 Tee, Diverging, Round (Conical Branch), with 45° Elbow, Branch 90° to Main (Jones and Sepsy 1969, Figure 19)

$A_c = A_s$

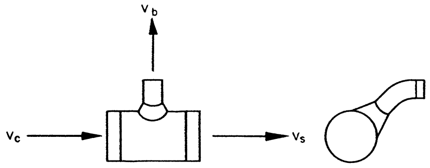

For tee geometry, see Fitting 5-10.

Branch											
V_b/V_s	0	0.2	0.4	0.6	0.8	1.0	1.2	1.4	1.6	1.8	2.0
$C_{c,b}$	1.0	0.94	0.88	0.84	0.80	0.82	0.84	0.87	0.90	0.95	1.02

For main loss coefficient ($C_{c,s}$), see Fitting 5-23.

© 2021 ASHRAE (www.ashrae.org). For personal use only. Additional reproduction, distribution, or transmission in either print or digital form is not permitted without ASHRAE's prior written permission.

5-15 Wye, 45°, Round, with 60° Elbow, Branch 90° to Main (Jones and Sepsy 1969, Figure 3)

$A_c = A_s$

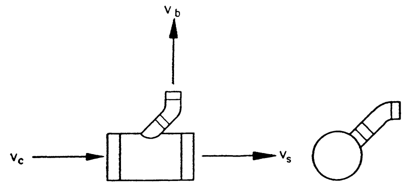

Branch											
V_b/V_c	0	0.2	0.4	0.6	0.8	1.0	1.2	1.4	1.6	1.8	2.0
$C_{c,b}$	1.0	0.88	0.77	0.68	0.65	0.69	0.73	0.88	1.14	1.54	2.2

For main loss coefficient ($C_{c,s}$), see Fitting 5-23.

5-16 Wye, 45°, Diverging, Round (Conical Branch), with 60° Elbow, Branch 90° to Main (Jones and Sepsy 1969, Figure 20)

$A_c = A_s$

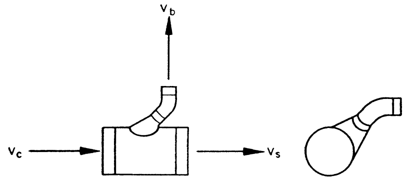

For wye geometry, see Fitting 5-11.

Branch											
V_b/V_c	0	0.2	0.4	0.6	0.8	1.0	1.2	1.4	1.6	1.8	2.0
$C_{c,b}$	1.0	0.82	0.63	0.52	0.45	0.42	0.41	0.40	0.41	0.45	0.56

For main loss coefficient ($C_{c,s}$), see Fitting 5-23.

© 2021 ASHRAE (www.ashrae.org). For personal use only. Additional reproduction, distribution, or transmission in either print or digital form is not permitted without ASHRAE's prior written permission.

5-17 Wye, 48°, Diverging, Conical Main and Branch, with 45° Elbow, Branch 90° to Main (Idelchik et al. 1986, Diagram 7-19)

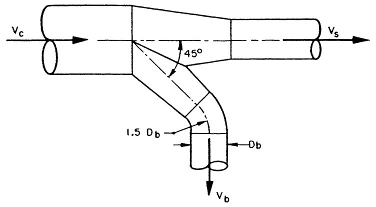

Branch									
V_b/V_c	0.2	0.4	0.6	0.7	0.8	0.9	1.0	1.1	1.2
$C_{c,b}$	0.76	0.60	0.52	0.50	0.51	0.52	0.56	0.61	0.68
V_b/V_c	1.4	1.6	1.8	2.0	2.2	2.4	2.6	2.8	3.0
$C_{c,b}$	0.86	1.1	1.4	1.8	2.2	2.6	3.1	3.7	4.2

Main										
V_s/V_c	0.2	0.4	0.6	0.8	1.0	1.2	1.4	1.6	1.8	2.0
$C_{c,s}$	0.14	0.06	0.05	0.09	0.18	0.30	0.46	0.64	0.84	1.0

5-18 Tee, Diverging, Round, with 60° Elbow, Branch 45° to Main (Jones and Sepsy 1969, Figure 22)

$A_c = A_s$

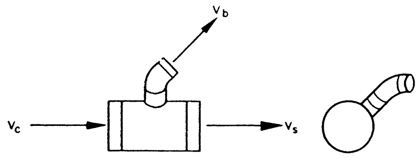

Branch											
V_b/V_c	0	0.2	0.4	0.6	0.8	1.0	1.2	1.4	1.6	1.8	2.0
$C_{c,b}$	1.0	1.06	1.15	1.29	1.45	1.65	1.89	2.2	2.5	2.9	3.3

For main loss coefficient ($C_{c,s}$), see Fitting 5-23.

© 2021 ASHRAE (www.ashrae.org). For personal use only. Additional reproduction, distribution, or transmission in either print or digital form is not permitted without ASHRAE's prior written permission.

5-19 Tee, Diverging, Round (Conical Branch), with 60° Elbow, Branch 45° to Main (Jones and Sepsy 1969, Figure 23)

$A_c = A_s$

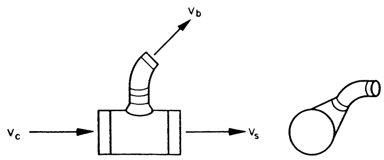

For tee geometry, see Fitting 5-10.

Branch											
V_b/V_c	0	0.2	0.4	0.6	0.8	1.0	1.2	1.4	1.6	1.8	2.0
$C_{c,b}$	1.0	0.95	0.90	0.86	0.81	0.79	0.79	0.81	0.86	0.96	1.10

For main loss coefficient ($C_{c,s}$), see Fitting 5-23.

5-20 Wye, 45°, Diverging, Round, with 30° Elbow, Branch 45° to Main (Jones and Sepsy 1969, Figure 2)

$A_c = A_s$

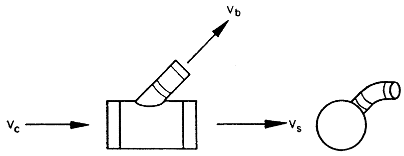

Branch											
V_b/V_c	0	0.2	0.4	0.6	0.8	1.0	1.2	1.4	1.6	1.8	2.0
$C_{c,b}$	1.0	0.84	0.72	0.62	0.54	0.50	0.56	0.71	0.92	1.22	1.66

For main loss coefficient ($C_{c,s}$), see Fitting 5-23.

5-21 Wye, 45°, Diverging, Round (Conical Branch), with 30° Elbow, Branch 45° to Main (Jones and Sepsy 1969, Figure 24)

$A_c = A_s$

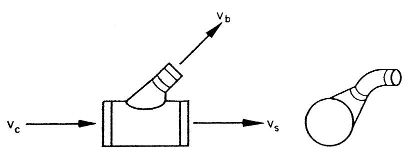

For wye geometry, see Fitting 5-11.

© 2021 ASHRAE (www.ashrae.org). For personal use only. Additional reproduction, distribution, or transmission in either print or digital form is not permitted without ASHRAE's prior written permission.

Branch

V_b/V_c	0	0.2	0.4	0.6	0.8	1.0	1.2	1.4	1.6	1.8	2.0
$C_{c,b}$	1.0	0.93	0.71	0.55	0.44	0.42	0.42	0.44	0.47	0.54	0.62

For main loss coefficient ($C_{c,s}$), see Fitting 5-23.

5-22 Tee, Diverging, Rectangular (Idelchik et al. 1986, Diagram 7-22)

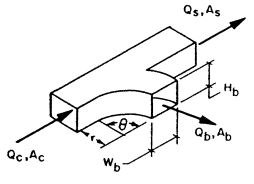

$\theta = 90°$
$r/W_b = 1.0$

Branch, $C_{c,b}$

		Q_b/Q_c								
A_b/A_s	A_b/A_c	0.1	0.2	0.3	0.4	0.5	0.6	0.7	0.8	0.9
0.25	0.25	0.55	0.50	0.60	0.85	1.2	1.8	3.1	4.4	6.0
0.33	0.25	0.35	0.35	0.50	0.80	1.3	2.0	2.8	3.8	5.0
0.5	0.5	0.62	0.48	0.40	0.40	0.48	0.60	0.78	1.1	1.5
0.67	0.5	0.52	0.40	0.32	0.30	0.34	0.44	0.62	0.92	1.4
1.0	0.5	0.44	0.38	0.38	0.41	0.52	0.68	0.92	1.2	1.6
1.0	1.0	0.67	0.55	0.46	0.37	0.32	0.29	0.29	0.30	0.37
1.33	1.0	0.70	0.60	0.51	0.42	0.34	0.28	0.26	0.26	0.29
2.0	1.0	0.60	0.52	0.43	0.33	0.24	0.17	0.15	0.17	0.21

Main, $C_{c,s}$

		Q_b/Q_c								
A_b/A_s	A_b/A_c	0.1	0.2	0.3	0.4	0.5	0.6	0.7	0.8	0.9
0.25	0.25	–0.01	–0.03	–0.01	0.05	0.13	0.21	0.29	0.38	0.46
0.33	0.25	0.08	0	–0.02	–0.01	0.02	0.08	0.16	0.24	0.34
0.5	0.5	–0.03	–0.06	–0.05	0	0.06	0.12	0.19	0.27	0.35
0.67	0.5	0.04	–0.02	–0.04	–0.03	–0.01	0.04	0.12	0.23	0.37
1.0	0.5	0.72	0.48	0.28	0.13	0.05	0.04	0.09	0.18	0.30
1.0	1.0	–0.02	–0.04	–0.04	–0.01	0.06	0.13	0.22	0.30	0.38
1.33	1.0	0.10	0	0.01	–0.03	–0.01	0.03	0.10	0.20	0.30
2.0	1.0	0.62	0.38	0.23	0.23	0.08	0.05	0.06	0.10	0.20

© 2021 ASHRAE (www.ashrae.org). For personal use only. Additional reproduction, distribution, or transmission in either print or digital form is not permitted without ASHRAE's prior written permission.

5-23 Wye, Diverging, Rectangular and Round (Idelchik et al. 1986, Diagram 7-21)

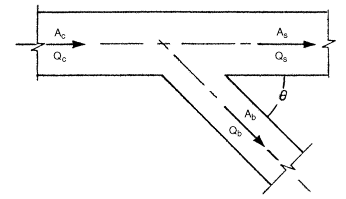

$A_c = A_s$

$H_b = H_c$
where H is height of rectangular duct

Main

V_s/V_c	0	0.1	0.2	0.3	0.4	0.5	0.6	0.8	1.0
$C_{c,s}$	0.40	0.32	0.26	0.20	0.14	0.10	0.06	0.02	0

θ = 30°

Branch, $C_{c,b}$

	Q_b/Q_c								
A_b/A_c	0.1	0.2	0.3	0.4	0.5	0.6	0.7	0.8	0.9
0.8	0.75	0.55	0.40	0.28	0.21	0.16	0.15	0.16	0.19
0.7	0.72	0.51	0.36	0.25	0.18	0.15	0.16	0.20	0.26
0.6	0.69	0.46	0.31	0.21	0.17	0.16	0.20	0.28	0.39
0.5	0.65	0.41	0.26	0.19	0.18	0.22	0.32	0.47	0.67
0.4	0.59	0.33	0.21	0.20	0.27	0.40	0.62	0.92	1.3
0.3	0.55	0.28	0.24	0.38	0.76	1.3	2.0	3.0	4.1
0.2	0.40	0.26	0.58	1.3	2.5	4.1	6.1	8.6	11.0
0.1	0.28	1.5	4.3	8.3	15.0	—	—	—	—

θ = 45°

Branch, $C_{c,b}$

	Q_b/Q_c								
A_b/A_c	0.1	0.2	0.3	0.4	0.5	0 6	0.7	0.8	0.9
0.8	0.78	0.62	0.49	0.40	0.34	0.31	0.32	0.35	0.40
0.7	0.71	0.59	0.47	0.38	0.34	0.32	0.35	0.41	0.50
0.6	0.74	0.56	0.44	0.37	0.35	0.36	0.43	0.54	0.68
0.5	0.71	0.52	0.41	0.38	0.40	0.45	0.59	0.78	1.0
0.4	0.66	0.47	0.40	0.43	0.54	0.69	0.95	1.3	1.7
0.3	0.66	0.48	0.52	0.73	1.2	1.8	2.7	3.7	4.9
0.2	0.56	0.56	1.0	1.8	3.2	4.9	7.1	9.6	13.0
0.1	0.60	2.1	5.1	9.3	16.0	—	—	—	—

© 2021 ASHRAE (www.ashrae.org). For personal use only. Additional reproduction, distribution, or transmission in either print or digital form is not permitted without ASHRAE's prior written permission.

θ = 60°

Branch, $C_{c,b}$

	Q_b/Q_c								
A_b/A_c	0.1	0.2	0.3	0.4	0.5	0.6	0.7	0.8	0.9
0.8	0.83	0.71	0.62	0.56	0.52	0.50	0.53	0.60	0.68
0.7	0.82	0.69	0.61	0.56	0.54	0.54	0.60	0.70	0.82
0.6	0.81	0.68	0.60	0.58	0.58	0.61	0.72	0.87	1.1
0.5	0.79	0.66	0.61	0.62	0.68	0.76	0.94	1.2	1.5
0.4	0.76	0.65	0.65	0.74	0.89	1.1	1.4	1.8	2.3
0.3	0.80	0.75	0.89	1.2	1.8	2.6	3.5	4.6	6.0
0.2	0.77	0.96	1.6	2.5	4.0	6.0	8.3	11.0	—
0.1	1.0	2.9	6.2	10.0	—	—	—	—	—

θ = 90°

Branch, $C_{c,b}$

	Q_b/Q_c								
A_b/A_c	0.1	0.2	0.3	0.4	0.5	0.6	0.7	0.8	0.9
0 8	0.95	0.92	0.92	0.93	0.94	0.95	1.1	1.2	1.4
0.7	0.95	0.94	0.95	0.98	1.0	1.1	1.2	1.4	1.6
0.6	0.96	0.97	1.0	1.1	1.1	1.2	1.4	1.7	2.0
0.5	0.97	1.0	1.1	1.2	1.4	1.5	1.8	2.1	2.5
0.4	0.99	1.1	1.3	1.5	1.7	2.0	2.4	3.0	3.6
0.3	1.1	1.4	1.8	2.3	3.2	4.3	5.5	6.9	8.5
0.2	1.3	1.9	2.9	4.1	6.2	8.5	11.0	—	—
0.1	2.1	4.8	8.9	14.0	—	—	—	—	—

5-24 Diverging Wye, Rectangular (Idelchik et al. 1986, Diagram 7-22)

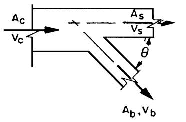

θ = 15° to 90°
and
$A_c = A_s + A_b$

Branch, $C_{c,b}$

	V_b/V_c											
θ, deg.	0.1	0.2	0.3	0.4	0.5	0.6	0.8	1.0	1.2	1.4	1.6	1.8	2.0
15	0.81	0.65	0.51	0.38	0.28	0.20	0.11	0.06	0.14	0.30	0.51	0.76	1.0
30	0.84	0.69	0.56	0.44	0.34	0.26	0.19	0.15	0.15	0.30	0.51	0.76	1.0
45	0.87	0.74	0.63	0.54	0.45	0.38	0.29	0.24	0.23	0.30	0.51	0.76	1.0
60	0.90	0.82	0.79	0.66	0.59	0.53	0.43	0.36	0.33	0.39	0.51	0.76	1.0
90	1.0	1.0	1.0	1.0	1.0	1.0	1.0	1.0	1.0	1.0	1.0	1.0	1.0

© 2021 ASHRAE (www.ashrae.org). For personal use only. Additional reproduction, distribution, or transmission in either print or digital form is not permitted without ASHRAE's prior written permission.

Main, $C_{c,s}$

θ, degrees	15-60	90				
	A_s/A_c	A_s/A_c				
V_s/V_c	0-1.0	0-0.4	0.5	0.6	0.7	≥0.8
0	1.0	1.0	1.0	1.0	1.0	1.0
0.1	0.81	0.81	0.81	0.81	0.81	0.81
0.2	0.64	0.64	0.64	0.64	0.64	0.64
0.3	0.50	0.50	0.52	0.52	0.50	0.50
0.4	0.36	0.36	0.40	0.38	0.37	0.36
0.5	0.25	0.25	0.30	0.28	0.27	0.25
0.6	0.16	0.16	0.23	0.20	0.18	0.16
0.8	0.04	0.04	0.17	0.10	0.07	0.04
1.0	0	0	0.20	0.10	0.05	0
1.2	0.07	0.07	0.36	0.21	0.14	0.07
1.4	0.39	0.39	0.79	0.59	0.39	—
1.6	0.90	0.90	1.4	1.2	—	—
1.8	1.8	1.8	2.4	—	—	—
2.0	3.2	3.2	4.0	—	—	—

5-25 Tee, Diverging, Rectangular Main to Round Tap (SMACNA 1981, Table 6-10T)

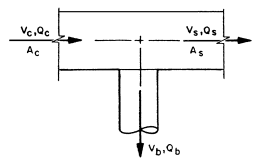

$A_c = A_s$

Branch, $C_{c,b}$

	Q_b/Q_s								
V_b/V_c	0.1	0.2	0.3	0.4	0.5	0.6	0.7	0.8	0.9
0.2	1.00								
0.4	1.01	1.07							
0.6	1.14	1.10	1.08						
0.8	1.18	1.31	1.12	1.13					
1.0	1.30	1.38	1.20	1.23	1.26				
1.2	1.46	1.58	1.45	1.31	1.39	1.48			
1.4	1.70	1.82	1.65	1.51	1.56	1.64	1.71		
1.6	1.93	2.06	2.00	1.85	1.70	1.76	1.80	1.88	
1.8	2.06	2.17	2.10	2.13	2.06	1.98	1.99	2.00	2.07

For main coefficient ($C_{c,s}$), see Fitting 5-23.

© 2021 ASHRAE (www.ashrae.org). For personal use only. Additional reproduction, distribution, or transmission in either print or digital form is not permitted without ASHRAE's prior written permission.

5-26 Tee, Diverging, Rectangular Main to Round Tap (Conical) (Inoue et al. 1980, Korst et al. 1950)

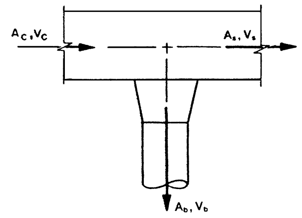

$A_c = A_s$

Branch						
V_b/V_c	0.40	0.50	0.75	1.0	1.3	1.5
$C_{c,b}$	0.80	0.83	0.90	1.0	1.1	1.4

For main coefficient ($C_{c,s}$), see Fitting 5-23.

5-27 Tee, Diverging, Rectangular Main, and Tap (45° Entry) (SMACNA 1981, Table 6-10N)

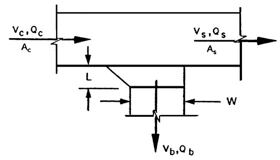

$L = 0.25W$, 3 in. min.
$A_c = A_s$

sRecommended[a]

Branch, $C_{c,b}$

V_b/V_c	Q_b/Q_s 0.1	0.2	0.3	0.4	0.5	0.6	0.7	0.8	0.9
0.2	0.91								
0.4	0.81	0.79							
0.6	0.77	0.72	0.70						
0.8	0.78	0.73	0.69	0.66					
1.0	0.78	0.98	0.85	0.79	0.74				
1.2	0.90	1.11	1.16	1.23	1.03	0.86			
1.4	1.19	1.22	1.26	1.29	1.54	0.25	0.92		
1.6	1.35	1.42	1.55	1.59	1.63	1.50	1.31	1.09	
1.8	1.44	1.50	1.75	1.74	1.72	2.24	1.63	1.40	1.17

For main coefficient ($C_{c,s}$), see Fitting 5-23.
[a]For performance study, see SMACNA (1987).

© 2021 ASHRAE (www.ashrae.org). For personal use only. Additional reproduction, distribution, or transmission in either print or digital form is not permitted without ASHRAE's prior written permission.

5-28 Tee, Diverging, Rectangular Main, and Tap[a] (SMACNA 1981, Table 10Q)

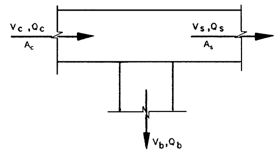

$A_c = A_s$

Branch, $C_{c,b}$

V_b/V_c	Q_b/Q_c 0.1	0.2	0.3	0.4	0.5	0.6	0.7	0.8	0.9
0.2	1.03								
0.4	1.04	1.01							
0 6	1.11	1.03	1.05						
0 8	1.16	1.21	1.17	1.12					
1.0	1.38	1.40	1.30	1.36	1.27				
1 2	1.52	1.61	1.68	1.91	1.47	1.66			
1 4	1.79	2.01	1.90	2.31	2.28	2.20	1.95		
1.6	2.07	2.28	2.13	2.71	2.99	2.81	2.09	2.20	
1.8	2.32	2.54	2.64	3.09	3.72	2.48	2.21	2.57	2.32

For main coefficient ($C_{c,s}$) see Fitting 5-23.
[a]For performance study see SMACNA (1987).

5-29 Tee, Diverging, Rectangular Main and Tap (45° Entry), with Damper (SMACNA 1981, Table 6-10P)

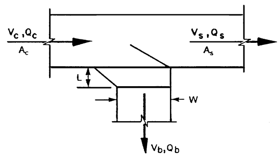

$L = 0.25W$, 3 in. min
$A_c = A_s$

Poor; should not be used.[a]

© 2021 ASHRAE (www.ashrae.org). For personal use only. Additional reproduction, distribution, or transmission in either print or digital form is not permitted without ASHRAE's prior written permission.

Branch, $C_{c,b}$

V_b/V_c	Q_b/Q_c 0.1	0.2	0.3	0.4	0.5	0.6	0.7	0.8	0.9
0.2	0.61								
0.4	0.46	0.61							
0.6	0.43	0.50	0.54						
0.8	0.39	0.43	0.62	0.53					
1.0	0.34	0.57	0.77	0.73	0.68				
1.2	0.37	0.64	0.85	0.98	1.07	0.83			
1.4	0.57	0.71	1.04	1.16	1.54	1.36	1.18		
1.6	0.89	1.08	1.28	1.30	1.69	2.09	1.81	1.47	
1.8	1.33	1.34	2.04	1.78	1.90	2.40	2.77	2.23	1.92

For main coefficient ($C_{c,s}$), see Fitting 5-31.
[a]For performance study, see SMACNA (1987).

5-30 Tee, Diverging, Rectangular Main and Tap, with Damper (SMACNA 1981, Table 6-10R)

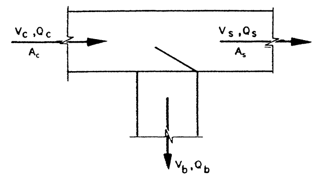

$A_c = A_s$

Poor; should not be used.[a]

Branch, $C_{c,b}$

V_b/V_c	Q_b/Q_c 0.1	0.2	0.3	0.4	0.5	0.6	0.7	0.8	0.9
0.2	0.58								
0.4	0.67	0.64							
0.6	0.78	0.76	0.75						
0.8	0.88	0.98	0.81	1.01					
1.0	1.12	1.05	1.08	1.18	1.29				
1.2	1.49	1.48	1.40	1.51	1.70	1.91			
1.4	2.10	2.21	2.25	2.29	2.32	2.48	2.53		
1.6	2.72	3.30	2.84	3.09	3.30	3.19	3.29	3.16	
1.8	3.42	4.58	3.65	3.92	4.20	4.15	4.14	4.10	4.05

For main coefficient ($C_{c,s}$) see Fitting 5-31.
[a]For performance study see SMACNA (1987).

© 2021 ASHRAE (www.ashrae.org). For personal use only. Additional reproduction, distribution, or transmission in either print or digital form is not permitted without ASHRAE's prior written permission.

5-31 Tee, Diverging, Rectangular, with Extractor (SMACNA 1981, Table 6-10S)

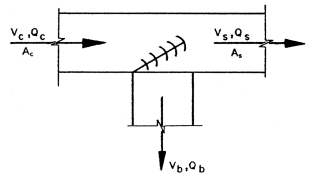

$A_c = A_s$

Poor; should not be used.[a]

Main									
V_b/V_c	0.2	0.4	0.6	0.8	1.0	1.2	1.4	1.6	1.8
$C_{c,s}$	0.03	0.04	0.07	0.12	0.13	0.14	0.27	0.30	0.25

Branch, $C_{c,b}$

V_b/V_c	Q_b/Q_c 0.1	0.2	0.3	0.4	0.5	0.6	0.7	0.8	0.9
0.2	0.60								
0.4	0.62	0.69							
0.6	0.74	0.80	0.82						
0.8	0.99	1.10	0.95	0.90					
1.0	1.48	1.12	1.41	1.24	1.21				
1.2	1.91	1.33	1.43	1.52	1.55	1.64			
1.4	2.47	1.67	1.70	2.04	1.86	1.98	2.47		
1.6	3.17	2.40	2.33	2.53	2.31	2.51	3.13	3.25	
1.8	3.85	3.37	2.89	3.23	3.09	3.03	3.30	3.74	4.11

[a]For performance study, see SMACNA (1987).

5-32 Symmetrical Wye, Dovetail, Rectangular (Idelchik et al. 1986, Diagram 7-24)

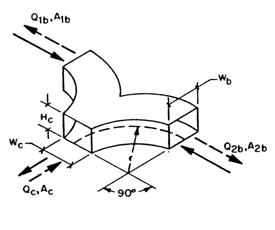

$r/W_c = 1.5$
$Q_{1b}/Q_c = Q_{2b}/Q_c = 0.5$

Converging		
A_{1b}/A_c or A_{2b}/A_c	0.50	1.0
$C_{c,1b}$ or $C_{c,2b}$	0.23	0.07

Diverging		
A_{1b}/A_c or A_{2b}/A_c	0.50	1.0
$C_{c,1b}$ or $C_{c,2b}$	0.30	0.25

© 2021 ASHRAE (www.ashrae.org). For personal use only. Additional reproduction, distribution, or transmission in either print or digital form is not permitted without ASHRAE's prior written permission.

5-33 Wye, Rectangular and Round (Idelchik et al. 1986, Diagram 7-30)

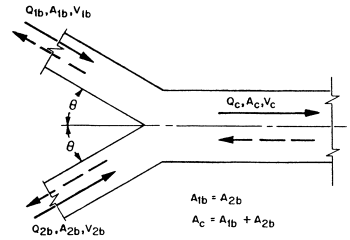

Converging — $C_{c,1b}$ or $C_{c,2b}$

	Q_{1b}/Q_c or Q_{2b}/Q_c										
θ, deg.	**0**	**0.1**	**0.2**	**03**	**0.4**	**0.5**	**0.6**	**0.7**	**0.8**	**0.9**	**1.0**
15	–2.6	–1.9	–1.3	–0.77	–0.30	0.10	0.41	0.67	0.85	0.97	1.0
30	–2.1	–1.5	–1.0	–0.53	–0.10	0.28	0.69	0.91	1.1	1.4	1.6
45	–1.3	–0.93	–0.55	–0.16	0.20	0.56	0.92	1.3	1.6	2.0	2.3

Diverging — $C_{c,1b}$ or $C_{c,2b}$

	V_{1b}/V_c or V_{2b}/V_c												
θ, deg.	**0.1**	**0.2**	**03**	**0.4**	**0.5**	**0.6**	**0.8**	**1.0**	**1.2**	**1.4**	**1.6**	**1.8**	**2.0**
15	0.81	0.65	0.51	0.38	0.28	0.20	0.11	0.06	0.14	0.30	0.51	0.76	1.0
30	0.84	0.69	0.56	0.44	0.34	0.26	0.19	0.15	0.15	0.30	0.51	0.76	1.0
45	0.87	0.74	0.63	0.54	0.45	0.38	0.29	0.24	0.23	0.30	0.51	0.76	1.0
60	0.90	0.82	0.79	0.66	0.59	0.53	0.43	0.36	0.33	0.39	0.51	0.76	1.0
90	1.0	1.0	1.0	1.0	1.0	1.0	1.0	1.0	1.0	1.0	1.0	1.0	1.0

© 2021 ASHRAE (www.ashrae.org). For personal use only. Additional reproduction, distribution, or transmission in either print or digital form is not permitted without ASHRAE's prior written permission.

5-34 Wye (Double), 45° Rectangular and Round (Idelchik et al. 1986, Diagram 7-27)

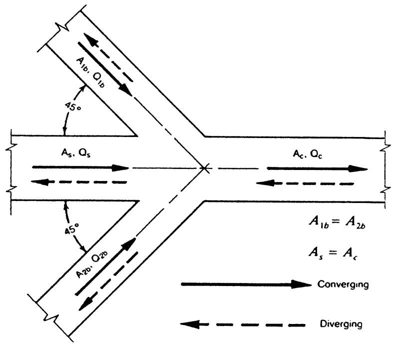

Converging Flow

Branch, $C_{c,b}$

	Q_{1b}/Q_c						
Q_{2b}/Q_{1b}	**0**	**0.1**	**0.2**	**0.3**	**0.4**	**0.5**	**0.6**
			$A_{1b}/A_c = 0.2$				
0.5	–1.0	–0.36	0.59	1.8	3.2	4.9	6.8
1.0	–1.0	–0.24	0.63	1.7	2.6	3.7	—
2.0	–1.0	–0.19	0.21	0.04	—	—	—
			$A_{1b}/A_c = 0.4$				
0.5	–1.0	–0.48	–0.02	0.58	0.92	1.3	16
1.0	–1.0	–0.36	0.17	0.55	0.72	0.78	—
2.0	–1.0	–0.18	0.16	–0.06	—	—	—
			$A_{1b}/A_c = 0.6$				
0.5	–1.0	–0.50	–0.07	0.31	0.60	0.82	0.92
1.0	–1.0	–0.37	0.12	0.55	0.60	0.52	—
2.0	–1.0	–0.18	0.26	0.16	—	—	—
			$A_{1b}/A_c = 1.0$				
0.5	–1.0	–0.51	–0.09	0.25	0.50	0.65	0.64
1.0	–1.0	–0.37	0.13	0.46	0.61	0.54	—
2.0	–1.0	–0.15	0.38	0.42	—	—	—

© 2021 ASHRAE (www.ashrae.org). For personal use only. Additional reproduction, distribution, or transmission in either print or digital form is not permitted without ASHRAE's prior written permission.

Main, $C_{c,s}$

	Q_s/Q_c										
Q_{2b}/Q_{1b}	**0**	**0.1**	**0.2**	**0.3**	**0.4**	**0.5**	**0.6**	**0.7**	**0.8**	**0.9**	**1.0**
					$A_{1b}/A_c = 0.2$						
0.5 & 2.0	–2.9	–1.9	–1.3	–0.80	–0.56	–0.23	–0.01	0.16	0.22	0.15	0
1.0	–2.5	–1.9	–1.3	–0.80	–0.42	–0.12	0.08	0.20	0.22	0.15	0
					$A_{1b}/A_c = 0.4$						
0.5 & 2.0	–0.98	–0.61	–0.30	–0.05	0.14	0.26	0.33	0.34	0.28	0.17	0
1.0	–0.77	–0.44	–0.16	0.05	0.21	0.31	0.36	0.35	0.29	0.17	0
					$A_{1b}/A_c = 0.6$						
0.5 & 2.0	–0.32	0.08	0.11	0.27	0.37	0.43	0.44	0.40	0.31	0.18	0
1.0	–0.18	–0.04	0.21	0.34	0.42	0.46	0.46	0.41	0.31	0.18	0
					$A_{1b}/A_c = 1.0$						
0.5 & 2.0	0.11	0.36	0.46	0.53	0.57	0.56	0.52	0.44	0.33	0.18	0
1.0	0.29	0.42	0.51	0.57	0.58	0.58	0.54	0.45	0.33	0.18	0

Diverging Flow: Use Fitting 5-23.

5-35 Cross, 90°, Rectangular and Round (Idelchik et al. 1986, Diagram 7-29)

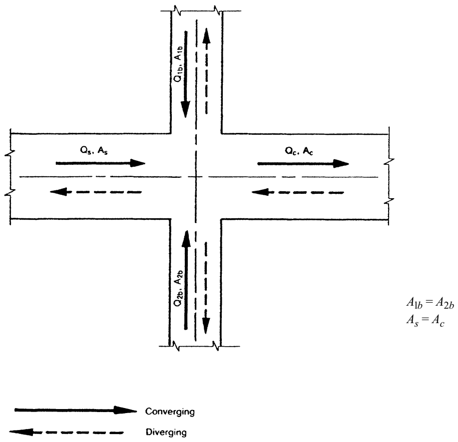

© 2021 ASHRAE (www.ashrae.org). For personal use only. Additional reproduction, distribution, or transmission in either print or digital form is not permitted without ASHRAE's prior written permission.

Converging Flow

Branch, $C_{c,b}$

	Q_{1b}/Q_c or Q_{2b}/Q_c						
Q_{2b}/Q_{1b}	**0**	**0.1**	**0.2**	**0.3**	**0.4**	**0.5**	**0.6**
			$A_{1b}/A_c = 0.2$				
0.5	–0.85	–0.10	1.1	2.7	4.8	7.3	10
1.0	–0.85	–0.05	1.4	3.1	5.1	7.4	—
2.0	–0.85	–0.31	1.8	3.4	—	—	—
			$A_{1b}/A_c = 0.4$				
0.5	–0 85	–0.29	0.34	1.0	1.8	2.6	3.4
1.0	–0.85	–0.14	0.60	1.3	2.1	2.7	—
2.0	–0.85	0.12	1.0	1.7	—	—	—
			$A_{1b}/A_c = 0.6$				
0.5	–0.85	–0.32	0.20	0.72	1.2	1.7	2.1
1.0	–0.85	–0.18	0.46	1.0	1.5	1.9	—
2.0	–0.85	0.09	0.88	1.4	—	—	—
			$A_{1b}/A_c = 0.8$				
0.5	–0.85	–0.33	0.13	0.61	1.0	1.4	1.7
1.0	–0.85	–0.18	0.41	0.91	1.3	1.5	—
2.0	–0.85	0.08	0.83	1.3	—	—	—
			$A_{1b}/A_c = 1.0$				
0.5	–0.85	–0.34	0.13	0.56	0.93	1.3	1.5
1.0	–0.85	–0.19	0.39	0.86	1.2	1.4	—
2.0	–0.85	0.07	0.81	1.2	—	—	—

Main

Q_s/Q_c	0	0.1	0.2	0.3	0.4	0.5
$C_{c,s}$	1.2	1.2	1.2	1.1	1.1	0.96
Q_s/Q_c	0.6	0.7	0.8	0.9	1.0	
$C_{c,s}$	0.85	0.72	0.56	0.39	0.20	

Diverging Flow: Use Fitting 5-23.

6 OBSTRUCTIONS

6-1 Damper, Butterfly, Round (Idelchik et al. 1986, Diagram 9-16; Zolotov 1967)

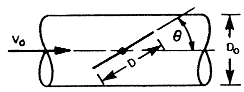

© 2021 ASHRAE (www.ashrae.org). For personal use only. Additional reproduction, distribution, or transmission in either print or digital form is not permitted without ASHRAE's prior written permission.

	C_o										
	θ, degrees										
D/D_o	0	10	20	30	40	50	60	70	75	80	85
0.5	019	0.27	0.37	0.49	0.61	0.74	0.86	0.96	0.99	1.0	1.0
0.6	0.19	0.32	0.48	0.69	0.94	1.2	1.5	1.7	1.8	1.9	1.9
0.7	0.19	0.37	0.64	1.0	1.5	2.1	2.8	3.5	3.7	3.9	4.1
0.8	0.19	0.45	0.87	1.6	2.6	4.1	6.1	8.4	9.4	10	10
0.9	0.19	0.54	1.2	2.5	5.0	9.6	17	30	38	45	50
1.0	0.19	0.67	1.8	4.4	11	32	113	—	—	—	—

6-2 Damper, Butterfly, Rectangular (Idelchik et al. 1986, Diagram 9-17; Zolotov 1967)

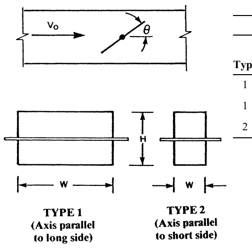

		C_o								
		θ, degrees								
Type	H/W	0	10	20	30	40	50	60	65	70
1	<0.25	0.04	0.30	1.1	3.0	8.0	23	60	100	190
1	0.25-1.0	0.08	0.33	1.2	3.3	9.0	26	70	128	210
2	>1.0	0.13	0.35	1.3	3.6	10	29	80	155	230

6-3 Damper, Gate, Round (Idelchik et al. 1986, Diagram 9-5)

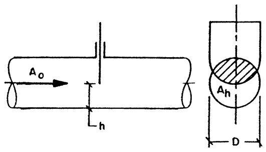

h/D	0.2	0.3	0.4	0.5	0.6	0.7	0.8	0.9
A_h/A_o	0.25	0.38	0.50	0.61	0.71	0.81	0.90	0.96
C_o	35	10	4.6	2.1	0.98	0.44	0.17	0.06

6-4 Damper, Gale, Rectangular (Idelchik et al. 1986, Diagram 8-5)

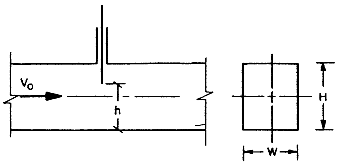

© 2021 ASHRAE (www.ashrae.org). For personal use only. Additional reproduction, distribution, or transmission in either print or digital form is not permitted without ASHRAE's prior written permission.

	h/H						
H/W	0.3	0.4	0.5	0.6	0.7	0.8	0.9
0.5	14	6.9	3.3	1.7	0.83	0.32	0.09
1.0	19	8.8	4.5	2.4	1.2	0.55	0.17
1.5	20	9.1	4.7	2.7	1.2	0.47	0.11
2.0	18	8.8	4.5	2.3	1.1	0.51	0.13

6-5 Damper, Rectangular, Parallel Blades (Brown and Fellows 1957)

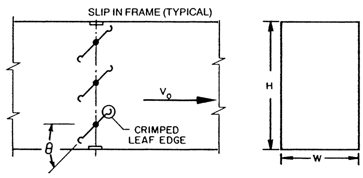

$$L/R = \frac{NW}{2(H+W)}$$

where
N = number of damper blades
W = duct dimension parallel to blade axis, in.
H = duct height, in.
L = sum of damper blade lengths, in.
R = perimeter of duct, in.

	C_o							
	θ, degrees							
L/R	0	10	20	30	40	50	60	70
0.3	0.52	0.79	1.4	2.3	5.0	9	14	32
0.4	0.52	0.85	1.5	2.4	5.0	9	16	38
0.5	0.52	0.92	1.5	2.4	5.0	9	18	45
0.6	0.52	0.92	1.5	2.4	5.4	9	21	45
0.8	0.52	0.92	1.5	2.5	5.4	9	22	55
1.0	0.52	1.0	1.6	2.6	5.4	10	24	65
1.5	0.52	1.0	1.6	2.7	5.4	10	28	102

6-6 Damper, Rectangular, Opposed Blades (Brown and Fellows 1957)

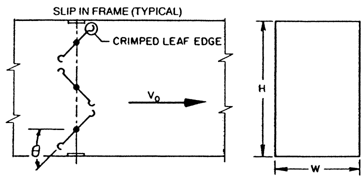

$$L/R = \frac{NW}{2(H+W)}$$

See Fitting 6-5 for definition of terms.

© 2021 ASHRAE (www.ashrae.org). For personal use only. Additional reproduction, distribution, or transmission in either print or digital form is not permitted without ASHRAE's prior written permission.

	C_o							
	θ, degrees							
L/R	0	10	20	30	40	50	60	70
0.3	0.52	0.85	2.1	4.1	9	21	73	284
0.4	0.52	0.92	2.2	5.0	11	28	100	332
0.5	0.52	1.0	2.3	5.4	13	33	122	377
0.6	0.52	1.0	2.3	6.0	14	38	148	411
0.8	0.52	1.1	2.4	6.6	18	54	188	495
1.0	0.52	1.2	2.7	7.3	21	65	245	547
1.5	0.52	1.4	3.2	9.0	28	107	361	677

6-7 Obstruction, Screen, Round and Rectangular (Idelchik et al. 1986, Diagram 8-6)

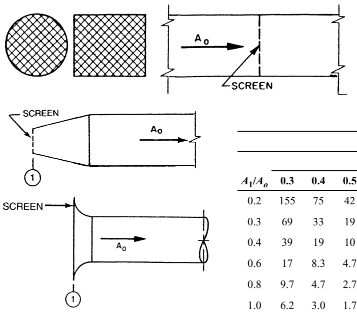

n = free area ratio of screen
A_o = area of duct
A_1 = cross-sectional area of duct or fitting where screen is located

	C_o							
	n							
A_1/A_o	0.3	0.4	0.5	0.6	0.7	0.8	0.9	1.0
0.2	155	75	42	24	15	8.0	3.5	0
0.3	69	33	19	11	6.4	3.6	1.6	0
0.4	39	19	10	6.1	3.6	2.0	0.88	0
0.6	17	8.3	4.7	2.7	1.6	0.89	0.39	0
0.8	9.7	4.7	2.7	1.5	0.91	0.50	0.22	0
1.0	6.2	3.0	1.7	0.97	0.58	0.32	0.14	0
1.2	4.3	2.1	1.2	0.67	0.40	0.22	0.10	0
1.4	3.2	1.5	0.87	0.49	0.30	0.16	0.07	0
1.6	2.4	1.2	0.66	0.38	0.23	0.12	0.05	0
2.0	1.6	0.75	0.43	0.24	0.15	0.08	0.04	0
2.5	0.99	0.48	0.27	0.16	0.09	0.05	0.02	0
3.0	0.69	0.33	0.19	0.11	0.06	0.04	0.02	0
4.0	0.39	0.19	0.11	0.06	0.04	0.02	0.01	0
6.0	0.17	0.08	0.05	0.03	0.02	0.01	0	0

© 2021 ASHRAE (www.ashrae.org). For personal use only. Additional reproduction, distribution, or transmission in either print or digital form is not permitted without ASHRAE's prior written permission.

6-8 Obstruction, Perforated Plate, Thick, Round, and Rectangular (Idelchik et al. 1986, Diagram 8-6)

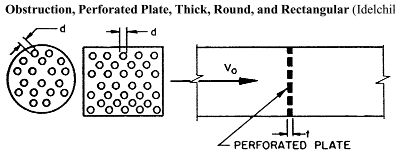

	C_o								
	n								
t/d	0.20	0.25	0.30	0.40	0.50	0.60	0.70	0.80	0.90
0.015	52	30	18	8.3	4.0	2.0	0.97	0.42	0.13
0.2	48	28	17	7.7	3.8	1.9	0.91	0.40	0.13
0.4	46	27	17	7.4	3.6	1.8	0.88	0.39	0.13
0.6	42	24	15	6.6	3.2	1.6	0.80	0.36	0.13

$t/d \geq 0.015$
$A_{or} = \pi d^2/4$
$n = \Sigma A_{or}/A_o$
where
A_o = area of duct
A_{or} = orifice area
d = diameter of perforated hole
n = free area ratio of plate, dimensionless
t = plate thickness

6-9 Obstruction, Smooth Cylinder in Round and Rectangular Ducts (Idelchik et al. 1986, Diagram 10-1)

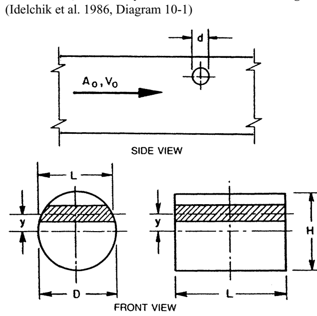

$S_m/A_o < 0.3$
$S_m = dL$
$Re' = dV_o/v$
$C_o = KC'_o$

	C'_o			
	S_m/A_o			
Re′	0.05	0.10	0.15	0.20
0.1	3.9	8.4	14	19
0.5	1.5	3.2	5.2	7.1
1	0.66	1.4	2.3	3.2
5	0.30	0.64	1.1	1.4
10	0.17	0.38	0.62	0.84
50	0.11	0.24	0.38	0.52
100	0.10	0.21	0.35	0.47
500 to 200,000	0.07	0.15	0.24	0.33
3×10^5	0.07	0.16	0.26	0.35
4×10^5	0.05	0.11	0.19	0.25
5×10^5	0.04	0.09	0.14	0.19
6×10^5 to 10^6	0.02	0.05	0.07	0.10

For obstruction offset from the centerline, use the following factors:

y/D or y/H	0	0.05	0.10	0.15	0.20	0.25	0.30	0.35	0.40
K	1.0	0.97	0.93	0.89	0.84	0.79	0.74	0.67	0.58

© 2021 ASHRAE (www.ashrae.org). For personal use only. Additional reproduction, distribution, or transmission in either print or digital form is not permitted without ASHRAE's prior written permission.

6-10 Round Duct, Depressed to Avoid an Obstruction (SMACNA 1981,Table 6-14I)

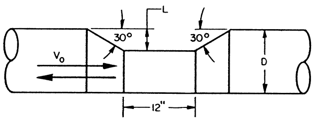

$L/D = 0.33$
$C_o = 0.24$

6-11 Rectangular Duct, Depressed to Avoid an Obstruction (SMACNA 1981, Table 6-14J)

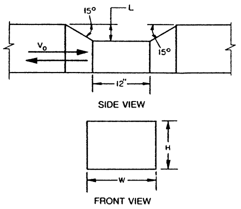

	C_o			
	L/H			
W/H	**0.125**	**0.15**	**0.25**	**030**
1.0	0.26	0.30	0.33	0.35
4.0	0.10	0.14	0.22	0.30

7 FAN-SYSTEM CONNECTIONS

7-1 Fans Discharging into a Plenum (AMCA 1973, Figure 19)

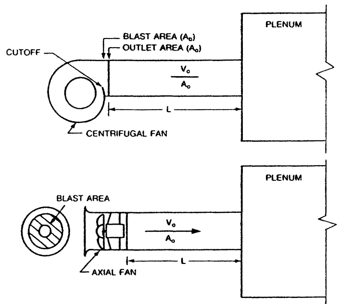

	C_o				
	L/L_e				
A_b/A_o	**0**	**0.12**	**0.25**	**0.5**	**≥1.0**
0.4	2.0	1.0	0.40	0.18	0
0.5	2.0	1.0	0.40	0.18	0
0.6	1.0	0.66	0.33	0.14	0
0.7	0.8	0.40	0.14	0	0
0.8	0.47	0.22	0.10	0	0
0.9	0.22	0.14	0	0	0
1.0	0	0	0	0	0

Calculate effective duct length.

$V_o > 2500$ fpm: $L_e = V\sqrt{A_o}/10{,}600$

$V_o \le 2500$ fpm: $L_e = \sqrt{A_o}/4.3$

where
V_o = duct velocity, fpm
L_e = effective duct length, ft
A_o = duct area, in.^{2}

© 2021 ASHRAE (www.ashrae.org). For personal use only. Additional reproduction, distribution, or transmission in either print or digital form is not permitted without ASHRAE's prior written permission.

7-2 Single Width Single Inlet (SWSI) Fan with an Outlet Duct Elbow (AMCA 1973, Figure 22)

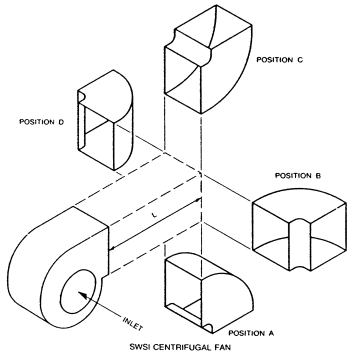

A_b = centrifugal fan blast area (see Fitting 7-1)
A_o = duct/outlet area (see Fitting 7-1)

To calculate effective duct length L_e, see Fitting 7-1.

		C_o				
	Outlet Elbow	L/L_e				
A_b/A_o	**Position**	**0**	**0.12**	**0.25**	**0.5**	**≥1.0**
0.4	A	3.2	2.7	1.8	0.84	0
	B	4.0	3.3	2.2	1.0	0
	C	5.8	4.8	3.2	1.5	0
	D	5.8	4.8	3.2	1.5	0
0.5	A	2.3	1.9	1.3	0.60	0
	B	2.8	2.4	1.6	0.72	0
	C	4.0	3.3	2.2	1.0	0
	D	4.0	3.3	2.2	1.0	0
0.6	A	1.6	1.3	0.88	0.40	0
	B	2.0	1.7	1.1	0.52	0
	C	2.9	2.4	1.6	0.76	0
	D	2.9	2.4	1.6	0.76	0
0.7	A	1.1	0.88	0.60	0.28	0
	B	1.3	1.1	0.72	0.36	0
	C	2.0	1.6	1.1	0.52	0
	D	2.0	1.6	1.1	0.52	0

© 2021 ASHRAE (www.ashrae.org). For personal use only. Additional reproduction, distribution, or transmission in either print or digital form is not permitted without ASHRAE's prior written permission.

		C_o				
	Outlet Elbow	L/L_e				
A_b/A_o	**Position**	**0**	**0.12**	**0.25**	**0.5**	**≥1.0**
0.8	A	0.76	0.64	0.44	0.20	0
	B	0.96	0.80	0.52	0.24	0
	C	1.4	1.2	0.76	0.36	0
	D	1.4	1.2	0.76	0.36	0
0.9	A	0.60	0.48	0.32	0.16	0
	B	0.76	0.64	0.44	0.20	0
	C	1.1	0.92	0.64	0.28	0
	D	1.1	0.92	0.64	0.28	0
1.0	A	0.56	0.48	0.32	0.16	0
	B	0.68	0.56	0.36	0.16	0
	C	1.0	0.84	0.56	0.26	0
	D	1.0	0.84	0.56	0.16	0

7-3 Double Width Double Inlet (DWDI) Fan with an Outlet Duct Elbow (AMCA 1973, Figure 22)

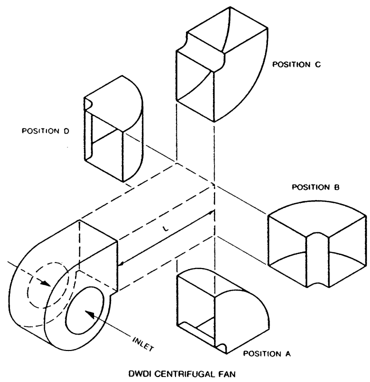

A_b = centrifugal fan blast area (see Fitting 7-1)
A_o = duct/outlet area (see Fitting 7-1)

To calculate effective duct length L_e, see Fitting 7-1.

© 2021 ASHRAE (www.ashrae.org). For personal use only. Additional reproduction, distribution, or transmission in either print or digital form is not permitted without ASHRAE's prior written permission.

		C_o				
	Outlet Elbow Posi-	L/L_e				
A_b/A_o	**tion**	**0**	**0.12**	**0.25**	**0.5**	**≥1.0**
0.4	A	3.2	2.7	1.8	0.84	0
	B	5.0	4.2	2.8	1.3	0
	C	5.8	4.8	3.2	1.5	0
	D	4.9	4.1	2.7	1.3	0
0.5	A	2.3	1.9	1.3	0.60	0
	B	3.6	3.0	2.0	0.90	0
	C	4 0	3-3	2.2	1.0	0
	D	3.4	2.8	19	0.88	0
0.6	A	1.6	1.3	0.88	0.40	0
	B	2.5	2.1	1.4	0.65	0
	C	2.9	2.4	1.6	0.76	0
	D	2.5	2.1	1.4	0.65	0
0.7	A	1.1	0.88	0.60	0.28	0
	B	1.7	1.4	0.90	0.45	0
	C	2 0	1.6	1.1	0.52	0
	D	1.7	1.4	0.92	0.44	0

		C_o				
	Outlet Elbow Posi-	L/L_e				
A_b/A_o	**tion**	**0**	**0.12**	**0.25**	**0.5**	**≥1.0**
0.8	A	0.76	0.64	0.44	0.20	0
	B	1.2	1.0	0.65	0.30	0
	C	1.4	1.2	0.76	0.36	0
	D	1.2	0.99	0.65	0.31	0
0.9	A	0.60	0.48	0.32	0.16	0
	B	0.95	0.80	0.55	0.25	0
	C	1.1	0.92	0.64	0.28	0
	D	0.95	0.78	0.54	0.24	0
1.0	A	0.56	0.48	0.32	0.16	0
	B	0.85	0.70	0.45	0.20	0
	C	1.0	0.84	0.56	0.28	0
	D	0.85	0.71	0.48	0.24	0

7-4 Nonuniform Elbow into a Fan Inlet Induced by a 90° Round Smooth Radius Elbow Without Vanes (AMCA 1973, Fig. 27)

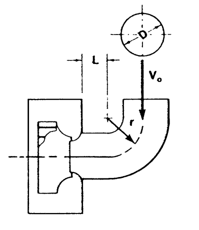

	C_o		
	L/D		
r/D	**0**	**2.0**	**≥5.0**
0.75	1.4	0.80	0.40
1.0	1.2	0.66	0.33
1.5	1.1	0.60	0.33
2.0	1.0	0.53	0.33
3.0	0.66	0.40	0.22

© 2021 ASHRAE (www.ashrae.org). For personal use only. Additional reproduction, distribution, or transmission in either print or digital form is not permitted without ASHRAE's prior written permission.

7-5 Nonuniform Elbow into a Fan Inlet Induced by 90° Mitered and Multipiece Elbows Without Vanes (AMCA 1973, Fig. 29)

Mitered

L/D	0	2.0	≥5.0
C_o	3.2	2.0	1.0

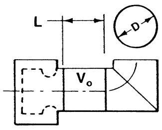

Three-Piece

	C_o		
	L/D		
r/D	0	2.0	≥5.0
0.50	2.5	1.6	0.80
0.75	1.6	1.0	0.47
1.0	1.2	0.66	0.33
1.5	1.1	0.60	0.33
2.0	1.0	0.53	0.33
3.0	0.80	0.47	0.26

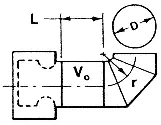

Four-Piece or more

	C_o		
	L/D		
r/D	0	2.0	≥5.0
0.50	1.8	1.0	0.53
0.75	1.4	0.80	0.40
1.0	1.2	0.66	0.33
1.5	1.1	0.60	0.33
2.0	1.0	0.53	0.33
3.0	0.66	0.40	0.22

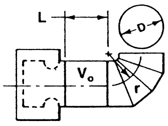

7-6 Nonuniform Elbow into a Fan Inlet Induced by a 90° Square Smooth Radius Elbow (AMCA 1973, Figure 35A)

Square Elbow with an Inlet Transition,[a] No Vanes

	C_o		
	L/D		
r/D	0	2.5	≥6.0
0.50	2.5	1.6	0.80
0.75	2.0	1.2	0.66
1.0	1.2	0.66	0.33
1.5	1.0	0.57	0.30
2.0	0.8	0.47	0.26

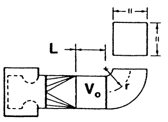

© 2021 ASHRAE (www.ashrae.org). For personal use only. Additional reproduction, distribution, or transmission in either print or digital form is not permitted without ASHRAE's prior written permission.

Square Elbow with an Inlet Transition,[a] Full Radius Vanes Equally Spaced

	C_o		
	L/D		
r/D	0	2.5	≥6.0
0.50	0.80	0.47	0.26
1.0	0.53	0.33	0.18
1.5	0.40	0.28	0.16
2.0	1.26	0.22	0.14

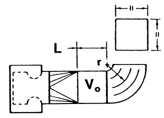

Square Elbow with an Inlet Transition,[a] Short Vanes per Fitting 3.8

	C_o		
	L/D		
r/D	0	2.5	≥6.0
0.50	0.80	0.47	0.26
1.0	0.53	0.33	0.18
1.5	0.40	0.28	0.16
2.0	0.26	0.22	0.14

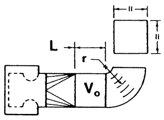

[a] The inside area of the square duct ($H \times H$) is equal to the inside area circumscribed by the fan inlet collar. The maximum angle of any converging element of the transition is 15° and, for a diverging element, 7.5°.

7-7 Fans Located in Plenums and Cabinet Enclosures (AMCA 1973, Figure 35A)

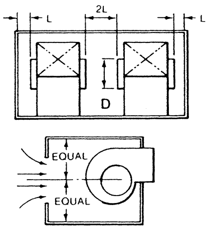

L	C_o
0.75 D	0.22
0.5 D	0.40
0.4 D	0.53
0.3 D	0.80
0.2 D	1.2

7-8 Fan Without an Outlet Diffuser (AMCA 1973, Figure 19)

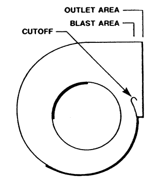

Poor; should not be used.

A_b/A_o	0.4	0.5	0.6	0.7	0.8	0.9	1.0
C_o	2.0	2.0	1.0	0.80	0.47	0.22	0

© 2021 ASHRAE (www.ashrae.org). For personal use only. Additional reproduction, distribution, or transmission in either print or digital form is not permitted without ASHRAE's prior written permission.

7-9 Plane Asymmetric Diffuser at Fan Outlet Without Ductwork (Idelchik et al. 1986, Diagram 11-11)

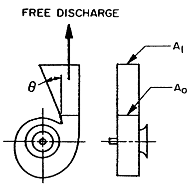

	C_o					
θ,	A_1/A_o					
degrees	1.5	2.0	2.5	3.0	3.5	4.0
10	0.51	0.34	0.25	0.21	0.18	0.17
15	0.54	0.36	0.27	0.24	0.22	0.20
20	0.55	0.38	0.31	0.27	0.25	0.24
25	0.59	0.43	0.37	0.35	0.33	0.33
30	0.63	0.50	0.46	0.44	0.43	0.42
35	0.65	0.56	0.53	0.52	0.51	0.50

If diffuser has a screen, use Fitting 6-7 to calculate screen resistance.

7-10 Pyramidal Diffuser at Fan Outlet Without Ductwork (Idelchik et al. 1986, Diagram 11-11)

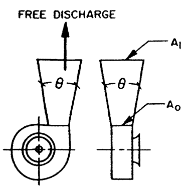

	C_o					
θ,	A_1/A_o					
degrees	1.5	2.0	2.5	3.0	3.5	4.0
10	0.54	0.42	0.37	0.34	0.32	0.31
15	0.67	0.58	0.53	0.51	0.50	0.51
20	0.75	0.67	0.65	0.64	0.64	0.65
25	0.80	0.74	0.72	0.70	0.70	0.72
30	0.85	0.78	0.76	0.75	0.75	0.76

If diffuser has a screen, use Fitting 6-7 to calculate screen resistance.

7-11 Plane Symmetric Diffuser at Fan Outlet with Ductwork (Idelchik et al. 1986, Diagram 5-12)

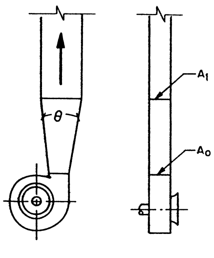

	C_o					
θ,	A_1/A_o					
degrees	1.5	2.0	2.5	3.0	3.5	4.0
10	0.05	0.07	0.09	0.10	0.11	0.11
15	0.06	0.09	0.11	0.13	0.13	0.14
20	0.07	0.10	0.13	0.15	0.16	0.16
25	0.08	0.13	0.16	0.19	0.21	0.23
30	0.16	0.29	0.39	0.32	0.34	0.35
35	0.24	0.34	0.39	0.44	0.48	0.50

© 2021 ASHRAE (www.ashrae.org). For personal use only. Additional reproduction, distribution, or transmission in either print or digital form is not permitted without ASHRAE's prior written permission.

7-12 Plane Asymmetric Diffuser at Fan Outlet with Ductwork (Idelchik et al. 1986, Diagram 5-13)

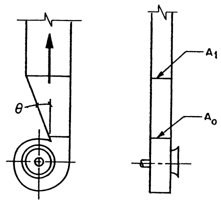

	C_o					
θ,	A_1/A_o					
degrees	1.5	2.8	2.5	3.0	3.5	4.0
10	0.08	0.09	0.10	0.10	0.11	0.11
15	0.10	0.11	0.12	0.13	0.14	0.15
20	0.12	0.14	0.15	0.16	0.17	0.18
25	0.15	0.18	0.21	0.23	0.25	0.26
30	0.18	0.25	0.30	0.33	0.35	0.35
35	0.21	0.31	0.38	0.41	0.43	0.44

7-13 Plane Asymmetric Diffuser at Fan Outlet with Ductwork (Idelchik et al. 1986, Diagram 5-14)

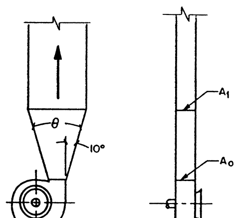

	C_o					
θ,	A_1/A_o					
degrees	1.5	2.8	2.5	3.0	3.5	4.0
10	0.05	0.08	0.11	0.13	0.13	0.14
15	0.06	0.10	0.12	0.14	0.15	0.15
20	0.07	0.11	0.14	0.15	0.16	0.16
25	0.09	0.14	0.18	0.20	0.21	0.22
30	0.13	0.18	0.23	0.26	0.28	0.29
35	0.15	0.23	0.28	0.33	0.35	0.36

7-14 Plane Asymmetric Diffuser at Fan Outlet with Ductwork (Idelchik et al. 1986, Diagram 5-15)

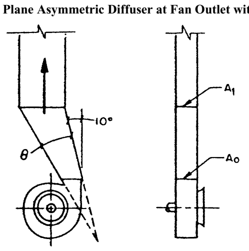

	C_o					
θ,	A_1/A_o					
degrees	1.5	2.8	2.5	3.0	3.5	4.0
10	0.11	0.13	0.14	0.14	0.14	0.14
15	0.13	0.15	0.16	0.17	0.18	0.18
20	0.19	0.22	0.24	0.26	0.28	0.30
25	0.29	0.32	0.35	0.37	0.39	0.40
30	0.36	0.42	0.46	0.49	0.51	0.51
35	0.44	0.54	0.61	0.64	0.66	0.66

© 2021 ASHRAE (www.ashrae.org). For personal use only. Additional reproduction, distribution, or transmission in either print or digital form is not permitted without ASHRAE's prior written permission.

7-15 Pyramidal Diffuser at Fan Outlet with Ductwork (Idelchik et al. 1986, Diagram 5-16)

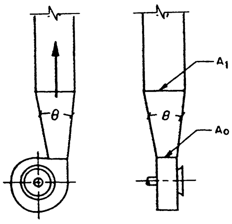

	C_o					
θ, degrees	A_1/A_o					
	1.5	**2.8**	**2.5**	**3.0**	**3.5**	**4.0**
10	0.10	0.18	0.21	0.23	0.24	0.25
15	0.23	0.33	0.38	0.40	0.42	0.44
20	0.31	0.43	0.48	0.53	0.56	0.58
25	0.36	0.49	0.55	0.58	0.62	0.64
30	0.42	0.53	0.59	0.64	0.67	0.69

8 References

ASHRAE. 2016. *ASHRAE Duct Fitting Database*, v. 6.00.01.

Idelchik, I.E., et al. 1986. *Handbook of hydraulic resistance*: *Coefficients of local resistance and of friction*. Translated from Russian by A. Barouch. Washington, DC: The U.S. Atomic Energy Commission and the National Science Foundation. https://www.nrc.gov/docs/ML1220/ML12209A041.pdf.

Locklin, D.W. 1950. Energy losses in 90-degree duct elbows. *ASHVE Trans.* 56:479.

Rozell, J.M. 1974. Duct turning vanes in 90° elbows. *ASHRAE Transactions* 80(2):53.

Jones, C.D., and C.F. Sepsy. 1969. An experimental study of losses in round miter elbows, miter tees and capped crosses. Transaction #2138. Semiannual ASHRAE Conference, San Francisco, CA.

AMCA. 1973. AMCA Publication 201, *Fans and systems*. Arlington Heights, IL: Air Movement and Control Association.

Brandt, A.D., and R.J. Steffy. 1946. *Energy losses at suction hoods*, 52:205.

SMACNA. n.d. Appendix A, Duct design tables and charts. In *HVAC systems duct design*.

Sepsy, C.F., and D.B. Pies. 1972. *Experimental study of the pressure losses in converging flow fittings used in exhaust systems*. Technical Report for National Institute for Occupational Safety and Health.

Korst, H.H., N.A. Buckley, S. Konzo, and R. W. Roose. 1950. *Fitting losses for extended-plenum forced air systems*. 56:259.

© 2021 ASHRAE (www.ashrae.org). For personal use only. Additional reproduction, distribution, or transmission in either print or digital form is not permitted without ASHRAE's prior written permission.

Appendix B

Simulation Output from Revit

```
Caminho:
Perda Total: 135,5502830318646

Secção: 52
Perda total: 31,877537439709485
Perda de carga em linha: 0,18383743970948344
Perda de carga localizada: 11,693700000000002
Perda de carga em acessórios: 20
Comprimento de conduta: 154,79999999999316
Caudal: 124,99999657825823
Velocidade: 3
Diâmetro: 125

Secção: 44
Perda total: 0,4583821077002957
Perda de carga em linha: 0,2868196077002957
Perda de carga localizada: 0,1715625
Perda de carga em acessórios: 0
Comprimento de conduta: 577,1446609405473
Caudal: 499,9999859273036
Velocidade: 3
Diâmetro: 250

Secção: 42
Perda total: 0,20478857649832338
Perda de carga em linha: 0,20478857649832338
Perda de carga localizada: 0
```

```
Perda de carga em acessórios: 0
Comprimento de conduta: 264,843586396148
Caudal: 624,9999178726473
Velocidade: 3,75
Diâmetro: 244

Secção: 41
Perda total: 62,736685839232535
Perda de carga em linha: 0,013609848643433413
Perda de carga localizada: 12,723075990589104
Perda de carga em acessórios: 50
Comprimento de conduta: 30,555175200013846
Caudal: 624,9999520715375
Velocidade: 3
Diâmetro: 273

Secção: 28
Perda total: 25,32214429989281
Perda de carga em linha: 1,2580650560659095
Perda de carga localizada: 24,0640792438269
Perda de carga em acessórios: 0
Comprimento de conduta: 1491,4248443480114
Caudal: 1124,999805467682
Velocidade: 4,5
Diâmetro: 299

Secção: 2
Perda total: 14,950744768831152
Perda de carga em linha: 1,6397822688311516
Perda de carga localizada: 13,3109625
Perda de carga em acessórios: 0
Comprimento de conduta: 1570,1059565883484
Caudal: 2089,9996347477336
Velocidade: 5,75
Diâmetro: 365

Perda Total: 135,5502830318646

#######################################
```

```
Caminho:
Perda Total: 137,26588124655996

Secção: 51
Perda total: 31,739476948706496
Perda de carga em linha: 0,21352694870649602
Perda de carga localizada: 11,52595
Perda de carga em acessórios: 20
Comprimento de conduta: 179,79999999999458
Caudal: 124,99999643535232
Velocidade: 3
Diâmetro: 125

Secção: 46
Perda total: 1,8536587056983467
Perda de carga em linha: 0,536058705698347
Perda de carga localizada: 1,3175999999999997
Perda de carga em acessórios: 0
Comprimento de conduta: 614,6446609407986
Caudal: 374,9999885532985
Velocidade: 3,5
Diâmetro: 200

Secção: 44
Perda total: 0,4583821077002957
Perda de carga em linha: 0,2868196077002957
Perda de carga localizada: 0,1715625
Perda de carga em acessórios: 0
Comprimento de conduta: 577,1446609405473
Caudal: 499,9999859273036
Velocidade: 3
Diâmetro: 250

Secção: 42
Perda total: 0,20478857649832338
Perda de carga em linha: 0,20478857649832338
Perda de carga localizada: 0
Perda de carga em acessórios: 0
Comprimento de conduta: 264,843586396148
Caudal: 624,9999178726473
```

```
Velocidade: 3,75
Diâmetro: 244

Secção: 41
Perda total: 62,736685839232535
Perda de carga em linha: 0,013609848643433413
Perda de carga localizada: 12,723075990589104
Perda de carga em acessórios: 50
Comprimento de conduta: 30,555175200013846
Caudal: 624,9999520715375
Velocidade: 3
Diâmetro: 273

Secção: 28
Perda total: 25,32214429989281
Perda de carga em linha: 1,2580650560659095
Perda de carga localizada: 24,0640792438269
Perda de carga em acessórios: 0
Comprimento de conduta: 1491,4248443480114
Caudal: 1124,999805467682
Velocidade: 4,5
Diâmetro: 299

Secção: 2
Perda total: 14,950744768831152
Perda de carga em linha: 1,6397822688311516
Perda de carga localizada: 13,3109625
Perda de carga em acessórios: 0
Comprimento de conduta: 1570,1059565883484
Caudal: 2089,9996347477336
Velocidade: 5,75
Diâmetro: 365

Perda Total: 137,26588124655996

########################################
Caminho:
Perda Total: 133,51185748817386

Secção: 50
```

```
Perda total: 27,27503945318629
Perda de carga em linha: 0,2135269487065012
Perda de carga localizada: 7,061512504479792
Perda de carga em acessórios: 20
Comprimento de conduta: 179,79999999999893
Caudal: 124,99999643535281
Velocidade: 3
Diâmetro: 125

Secção: 47
Perda total: 0,7104137371341033
Perda de carga em linha: 0,2620637371341033
Perda de carga localizada: 0,44835
Perda de carga em acessórios: 0
Comprimento de conduta: 674,9999999998704
Caudal: 249,9999925080428
Velocidade: 2,25
Diâmetro: 200

Secção: 46
Perda total: 1,8536587056983467
Perda de carga em linha: 0,536058705698347
Perda de carga localizada: 1,3175999999999997
Perda de carga em acessórios: 0
Comprimento de conduta: 614,6446609407986
Caudal: 374,9999885532985
Velocidade: 3,5
Diâmetro: 200

Secção: 44
Perda total: 0,4583821077002957
Perda de carga em linha: 0,2868196077002957
Perda de carga localizada: 0,1715625
Perda de carga em acessórios: 0
Comprimento de conduta: 577,1446609405473
Caudal: 499,9999859273036
Velocidade: 3
Diâmetro: 250

Secção: 42
```

```
Perda total: 0,20478857649832338
Perda de carga em linha: 0,20478857649832338
Perda de carga localizada: 0
Perda de carga em acessórios: 0
Comprimento de conduta: 264,843586396148
Caudal: 624,9999178726473
Velocidade: 3,75
Diâmetro: 244

Secção: 41
Perda total: 62,736685839232535
Perda de carga em linha: 0,013609848643433413
Perda de carga localizada: 12,723075990589104
Perda de carga em acessórios: 50
Comprimento de conduta: 30,555175200013846
Caudal: 624,9999520715375
Velocidade: 3
Diâmetro: 273

Secção: 28
Perda total: 25,32214429989281
Perda de carga em linha: 1,2580650560659095
Perda de carga localizada: 24,0640792438269
Perda de carga em acessórios: 0
Comprimento de conduta: 1491,4248443480114
Caudal: 1124,999805467682
Velocidade: 4,5
Diâmetro: 299

Secção: 2
Perda total: 14,950744768831152
Perda de carga em linha: 1,6397822688311516
Perda de carga localizada: 13,3109625
Perda de carga em acessórios: 0
Comprimento de conduta: 1570,1059565883484
Caudal: 2089,9996347477336
Velocidade: 5,75
Diâmetro: 365

Perda Total: 133,51185748817386
```

```
######################################

Caminho:
Perda Total: 131,64736625819086

Secção: 49
Perda total: 25,410548223203293
Perda de carga em linha: 0,922473223203293
Perda de carga localizada: 4,488075
Perda de carga em acessórios: 20
Comprimento de conduta: 776,7669914111463
Caudal: 124,99999573419305
Velocidade: 3
Diâmetro: 125

Secção: 47
Perda total: 0,7104137371341033
Perda de carga em linha: 0,2620637371341033
Perda de carga localizada: 0,44835
Perda de carga em acessórios: 0
Comprimento de conduta: 674,9999999998704
Caudal: 249,9999925080428
Velocidade: 2,25
Diâmetro: 200

Secção: 46
Perda total: 1,8536587056983467
Perda de carga em linha: 0,536058705698347
Perda de carga localizada: 1,3175999999999997
Perda de carga em acessórios: 0
Comprimento de conduta: 614,6446609407986
Caudal: 374,9999885532985
Velocidade: 3,5
Diâmetro: 200

Secção: 44
Perda total: 0,4583821077002957
Perda de carga em linha: 0,2868196077002957
Perda de carga localizada: 0,1715625
```

```
Perda de carga em acessórios: 0
Comprimento de conduta: 577,1446609405473
Caudal: 499,9999859273036
Velocidade: 3
Diâmetro: 250

Secção: 42
Perda total: 0,20478857649832338
Perda de carga em linha: 0,20478857649832338
Perda de carga localizada: 0
Perda de carga em acessórios: 0
Comprimento de conduta: 264,843586396148
Caudal: 624,9999178726473
Velocidade: 3,75
Diâmetro: 244

Secção: 41
Perda total: 62,736685839232535
Perda de carga em linha: 0,013609848643433413
Perda de carga localizada: 12,723075990589104
Perda de carga em acessórios: 50
Comprimento de conduta: 30,555175200013846
Caudal: 624,9999520715375
Velocidade: 3
Diâmetro: 273

Secção: 28
Perda total: 25,32214429989281
Perda de carga em linha: 1,2580650560659095
Perda de carga localizada: 24,0640792438269
Perda de carga em acessórios: 0
Comprimento de conduta: 1491,4248443480114
Caudal: 1124,999805467682
Velocidade: 4,5
Diâmetro: 299

Secção: 2
Perda total: 14,950744768831152
Perda de carga em linha: 1,6397822688311516
Perda de carga localizada: 13,3109625
```

Perda de carga em acessórios: 0
Comprimento de conduta: 1570,1059565883484
Caudal: 2089,9996347477336
Velocidade: 5,75
Diâmetro: 365

Perda Total: 131,64736625819086

######################################

Caminho:
Perda Total: 156,21687236073873

Secção: 54
Perda total: 53,00250887628391
Perda de carga em linha: 0,13799628908382372
Perda de carga localizada: 32,86451258720009
Perda de carga em acessórios: 20
Comprimento de conduta: 116,19953793924056
Caudal: 124,99999718890547
Velocidade: 3
Diâmetro: 125

Secção: 42
Perda total: 0,20478857649832338
Perda de carga em linha: 0,20478857649832338
Perda de carga localizada: 0
Perda de carga em acessórios: 0
Comprimento de conduta: 264,843586396148
Caudal: 624,9999178726473
Velocidade: 3,75
Diâmetro: 244

Secção: 41
Perda total: 62,736685839232535
Perda de carga em linha: 0,013609848643433413
Perda de carga localizada: 12,723075990589104
Perda de carga em acessórios: 50
Comprimento de conduta: 30,555175200013846
Caudal: 624,9999520715375

```
Velocidade: 3
Diâmetro: 273

Secção: 28
Perda total: 25,32214429989281
Perda de carga em linha: 1,2580650560659095
Perda de carga localizada: 24,0640792438269
Perda de carga em acessórios: 0
Comprimento de conduta: 1491,4248443480114
Caudal: 1124,999805467682
Velocidade: 4,5
Diâmetro: 299

Secção: 2
Perda total: 14,950744768831152
Perda de carga em linha: 1,6397822688311516
Perda de carga localizada: 13,3109625
Perda de carga em acessórios: 0
Comprimento de conduta: 1570,1059565883484
Caudal: 2089,9996347477336
Velocidade: 5,75
Diâmetro: 365

Perda Total: 156,21687236073873

#######################################

Caminho:
Perda Total: 168,68081608107167

Secção: 40
Perda total: 42,73758072563451
Perda de carga em linha: 1,40176310746388
Perda de carga localizada: 21,33581761817063
Perda de carga em acessórios: 20
Comprimento de conduta: 1180,352214316686
Caudal: 124,9999955118421
Velocidade: 3
Diâmetro: 125
```

```
Secção: 30
Perda total: 85,6703462867132
Perda de carga em linha: 3,338821062869485
Perda de carga localizada: 32,33152522384371
Perda de carga em acessórios: 50
Comprimento de conduta: 2840,0203725967103
Caudal: 499,99994374340093
Velocidade: 4,25
Diâmetro: 210

Secção: 28
Perda total: 25,32214429989281
Perda de carga em linha: 1,2580650560659095
Perda de carga localizada: 24,0640792438269
Perda de carga em acessórios: 0
Comprimento de conduta: 1491,4248443480114
Caudal: 1124,999805467682
Velocidade: 4,5
Diâmetro: 299

Secção: 2
Perda total: 14,950744768831152
Perda de carga em linha: 1,6397822688311516
Perda de carga localizada: 13,3109625
Perda de carga em acessórios: 0
Comprimento de conduta: 1570,1059565883484
Caudal: 2089,9996347477336
Velocidade: 5,75
Diâmetro: 365

Perda Total: 168,68081608107167
Caminho Critico

#######################################

Caminho:
Perda Total: 163,2266846281576

Secção: 38
Perda total: 33,106902478173254
```

```
Perda de carga em linha: 1,5809524781732514
Perda de carga localizada: 11,52595
Perda de carga em acessórios: 20
Comprimento de conduta: 1331,2383158074617
Caudal: 124,99999546681397
Velocidade: 3
Diâmetro: 125

Secção: 32
Perda total: 4,176546794547198
Perda de carga em linha: 0,3202030445471977
Perda de carga localizada: 3,8563437499999997
Perda de carga em acessórios: 0
Comprimento de conduta: 367,14466094068814
Caudal: 374,9999890625896
Velocidade: 3,5
Diâmetro: 200

Secção: 30
Perda total: 85,6703462867132
Perda de carga em linha: 3,338821062869485
Perda de carga localizada: 32,33152522384371
Perda de carga em acessórios: 50
Comprimento de conduta: 2840,0203725967103
Caudal: 499,99994374340093
Velocidade: 4,25
Diâmetro: 210

Secção: 28
Perda total: 25,32214429989281
Perda de carga em linha: 1,2580650560659095
Perda de carga localizada: 24,0640792438269
Perda de carga em acessórios: 0
Comprimento de conduta: 1491,4248443480114
Caudal: 1124,999805467682
Velocidade: 4,5
Diâmetro: 299

Secção: 2
Perda total: 14,950744768831152
```

```
Perda de carga em linha: 1,6397822688311516
Perda de carga localizada: 13,3109625
Perda de carga em acessórios: 0
Comprimento de conduta: 1570,1059565883484
Caudal: 2089,9996347477336
Velocidade: 5,75
Diâmetro: 365

Perda Total: 163,2266846281576

#######################################

Caminho:
Perda Total: 155,14567021681813

Secção: 36
Perda total: 23,774217430790955
Perda de carga em linha: 1,0978424307909531
Perda de carga localizada: 2,676375
Perda de carga em acessórios: 20
Comprimento de conduta: 924,4363311140326
Caudal: 124,99999560439954
Velocidade: 3
Diâmetro: 125

Secção:
Perda total: 0
Perda de carga em linha: 0
Perda de carga localizada: 0
Perda de carga em acessórios: 0
Comprimento de conduta: 0
Caudal: 249,99999299743405
Velocidade: 2,25
Diâmetro: 200

Secção: 33
Perda total: 1,251670636042809
Perda de carga em linha: 0,1239331360428092
Perda de carga localizada: 1,1277374999999998
Perda de carga em acessórios: 0
```

```
Comprimento de conduta: 319,2157287525525
Caudal: 249,99999299743405
Velocidade: 2,25
Diâmetro: 200

Secção: 32
Perda total: 4,176546794547198
Perda de carga em linha: 0,3202030445471977
Perda de carga localizada: 3,8563437499999997
Perda de carga em acessórios: 0
Comprimento de conduta: 367,14466094068814
Caudal: 374,9999890625896
Velocidade: 3,5
Diâmetro: 200

Secção: 30
Perda total: 85,6703462867132
Perda de carga em linha: 3,338821062869485
Perda de carga localizada: 32,33152522384371
Perda de carga em acessórios: 50
Comprimento de conduta: 2840,0203725967103
Caudal: 499,99994374340093
Velocidade: 4,25
Diâmetro: 210

Secção: 28
Perda total: 25,32214429989281
Perda de carga em linha: 1,2580650560659095
Perda de carga localizada: 24,0640792438269
Perda de carga em acessórios: 0
Comprimento de conduta: 1491,4248443480114
Caudal: 1124,999805467682
Velocidade: 4,5
Diâmetro: 299

Secção: 2
Perda total: 14,950744768831152
Perda de carga em linha: 1,6397822688311516
Perda de carga localizada: 13,3109625
Perda de carga em acessórios: 0
```

```
Comprimento de conduta: 1570,1059565883484
Caudal: 2089,9996347477336
Velocidade: 5,75
Diâmetro: 365

Perda Total: 155,14567021681813

######################################

Caminho:
Perda Total: 162,3369871928372

Secção: 37
Perda total: 30,96553440681003
Perda de carga em linha: 2,0923219286256165
Perda de carga localizada: 8,873212478184413
Perda de carga em acessórios: 20
Comprimento de conduta: 1761,836082264166
Caudal: 124,99999561567363
Velocidade: 3
Diâmetro: 125

Secção:
Perda total: 0
Perda de carga em linha: 0
Perda de carga localizada: 0
Perda de carga em acessórios: 0
Comprimento de conduta: 0
Caudal: 249,99999299743405
Velocidade: 2,25
Diâmetro: 200

Secção: 33
Perda total: 1,251670636042809
Perda de carga em linha: 0,1239331360428092
Perda de carga localizada: 1,1277374999999998
Perda de carga em acessórios: 0
Comprimento de conduta: 319,2157287525525
Caudal: 249,99999299743405
Velocidade: 2,25
```

```
Diâmetro: 200

Secção: 32
Perda total: 4,176546794547198
Perda de carga em linha: 0,3202030445471977
Perda de carga localizada: 3,8563437499999997
Perda de carga em acessórios: 0
Comprimento de conduta: 367,14466094068814
Caudal: 374,9999890625896
Velocidade: 3,5
Diâmetro: 200

Secção: 30
Perda total: 85,6703462867132
Perda de carga em linha: 3,338821062869485
Perda de carga localizada: 32,33152522384371
Perda de carga em acessórios: 50
Comprimento de conduta: 2840,0203725967103
Caudal: 499,99994374340093
Velocidade: 4,25
Diâmetro: 210

Secção: 28
Perda total: 25,32214429989281
Perda de carga em linha: 1,2580650560659095
Perda de carga localizada: 24,0640792438269
Perda de carga em acessórios: 0
Comprimento de conduta: 1491,4248443480114
Caudal: 1124,999805467682
Velocidade: 4,5
Diâmetro: 299

Secção: 2
Perda total: 14,950744768831152
Perda de carga em linha: 1,6397822688311516
Perda de carga localizada: 13,3109625
Perda de carga em acessórios: 0
Comprimento de conduta: 1570,1059565883484
Caudal: 2089,9996347477336
Velocidade: 5,75
```

```
Diâmetro: 365

Perda Total: 162,3369871928372

#######################################

Caminho:
Perda Total: 115,48058201935689

Secção: 23
Perda total: 31,734883590096892
Perda de carga em linha: 0,20893359009689227
Perda de carga localizada: 11,52595
Perda de carga em acessórios: 20
Comprimento de conduta: 175,93217028103035
Caudal: 124,99999643013341
Velocidade: 3
Diâmetro: 125

Secção: 18
Perda total: 1,8536587056983467
Perda de carga em linha: 0,536058705698347
Perda de carga localizada: 1,3175999999999997
Perda de carga em acessórios: 0
Comprimento de conduta: 614,6446609407986
Caudal: 374,9999885532985
Velocidade: 3,5
Diâmetro: 200

Secção: 16
Perda total: 0,4583821077002957
Perda de carga em linha: 0,2868196077002957
Perda de carga localizada: 0,1715625
Perda de carga em acessórios: 0
Comprimento de conduta: 577,1446609405473
Caudal: 499,9999859273036
Velocidade: 3
Diâmetro: 250

Secção: 14
```

```
Perda total: 50,18131650847627
Perda de carga em linha: 0,1813165084762731
Perda de carga localizada: 0
Perda de carga em acessórios: 50
Comprimento de conduta: 234,48824733676923
Caudal: 624,9999234949214
Velocidade: 3,75
Diâmetro: 244

Secção: 13
Perda total: 3,0681841973325845
Perda de carga em linha: 0,026952947332584687
Perda de carga localizada: 3,04123125
Perda de carga em acessórios: 0
Comprimento de conduta: 50,55517541489892
Caudal: 624,999942794674
Velocidade: 3,25
Diâmetro: 266

Secção: 4
Perda total: 10,09633486602805
Perda de carga em linha: 5,06383486602805
Perda de carga localizada: 5,0325
Perda de carga em acessórios: 0
Comprimento de conduta: 4267,019410134665
Caudal: 964,9998081882068
Velocidade: 5
Diâmetro: 266

Secção: 3
Perda total: 3,1370772751933056
Perda de carga em linha: 0,1053772751933059
Perda de carga localizada: 3,0317
Perda de carga em acessórios: 0
Comprimento de conduta: 397,93176240001156
Caudal: 964,9999232248229
Velocidade: 2,75
Diâmetro: 365

Secção: 2
```

```
Perda total: 14,950744768831152
Perda de carga em linha: 1,6397822688311516
Perda de carga localizada: 13,3109625
Perda de carga em acessórios: 0
Comprimento de conduta: 1570,1059565883484
Caudal: 2089,9996347477336
Velocidade: 5,75
Diâmetro: 365

Perda Total: 115,48058201935689

#######################################

Caminho:
Perda Total: 109,8620670309878

Secção: 21
Perda total: 25,40595486459369
Perda de carga em linha: 0,9178798645936885
Perda de carga localizada: 4,488075
Perda de carga em acessórios: 20
Comprimento de conduta: 772,8991616921816
Caudal: 124,99999573419316
Velocidade: 3
Diâmetro: 125

Secção: 19
Perda total: 0,7104137371341033
Perda de carga em linha: 0,2620637371341033
Perda de carga localizada: 0,44835
Perda de carga em acessórios: 0
Comprimento de conduta: 674,9999999998704
Caudal: 249,9999925080428
Velocidade: 2,25
Diâmetro: 200

Secção: 18
Perda total: 1,8536587056983467
Perda de carga em linha: 0,536058705698347
Perda de carga localizada: 1,3175999999999997
```

```
Perda de carga em acessórios: 0
Comprimento de conduta: 614,6446609407986
Caudal: 374,9999885532985
Velocidade: 3,5
Diâmetro: 200

Secção: 16
Perda total: 0,4583821077002957
Perda de carga em linha: 0,2868196077002957
Perda de carga localizada: 0,1715625
Perda de carga em acessórios: 0
Comprimento de conduta: 577,1446609405473
Caudal: 499,9999859273036
Velocidade: 3
Diâmetro: 250

Secção: 14
Perda total: 50,18131650847627
Perda de carga em linha: 0,1813165084762731
Perda de carga localizada: 0
Perda de carga em acessórios: 50
Comprimento de conduta: 234,48824733676923
Caudal: 624,9999234949214
Velocidade: 3,75
Diâmetro: 244

Secção: 13
Perda total: 3,0681841973325845
Perda de carga em linha: 0,026952947332584687
Perda de carga localizada: 3,04123125
Perda de carga em acessórios: 0
Comprimento de conduta: 50,55517541489892
Caudal: 624,999942794674
Velocidade: 3,25
Diâmetro: 266

Secção: 4
Perda total: 10,09633486602805
Perda de carga em linha: 5,06383486602805
Perda de carga localizada: 5,0325
```

```
Perda de carga em acessórios: 0
Comprimento de conduta: 4267,019410134665
Caudal: 964,9998081882068
Velocidade: 5
Diâmetro: 266

Secção: 3
Perda total: 3,1370772751933056
Perda de carga em linha: 0,1053772751933059
Perda de carga localizada: 3,0317
Perda de carga em acessórios: 0
Comprimento de conduta: 397,93176240001156
Caudal: 964,9999232248229
Velocidade: 2,75
Diâmetro: 365

Secção: 2
Perda total: 14,950744768831152
Perda de carga em linha: 1,6397822688311516
Perda de carga localizada: 13,3109625
Perda de carga em acessórios: 0
Comprimento de conduta: 1570,1059565883484
Caudal: 2089,9996347477336
Velocidade: 5,75
Diâmetro: 365

Perda Total: 109,8620670309878

#######################################

Caminho:
Perda Total: 111,72655826084181

Secção: 22
Perda total: 27,27044609444771
Perda de carga em linha: 0,20893359009689808
Perda de carga localizada: 7,0615125043508105
Perda de carga em acessórios: 20
Comprimento de conduta: 175,93217028103524
Caudal: 124,99999643013194
```

```
Velocidade: 3
Diâmetro: 125

Secção: 19
Perda total: 0,7104137371341033
Perda de carga em linha: 0,2620637371341033
Perda de carga localizada: 0,44835
Perda de carga em acessórios: 0
Comprimento de conduta: 674,9999999998704
Caudal: 249,9999925080428
Velocidade: 2,25
Diâmetro: 200

Secção: 18
Perda total: 1,8536587056983467
Perda de carga em linha: 0,536058705698347
Perda de carga localizada: 1,3175999999999997
Perda de carga em acessórios: 0
Comprimento de conduta: 614,6446609407986
Caudal: 374,9999885532985
Velocidade: 3,5
Diâmetro: 200

Secção: 16
Perda total: 0,4583821077002957
Perda de carga em linha: 0,2868196077002957
Perda de carga localizada: 0,1715625
Perda de carga em acessórios: 0
Comprimento de conduta: 577,1446609405473
Caudal: 499,9999859273036
Velocidade: 3
Diâmetro: 250

Secção: 14
Perda total: 50,18131650847627
Perda de carga em linha: 0,1813165084762731
Perda de carga localizada: 0
Perda de carga em acessórios: 50
Comprimento de conduta: 234,48824733676923
Caudal: 624,9999234949214
```

```
Velocidade: 3,75
Diâmetro: 244

Secção: 13
Perda total: 3,0681841973325845
Perda de carga em linha: 0,026952947332584687
Perda de carga localizada: 3,04123125
Perda de carga em acessórios: 0
Comprimento de conduta: 50,55517541489892
Caudal: 624,999942794674
Velocidade: 3,25
Diâmetro: 266

Secção: 4
Perda total: 10,09633486602805
Perda de carga em linha: 5,06383486602805
Perda de carga localizada: 5,0325
Perda de carga em acessórios: 0
Comprimento de conduta: 4267,019410134665
Caudal: 964,9998081882068
Velocidade: 5
Diâmetro: 266

Secção: 3
Perda total: 3,1370772751933056
Perda de carga em linha: 0,1053772751933059
Perda de carga localizada: 3,0317
Perda de carga em acessórios: 0
Comprimento de conduta: 397,93176240001156
Caudal: 964,9999232248229
Velocidade: 2,75
Diâmetro: 365

Secção: 2
Perda total: 14,950744768831152
Perda de carga em linha: 1,6397822688311516
Perda de carga localizada: 13,3109625
Perda de carga em acessórios: 0
Comprimento de conduta: 1570,1059565883484
Caudal: 2089,9996347477336
```

Velocidade: 5,75
Diâmetro: 365

Perda Total: 111,72655826084181

######################################

Caminho:
Perda Total: 113,76498380466154

Secção: 24
Perda total: 31,87294408109988
Perda de carga em linha: 0,17924408109987905
Perda de carga localizada: 11,693700000000002
Perda de carga em acessórios: 20
Comprimento de conduta: 150,93217028102842
Caudal: 124,99999657026508
Velocidade: 3
Diâmetro: 125

Secção: 16
Perda total: 0,4583821077002957
Perda de carga em linha: 0,2868196077002957
Perda de carga localizada: 0,1715625
Perda de carga em acessórios: 0
Comprimento de conduta: 577,1446609405473
Caudal: 499,9999859273036
Velocidade: 3
Diâmetro: 250

Secção: 14
Perda total: 50,18131650847627
Perda de carga em linha: 0,1813165084762731
Perda de carga localizada: 0
Perda de carga em acessórios: 50
Comprimento de conduta: 234,48824733676923
Caudal: 624,9999234949214
Velocidade: 3,75
Diâmetro: 244

```
Secção: 13
Perda total: 3,0681841973325845
Perda de carga em linha: 0,026952947332584687
Perda de carga localizada: 3,04123125
Perda de carga em acessórios: 0
Comprimento de conduta: 50,55517541489892
Caudal: 624,999942794674
Velocidade: 3,25
Diâmetro: 266

Secção: 4
Perda total: 10,09633486602805
Perda de carga em linha: 5,06383486602805
Perda de carga localizada: 5,0325
Perda de carga em acessórios: 0
Comprimento de conduta: 4267,019410134665
Caudal: 964,9998081882068
Velocidade: 5
Diâmetro: 266

Secção: 3
Perda total: 3,1370772751933056
Perda de carga em linha: 0,1053772751933059
Perda de carga localizada: 3,0317
Perda de carga em acessórios: 0
Comprimento de conduta: 397,93176240001156
Caudal: 964,9999232248229
Velocidade: 2,75
Diâmetro: 365

Secção: 2
Perda total: 14,950744768831152
Perda de carga em linha: 1,6397822688311516
Perda de carga localizada: 13,3109625
Perda de carga em acessórios: 0
Comprimento de conduta: 1570,1059565883484
Caudal: 2089,9996347477336
Velocidade: 5,75
Diâmetro: 365
```

```
Perda Total: 113,76498380466154

#######################################

Caminho:
Perda Total: 134,43157312601528

Secção: 26
Perda total: 52,99791551015392
Perda de carga em linha: 0,133402930474219
Perda de carga localizada: 32,864512579679705
Perda de carga em acessórios: 20
Comprimento de conduta: 112,33170822027553
Caudal: 124,99999713921746
Velocidade: 3
Diâmetro: 125

Secção: 14
Perda total: 50,18131650847627
Perda de carga em linha: 0,1813165084762731
Perda de carga localizada: 0
Perda de carga em acessórios: 50
Comprimento de conduta: 234,48824733676923
Caudal: 624,9999234949214
Velocidade: 3,75
Diâmetro: 244

Secção: 13
Perda total: 3,0681841973325845
Perda de carga em linha: 0,026952947332584687
Perda de carga localizada: 3,04123125
Perda de carga em acessórios: 0
Comprimento de conduta: 50,55517541489892
Caudal: 624,999942794674
Velocidade: 3,25
Diâmetro: 266

Secção: 4
Perda total: 10,09633486602805
Perda de carga em linha: 5,06383486602805
```

```
Perda de carga localizada: 5,0325
Perda de carga em acessórios: 0
Comprimento de conduta: 4267,019410134665
Caudal: 964,9998081882068
Velocidade: 5
Diâmetro: 266

Secção: 3
Perda total: 3,1370772751933056
Perda de carga em linha: 0,1053772751933059
Perda de carga localizada: 3,0317
Perda de carga em acessórios: 0
Comprimento de conduta: 397,93176240001156
Caudal: 964,9999232248229
Velocidade: 2,75
Diâmetro: 365

Secção: 2
Perda total: 14,950744768831152
Perda de carga em linha: 1,6397822688311516
Perda de carga localizada: 13,3109625
Perda de carga em acessórios: 0
Comprimento de conduta: 1570,1059565883484
Caudal: 2089,9996347477336
Velocidade: 5,75
Diâmetro: 365

Perda Total: 134,43157312601528

#######################################

Caminho:
Perda Total: 110,17891734523124

Secção: 12
Perda total: 32,95626995260991
Perda de carga em linha: 1,858844744336975
Perda de carga localizada: 11,09742520827293
Perda de carga em acessórios: 20
Comprimento de conduta: 1565,2370206965368
```

```
Caudal: 124,99999576882671
Velocidade: 3
Diâmetro: 125

Secção: 8
Perda total: 49,038490482568825
Perda de carga em linha: 3,2135654825688236
Perda de carga localizada: 15,824925
Perda de carga em acessórios: 30
Comprimento de conduta: 3419,69543411155
Caudal: 249,99997288871415
Velocidade: 3,25
Diâmetro: 169

Secção: 4
Perda total: 10,09633486602805
Perda de carga em linha: 5,06383486602805
Perda de carga localizada: 5,0325
Perda de carga em acessórios: 0
Comprimento de conduta: 4267,019410134665
Caudal: 964,9998081882068
Velocidade: 5
Diâmetro: 266

Secção: 3
Perda total: 3,1370772751933056
Perda de carga em linha: 0,1053772751933059
Perda de carga localizada: 3,0317
Perda de carga em acessórios: 0
Comprimento de conduta: 397,93176240001156
Caudal: 964,9999232248229
Velocidade: 2,75
Diâmetro: 365

Secção: 2
Perda total: 14,950744768831152
Perda de carga em linha: 1,6397822688311516
Perda de carga localizada: 13,3109625
Perda de carga em acessórios: 0
Comprimento de conduta: 1570,1059565883484
```

```
Caudal: 2089,9996347477336
Velocidade: 5,75
Diâmetro: 365

Perda Total: 110,17891734523124

#######################################

Caminho:
Perda Total: 101,29819448911282

Secção: 10
Perda total: 22,981360484870816
Perda de carga em linha: 1,1696604848708163
Perda de carga localizada: 1,8117
Perda de carga em acessórios: 20
Comprimento de conduta: 984,9106000612672
Caudal: 124,9999955802214
Velocidade: 3
Diâmetro: 125

Secção: 9
Perda total: 1,0941866116206707
Perda de carga em linha: 0,0015241116206706955
Perda de carga localizada: 1,0926624999999999
Perda de carga em acessórios: 0
Comprimento de conduta: 4,999964195817894
Caudal: 124,99999448854102
Velocidade: 1,75
Diâmetro: 169

Secção: 8
Perda total: 49,038490482568825
Perda de carga em linha: 3,2135654825688236
Perda de carga localizada: 15,824925
Perda de carga em acessórios: 30
Comprimento de conduta: 3419,69543411155
Caudal: 249,99997288871415
Velocidade: 3,25
Diâmetro: 169
```

```
Secção: 4
Perda total: 10,09633486602805
Perda de carga em linha: 5,06383486602805
Perda de carga localizada: 5,0325
Perda de carga em acessórios: 0
Comprimento de conduta: 4267,019410134665
Caudal: 964,9998081882068
Velocidade: 5
Diâmetro: 266

Secção: 3
Perda total: 3,1370772751933056
Perda de carga em linha: 0,1053772751933059
Perda de carga localizada: 3,0317
Perda de carga em acessórios: 0
Comprimento de conduta: 397,93176240001156
Caudal: 964,9999232248229
Velocidade: 2,75
Diâmetro: 365

Secção: 2
Perda total: 14,950744768831152
Perda de carga em linha: 1,6397822688311516
Perda de carga localizada: 13,3109625
Perda de carga em acessórios: 0
Comprimento de conduta: 1570,1059565883484
Caudal: 2089,9996347477336
Velocidade: 5,75
Diâmetro: 365

Perda Total: 101,29819448911282

#######################################

Caminho:
Perda Total: 76,27900723025869

Secção: 6
Perda total: 48,09485032020618
```

```
Perda de carga em linha: 6,737606570206184
Perda de carga localizada: 21,357243749999995
Perda de carga em acessórios: 20
Comprimento de conduta: 9573,089743490138
Caudal: 89,99999673887346
Velocidade: 2,25
Diâmetro: 125

Secção: 4
Perda total: 10,09633486602805
Perda de carga em linha: 5,06383486602805
Perda de carga localizada: 5,0325
Perda de carga em acessórios: 0
Comprimento de conduta: 4267,019410134665
Caudal: 964,9998081882068
Velocidade: 5
Diâmetro: 266

Secção: 3
Perda total: 3,1370772751933056
Perda de carga em linha: 0,1053772751933059
Perda de carga localizada: 3,0317
Perda de carga em acessórios: 0
Comprimento de conduta: 397,93176240001156
Caudal: 964,9999232248229
Velocidade: 2,75
Diâmetro: 365

Secção: 2
Perda total: 14,950744768831152
Perda de carga em linha: 1,6397822688311516
Perda de carga localizada: 13,3109625
Perda de carga em acessórios: 0
Comprimento de conduta: 1570,1059565883484
Caudal: 2089,9996347477336
Velocidade: 5,75
Diâmetro: 365

Perda Total: 76,27900723025869
```

```
#######################################
```

Appendix C

Duct Pressure Loss Report

Duct Pressure Loss Report

Project Name	CONSTRUÇÃO DE UNIDADE HOSPITALAR
Project Issue Date	SETEMBRO 2024
Project Status	LICENCIAMENTO
Client Name	REMOTO & PRESENTE S.A.
Project Address	AVENIDA DOM MENDO, MAIA
Project Number	1585
Organization Name	ASL
Organization Description	
Building Name	
Author	SNC
IfcSite GUID	
IfcBuilding GUID	
IfcProject GUID	
04-COD-Esp	
Run Time	26/05/2025 11:53:10

Mechanical ASL-MEC-DS-ACO.GALV-AR NOVO 107

System Information	
System Classification	Supply Air
System Type	ASL-MEC-DS-ACO.GALV-AR NOVO
System Name	Mechanical ASL-MEC-DS-ACO.GALV-AR NOVO 107
Abbreviation	

Total Pressure Loss Calculations by Sections

Section	Element	Flow	Size	Velocity	Velocity Pressure	Length	Loss Coefficient	Friction	Equivalent Diameter	Diameter	Free Size	Height	Hydraulic Diameter	Overall Size	Reynolds number	Width	Total Pressure Loss	Section Pressure Loss
220	Duct	100 m^3/h	125 mmx200 mm	1.5 m/s	-	0.629	-	0.24 Pa/m	-	-	125 mmx200 mm	200 mm	154 mm	185 mmx260 mm	15317.92863	125 mm	0.1 Pa	0.1 Pa
	Fittings	100 m^3/h	-	1.5 m/s	1.3 Pa	-	0	-	-	-	-	-	-	-	-	-	0.0 Pa	
	Air Terminal	100 m^3/h	-	-	-	-	-	-	-	-	-	-	-	-	-	-	0.0 Pa	

Critical Path : ; Total Pressure Loss : 0.0 Pa

Detail Information of Straight Segment by Sections

Section	Element ID	Flow	Size	Velocity	Velocity Pressure	Length	Pressure Loss	Total Pressure Loss
220	8176914	100 m^3/h	125 mmx200 mm	1.5 m/s	1.3 Pa	0.629	0.1 Pa	0.1 Pa

Fitting and Accessory Loss Coefficient Summary by Sections

Section	Element ID	Loss Method	ASHRAE Table	Loss Coefficient	Pressure Loss	Total Pressure Loss
220	8176911	Coefficient from ASHRAE Table	CD6-4	0	0.0 Pa	0.0 Pa

Mechanical ASL-MEC-DS-ACO.GALV-AR NOVO 15

System Information	
System Classification	Supply Air
System Type	ASL-MEC-DS-ACO.GALV-AR NOVO
System Name	Mechanical ASL-MEC-DS-ACO.GALV-AR NOVO 15
Abbreviation	

Total Pressure Loss Calculations by Sections

Section	Element	Flow	Size	Velocity	Velocity Pressure	Length	Loss Coefficient	Friction	Equivalent Diameter	Diameter	Free Size	Height	Hydraulic Diameter	Overall Size	Reynolds number	Width	Total Pressure Loss	Section Pressure Loss
179	Duct	100 m^3/h	125 mmx200 mm	1.5 m/s	-	0.629	-	0.24 Pa/m	-	-	125 mmx200 mm	200 mm	154 mm	185 mmx260 mm	15317.92863	125 mm	0.1 Pa	0.1 Pa
	Fittings	100 m^3/h	-	1.5 m/s	1.3 Pa	-	0	-	-	-	-	-	-	-	-	-	0.0 Pa	
	Air Terminal	100 m^3/h	-	-	-	-	-	-	-	-	-	-	-	-	-	-	0.0 Pa	

Critical Path : ; Total Pressure Loss : 0.0 Pa

Detail Information of Straight Segment by Sections

Section	Element ID	Flow	Size	Velocity	Velocity Pressure	Length	Pressure Loss	Total Pressure Loss
179	5140485	100 m^3/h	125 mmx200 mm	1.5 m/s	1.3 Pa	0.629	0.1 Pa	0.1 Pa

Fitting and Accessory Loss Coefficient Summary by Sections

Section	Element ID	Loss Method	ASHRAE Table	Loss Coefficient	Pressure Loss	Total Pressure Loss
179	5139468	Coefficient from ASHRAE Table	CD6-4	0	0.0 Pa	0.0 Pa

Mechanical ASL-MEC-DS-ACO.GALV-AR NOVO 27

System Information	
System Classification	Supply Air
System Type	ASL-MEC-DS-ACO.GALV-AR NOVO
System Name	Mechanical ASL-MEC-DS-ACO.GALV-AR NOVO 27
Abbreviation	

Total Pressure Loss Calculations by Sections

Section	Element	Flow	Size	Velocity	Velocity Pressure	Length	Loss Coefficient	Friction	Equivalent Diameter	Diameter	Free Size	Height	Hydraulic Diameter	Overall Size	Reynolds number	Width	Total Pressure Loss	Section Pressure Loss
1	Duct	0 m^3/h	1450 mmx350 mm	0.0 m/s	-	0.715	-	0.00 Pa/m	-	-	1450 mmx350 mm	350 mm	564 mm	1450 mmx350 mm	0	1450 mm	0.0 Pa	0.0 Pa
	Air Terminal	0 m^3/h	-	-	-	-	-	-	-	-	-	-	-	-	-	-	0.0 Pa	

Critical Path : ; Total Pressure Loss : 0.0 Pa

Detail Information of Straight Segment by Sections

Section	Element ID	Flow	Size	Velocity	Velocity Pressure	Length	Pressure Loss	Total Pressure Loss
1	6726528	0 m^3/h	1450 mmx350 mm	0.0 m/s	0.0 Pa	0.715	0.0 Pa	0.0 Pa

Fitting and Accessory Loss Coefficient Summary by Sections

Section	Element ID	Loss Method	ASHRAE Table	Loss Coefficient	Pressure Loss	Total Pressure Loss

Mechanical ASL-MEC-DS-ACO.GALV-AR NOVO 35

System Information	
System Classification	Supply Air
System Type	ASL-MEC-DS-ACO.GALV-AR NOVO
System Name	Mechanical ASL-MEC-DS-ACO.GALV-AR NOVO 35
Abbreviation	

Total Pressure Loss Calculations by Sections

Section	Element	Flow	Size	Velocity	Velocity Pressure	Length	Loss Coefficient	Friction	Equivalent Diameter	Diameter	Free Size	Height	Hydraulic Diameter	Overall Size	Reynolds number	Width	Total Pressure Loss	Section Pressure Loss

Critical Path : ; Total Pressure Loss : 0.0 Pa

Detail Information of Straight Segment by Sections

Section	Element ID	Flow	Size	Velocity	Velocity Pressure	Length	Pressure Loss	Total Pressure Loss

Fitting and Accessory Loss Coefficient Summary by Sections

Section	Element ID	Loss Method	ASHRAE Table	Loss Coefficient	Pressure Loss	Total Pressure Loss

Mechanical ASL-MEC-DS-ACO.GALV-EXAUSTAO 4

System Information	
System Classification	Exhaust Air
System Type	ASL-MEC-DS-ACO.GALV-EXAUSTAO
System Name	Mechanical ASL-MEC-DS-ACO.GALV-EXAUSTAO 4
Abbreviation	

Total Pressure Loss Calculations by Sections

Section	Element	Flow	Size	Velocity	Velocity Pressure	Length	Loss Coefficient	Friction	Equivalent Diameter	Diameter	Free Size	Height	Hydraulic Diameter	Overall Size	Reynolds number	Width	Total Pressure Loss	Section Pressure Loss

Critical Path : ; Total Pressure Loss : 0.0 Pa

Detail Information of Straight Segment by Sections

Section	Element ID	Flow	Size	Velocity	Velocity Pressure	Length	Pressure Loss	Total Pressure Loss

Fitting and Accessory Loss Coefficient Summary by Sections

Section	Element ID	Loss Method	ASHRAE Table	Loss Coefficient	Pressure Loss	Total Pressure Loss

Mechanical ASL-MEC-DS-ACO.GALV-EXAUSTAO 5

System Information	
System Classification	Exhaust Air
System Type	ASL-MEC-DS-ACO.GALV-EXAUSTAO
System Name	Mechanical ASL-MEC-DS-ACO.GALV-EXAUSTAO 5
Abbreviation	

Total Pressure Loss Calculations by Sections

					Velocity		Loss		Equivalent		Free		Hydraulic	Overall	Reynolds		Total	

Section	Element	Flow	Size	Velocity	Pressure	Length	Coefficient	Friction	Diameter	Diameter	Size	Height	Diameter	Size	number	Width	Pressure Loss	Section Pressure Loss

Critical Path : ; Total Pressure Loss : 0.0 Pa

Detail Information of Straight Segment by Sections

Section	Element ID	Flow	Size	Velocity	Velocity Pressure	Length	Pressure Loss	Total Pressure Loss

Fitting and Accessory Loss Coefficient Summary by Sections

Section	Element ID	Loss Method	ASHRAE Table	Loss Coefficient	Pressure Loss	Total Pressure Loss

Mechanical ASL-MEC-DS-ACO.GALV-EXTRACAO GERAIS 1

System Information	
System Classification	Exhaust Air
System Type	ASL-MEC-DS-ACO.GALV-EXTRACAO GERAIS
System Name	Mechanical ASL-MEC-DS-ACO.GALV-EXTRACAO GERAIS 1
Abbreviation	

Total Pressure Loss Calculations by Sections

Section	Element	Flow	Size	Velocity	Velocity Pressure	Length	Loss Coefficient	Friction	Equivalent Diameter	Diameter	Free Size	Height	Hydraulic Diameter	Overall Size	Reynolds number	Width	Total Pressure Loss	Section Pressure Loss
220	Fittings	100 m^3/h	-	1.5 m/s	1.3 Pa	-	0	-	-	-	-	-	-	-	-	-	0.0 Pa	0.0 Pa

Critical Path : ; Total Pressure Loss : 0.0 Pa

Detail Information of Straight Segment by Sections

Section	Element ID	Flow	Size	Velocity	Velocity Pressure	Length	Pressure Loss	Total Pressure Loss

Fitting and Accessory Loss Coefficient Summary by Sections

Section	Element ID	Loss Method	ASHRAE Table	Loss Coefficient	Pressure Loss	Total Pressure Loss
220	8176911	Coefficient from ASHRAE Table	CD6-4	0	0.0 Pa	0.0 Pa

Mechanical ASL-MEC-DS-ACO.GALV-EXTRACAO GERAIS 10

System Information	
System Classification	Exhaust Air
System Type	ASL-MEC-DS-ACO.GALV-EXTRACAO GERAIS
System Name	Mechanical ASL-MEC-DS-ACO.GALV-EXTRACAO GERAIS 10
Abbreviation	

Total Pressure Loss Calculations by Sections

Section	Element	Flow	Size	Velocity	Velocity Pressure	Length	Loss Coefficient	Friction	Equivalent Diameter	Diameter	Free Size	Height	Hydraulic Diameter	Overall Size	Reynolds number	Width	Total Pressure Loss	Section Pressure Loss

Critical Path : ; Total Pressure Loss : 0.0 Pa

Detail Information of Straight Segment by Sections

Section	Element ID	Flow	Size	Velocity	Velocity Pressure	Length	Pressure Loss	Total Pressure Loss

Fitting and Accessory Loss Coefficient Summary by Sections

Section	Element ID	Loss Method	ASHRAE Table	Loss Coefficient	Pressure Loss	Total Pressure Loss

Mechanical ASL-MEC-DS-ACO.GALV-EXTRACAO GERAIS 13

System Information	
System Classification	Exhaust Air
System Type	ASL-MEC-DS-ACO.GALV-EXTRACAO GERAIS
System Name	Mechanical ASL-MEC-DS-ACO.GALV-EXTRACAO GERAIS 13
Abbreviation	

Total Pressure Loss Calculations by Sections

Section	Element	Flow	Size	Velocity	Velocity Pressure	Length	Loss Coefficient	Friction	Equivalent Diameter	Diameter	Free Size	Height	Hydraulic Diameter	Overall Size	Reynolds number	Width	Total Pressure Loss	Section Pressure Loss
179	Fittings	100 m^3/h	-	1.5 m/s	1.3 Pa	-	0	-	-	-	-	-	-	-	-	-	0.0 Pa	0.0 Pa

Critical Path : ; Total Pressure Loss : 0.0 Pa

Detail Information of Straight Segment by Sections

Section	Element ID	Flow	Size	Velocity	Velocity Pressure	Length	Pressure Loss	Total Pressure Loss

Fitting and Accessory Loss Coefficient Summary by Sections

Section	Element ID	Loss Method	ASHRAE Table	Loss Coefficient	Pressure Loss	Total Pressure

						Loss
179	5139468	Coefficient from ASHRAE Table	CD6-4	0	0.0 Pa	0.0 Pa

Mechanical ASL-MEC-DS-ACO.GALV-EXTRACAO SUJOS 6

System Information	
System Classification	Exhaust Air
System Type	ASL-MEC-DS-ACO.GALV-EXTRACAO SUJOS
System Name	Mechanical ASL-MEC-DS-ACO.GALV-EXTRACAO SUJOS 6
Abbreviation	

Total Pressure Loss Calculations by Sections																	
Section	Element	Flow	Size	Velocity	Velocity Pressure	Length	Loss Coefficient	Friction	Equivalent Diameter	Diameter	Free Size	Height	Hydraulic Diameter	Overall Size	Reynolds number	Width	Total Pressure Loss	Section Pressure Loss
Critical Path : ; Total Pressure Loss : 0.0 Pa																		

Detail Information of Straight Segment by Sections								
Section	Element ID	Flow	Size	Velocity	Velocity Pressure	Length	Pressure Loss	Total Pressure Loss

Fitting and Accessory Loss Coefficient Summary by Sections						
Section	Element ID	Loss Method	ASHRAE Table	Loss Coefficient	Pressure Loss	Total Pressure Loss

Mechanical ASL-MEC-DS-ACO.GALV-INSUFLACAO 1

System Information	
System Classification	Supply Air
System Type	ASL-MEC-DS-ACO.GALV-INSUFLACAO
System Name	Mechanical ASL-MEC-DS-ACO.GALV-INSUFLACAO 1
Abbreviation	

Total Pressure Loss Calculations by Sections																		
Section	Element	Flow	Size	Velocity	Velocity Pressure	Length	Loss Coefficient	Friction	Equivalent Diameter	Diameter	Free Size	Height	Hydraulic Diameter	Overall Size	Reynolds number	Width	Total Pressure Loss	Section Pressure Loss
Critical Path : ; Total Pressure Loss : 0.0 Pa																		

Detail Information of Straight Segment by Sections								
Section	Element ID	Flow	Size	Velocity	Velocity Pressure	Length	Pressure Loss	Total Pressure Loss

Fitting and Accessory Loss Coefficient Summary by Sections						
Section	Element ID	Loss Method	ASHRAE Table	Loss Coefficient	Pressure Loss	Total Pressure Loss

Mechanical ASL-MEC-DS-ACO.GALV-INSUFLACAO 109

System Information	
System Classification	Supply Air
System Type	ASL-MEC-DS-ACO.GALV-INSUFLACAO
System Name	Mechanical ASL-MEC-DS-ACO.GALV-INSUFLACAO 109
Abbreviation	

Total Pressure Loss Calculations by Sections																		
Section	Element	Flow	Size	Velocity	Velocity Pressure	Length	Loss Coefficient	Friction	Equivalent Diameter	Diameter	Free Size	Height	Hydraulic Diameter	Overall Size	Reynolds number	Width	Total Pressure Loss	Section Pressure Loss
Critical Path : ; Total Pressure Loss : 0.0 Pa																		

Detail Information of Straight Segment by Sections								
Section	Element ID	Flow	Size	Velocity	Velocity Pressure	Length	Pressure Loss	Total Pressure Loss

Fitting and Accessory Loss Coefficient Summary by Sections						
Section	Element ID	Loss Method	ASHRAE Table	Loss Coefficient	Pressure Loss	Total Pressure Loss

Mechanical ASL-MEC-DS-ACO.GALV-INSUFLACAO 112

System Information	
System Classification	Supply Air
System Type	ASL-MEC-DS-ACO.GALV-INSUFLACAO
System Name	Mechanical ASL-MEC-DS-ACO.GALV-INSUFLACAO 112
Abbreviation	

Total Pressure Loss Calculations by Sections																		
Section	Element	Flow	Size	Velocity	Velocity Pressure	Length	Loss Coefficient	Friction	Equivalent Diameter	Diameter	Free Size	Height	Hydraulic Diameter	Overall Size	Reynolds number	Width	Total Pressure Loss	Section Pressure Loss

Critical Path : ; Total Pressure Loss : 0.0 Pa

Detail Information of Straight Segment by Sections								
Section	Element ID	Flow	Size	Velocity	Velocity Pressure	Length	Pressure Loss	Total Pressure Loss

Fitting and Accessory Loss Coefficient Summary by Sections						
Section	Element ID	Loss Method	ASHRAE Table	Loss Coefficient	Pressure Loss	Total Pressure Loss

Mechanical ASL-MEC-DS-ACO.GALV-INSUFLACAO 117

System Information	
System Classification	Supply Air
System Type	ASL-MEC-DS-ACO.GALV-INSUFLACAO
System Name	Mechanical ASL-MEC-DS-ACO.GALV-INSUFLACAO 117
Abbreviation	

Total Pressure Loss Calculations by Sections																	
Section	Element	Flow	Size	Velocity	Velocity Pressure	Length	Loss Coefficient	Friction	Equivalent Diameter	Diameter	Free Size	Height	Hydraulic Diameter	Overall Size	Reynolds number	Width	Total Pressure Loss	Section Pressure Loss
Critical Path : ; Total Pressure Loss : 0.0 Pa																		

Detail Information of Straight Segment by Sections								
Section	Element ID	Flow	Size	Velocity	Velocity Pressure	Length	Pressure Loss	Total Pressure Loss

Fitting and Accessory Loss Coefficient Summary by Sections						
Section	Element ID	Loss Method	ASHRAE Table	Loss Coefficient	Pressure Loss	Total Pressure Loss

Mechanical ASL-MEC-DS-ACO.GALV-INSUFLACAO 12

System Information	
System Classification	Supply Air
System Type	ASL-MEC-DS-ACO.GALV-INSUFLACAO
System Name	Mechanical ASL-MEC-DS-ACO.GALV-INSUFLACAO 12
Abbreviation	

Total Pressure Loss Calculations by Sections																		
Section	Element	Flow	Size	Velocity	Velocity Pressure	Length	Loss Coefficient	Friction	Equivalent Diameter	Diameter	Free Size	Height	Hydraulic Diameter	Overall Size	Reynolds number	Width	Total Pressure Loss	Section Pressure Loss
Critical Path : ; Total Pressure Loss : 0.0 Pa																		

Detail Information of Straight Segment by Sections								
Section	Element ID	Flow	Size	Velocity	Velocity Pressure	Length	Pressure Loss	Total Pressure Loss

Fitting and Accessory Loss Coefficient Summary by Sections						
Section	Element ID	Loss Method	ASHRAE Table	Loss Coefficient	Pressure Loss	Total Pressure Loss

Mechanical ASL-MEC-DS-ACO.GALV-INSUFLACAO 123

System Information	
System Classification	Supply Air
System Type	ASL-MEC-DS-ACO.GALV-INSUFLACAO
System Name	Mechanical ASL-MEC-DS-ACO.GALV-INSUFLACAO 123
Abbreviation	

Total Pressure Loss Calculations by Sections																		
Section	Element	Flow	Size	Velocity	Velocity Pressure	Length	Loss Coefficient	Friction	Equivalent Diameter	Diameter	Free Size	Height	Hydraulic Diameter	Overall Size	Reynolds number	Width	Total Pressure Loss	Section Pressure Loss
Critical Path : ; Total Pressure Loss : 0.0 Pa																		

Detail Information of Straight Segment by Sections								
Section	Element ID	Flow	Size	Velocity	Velocity Pressure	Length	Pressure Loss	Total Pressure Loss

Fitting and Accessory Loss Coefficient Summary by Sections						
Section	Element ID	Loss Method	ASHRAE Table	Loss Coefficient	Pressure Loss	Total Pressure Loss

Mechanical ASL-MEC-DS-ACO.GALV-INSUFLACAO 13

System Information	
System Classification	Supply Air
System Type	ASL-MEC-DS-ACO.GALV-INSUFLACAO
System Name	Mechanical ASL-MEC-DS-ACO.GALV-INSUFLACAO 13
Abbreviation	

Total Pressure Loss Calculations by Sections																		
Section	Element	Flow	Size	Velocity	Velocity Pressure	Length	Loss Coefficient	Friction	Equivalent Diameter	Diameter	Free Size	Height	Hydraulic Diameter	Overall Size	Reynolds number	Width	Total Pressure Loss	Section Pressure Loss
Critical Path : ; Total Pressure Loss : 0.0 Pa																		

Detail Information of Straight Segment by Sections								
Section	Element ID	Flow	Size	Velocity	Velocity Pressure	Length	Pressure Loss	Total Pressure Loss

Fitting and Accessory Loss Coefficient Summary by Sections						
Section	Element ID	Loss Method	ASHRAE Table	Loss Coefficient	Pressure Loss	Total Pressure Loss

Mechanical ASL-MEC-DS-ACO.GALV-INSUFLACAO 14

System Information	
System Classification	Supply Air
System Type	ASL-MEC-DS-ACO.GALV-INSUFLACAO
System Name	Mechanical ASL-MEC-DS-ACO.GALV-INSUFLACAO 14
Abbreviation	

Total Pressure Loss Calculations by Sections																		
Section	Element	Flow	Size	Velocity	Velocity Pressure	Length	Loss Coefficient	Friction	Equivalent Diameter	Diameter	Free Size	Height	Hydraulic Diameter	Overall Size	Reynolds number	Width	Total Pressure Loss	Section Pressure Loss
Critical Path : ; Total Pressure Loss : 0.0 Pa																		

Detail Information of Straight Segment by Sections								
Section	Element ID	Flow	Size	Velocity	Velocity Pressure	Length	Pressure Loss	Total Pressure Loss

Fitting and Accessory Loss Coefficient Summary by Sections						
Section	Element ID	Loss Method	ASHRAE Table	Loss Coefficient	Pressure Loss	Total Pressure Loss

Mechanical ASL-MEC-DS-ACO.GALV-INSUFLACAO 15

System Information	
System Classification	Supply Air
System Type	ASL-MEC-DS-ACO.GALV-INSUFLACAO
System Name	Mechanical ASL-MEC-DS-ACO.GALV-INSUFLACAO 15
Abbreviation	

Total Pressure Loss Calculations by Sections																		
Section	Element	Flow	Size	Velocity	Velocity Pressure	Length	Loss Coefficient	Friction	Equivalent Diameter	Diameter	Free Size	Height	Hydraulic Diameter	Overall Size	Reynolds number	Width	Total Pressure Loss	Section Pressure Loss
Critical Path : ; Total Pressure Loss : 0.0 Pa																		

Detail Information of Straight Segment by Sections								
Section	Element ID	Flow	Size	Velocity	Velocity Pressure	Length	Pressure Loss	Total Pressure Loss

Fitting and Accessory Loss Coefficient Summary by Sections						
Section	Element ID	Loss Method	ASHRAE Table	Loss Coefficient	Pressure Loss	Total Pressure Loss

Mechanical ASL-MEC-DS-ACO.GALV-INSUFLACAO 17

System Information	
System Classification	Supply Air
System Type	ASL-MEC-DS-ACO.GALV-INSUFLACAO
System Name	Mechanical ASL-MEC-DS-ACO.GALV-INSUFLACAO 17
Abbreviation	

Total Pressure Loss Calculations by Sections																		
Section	Element	Flow	Size	Velocity	Velocity Pressure	Length	Loss Coefficient	Friction	Equivalent Diameter	Diameter	Free Size	Height	Hydraulic Diameter	Overall Size	Reynolds number	Width	Total Pressure Loss	Section Pressure Loss
Critical Path : ; Total Pressure Loss : 0.0 Pa																		

Detail Information of Straight Segment by Sections								
Section	Element ID	Flow	Size	Velocity	Velocity Pressure	Length	Pressure Loss	Total Pressure Loss

Fitting and Accessory Loss Coefficient Summary by Sections						
Section	Element ID	Loss Method	ASHRAE Table	Loss Coefficient	Pressure Loss	Total Pressure Loss

Mechanical ASL-MEC-DS-ACO.GALV-INSUFLACAO 18

System Information	
System Classification	Supply Air
System Type	ASL-MEC-DS-ACO.GALV-INSUFLACAO
System Name	Mechanical ASL-MEC-DS-ACO.GALV-INSUFLACAO 18
Abbreviation	

Total Pressure Loss Calculations by Sections																	
Section	Element	Flow	Size	Velocity	Velocity Pressure	Length	Loss Coefficient	Friction	Equivalent Diameter	Diameter	Free Size	Height	Hydraulic Diameter	Overall Size	Reynolds number	Width	Total Pressure Loss	Section Pressure Loss
Critical Path : ; Total Pressure Loss : 0.0 Pa																		

Detail Information of Straight Segment by Sections								
Section	Element ID	Flow	Size	Velocity	Velocity Pressure	Length	Pressure Loss	Total Pressure Loss

Fitting and Accessory Loss Coefficient Summary by Sections						
Section	Element ID	Loss Method	ASHRAE Table	Loss Coefficient	Pressure Loss	Total Pressure Loss

Mechanical ASL-MEC-DS-ACO.GALV-INSUFLACAO 2

System Information	
System Classification	Supply Air
System Type	ASL-MEC-DS-ACO.GALV-INSUFLACAO
System Name	Mechanical ASL-MEC-DS-ACO.GALV-INSUFLACAO 2
Abbreviation	

Total Pressure Loss Calculations by Sections																		
Section	Element	Flow	Size	Velocity	Velocity Pressure	Length	Loss Coefficient	Friction	Equivalent Diameter	Diameter	Free Size	Height	Hydraulic Diameter	Overall Size	Reynolds number	Width	Total Pressure Loss	Section Pressure Loss
Critical Path : ; Total Pressure Loss : 0.0 Pa																		

Detail Information of Straight Segment by Sections								
Section	Element ID	Flow	Size	Velocity	Velocity Pressure	Length	Pressure Loss	Total Pressure Loss

Fitting and Accessory Loss Coefficient Summary by Sections						
Section	Element ID	Loss Method	ASHRAE Table	Loss Coefficient	Pressure Loss	Total Pressure Loss

Mechanical ASL-MEC-DS-ACO.GALV-INSUFLACAO 3

System Information	
System Classification	Supply Air
System Type	ASL-MEC-DS-ACO.GALV-INSUFLACAO
System Name	Mechanical ASL-MEC-DS-ACO.GALV-INSUFLACAO 3
Abbreviation	

Total Pressure Loss Calculations by Sections																		
Section	Element	Flow	Size	Velocity	Velocity Pressure	Length	Loss Coefficient	Friction	Equivalent Diameter	Diameter	Free Size	Height	Hydraulic Diameter	Overall Size	Reynolds number	Width	Total Pressure Loss	Section Pressure Loss
Critical Path : ; Total Pressure Loss : 0.0 Pa																		

Detail Information of Straight Segment by Sections								
Section	Element ID	Flow	Size	Velocity	Velocity Pressure	Length	Pressure Loss	Total Pressure Loss

Fitting and Accessory Loss Coefficient Summary by Sections						
Section	Element ID	Loss Method	ASHRAE Table	Loss Coefficient	Pressure Loss	Total Pressure Loss

Mechanical ASL-MEC-DS-ACO.GALV-INSUFLACAO 35

System Information	
System Classification	Supply Air
System Type	ASL-MEC-DS-ACO.GALV-INSUFLACAO
System Name	Mechanical ASL-MEC-DS-ACO.GALV-INSUFLACAO 35
Abbreviation	

Total Pressure Loss Calculations by Sections																		
Section	Element	Flow	Size	Velocity	Velocity Pressure	Length	Loss Coefficient	Friction	Equivalent Diameter	Diameter	Free Size	Height	Hydraulic Diameter	Overall Size	Reynolds number	Width	Total Pressure Loss	Section Pressure Loss
Critical Path : ; Total Pressure Loss : 0.0 Pa																		

Detail Information of Straight Segment by Sections								
Section	Element ID	Flow	Size	Velocity	Velocity Pressure	Length	Pressure Loss	Total Pressure Loss

Fitting and Accessory Loss Coefficient Summary by Sections						
Section	Element ID	Loss Method	ASHRAE Table	Loss Coefficient	Pressure Loss	Total Pressure Loss

Mechanical ASL-MEC-DS-ACO.GALV-INSUFLACAO 5

System Information	
System Classification	Supply Air
System Type	ASL-MEC-DS-ACO.GALV-INSUFLACAO
System Name	Mechanical ASL-MEC-DS-ACO.GALV-INSUFLACAO 5
Abbreviation	

Total Pressure Loss Calculations by Sections																		
Section	Element	Flow	Size	Velocity	Velocity Pressure	Length	Loss Coefficient	Friction	Equivalent Diameter	Diameter	Free Size	Height	Hydraulic Diameter	Overall Size	Reynolds number	Width	Total Pressure Loss	Section Pressure Loss
Critical Path : ; Total Pressure Loss : 0.0 Pa																		

Detail Information of Straight Segment by Sections								
Section	Element ID	Flow	Size	Velocity	Velocity Pressure	Length	Pressure Loss	Total Pressure Loss

Fitting and Accessory Loss Coefficient Summary by Sections						
Section	Element ID	Loss Method	ASHRAE Table	Loss Coefficient	Pressure Loss	Total Pressure Loss

Mechanical ASL-MEC-DS-ACO.GALV-INSUFLACAO 6

System Information	
System Classification	Supply Air
System Type	ASL-MEC-DS-ACO.GALV-INSUFLACAO
System Name	Mechanical ASL-MEC-DS-ACO.GALV-INSUFLACAO 6
Abbreviation	

Total Pressure Loss Calculations by Sections																		
Section	Element	Flow	Size	Velocity	Velocity Pressure	Length	Loss Coefficient	Friction	Equivalent Diameter	Diameter	Free Size	Height	Hydraulic Diameter	Overall Size	Reynolds number	Width	Total Pressure Loss	Section Pressure Loss
Critical Path : ; Total Pressure Loss : 0.0 Pa																		

Detail Information of Straight Segment by Sections								
Section	Element ID	Flow	Size	Velocity	Velocity Pressure	Length	Pressure Loss	Total Pressure Loss

Fitting and Accessory Loss Coefficient Summary by Sections						
Section	Element ID	Loss Method	ASHRAE Table	Loss Coefficient	Pressure Loss	Total Pressure Loss

Mechanical ASL-MEC-DS-ACO.GALV-INSUFLACAO 7

System Information	
System Classification	Supply Air
System Type	ASL-MEC-DS-ACO.GALV-INSUFLACAO
System Name	Mechanical ASL-MEC-DS-ACO.GALV-INSUFLACAO 7
Abbreviation	

Total Pressure Loss Calculations by Sections																		
Section	Element	Flow	Size	Velocity	Velocity Pressure	Length	Loss Coefficient	Friction	Equivalent Diameter	Diameter	Free Size	Height	Hydraulic Diameter	Overall Size	Reynolds number	Width	Total Pressure Loss	Section Pressure Loss
Critical Path : ; Total Pressure Loss : 0.0 Pa																		

Detail Information of Straight Segment by Sections								
Section	Element ID	Flow	Size	Velocity	Velocity Pressure	Length	Pressure Loss	Total Pressure Loss

Fitting and Accessory Loss Coefficient Summary by Sections						
Section	Element ID	Loss Method	ASHRAE Table	Loss Coefficient	Pressure Loss	Total Pressure Loss

Mechanical ASL-MEC-DS-ACO.GALV-INSUFLACAO 98

System Information	
System Classification	Supply Air
System Type	ASL-MEC-DS-ACO.GALV-INSUFLACAO
System Name	Mechanical ASL-MEC-DS-ACO.GALV-INSUFLACAO 98
Abbreviation	

Total Pressure Loss Calculations by Sections																		
Section	Element	Flow	Size	Velocity	Velocity Pressure	Length	Loss Coefficient	Friction	Equivalent Diameter	Diameter	Free Size	Height	Hydraulic Diameter	Overall Size	Reynolds number	Width	Total Pressure Loss	Section Pressure Loss

Critical Path : ; Total Pressure Loss : 0.0 Pa

Detail Information of Straight Segment by Sections								
Section	Element ID	Flow	Size	Velocity	Velocity Pressure	Length	Pressure Loss	Total Pressure Loss

Fitting and Accessory Loss Coefficient Summary by Sections						
Section	Element ID	Loss Method	ASHRAE Table	Loss Coefficient	Pressure Loss	Total Pressure Loss

Mechanical ASL-MEC-DS-ACO.GALV-RETORNO_E 17

System Information	
System Classification	Exhaust Air
System Type	ASL-MEC-DS-ACO.GALV-RETORNO_E
System Name	Mechanical ASL-MEC-DS-ACO.GALV-RETORNO_E 17
Abbreviation	

Total Pressure Loss Calculations by Sections																	
Section	Element	Flow	Size	Velocity	Velocity Pressure	Length	Loss Coefficient	Friction	Equivalent Diameter	Diameter	Free Size	Height	Hydraulic Diameter	Overall Size	Reynolds number	Width	Total Pressure Loss	Section Pressure Loss
Critical Path : ; Total Pressure Loss : 0.0 Pa																		

Detail Information of Straight Segment by Sections								
Section	Element ID	Flow	Size	Velocity	Velocity Pressure	Length	Pressure Loss	Total Pressure Loss

Fitting and Accessory Loss Coefficient Summary by Sections						
Section	Element ID	Loss Method	ASHRAE Table	Loss Coefficient	Pressure Loss	Total Pressure Loss

Mechanical ASL-MEC-DS-ACO.GALV-RETORNO_R 132

System Information	
System Classification	Return Air
System Type	ASL-MEC-DS-ACO.GALV-RETORNO_R
System Name	Mechanical ASL-MEC-DS-ACO.GALV-RETORNO_R 132
Abbreviation	

Total Pressure Loss Calculations by Sections																		
Section	Element	Flow	Size	Velocity	Velocity Pressure	Length	Loss Coefficient	Friction	Equivalent Diameter	Diameter	Free Size	Height	Hydraulic Diameter	Overall Size	Reynolds number	Width	Total Pressure Loss	Section Pressure Loss
Critical Path : ; Total Pressure Loss : 0.0 Pa																		

Detail Information of Straight Segment by Sections								
Section	Element ID	Flow	Size	Velocity	Velocity Pressure	Length	Pressure Loss	Total Pressure Loss

Fitting and Accessory Loss Coefficient Summary by Sections						
Section	Element ID	Loss Method	ASHRAE Table	Loss Coefficient	Pressure Loss	Total Pressure Loss

Mechanical ASL-MEC-DS-ACO.GALV-RETORNO_R 134

System Information	
System Classification	Return Air
System Type	ASL-MEC-DS-ACO.GALV-RETORNO_R
System Name	Mechanical ASL-MEC-DS-ACO.GALV-RETORNO_R 134
Abbreviation	

Total Pressure Loss Calculations by Sections																		
Section	Element	Flow	Size	Velocity	Velocity Pressure	Length	Loss Coefficient	Friction	Equivalent Diameter	Diameter	Free Size	Height	Hydraulic Diameter	Overall Size	Reynolds number	Width	Total Pressure Loss	Section Pressure Loss
Critical Path : ; Total Pressure Loss : 0.0 Pa																		

Detail Information of Straight Segment by Sections								
Section	Element ID	Flow	Size	Velocity	Velocity Pressure	Length	Pressure Loss	Total Pressure Loss

Fitting and Accessory Loss Coefficient Summary by Sections						
Section	Element ID	Loss Method	ASHRAE Table	Loss Coefficient	Pressure Loss	Total Pressure Loss

Mechanical ASL-MEC-DS-ACO.GALV-RETORNO_R 16

System Information	
System Classification	Return Air
System Type	ASL-MEC-DS-ACO.GALV-RETORNO_R
System Name	Mechanical ASL-MEC-DS-ACO.GALV-RETORNO_R 16
Abbreviation	

Total Pressure Loss Calculations by Sections																	
Section	Element	Flow	Size	Velocity	Velocity Pressure	Length	Loss Coefficient	Friction	Equivalent Diameter	Diameter	Free Size	Height	Hydraulic Diameter	Overall Size	Reynolds number	Width	Total Pressure Loss	Section Pressure Loss
Critical Path : ; Total Pressure Loss : 0.0 Pa																		

Detail Information of Straight Segment by Sections								
Section	Element ID	Flow	Size	Velocity	Velocity Pressure	Length	Pressure Loss	Total Pressure Loss

Fitting and Accessory Loss Coefficient Summary by Sections						
Section	Element ID	Loss Method	ASHRAE Table	Loss Coefficient	Pressure Loss	Total Pressure Loss

Mechanical ASL-MEC-DS-ACO.GALV-RETORNO_R 162

System Information	
System Classification	Return Air
System Type	ASL-MEC-DS-ACO.GALV-RETORNO_R
System Name	Mechanical ASL-MEC-DS-ACO.GALV-RETORNO_R 162
Abbreviation	

Total Pressure Loss Calculations by Sections																		
Section	Element	Flow	Size	Velocity	Velocity Pressure	Length	Loss Coefficient	Friction	Equivalent Diameter	Diameter	Free Size	Height	Hydraulic Diameter	Overall Size	Reynolds number	Width	Total Pressure Loss	Section Pressure Loss
Critical Path : ; Total Pressure Loss : 0.0 Pa																		

Detail Information of Straight Segment by Sections								
Section	Element ID	Flow	Size	Velocity	Velocity Pressure	Length	Pressure Loss	Total Pressure Loss

Fitting and Accessory Loss Coefficient Summary by Sections						
Section	Element ID	Loss Method	ASHRAE Table	Loss Coefficient	Pressure Loss	Total Pressure Loss

Mechanical ASL-MEC-DS-ACO.GALV-RETORNO_R 18

System Information	
System Classification	Return Air
System Type	ASL-MEC-DS-ACO.GALV-RETORNO_R
System Name	Mechanical ASL-MEC-DS-ACO.GALV-RETORNO_R 18
Abbreviation	

Total Pressure Loss Calculations by Sections																		
Section	Element	Flow	Size	Velocity	Velocity Pressure	Length	Loss Coefficient	Friction	Equivalent Diameter	Diameter	Free Size	Height	Hydraulic Diameter	Overall Size	Reynolds number	Width	Total Pressure Loss	Section Pressure Loss
Critical Path : ; Total Pressure Loss : 0.0 Pa																		

Detail Information of Straight Segment by Sections								
Section	Element ID	Flow	Size	Velocity	Velocity Pressure	Length	Pressure Loss	Total Pressure Loss

Fitting and Accessory Loss Coefficient Summary by Sections						
Section	Element ID	Loss Method	ASHRAE Table	Loss Coefficient	Pressure Loss	Total Pressure Loss

Mechanical ASL-MEC-DS-ACO.GALV-RETORNO_R 302

System Information	
System Classification	Return Air
System Type	ASL-MEC-DS-ACO.GALV-RETORNO_R
System Name	Mechanical ASL-MEC-DS-ACO.GALV-RETORNO_R 302
Abbreviation	

Total Pressure Loss Calculations by Sections																		
Section	Element	Flow	Size	Velocity	Velocity Pressure	Length	Loss Coefficient	Friction	Equivalent Diameter	Diameter	Free Size	Height	Hydraulic Diameter	Overall Size	Reynolds number	Width	Total Pressure Loss	Section Pressure Loss
Critical Path : ; Total Pressure Loss : 0.0 Pa																		

Detail Information of Straight Segment by Sections								
Section	Element ID	Flow	Size	Velocity	Velocity Pressure	Length	Pressure Loss	Total Pressure Loss

Fitting and Accessory Loss Coefficient Summary by Sections						
Section	Element ID	Loss Method	ASHRAE Table	Loss Coefficient	Pressure Loss	Total Pressure Loss

Mechanical ASL-MEC-DS-ACO.GALV-RETORNO_R 304

System Information	
System Classification	Return Air
System Type	ASL-MEC-DS-ACO.GALV-RETORNO_R
System Name	Mechanical ASL-MEC-DS-ACO.GALV-RETORNO_R 304
Abbreviation	

Total Pressure Loss Calculations by Sections

Section	Element	Flow	Size	Velocity	Velocity Pressure	Length	Loss Coefficient	Friction	Equivalent Diameter	Diameter	Free Size	Height	Hydraulic Diameter	Overall Size	Reynolds number	Width	Total Pressure Loss	Section Pressure Loss
Critical Path : ; Total Pressure Loss : 0.0 Pa																		

Detail Information of Straight Segment by Sections

Section	Element ID	Flow	Size	Velocity	Velocity Pressure	Length	Pressure Loss	Total Pressure Loss

Fitting and Accessory Loss Coefficient Summary by Sections

Section	Element ID	Loss Method	ASHRAE Table	Loss Coefficient	Pressure Loss	Total Pressure Loss

Mechanical ASL-MEC-DS-ACO.GALV-RETORNO_R 35

System Information	
System Classification	Return Air
System Type	ASL-MEC-DS-ACO.GALV-RETORNO_R
System Name	Mechanical ASL-MEC-DS-ACO.GALV-RETORNO_R 35
Abbreviation	

Total Pressure Loss Calculations by Sections

Section	Element	Flow	Size	Velocity	Velocity Pressure	Length	Loss Coefficient	Friction	Equivalent Diameter	Diameter	Free Size	Height	Hydraulic Diameter	Overall Size	Reynolds number	Width	Total Pressure Loss	Section Pressure Loss
Critical Path : ; Total Pressure Loss : 0.0 Pa																		

Detail Information of Straight Segment by Sections

Section	Element ID	Flow	Size	Velocity	Velocity Pressure	Length	Pressure Loss	Total Pressure Loss

Fitting and Accessory Loss Coefficient Summary by Sections

Section	Element ID	Loss Method	ASHRAE Table	Loss Coefficient	Pressure Loss	Total Pressure Loss

Mechanical ASL-MEC-DS-ACO.GALV-RETORNO_R 37

System Information	
System Classification	Return Air
System Type	ASL-MEC-DS-ACO.GALV-RETORNO_R
System Name	Mechanical ASL-MEC-DS-ACO.GALV-RETORNO_R 37
Abbreviation	

Total Pressure Loss Calculations by Sections

Section	Element	Flow	Size	Velocity	Velocity Pressure	Length	Loss Coefficient	Friction	Equivalent Diameter	Diameter	Free Size	Height	Hydraulic Diameter	Overall Size	Reynolds number	Width	Total Pressure Loss	Section Pressure Loss
Critical Path : ; Total Pressure Loss : 0.0 Pa																		

Detail Information of Straight Segment by Sections

Section	Element ID	Flow	Size	Velocity	Velocity Pressure	Length	Pressure Loss	Total Pressure Loss

Fitting and Accessory Loss Coefficient Summary by Sections

Section	Element ID	Loss Method	ASHRAE Table	Loss Coefficient	Pressure Loss	Total Pressure Loss

Mechanical ASL-MEC-DS-ACO.GALV-RETORNO_R 38

System Information	
System Classification	Return Air
System Type	ASL-MEC-DS-ACO.GALV-RETORNO_R
System Name	Mechanical ASL-MEC-DS-ACO.GALV-RETORNO_R 38
Abbreviation	

Total Pressure Loss Calculations by Sections

Section	Element	Flow	Size	Velocity	Velocity Pressure	Length	Loss Coefficient	Friction	Equivalent Diameter	Diameter	Free Size	Height	Hydraulic Diameter	Overall Size	Reynolds number	Width	Total Pressure Loss	Section Pressure Loss
Critical Path : ; Total Pressure Loss : 0.0 Pa																		

Detail Information of Straight Segment by Sections

Section	Element ID	Flow	Size	Velocity	Velocity Pressure	Length	Pressure Loss	Total Pressure Loss

Fitting and Accessory Loss Coefficient Summary by Sections						
Section	Element ID	Loss Method	ASHRAE Table	Loss Coefficient	Pressure Loss	Total Pressure Loss

Mechanical ASL-MEC-DS-ACO.GALV-RETORNO_R 39

System Information	
System Classification	Return Air
System Type	ASL-MEC-DS-ACO.GALV-RETORNO_R
System Name	Mechanical ASL-MEC-DS-ACO.GALV-RETORNO_R 39
Abbreviation	

Total Pressure Loss Calculations by Sections																	
Section	Element	Flow	Size	Velocity	Velocity Pressure	Length	Loss Coefficient	Friction	Equivalent Diameter	Diameter	Free Size	Height	Hydraulic Diameter	Overall Size	Reynolds number	Width	Total Pressure Loss	Section Pressure Loss
Critical Path : ; Total Pressure Loss : 0.0 Pa																		

Detail Information of Straight Segment by Sections								
Section	Element ID	Flow	Size	Velocity	Velocity Pressure	Length	Pressure Loss	Total Pressure Loss

Fitting and Accessory Loss Coefficient Summary by Sections						
Section	Element ID	Loss Method	ASHRAE Table	Loss Coefficient	Pressure Loss	Total Pressure Loss

Mechanical ASL-MEC-DS-ACO.GALV-RETORNO_R 42

System Information	
System Classification	Return Air
System Type	ASL-MEC-DS-ACO.GALV-RETORNO_R
System Name	Mechanical ASL-MEC-DS-ACO.GALV-RETORNO_R 42
Abbreviation	

Total Pressure Loss Calculations by Sections																	
Section	Element	Flow	Size	Velocity	Velocity Pressure	Length	Loss Coefficient	Friction	Equivalent Diameter	Diameter	Free Size	Height	Hydraulic Diameter	Overall Size	Reynolds number	Width	Total Pressure Loss	Section Pressure Loss
Critical Path : ; Total Pressure Loss : 0.0 Pa																		

Detail Information of Straight Segment by Sections								
Section	Element ID	Flow	Size	Velocity	Velocity Pressure	Length	Pressure Loss	Total Pressure Loss

Fitting and Accessory Loss Coefficient Summary by Sections						
Section	Element ID	Loss Method	ASHRAE Table	Loss Coefficient	Pressure Loss	Total Pressure Loss

Mechanical ASL-MEC-DS-ACO.GALV-RETORNO_R 50

System Information	
System Classification	Return Air
System Type	ASL-MEC-DS-ACO.GALV-RETORNO_R
System Name	Mechanical ASL-MEC-DS-ACO.GALV-RETORNO_R 50
Abbreviation	

Total Pressure Loss Calculations by Sections																	
Section	Element	Flow	Size	Velocity	Velocity Pressure	Length	Loss Coefficient	Friction	Equivalent Diameter	Diameter	Free Size	Height	Hydraulic Diameter	Overall Size	Reynolds number	Width	Total Pressure Loss	Section Pressure Loss
Critical Path : ; Total Pressure Loss : 0.0 Pa																		

Detail Information of Straight Segment by Sections								
Section	Element ID	Flow	Size	Velocity	Velocity Pressure	Length	Pressure Loss	Total Pressure Loss

Fitting and Accessory Loss Coefficient Summary by Sections						
Section	Element ID	Loss Method	ASHRAE Table	Loss Coefficient	Pressure Loss	Total Pressure Loss

Mechanical ASL-MEC-DS-ACO.GALV-RETORNO_R 53

System Information	
System Classification	Return Air
System Type	ASL-MEC-DS-ACO.GALV-RETORNO_R
System Name	Mechanical ASL-MEC-DS-ACO.GALV-RETORNO_R 53
Abbreviation	

Total Pressure Loss Calculations by Sections																	
Section	Element	Flow	Size	Velocity	Velocity Pressure	Length	Loss Coefficient	Friction	Equivalent Diameter	Diameter	Free Size	Height	Hydraulic Diameter	Overall Size	Reynolds number	Width	Total Pressure Loss	Section Pressure Loss

Critical Path : ; Total Pressure Loss : 0.0 Pa

Detail Information of Straight Segment by Sections							
Section	Element ID	Flow	Size	Velocity	Velocity Pressure	Length	Pressure Loss	Total Pressure Loss

Fitting and Accessory Loss Coefficient Summary by Sections						
Section	Element ID	Loss Method	ASHRAE Table	Loss Coefficient	Pressure Loss	Total Pressure Loss

Mechanical ASL-MEC-DS-ACO.GALV-RETORNO_R 64

System Information	
System Classification	Return Air
System Type	ASL-MEC-DS-ACO.GALV-RETORNO_R
System Name	Mechanical ASL-MEC-DS-ACO.GALV-RETORNO_R 64
Abbreviation	

Total Pressure Loss Calculations by Sections																	
Section	Element	Flow	Size	Velocity	Velocity Pressure	Length	Loss Coefficient	Friction	Equivalent Diameter	Diameter	Free Size	Height	Hydraulic Diameter	Overall Size	Reynolds number	Width	Total Pressure Loss	Section Pressure Loss
Critical Path : ; Total Pressure Loss : 0.0 Pa																		

Detail Information of Straight Segment by Sections								
Section	Element ID	Flow	Size	Velocity	Velocity Pressure	Length	Pressure Loss	Total Pressure Loss

Fitting and Accessory Loss Coefficient Summary by Sections						
Section	Element ID	Loss Method	ASHRAE Table	Loss Coefficient	Pressure Loss	Total Pressure Loss

Mechanical ASL-MEC-DS-ACO.GALV-RETORNO_R 69

System Information	
System Classification	Return Air
System Type	ASL-MEC-DS-ACO.GALV-RETORNO_R
System Name	Mechanical ASL-MEC-DS-ACO.GALV-RETORNO_R 69
Abbreviation	

Total Pressure Loss Calculations by Sections																		
Section	Element	Flow	Size	Velocity	Velocity Pressure	Length	Loss Coefficient	Friction	Equivalent Diameter	Diameter	Free Size	Height	Hydraulic Diameter	Overall Size	Reynolds number	Width	Total Pressure Loss	Section Pressure Loss
Critical Path : ; Total Pressure Loss : 0.0 Pa																		

Detail Information of Straight Segment by Sections								
Section	Element ID	Flow	Size	Velocity	Velocity Pressure	Length	Pressure Loss	Total Pressure Loss

Fitting and Accessory Loss Coefficient Summary by Sections						
Section	Element ID	Loss Method	ASHRAE Table	Loss Coefficient	Pressure Loss	Total Pressure Loss

Mechanical ASL-MEC-DS-ACO.GALV-RETORNO_R 76

System Information	
System Classification	Return Air
System Type	ASL-MEC-DS-ACO.GALV-RETORNO_R
System Name	Mechanical ASL-MEC-DS-ACO.GALV-RETORNO_R 76
Abbreviation	

Total Pressure Loss Calculations by Sections																		
Section	Element	Flow	Size	Velocity	Velocity Pressure	Length	Loss Coefficient	Friction	Equivalent Diameter	Diameter	Free Size	Height	Hydraulic Diameter	Overall Size	Reynolds number	Width	Total Pressure Loss	Section Pressure Loss
Critical Path : ; Total Pressure Loss : 0.0 Pa																		

Detail Information of Straight Segment by Sections								
Section	Element ID	Flow	Size	Velocity	Velocity Pressure	Length	Pressure Loss	Total Pressure Loss

Fitting and Accessory Loss Coefficient Summary by Sections						
Section	Element ID	Loss Method	ASHRAE Table	Loss Coefficient	Pressure Loss	Total Pressure Loss

Mechanical ASL-MEC-DS-ACO.GALV-RETORNO_R 84

System Information	
System Classification	Return Air
System Type	ASL-MEC-DS-ACO.GALV-RETORNO_R
System Name	Mechanical ASL-MEC-DS-ACO.GALV-RETORNO_R 84
Abbreviation	

Total Pressure Loss Calculations by Sections																		
Section	Element	Flow	Size	Velocity	Velocity Pressure	Length	Loss Coefficient	Friction	Equivalent Diameter	Diameter	Free Size	Height	Hydraulic Diameter	Overall Size	Reynolds number	Width	Total Pressure Loss	Section Pressure Loss
Critical Path : ; Total Pressure Loss : 0.0 Pa																		

Detail Information of Straight Segment by Sections								
Section	Element ID	Flow	Size	Velocity	Velocity Pressure	Length	Pressure Loss	Total Pressure Loss

Fitting and Accessory Loss Coefficient Summary by Sections						
Section	Element ID	Loss Method	ASHRAE Table	Loss Coefficient	Pressure Loss	Total Pressure Loss

Mechanical ASL-MEC-DS-ACO.GALV-RETORNO_R 87

System Information	
System Classification	Return Air
System Type	ASL-MEC-DS-ACO.GALV-RETORNO_R
System Name	Mechanical ASL-MEC-DS-ACO.GALV-RETORNO_R 87
Abbreviation	

Total Pressure Loss Calculations by Sections																		
Section	Element	Flow	Size	Velocity	Velocity Pressure	Length	Loss Coefficient	Friction	Equivalent Diameter	Diameter	Free Size	Height	Hydraulic Diameter	Overall Size	Reynolds number	Width	Total Pressure Loss	Section Pressure Loss
Critical Path : ; Total Pressure Loss : 0.0 Pa																		

Detail Information of Straight Segment by Sections								
Section	Element ID	Flow	Size	Velocity	Velocity Pressure	Length	Pressure Loss	Total Pressure Loss

Fitting and Accessory Loss Coefficient Summary by Sections						
Section	Element ID	Loss Method	ASHRAE Table	Loss Coefficient	Pressure Loss	Total Pressure Loss

Appendix D

Pressure Loss Manual Excel Sheet

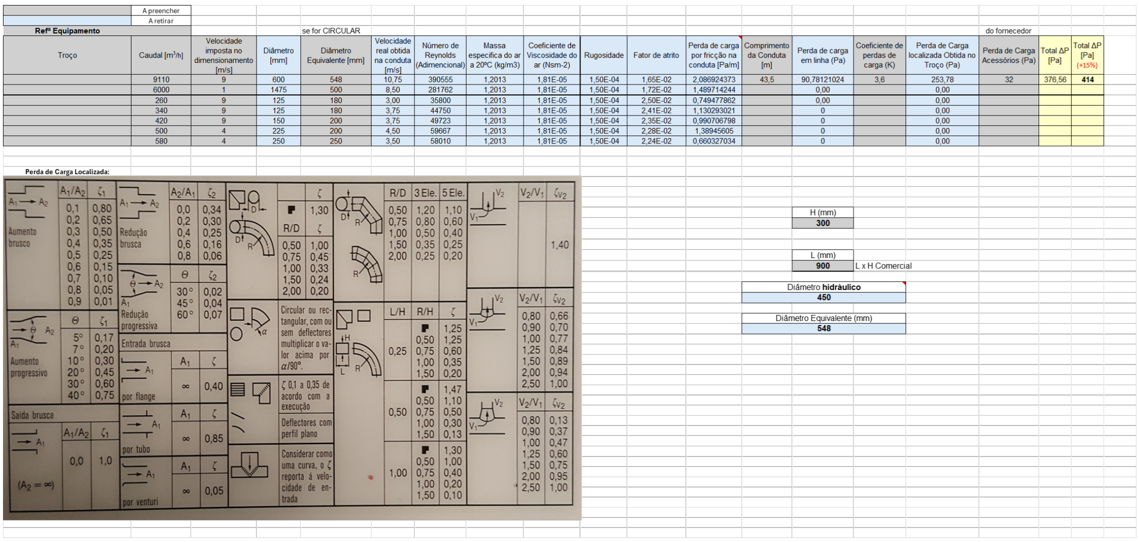

	A preencher
	A retirar

Refª Equipamento — se for CIRCULAR — do fornecedor

Troço	Caudal [m³/h]	Velocidade imposta no dimensionamento [m/s]	Diâmetro [mm]	Diâmetro Equivalente [mm]	Velocidade real obtida na conduta [m/s]	Número de Reynolds (Adimencional)	Massa especifica do ar a 20ºC (kg/m3)	Coeficiente de Viscosidade do ar (Nsm-2)	Rugosidade	Fator de atrito	Perda de carga por fricção na conduta [Pa/m]	Comprimento da Conduta [m]	Perda de carga em linha (Pa)	Coeficiente de perdas de carga (K)	Perda de Carga localizada Obtida no Troço (Pa)	Perda de Carga Acessórios (Pa)	Total ΔP [Pa]	Total ΔP [Pa] (+15%)
	9110	9	600	548	10,75	390555	1,2013	1,81E-05	1,50E-04	1,65E-02	2,086924373	43,5	90,78121024	3,6	253,78	32	376,56	**414**
	6000	1	1475	500	8,50	281762	1,2013	1,81E-05	1,50E-04	1,72E-02	1,489714244		0,00		0,00			
	260	9	125	180	3,00	35800	1,2013	1,81E-05	1,50E-04	2,50E-02	0,749477862		0,00		0,00			
	340	9	125	180	3,75	44750	1,2013	1,81E-05	1,50E-04	2,41E-02	1,130293021		0		0,00			
	420	9	150	200	3,75	49723	1,2013	1,81E-05	1,50E-04	2,35E-02	0,990706798		0		0,00			
	500	4	225	200	4,50	59667	1,2013	1,81E-05	1,50E-04	2,28E-02	1,38945605		0		0,00			
	580	4	250	250	3,50	58010	1,2013	1,81E-05	1,50E-04	2,24E-02	0,660327034		0		0,00			

Perda de Carga Localizada:

H (mm)
300

L (mm)	
900	L x H Comercial

Diâmetro **hidráulico**
450

Diâmetro Equivalente (mm)
548

Figure D.1: Manual Excel Sheet for Pressure Loss Calculations

Appendix E

Revit Automation Tool Workshop

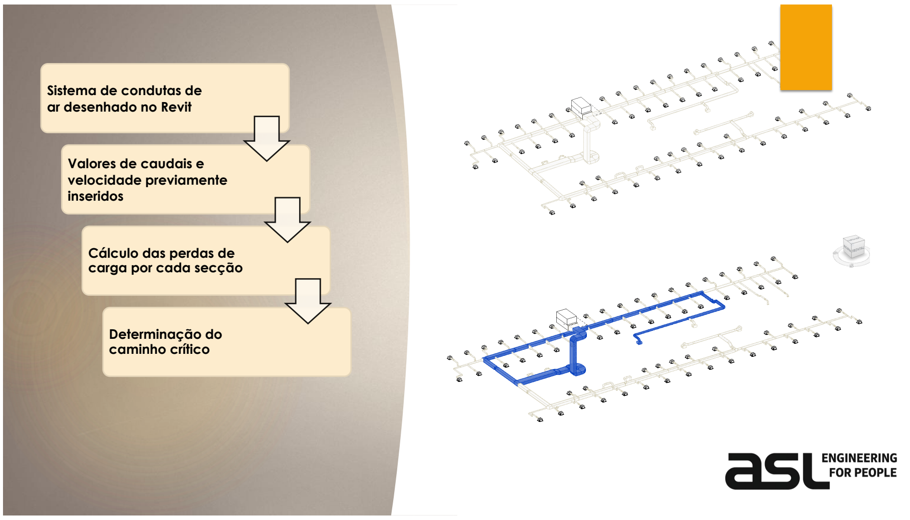

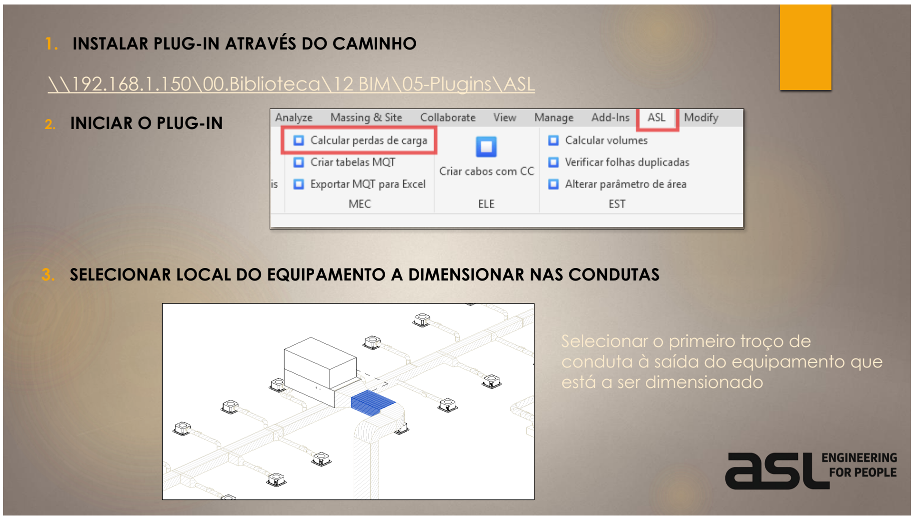
1. INSTALAR PLUG-IN ATRAVÉS DO CAMINHO
\\192.168.1.150\00.Biblioteca\12 BIM\05-Plugins\ASL
2. INICIAR O PLUG-IN
Analyze Massing & Site Collaborate View Manage Add-Ins ASL Modify
Calcular perdas de carga
Criar tabelas MQT
Exportar MQT para Excel
MEC
Criar cabos com CC
ELE
Calcular volumes
Verificar folhas duplicadas
Alterar parâmetro de área
EST
3. SELECIONAR LOCAL DO EQUIPAMENTO A DIMENSIONAR NAS CONDUTAS
Selecionar o primeiro troço de conduta à saída do equipamento que está a ser dimensionado
asl ENGINEERING FOR PEOPLE

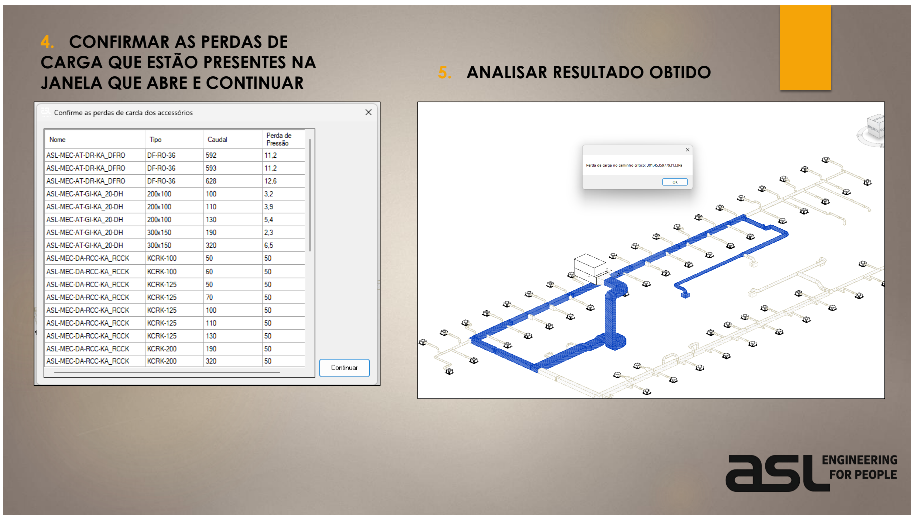
4. CONFIRMAR AS PERDAS DE CARGA QUE ESTÃO PRESENTES NA JANELA QUE ABRE E CONTINUAR
Confirme as perdas de carda dos accessórios
Nome Tipo Caudal Perda de Pressão
ASL-MEC-AT-DR-KA_DFRO DF-RO-36 592 11,2
ASL-MEC-AT-DR-KA_DFRO DF-RO-36 593 11,2
ASL-MEC-AT-DR-KA_DFRO DF-RO-36 628 12,6
ASL-MEC-AT-GI-KA_20-DH 200x100 100 3,2
ASL-MEC-AT-GI-KA_20-DH 200x100 110 3,9
ASL-MEC-AT-GI-KA_20-DH 200x100 130 5,4
ASL-MEC-AT-GI-KA_20-DH 300x150 190 2,3
ASL-MEC-AT-GI-KA_20-DH 300x150 320 6,5
ASL-MEC-DA-RCC-KA_RCCK KCRK-100 50 50
ASL-MEC-DA-RCC-KA_RCCK KCRK-100 60 50
ASL-MEC-DA-RCC-KA_RCCK KCRK-125 50 50
ASL-MEC-DA-RCC-KA_RCCK KCRK-125 70 50
ASL-MEC-DA-RCC-KA_RCCK KCRK-125 100 50
ASL-MEC-DA-RCC-KA_RCCK KCRK-125 110 50
ASL-MEC-DA-RCC-KA_RCCK KCRK-125 130 50
ASL-MEC-DA-RCC-KA_RCCK KCRK-200 190 50
ASL-MEC-DA-RCC-KA_RCCK KCRK-200 320 50
Continuar
5. ANALISAR RESULTADO OBTIDO
asl ENGINEERING FOR PEOPLE

Appendix F

Maintenance Tasks Manual

G Trabalhos de inspeção e manutenção – Vista geral

Indicação
A tabela seguinte apresenta os requisitos do fabricante relativamente aos intervalos mínimos de inspeção e manutenção. Se as disposições e diretivas nacionais exigirem intervalos e inspeção e manutenção mais curtos, nesses casos cumpra os intervalos exigidos por lei.

N.º	Trabalhos	Inspeção (anual)	Manutenção (no mín. a cada 2 anos)
1	Desligue o produto da rede elétrica e feche a alimentação de gás.	X	X
2	Desinstale a envolvente frontal.	X	X
3	Verifique visualmente se o circuito de aquecimento está estanque e verifique também o funcionamento do purgador automático.	X	X
4	Faça uma verificação visual da válvula de segurança. Não se pode detetar qualquer tampão ou ligação fixa do tubo na válvula de segurança. Certifique-se de que a válvula de segurança, o funil de descarga e o tubo são os corretos. O funil de descarga tem de ser visível. Não pode existir qualquer dispositivo de corte entre a caldeira de condensação a gás e a válvula de segurança.	X	X
5	Desmonte o grupo do queimador		X
6	Limpe a câmara de combustão e lave também o sifão para condensados.		X
7	Limpe o queimador e verifique se está danificado.		X
8	Verifique a distância dos elétrodos entre si e entre o queimador.		X
9	Verifique se existe formação de depósitos nos elétrodos. Se necessário, substitua os elétrodos.		X
10	Verifique as juntas do depósito de condensados e a abertura de inspeção quanto a danos. Substitua as juntas danificadas.	X	X
11	Limpe o acumulador de condensados.	X	X
12	Verifique a mangueira para o controlador da pressão dos gases queimados quanto a sujidade e estanqueidade.	X	X

0020193890_04 Manual de instalação e manutenção 37

Figure F.1: Maintenance Tasks Manual (Part One).

N.º	Trabalhos	Inspeção (anual)	Manutenção (no mín. a cada 2 anos)
13	Verifique as mangueiras para o controlador da pressão do ar de combustão quanto a sujidade e estanqueidade.	X	X
14	Verifique o filtro de pó na caixa do ar de alimentação quanto a sujidade e danos. Se necessário, substitua o filtro de pó.	X	X
15	Instale novamente o grupo do queimador. **Atenção: substitua as juntas!**		X
16	Verifique o sifão para condensados no produto e, se necessário, encha o sifão	X	X
17	Abra a válvula de corte do gás, conecte novamente o produto à rede elétrica e ligue-o.	X	X
18	Execute um funcionamento de teste do aparelho e do sistema de aquecimento incl. a preparação de AQS e, se necessário, purgue a instalação uma segunda vez.	X	X
19	Verifique o comportamento da ignição e do queimador em **d.44**	X	X
20	Verifique o teor de CO_2 e, se necessário, regule-o.	X	X
21	Verifique o aparelho quanto a fugas do lado do gás, da exaustão, da água quente e dos condensados, elimine-os, se necessário.		X
22	Verifique todos os dispositivos de segurança.	X	X
23	Verifique o funcionamento do controlador da pressão dos gases queimados através de um congestionamento total dos gases queimados com ventilador dos gases queimados. Efetue uma verificação visual de todas as mangueiras e niples de medição.		X
24	Verifique os dispositivos de regulação (regulador externo) e, se necessário, regule-os novamente.	X	X
25	Efetue uma medição da carga.		X
26	Se existente: faça a manutenção do acumulador de água quente sanitária.		a cada 5 anos, independentemente do gerador de calor
27	Registe em protocolo a inspeção/manutenção efetuada.	X	X
28	Instale a envolvente frontal.	X	X
29	Verifique a pressão da instalação e, se necessário, corrija-a	X	X
30	Verifique o estado geral do aparelho. Remova a sujidade geral existente no produto.	X	X

Figure F.2: Maintenance Tasks Manual (Part Two).

Appendix G

Automatic Maintenance Report

De: isabelazevedo.asl@gmail.com
Para: up2020068802up.pt
Assunto: Relatório de Tarefas Concluídas - junho/2025
Data: 13/07/2025

Relatório das tarefas concluídas no mês atual:

Data: 13/06/2025 Utilizador: Isabel Azevedo Categoria: Bombas circuladoras Descrição da tarefa: Verificar ruídos e vibrações da bomba Observações:

—

Data: 13/06/2025 Utilizador: Isabel Azevedo Categoria: Bombas circuladoras Descrição da tarefa: Verificar estanquidade do empanque e juntas Observações:

—

Data: 13/06/2025 Utilizador: Isabel Azevedo Categoria: Bombas circuladoras Descrição da tarefa: Verificar alinhamento e aperto do chassis da bomba Observações: Verificar registos anteriores

—

Data: 13/06/2025 Utilizador: Isabel Azevedo Categoria: Bombas circuladoras Descrição da tarefa: Verificar estado dos rolamentos Observações:

—

Data: 13/06/2025 Utilizador: Isabel Azevedo Categoria: Bombas circuladoras Descrição da tarefa: Verificar aquecimentos anormais Observações:

—

Data: 13/06/2025 Utilizador: Isabel Azevedo Categoria: Bombas circuladoras Descrição da tarefa: Verificar sistema de arrefecimento Observações:

—

Appendix H

Boiler Specifications Manual

Dimensões

	VKK 806/3- VKK 1206/3-E VKK 1606/3-E	VKK 2006/3-E VKK 2406/3-E VKK 2806/3-E
A	1.168	1.478
B	1.240	1.550
C	150	200
D	130	130

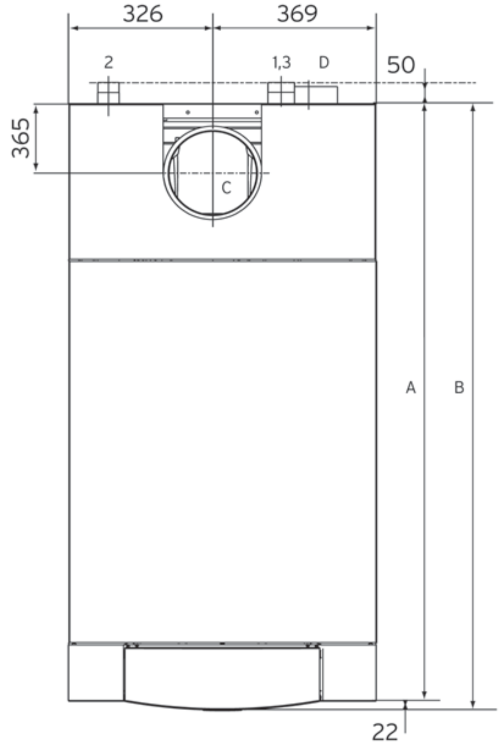

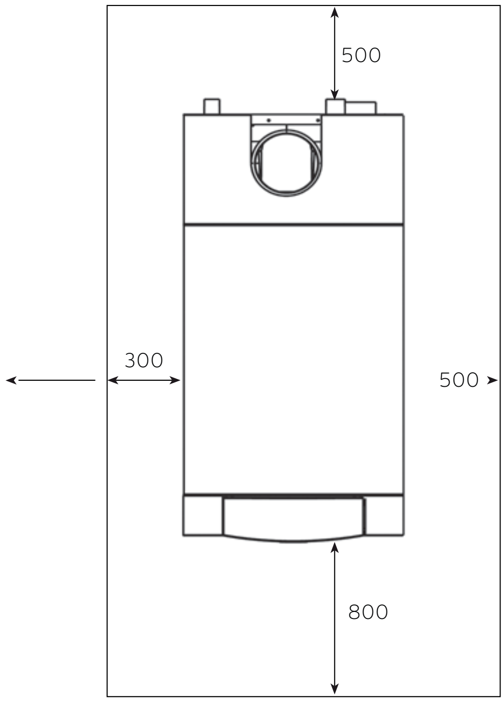

Distâncias mínimas na montagem
para facilitar a manutenção.

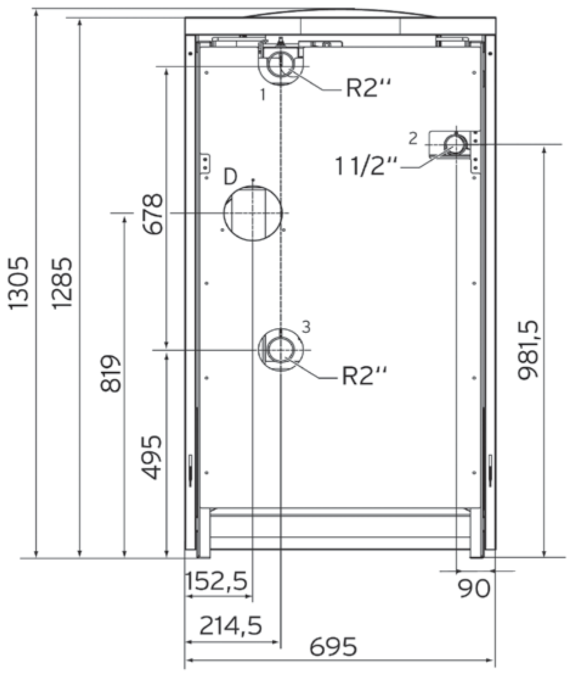

Legenda
1 Ligação de avanço de aquecimento
2 Ligação de gás
3 Ligação de retorno do aquecimento
C Ligação de exaustão de gases
D Ligação de entrada de ar

Dados técnicos

ecoCRAFT exclusiv

	Condições	Unidade	ecoCRAFT exclusiv					
			VKK 806/3-E	VKK 1206/3-E	VKK 1606/3-E	VKK 2006/3-E	VKK 2406/3-E	VKK 2806/3-E
Etiqueta Energética			A	A	A	A	A	A
Dados técnicos								
Potência útil mín.-máx.	40/30 °C	kW	14,7-84,1	23,1-121,8	28,4-168,2	46,2-210,2	50,4-252,2	54,7-294,3
Potencia útil mín.-máx.	60/40 °C	kW	14,1-80,4	22,1-116,5	27,1-160,8	44,2-201,0	48,2-241,2	52,3-281,4
Potencia útil mín.-máx.	80/60 °C	kW	13,6-77,9	21,3-112,9	26,2-155,8	43,1-196,8	47,0-236,2	51,0-275,5
Campo de modulação		%	17,5 - 100	19 - 100	17 - 100	22 - 100	20 - 100	19 - 100
Poder calorífico nom.		kW	80,0	115,9	160,0	200,0	240,0	280,0
Rendimento útil	40/30 °C	%	105,1	105,1	105,1	105,1	105,1	105,1
Rendimento útil	60/40 °C	%	100,5	100,5	100,5	100,5	100,5	100,5
Rendimento útil	80/60 °C	%	97,5	97,5	97,5	98,4	98,4	98,4
Rendimento útil [1]	75/60 °C	%	106,0	106,0	106,0	106,0	106,0	106,0
Rendimento útil [1]	40/30 °C	%	110	110	110	110	110	110
Rend. standard [3]	30%[2]	%	108	108	108	108	108	108
Aquecimento								
Campo de Ta ajustáveis		°C	35 - 85	35 - 85	35 - 85	35 - 85	35 - 85	35 - 85
Temperatura máxima		°C	85	85	85	85	85	85
Caudal	Δt = 20K	L/h	3.442	4.986	6.883	8.604	10.325	12.046
Perda de carga		mbar	80	85	90	95	100	105
Pressão máxima		bar	6	6	6	6	6	6
Projeto								
Valores mínimos de								
água em circulação[4]								
Mínima potência	Δt = 25K		14	22	27	44	48	53
		kW	0,49	0,54	0,66	1,08	1,18	1,28
Potência de arranque		m3/h	20	44	52	77	85	105
		kW	0,7	1,09	1,26	1,88	2,1	2,58
Máxima potência		m3/h	80	116	160	200	240	280
		kW	2,75	4,12	5,5	6,87	8,25	9,62
Volume de água	Δt = 20K	m3/h	3.442	4.986	6.883	8.604	10.325	12.046
Perda de carga	Δt = 20K	L/h	80	85	90	95	100	105
Dep. equilíbrio rec. [4]		mbar	WH 95	WH 160	WH 160	WH 280	WH 280	WH 280
Ligações								
Ligações ida/retorno			R2"	R2"	R2"	R2"	R2"	R2"
Ligações condensados		Ø mm	21	21	21	21	21	21
Ligação de gás			1 1/2"	1 1/2"	1 1/2"	1 1/2"	1 1/2"	1 1/2"
Conduta de exaustão								
Ligação de saída de gases		mm	150	150	150	200	200	200
Pressão de tiragem		Pa	100,0	100,0	150,0	150,0	150,0	150,0
Tipos de instalação	C_{33}, C_{43}, C_{53}, C_{83}, B_{23}, B_{23P}							
Dimensões								
Vol. água na caldeira		L	5,74	8,07	10,4	12,73	15,05	17,37
Altura		mm	1.285	1.285	1.285	1.285	1.285	1.285
Largura		mm	695	695	695	695	695	695
Profundidade		mm	1.240	1.240	1.240	1.550	1.550	1.550
Peso								
Com embalagem		kg	260	280	295	340	360	375
Sem embalagem		kg	200	220	235	275	295	310
Sem embalagem, c/ água		kg	210	235	255	300	320	340
Ligação elétrica								
Tensão/Frequência		V/Hz	230 / 50	230 / 50	230 / 50	230 / 50	230 / 50	230 / 50
Potência absorvida		W	260	260	320	320	320	320
Grau de proteção			IP 20	IP 20	IP 20	IP 20	IP 20	IP 20
Combustão								
Categoria			I2H	I2H	I2H	I2H	I2	I2H
Caudal PDCs mín./máx.		g/s	6,3 / 35,4	10 / 51,2	12,2 / 70,7	19,9 / 88,4	21,7 / 106,1	23,5 / 123,8
Ta PDCs mín./máx.	80/60 °C	°C	60-65 / 65-70	60-65 / 65-70	60-65 / 65-70	60-65 / 65-70	60-65 / 65-70	60-65 / 65-70
Perdas em repouso	70 °C	%	< 0,4	< 0,4	< 0,4	< 0,4	< 0,4	< 0,4
Emiss. CO2 mín./máx.	G20	%	9,1 / 9,3	9,1 / 9,3	9,1 / 9,3	9,1 / 9,3	9,1 / 9,3	9,1 / 9,3
Classe NOx			5	5	5	5	5	5
Emissões NOx		mg/kWh	< 60	< 60	< 60	< 60	< 60	< 60
Emissões CO		mg/kWh	< 20	< 20	< 20	< 20	< 20	< 20
Água de condensação	40/30 °C	L/h	13	20	27	34	40	47
Valor pH condensação	aprox.		3,5-4,0	3,5-4,0	3,5-4,0	3,5-4,0	3,5-4,0	3,5-4,0
Consumo de gás	15 °C/1013	m3/h	8,5	12,3	16,9	21,2	25,4	29,6
Homologação CE			0063BS3740					

1) DIN 4702, parte 8
2) EN 483
3) De acordo com a Diretiva Europeia 92/42/CEE
4) Não é necessário um depósito de inércia ou de equilíbrio mas, de acordo com a temperatura de trabalho, é necessário verificar em projeto se é possível garantir o caudal mínimo.

Appendix I

Life Cycle Costs Report

Ano a Avaliar

35

Nome	Soma de Valor
Custo Eletricidade MWh	61,00
Custo Gás Natural MWh	41,00
Horas de Funcionamento por Dia	24,00

2163,2
Consumo Gás Anual (MWh)

2,80
Consumo Eletricidade Anual (MWh)

0,0 €
Custo de Aquisição

734,0 €
Custo de Manutenção Anual

88.863,6 €
Custo Energia Anual

89.597,6 €
Custo no Ano a Avaliar

228.004,0 €
Custo Acumulado até ao Ano a avaliar

Intervalo de Anos

0 40

3.871.410,0 €
Custos Acumulados Totais

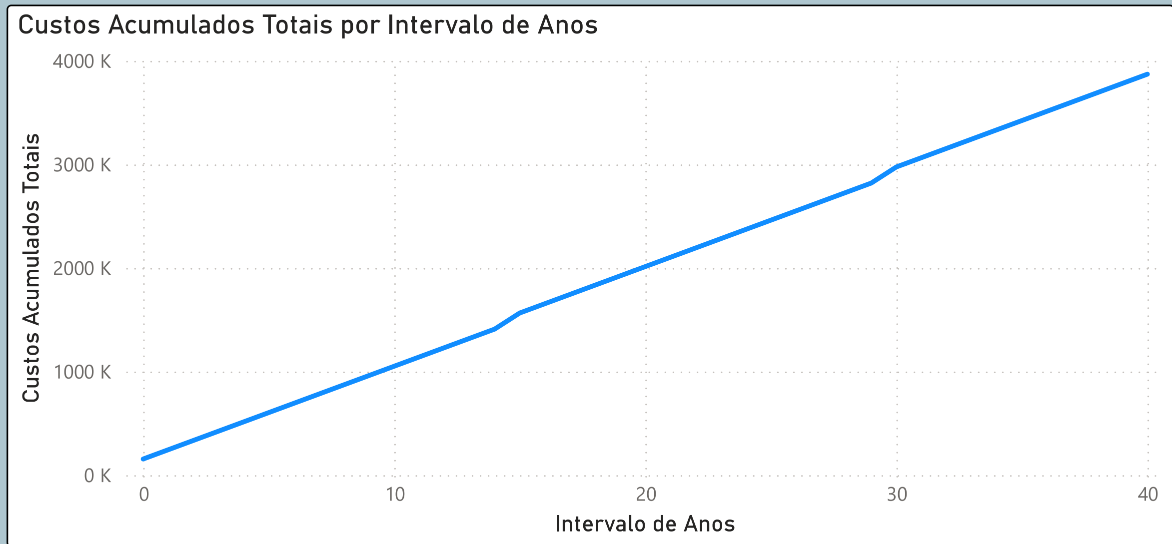

Appendix J

Life Cycle Costs Report

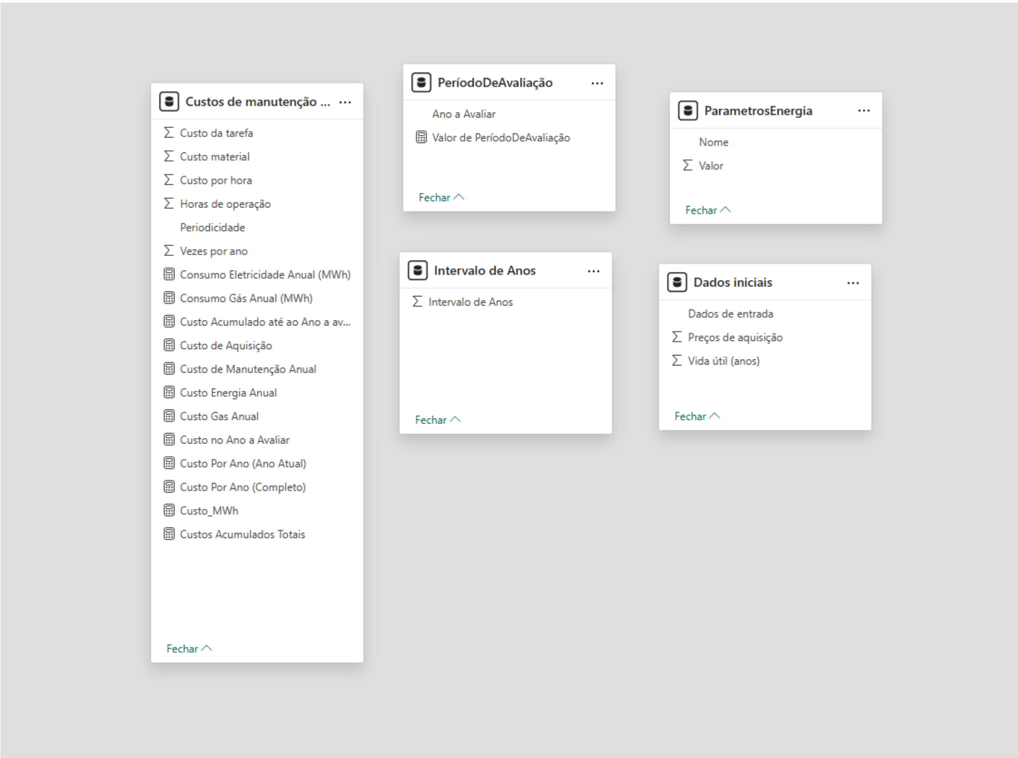

Figure J.1: LCCA tool in Power BI blocks.